UNIVERSITY OF MINING AND GEOLOGY "ST. IVAN RILSKI"

JOURNAL

OF

MINING AND GEOLOGICAL SCIENCES

Volume 60
Part II: MINING, TECHNOLOGY AND MINERAL PROCESSING

Publishing House "St. Ivan Rilski"
Sofia, 2017

ISSN 2535-1184

www.mgu.bg

C O N T E N T S

С Ъ Д Ъ Р Ж А Н И Е

COMPUTATIONAL POTHOLE MINING SUBSIDENCE ANALYSIS

Nandor Tamaskovics[1], Pavel Pavlov[2], Lyuben Totev[2], Detlev Tondera[1]

[1] Geotechnical Institute, TU Bergakademie Freiberg, Freiberg, Germany
[2] University of Mining and Geology „St. Ivan Rilski", Sofia, Bulgaria

ABSTRACT: The use of sites over old or active mining regions or with natural openings in the ground includes an elevated technical risk, as constructions can be constrained due to unplanned deformations of the subsoil. Typical failure modes include pothole subsidence or earthfalls, when failing soil masses are displaced and loosened stepwise toward a collapsing opening in the ground. The displacement process continues until a stable static equilibrium is reached and a further propagation of displacements is prevented. To determine the failure probability on a given site due to pothole subsidence, an efficient computational prognosis method for the practical estimation of the expected subsidence volume is required and proposed that is based on simple geotechnical assumptions.

Keywords: mine, subsidence, pot-hole, deformation, prognosis, numerical method

ИЗЧИСЛИТЕЛЕН АНАЛИЗ ПРИ СЛЯГАНЕТО НА МУЛДА

Нандор Тамашкович[1], Павел Павлов[2], Любен Тотев[2], Детлев Тондера[1]
[1] Геотехнически институт , ТУ - Минна академия , Фрайберг , Германия
[2] Минно-геоложки университет „Св. Иван Рилски ", София , България

РЕЗЮМЕ: Използването на терени, разположени над стари или действащи рудници или такива с естествени отвори на повърхността предполага повишен технически риск. Строителството може да бъде възпрепятствано поради непланирани деформации на грунтовия слой. Обичайните начини на пропадане включват пропадане на отвора в горнището на мулдата или поява на срутища, при които пластове земна маса се деформират и постепенно се изместват, придвижвайки се към обрушващ се отвор. Процесът на пропадане продължава, докато се достигне стабилно статично равновесие и се предотврати по-нататъшното разпространение на деформациите. За да се определи вероятността за поддаване на даден участък в резултат от пропадане на отвора на мулдата, е необходимо да се предложи ефективен изчислителен прогностичен метод за практическото изчисление на очаквания обем, на слягане.

Ключови думи: мулда, слягане, отвор в горнището, деформация, прогноза, цифров метод

Introduction

The use of sites over old or active mining regions or of sites with natural openings in the ground includes an elevated technical risk, as constructions can be constrained due to unplanned deformations of the subsoil. Typical failure modes include pothole subsidence or earthfalls, when failing soil masses are displaced and loosened stepwise toward a collapsing opening in the ground. The displacement process continues until a stable static equilibrium is reached and a further propagation of displacements is prevented.

To determine the failure probability on a given site due to pothole subsidence, an efficient computational prognosis method for the practical estimation of the expected subsidence volume is required and proposed that is based on simple geotechnical assumptions. In computational methods for potential pothole subsidence analysis, the emphasis is not on the time required until a failure happens but on the development of a static equilibrium stopping a further extension of the failure zone.

Computational pothole subsidence analysis

The different theoretical approaches proposed for the computational pothole subsidence analysis have been categorized by Fenk et al. (2004) into failure volume balance methods, force equilibrium methods, arch failure methods, and complex methods. The practical application of computational methods for pothole subsidence analysis proves to be difficult, as information on the structure of the ground and on the spatial distribution of material specific parameters is limited and an additional geotechnical ground prospection is often not feasible.

In the mechanical process of a pothole subsidence, the tensile strength of the material in the subsoil has very high importance. The driving force behind the failure mechanism is given by the gravity forces directed vertically downwards. During the extension of a pothole failure zone, sequential partial failures take place. After a partial failure, the occurring changes in the stress state are temporarily supported by the neighbouring subsoil regions for a certain time period, but the extension of the pothole failure zone probably slowly continues until a stable static and volumetric equilibrium is reached. These assumptions are backed by the common field experience that pothole failures typically take several decades to

centuries to develop and reach the ground surface.

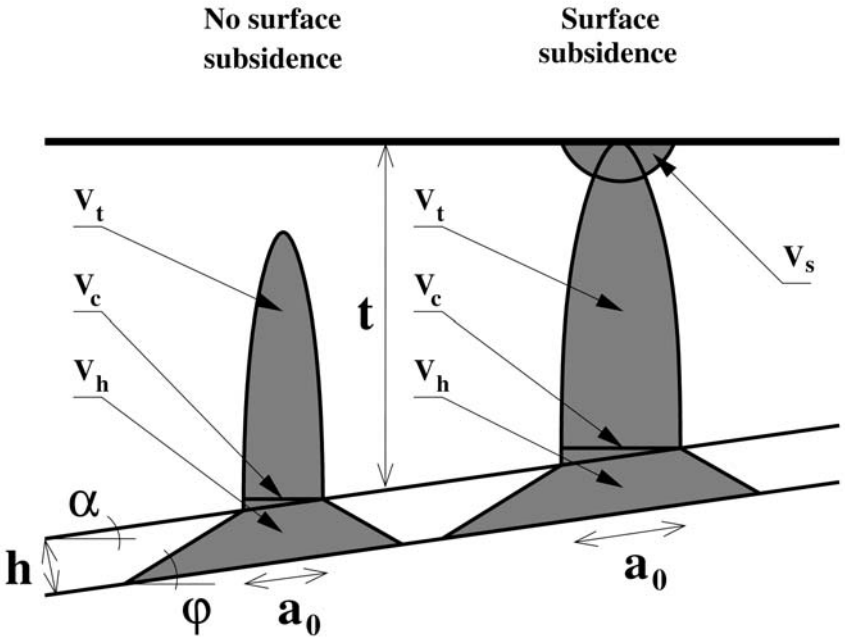

Fig. 1. Pothole surface subsidence concept

The very simple and robust theoretical concept of the failure volume balance method (FVBM) can be seen in Figure 1. In an artificial or natural void space with the height of h and inclination α, a local failure takes place on the roof over a length of a_0. The void space is filled by failing masses in the subsoil over the failure zone in the roof, where the initial volume V_h develops with a typical bulk friction angle φ. In the subsoil, a failure zone with the volume of V_c and V_t develops towards the ground surface. If the ground surface has been reached by the failure mechanism and a static equilibrium has not been reached, an additional surface failure volume V_s must be included into the volumetric balance. During the failure process, the moving and failing masses with the volume V_c, V_t and eventually V_s, the volume is increased with a material specific loosening factor s. The theoretical concept of the failure volume balance method (FSVM) is based on the governing volume conservation equation

$$V_t + V_c + V_h = s \cdot (V_t + V_c + V_s) \ , \ [m^3] \ .$$

Re-formulating the governing equation of volume conservation for the volume V_s of the pothole subsidence failure on the ground surface, the equation takes the form

$$V_s = \frac{1}{s} \cdot (V_t + V_c + V_h) - (V_t + V_c) \ , \ [m^3] \ \geq \ 0 \ .$$

Re-arranging the terms for the condition that the volume of surface failure vanishes V_s=0, an equation for the minimum height of the subsoil overburden t_{min} can be derived, when no subsidence volume is expected to appear on the ground surface

$$V_t(t_{min}) = \frac{V_h}{s - 1} - V_c \ , \ [m^3] \ .$$

The simple theoretical framework of the failure volume balance method (FVBM) uses only the failure length of a_0 in the void space roof, the inclination α and height h of the void space, the typical bulk friction angle φ in the subsoil, the loosening factor s, and the geometrical configuration of the failure as its input parameters.

Depending on the regarded plane or spatial geometrical configuration, different analytical concepts for the mathematical formulation of the initial failure zone in the failing void space V_h and for the volume in the failing subsoil V_c and V_t have been proposed by Meier et al. (2005) and Tamáskovics et al. (2017).

From information on the void space configuration, subsoil height over the failing void space, and observed failure volumes on the ground surface, the specific parameters of the missing material can be estimated with back calculation. With the small number of process parameters, the robustness of the method increases, since the input values can be determined with higher accuracy.

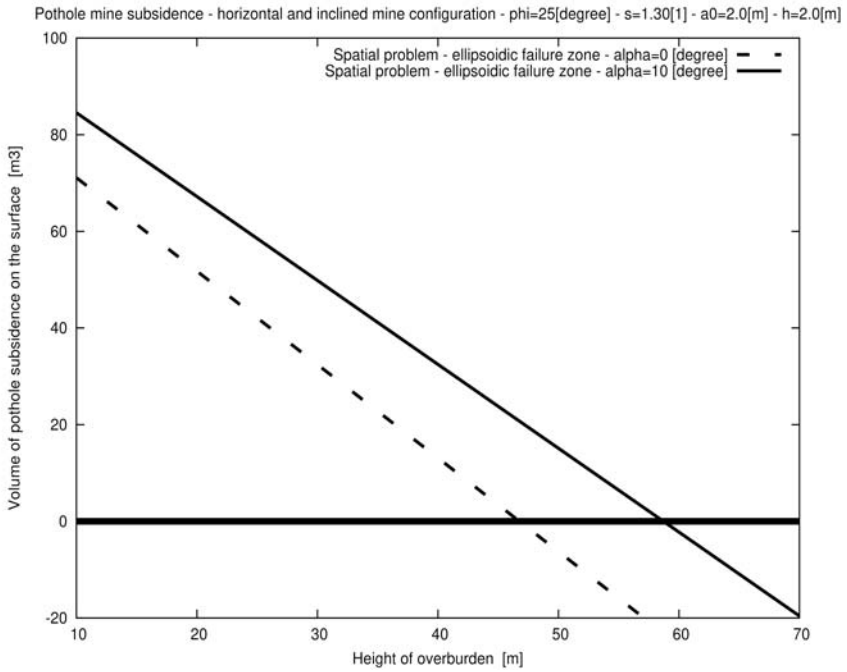

Fig. 2. Computational pothole surface subsidence prognosis

Practical application

For a practical three-dimensional case, a computational pothole mine subsidence analysis has been carried out. The friction angle for the bulk mass in the primary volume with a failing roof extension of a_0=2.0 m and a height of h=2.0 m has been assumed with φ=25°. The loosening factor for the failing volume in the subsoil with a half ellipsoid form over the primary volume with a cone frustum form has been introduced with s=1.3 [1]. The inclination of the failing void space was assumed with α=0° and α=10°.

The computational results can be seen in Figure 2. With low values for the height of the overburden t over the failing void space, a positive volume for the pothole subsidence on the ground surface V_s is calculated. Negative values mean no volume subsidence on the ground surface. The short computational analysis example clearly shows the great advantage and potential of the failure volume balance method (FSVM) for practical applications.

Summary and conclusions

Technical risk is involved in the use of sites that are either over old or active mining regions or are with natural openings in the ground, since unplanned deformations of the subsoil can lead to constraints in the constructions. The failure modes include pothole subsidence or earthfalls, when failing soil masses are displaced and loosened stepwise toward a collapsing opening in the ground. The process continues until a stable static equilibrium is reached and a further propagation of displacements is prevented.

To determine the failure probability on a given site due to pothole subsidence, it is necessary to estimate the expected subsidence volume; for this purpose, an efficient computational prognosis method is proposed that is based on simple geotechnical assumptions. In computational methods for potential pothole subsidence analysis, the emphasis is not on the time required until a failure happens but on the development of a static equilibrium that stops the further extension of the failure zone.

The simple theoretical framework of the failure volume balance method (FVBM) uses only the failure length of a_0 in the void space roof, the inclination α and height h of the void space, the typical bulk friction angle φ in the subsoil, the loosening factor s, and the geometrical configuration of the failure as its input parameters. With the small number of process parameters, the robustness of the method increases, since the input values can be determined with higher accuracy.

References

Fenk, J., W. Ast. Geotechnische Einschätzung bruchgefährdeten Baugrunds. Geotechnik, vol.27 (2004), no.1, p.59-65.

Hundt, R. Erdfalltektonik. Verlag von Wilhelm Knapp, Halle (Saale), 1950, p.137.

Meier, J.; G. Meier. Modifikation von Tagesbruchprognosen. Geotechnik, vol.28 (2005), no.2, p.119-125.

Tamáskovics, N., G. Meier, S. Braun, B. Schlesinger. Statistisches Konzept zur Risikoanalyse von Tagesbrüchen über natürlichen und künstlichen Hohlräumen, in J. Benndorf, (ed.): Abschrift 18. Geokinematischer Tag, Freiberg, 2017.

This article was reviewed by Assoc. Prof. Dr. Elena Vlasseva and Prof. Dr. Nikolay Jechev.

TECHNOLOGY FOR BACKFILLING OF THE MINED-OUT AREAS WITH PASTE FILL APPLIED AT DUNDEE PRECIOUS METALS CHELOPECH

Emilia Todorova[1], Ivan Avramov[1], Ivan Georgakiev[1]

[1]Dundee Precious Metals Chelopech, Emilia.Todorova@dundeeprecious.com, Ivan.Avramov@dundeeprecious.com, Ivan.Georgakiev@dundeeprecious.com

ABSTRACT. This article covers the methods for backfilling of mined out areas with paste fill (PF), used at Dundee Precious Metals Chelopech. Described are the onsite Paste Plant; Paste Reticulation System, the paste fill control system, methods used for barricading the ramp accesses to the mined out areas (production stopes), as well as paste quality control methods. Presented are also the major paste fill parameters.

Keywords: paste plant, work parameters, barricades, quality control, samples, solid content, cement

ТЕХНОЛОГИЯ ЗА ЗАПЪЛВАНЕ НА ИЗЗЕТИТЕ ДОБИВНИ ПРОСТРАНСТВА С ПАСТОВО ЗАПЪЛНЕНИЕ, ПРИЛАГАНА В „ДЪНДИ ПРЕШЪС МЕТАЛС ЧЕЛОПЕЧ“ ЕАД

Емилия Тодорова[1], Иван Аврамов[1], Иван Георгакиев[1]

[1]„Дънди Прешъс Металс Челопеч“ ЕАД, Emilia.Todorova@dundeeprecious.com, Ivan.Avramov@dundeeprecious.com, Ivan.Georgakiev@dundeeprecious.com

РЕЗЮМЕ. В тази статия се разглеждат методите за запълване на иззетите добивни пространства с пастово запълнение (ПЗ), прилагани в „Дънди Прешъс Металс Челопеч” ЕАД. Описват се разположените на територията на предприятието Фабрика за пастов материал, Системата за мрежовидно разпределение на пастовия материал, системата за управление на пастовото запълване, използваните методи за преграждане на рамповия достъп до иззетите добивни площи (производствени крепежи), а също и методите за управление на качеството на пастовия материал. Представени са също и основните параметри при пастовото запълнение.

Ключови думи: фабрика за пастов материал, работтни параметри, прегражения, контрол на качеството, образци, съдържание на твърди частици, цимент

Introduction

Chelopech mine is an underground mine for mining of copper-gold ore. With the development of the mining works in depth, in 2005, the sublevel caving system was replaced by chamber-and-pillar system with backfilling.

Since the introduction of the chamber-and-pillar system of backfilling, the technology for backfilling of the mined-out areas has passed through the following stages:

Stage 1: Until 2008, ore mining was carried out through primary chambers where the sterile rock mass, generated by the driven mining workings in the mine, was temporarily stored.

Stage 2: In 2007, an installation for the production of cement milk that is used for the production of cemented rock fill (CRF) was put into operation. CRF is a mixture of cement milk and basic filler of sterile rock mass. The sterile rock is produced from the driven mining workings in the mine and the mined-out primary chambers temporarily filled with sterile rock mass. This type of backfilling was in operation till 2013 and afterwards its application was stopped.

Stage 3: 2008 saw the completion of the installation for the production of hydraulic hardening fill (HHF) at the north site of Chelopech mine. HHF is a mixture of cyclone flotation tailings from the processing factory, water and cement. From 2008 to the middle of 2010, the main backfilling of the mine was CRF and HHF.

Stage 4: The process for optimization of the surface installation was completed by September 2010 and the hydraulic fill was replaced by paste fill (PF). The paste fill is a mixture of compressed and filtrated flotation tailings with weight content of solid particles between 68% and 75.5% and binding substance - sulphate-resistant cement.

The introduction of PF aims at improving the quality of the backfilling, decreasing the quantity of the binding substance (cement) and increasing the utilisation of the waste product.

PF with a different percentage of cement is used during the backfilling process of the mined-out areas depending on the necessary parameters for sustainability of the artificial massif of backfilling. To reach the set parameters of the finished hardened product requires certain time for the cement to bind and for to acquire the necessary strength. Only after that is it possible to proceed with the next stage - the mining-out the adjacent chamber (Fig. 1 and Fig. 2).

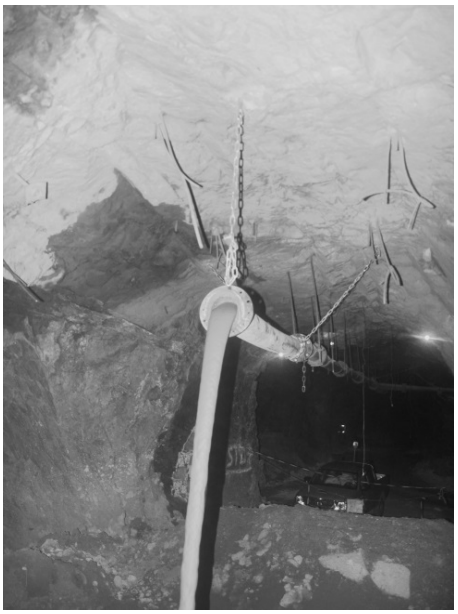

Fig.1. The process of backfilling of a chamber

Fig. 2. Surface of a chamber filled with paste fill

Installation for the production of paste fill

The after-flotation tailings from the processing factory are thickened in a cone thickener and transported via a pipeline to the installation for the production of paste fill which is situated on the north site of Chelopech mine (Fig. 3). The waste is fed into a buffer container with a volume of 1045 m^3 and has a weight content of solid particles 50%-60%.

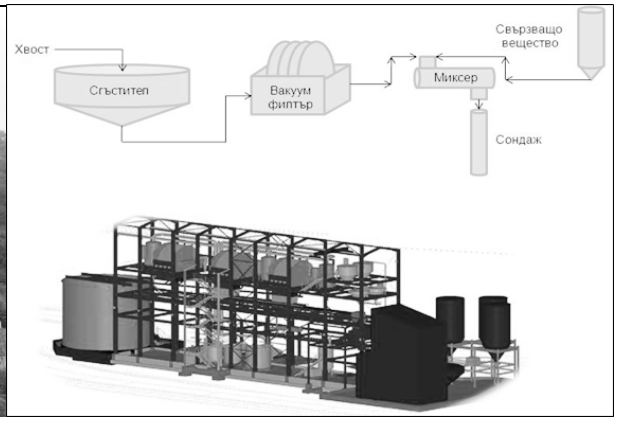

a) Surface filling complex

b) Principle scheme of the installation for paste fill (PF)

Fig.3. Installation for the production of paste fill

Through a pipeline, the material is transported to two Bokela disc vacuum filters (Fig. 4) which de-water the mixture to about 80% content of the hard substance. Flocculant water solution is added to the tub of each vacuum filter in order to better catch the particles of the waste, to clear the waste waters, and to increase the productivity of the filters.

The dried waste is supplied by a belt conveyor (Fig. 5) to the mixer for continuous mixing (Fig. 6). The cement and the unfiltered waste are added in the mixer together with the dried waste.

The dry binding substance (in this case sulphate resistant cement, strength class 42.5) is transported to the mixer via a pipeline with compressed air. The unfiltered waste is added from the buffer container to dilute the waste to the planned content of solid particles.

Productivity and production parameters

1. ***Productivity***:
   - Daily productivity of the paste fill (m^3/day): ~2 500 m^3/day
   - Monthly productivity of the paste fill (m^3/h): ~52 500 m^3/month
   - Annual productivity of the paste fill (m^3/h): ~680 000 m^3/year
   - Mean quantity of the sulphate resistant cement (t/year): ~40 000 t/year
   - Total flotation tailings generated by the factory (t): ~1 900 000 t
   - Total flotation tailings used for backfilling (t): ~800 000 t/year, which is 40% from the overall waste.

Fig. 4. Disc vacuum filter

Fig. 5. Belt conveyor for supplying the filtered waste

Fig. 6. Mixer for mixing the filtered waste, dry cement, and unfiltered waste

2. ***Production parameters:***

The parameters for backfilling of each chamber are described in the detailed design on the basis of tested recipes, ensuring the necessary strength parameters of the hardened filling material, and respectively, the non-problematic and safe future mining-out of the adjacent secondary stalls.

- Targeted pack compression of the ready product – maximum 240 mm;
- Level of the material in the borehole/boreholes: 230 – 250 m;
- Content of the solid particles in the borehole (%):
  - Minimum: ≥ 68%;
  - Targeted: 75.5%
- Content of the cement (%): *2% ÷ 8%.* [1]

[1] The cement content in the paste fill is different for each chamber and is determined on the basis of the width, length and height of the uncovered surface of the fill from the adjacent secondary stall.

System for transportation of the fill to the mined out areas

The system for transportation of the fill consists of two inclined boreholes driven from the surface to level 448 underground, a pipeline installation along the main haulage tunnels and preparatory cuts, and short boreholes between the separate sublevels.

The wellheads on the surface are situated immediately next to the surface installation for the preparation of the filling material and have a length of 300 m and a diameter of 300 mm. They are cased with metal and polyurethane pipes. The polyurethane pipes are with an external diameter of 225 mm and an internal diameter of 134.8 mm.

The pipeline installation along the main mining workings is implemented via 8” metal pipes, mounted on the ceiling of the workings (Fig. 7). The pipeline installation along the preparatory cuts to the chambers is via 10” polyurethane pipes for high pressure.

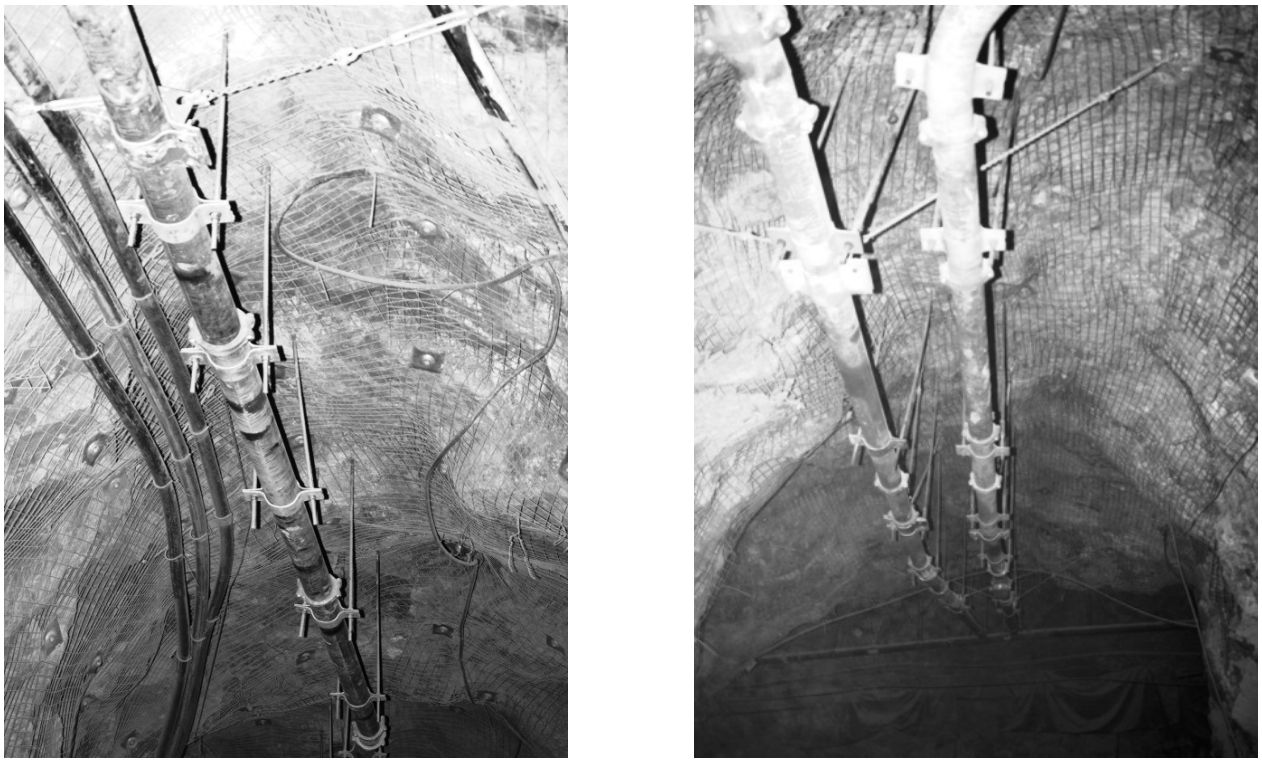

Fig.7. Metal pipeline for the supply of paste fill

Control and management system of the filling process

All available tools and functions for the management of the paste fill are ensured by the SCADA software system for process management. The operator monitors, controls and manages the filling process of the pit chambers from the control room.

SCADA provides for:

- Remote start and stop, as well as for emergency stopping.
- Visualisation of the paste fill cycle on a display;
- Visualisation of the planned and real parameters of the filling;
- Monitoring of the state of the electrical engines, including the indications for failures;
- Archiving the data for the backfilling.

Barricades

The barricades are used for closing the ramp accesses to the empty space in the mined-out areas in order to prevent spilling of the paste fill on the underground infrastructure of the pit. The barricades are built from reinforced net and shotcrete with a width of 300mm ÷ 500mm and strengthened with fibers.

The barricades (Fig. 9) are constructed in each entry that has been cut off for access to the chamber and that has to be filled in; they are situated on the lower and intermediate horizons. The detailed design for filling of each chamber with paste fill contains information about the type, parameters, and location of the barricades.

Quality control of the paste fill

1. Stability of the rock mass from hardening paste fill when mining out adjacent chamber/s

The artificial monolith mass of hardening paste fill should guarantee the overall stability in order to be able to withstand sufficient loads and to remain stable in the presence of free open space during the further mining-out of the adjacent stalls (Stefanov, Dr., 1993).

The necessary targeted strength of the paste fill is defined through computer modelling done by Revel Resources PTY LTD which is reflected in the technical report Chelopech Mining Paste Fill Exposure Stability Analysis (2011).

Preliminary assessment of the necessary stability of the artificial mass according to its open area is prepared for each chamber to be filled in (Fig. 10). This assessment takes into consideration:

- The height of the open area of the artificial mass of filling.
- The width of the open area of the artificial mass of filling.
- The length of the open area of the artificial mass of filling.

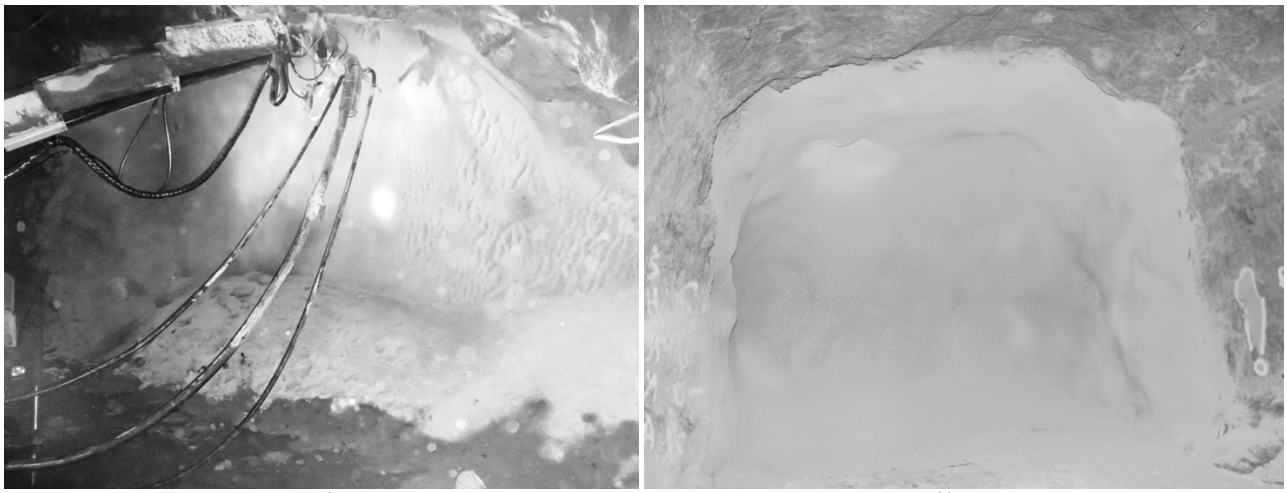

a) *b)*

Fig.9: a) Barricade in the process of sprinkling with shotcrete; b) Completed barricade

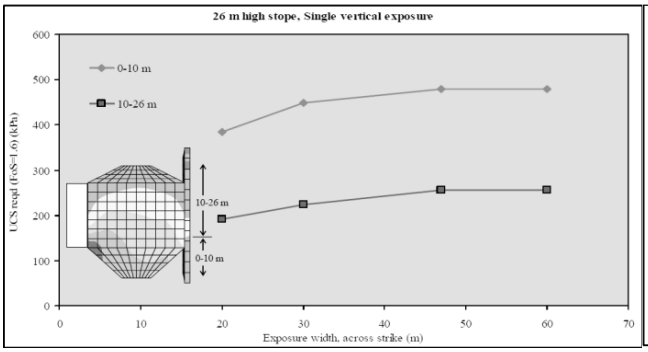

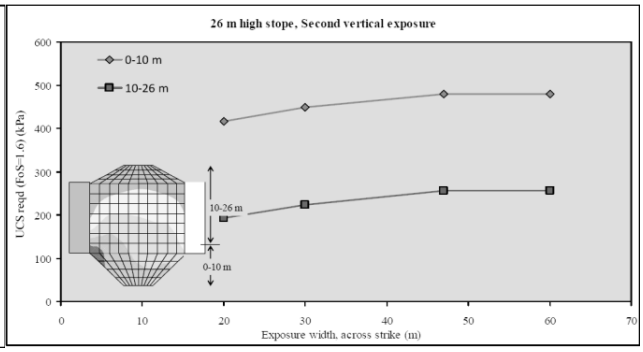

a) *b)*

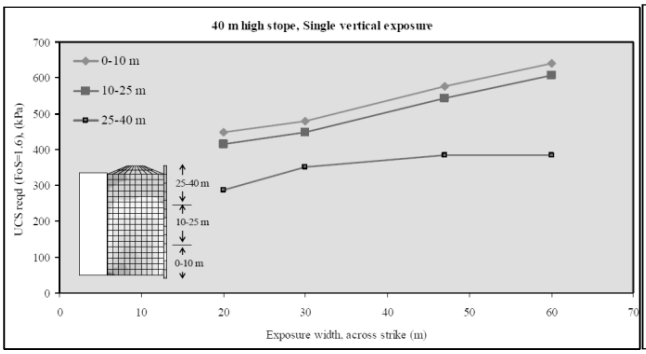

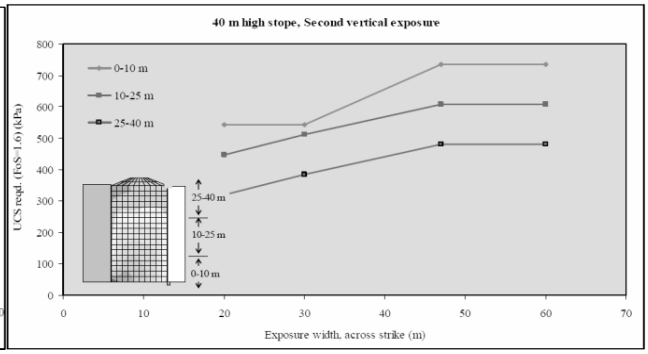

c) *d)*

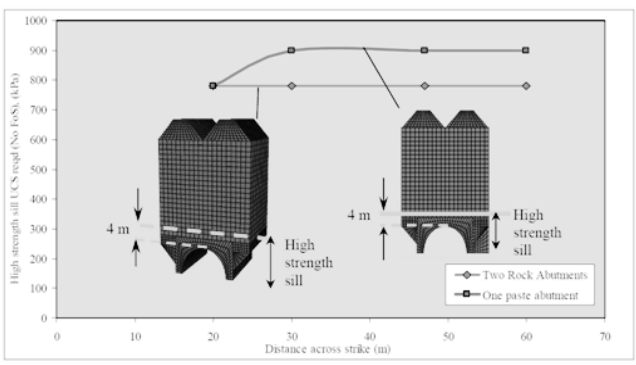

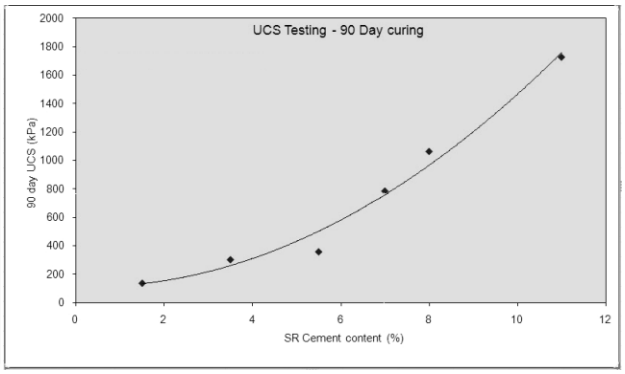

e) *f)*

Fig.10: a), c) – Targeted strength of the fill in case of one vertical open area; b), d) - Targeted strength of the fill in case of two vertical open areas; e) Targeted strength of uniaxial pressure (UP) of the PF with an open area at the base of the chamber; f) Graph for defining the percentage of the cement content

2. Sampling of the fill and strength tests

A local database has been collected on the behavior of the artificial pillars from hardening fill for the specific conditions.

In order to define the quality of the fill, samples are taken in plastic cylindrical containers with dimensions width/length – 100/200mm. The samples are taken from the installation for paste fill at the point of backfilling immediately after the mixer. The samples mature in special containers which maintain constant temperature and humidity to maximally resemble the conditions in the pit. The samples are left to gather strength for 7, 28, 56, 90 or 360 days respectively and after that are tested for uniaxial pressure (Fig.11).

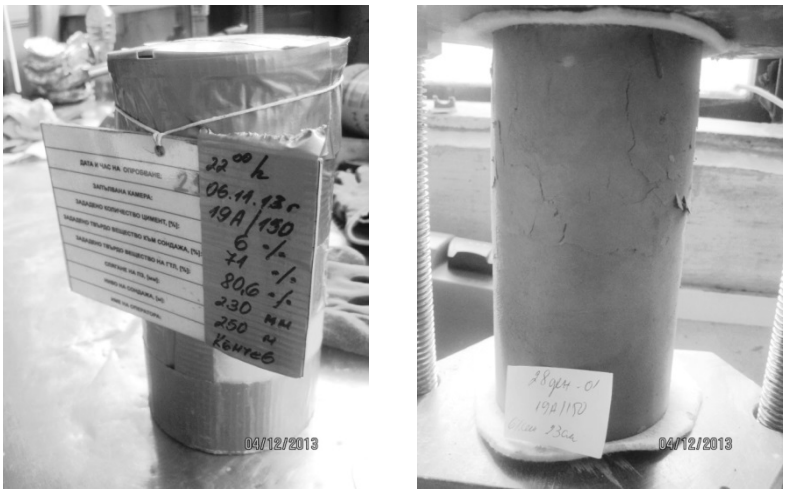

Fig.11. Sample from paste fill tested for uniaxial strength in laboratory conditions

- Each sample is taken out of its container (in laboratory conditions) and checks for disruptions are made. The state of each sample prior to the test is described.
- The height and width of each sample is measured prior to the test.
- An even load of 0.5 mm / min is applied throughout the test.
- The type of disturbance is recorded for each sample.
- The humid weight of the disturbed sample is measured after the end of the test.
- The disturbed sample is dried in a furnace for at least 24 hours at a temperature of 100°C and the dry weight it measured.
- A comparison is made between the dry and moist sample in order to define the unit weight.

The information from the samples is important and provides preliminary information about the behavior of the artificial mass at its exposed surface.

3. Defining the pack compression of the ready product

The test for defining the pack compression is an important parameter in the control programme and gives information about the quality and mobility of the fill which is supplied underground. The targeted pack compression of the ready product is between 200 mm and 240 mm and is defined in the detailed designs for the filling of the individual chambers. The Abrams cone is used for testing the paste fill for subsidence (fig.12).

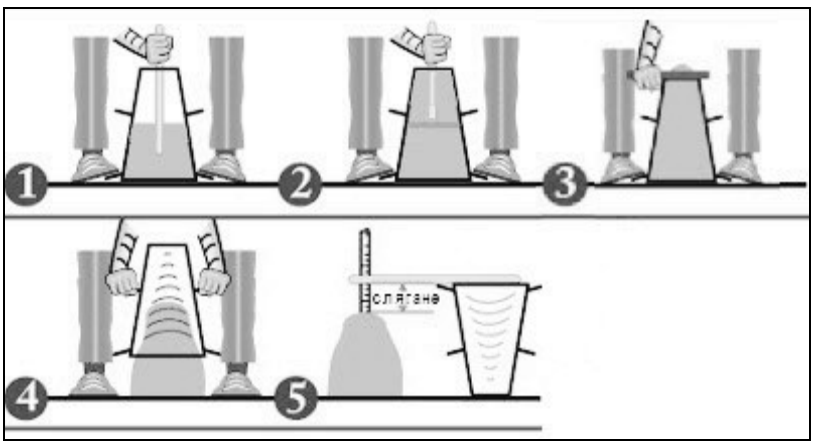

Fig.12. Defining the pack compression of the ready product using the Abrams cone

Conclusion

Backfilling is an important element for the development of the Chelopech mine and for the effective sustaining of the 2 200 000 t annual ore output. Concurrently with the backfilling of the mined-out areas in the pit, the PF should guarantee stability with regard to the various dimensions of the subsequently exposed walls of the artificial pillar formed after its hardening.

The advantages of the paste fill in comparison to the hydraulic fill are as follows:

1. Reduced quantity of the binding substance for obtaining the necessary strength of the hardened fill;
2. Lower speed of the transportation of the fill to the mined-out areas in the stalls which leads to a considerable decrease in the wearing-out of the pipeline system;
3. Shorter time for achieving early strength;
4. Smaller quantities of water generated in the water drainage system of the pit;
5. Simpler design of the barricades of the ramp accesses to the mined-out chambers;
6. Better utilisation of the waste product from the mineral processing.

Under the conditions of continuous development of the mining works in depth at the planned output of the pit, the filling of mined-out areas is a dynamic system that undergoes changes; therefore, optimisation solutions and formulations are sought that lead to safer work, continuity, stability, efficiency, economy, and flexibility of both the process and the mining technology as a whole.

References

Стефанов, Др. Подземен рудодобив. 1993. - 393 с. (Stefanov, Dr. Podzemen rudodobiv, 1993. - 393 p.)

Revel Resources PTY LTD, Chelopech Mine Paste Fill Exposure Stability Analysis (P156-Ro1), consultants report, February 2011. - 59 p.

Annual detailed design for mining and mineral processing of gold-copper ores at the Chelopech mine, 2014. - 131 p.

Designs, presentations and work procedures at Dundee Precious Metals Inc.

This article was reviewed by Assoc. Prof. Dr. Pavel Pavlov and Prof. Dr. Nikolay Jechev.

A REVIEW OF COMBINING OPEN-PIT AND UNDERGROUND MINING METHODS AROUND THE WORLD

Stefan Zehirov[1], Dimitar Kaykov[2], Ivaylo Koprev[3]

[1] University of Mining and Geology "St. Ivan Rilski", 1700 Sofia, e-mail: zehirov83@yahoo.com
[2] University of Mining and Geology "St. Ivan Rilski", 1700 Sofia, e-mail: ddv_kai@abv.bg
[3] University of Mining and Geology "St. Ivan Rilski", 1700 Sofia, e-mail: ivomad@abv.bg

ABSTRACT. Currently, some of the largest and most influential open-pit mines in the world are planning, or are in the process of implementing, the underground mining method. This leads to transitioning to underground mining or to concurrently combining open-cast and underground operations. Those mines deal with the extraction of expensive ores, such as copper, gold, diamond, etc. This is why profitability, the expensive price of the mined ores, and the depletion of the deposits close to the surface of some open-pit mines are the main factors of such technological changes.

Keywords: open-pit mines, underground mines, transition, combined mining methods

КОМБИНИРАНЕ НА ОТКРИТИЯ И ПОДЗЕМЕНИЯ СПОСОБ НА РАЗРАБОТВАНЕ В СВЕТОВЕН ПЛАН

Стефан Зехиров[1], Димитър Кайков[2], Ивайло Копрев[3]

[1] Минно-геоложки университет „Св. Иван Рилски", 1700 София, e-mail: zehirov83@yahoo.com
[2] Минно-геоложки университет „Св. Иван Рилски", 1700 София, e-mail: ddv_kai@abv.bg
[3] Минно-геоложки университет „Св. Иван Рилски", 1700 София, e-mail: ivomad@abv.bg

РЕЗЮМЕ. В настоящия момент някои от откритите рудници, които са най-големите в световен план и оказват най-значително влияние върху цените на материалите, планират или са в процес на внедряване на подземно разработване на находището. Това води до преминаване от открит към подземен способ на разработване или до комбинирането на открит и подземен добив едновременно. Тези рудници извличат скъпи материали като мед, злато, диаманти и др. Основните фактори за осъществяване на такава технологична промяна при откритие рудници са реализирането на по-висока печалба, високата цена на добиваните материали и изчерпването на рудата в близост до повърхността в някои открити рудници.

Ключови думи: открит рудник, подземен рудник, преминаване, комбиниран добив

Introduction

The application of a suitable mining method has always been a topical problem. The dynamic conditions of our time impose specific requirements for the processes of mining mineral resources. The geological conditions, economical changes and the improvement of mining technology and techniques are few of the factors which determine the choice of mining method. In order to prosper, each mining organization needs to consider the possibilities of utilizing underground or open-pit mining or combining both methods depending on the conditions, as well as to look for certain tendencies in a global scale for a preferred method.

Factors influencing the choice of mining methods

The main factors which determine the mining process are the geological conditions, the level of technological development, and the ecological and economical aspects. These factors are interdependent. The geological conditions are related to certain spatial and quality parameters, such as depth, size, type, and quality of the minerals in the deposit. While the parameters representing depth and type are fixed, the spatial parameters of the deposit depend on the level of development of the mining technology and mechanization, as well as on the current economical condition, production costs, and the selling prices. This is why boundaries of the deposit and differentiation between resources and reserves are not fixed during the life of the mine. The ecological and social aspects of mining are also an important group of factors which affect the choice of a suitable mining technology that ensures safe and healthy conditions during the mining process, especially when mining takes place near residential areas. All these groups of factors influence the choice of the mining method in a complex manner.

Combining open-pit and underground mining

There are two main cases of utilizing open-pit and underground methods of ore extraction: 1) utilizing open-pit or underground mining separately for a single ore body and 2) combining both methods simultaneously.

In the first case, both open-cast and underground mining are utilized sequentially by transitioning between the methods. Transitioning from open-cast to underground mining is a popular and preferred method for further ore extraction. The stripping ratio is a commonly used index which gives information about the profitability of the mining operations and the maximum volume of overburden. A variation of the stripping ratio could directly yield the comparison between the costs of underground mining operations and open-cast operations. Transportation costs should also be taken into account, as well as the productivity of the dumpers per shift, which depends on the number of work cycles during the shift. Deep open-pit mines have the problem of increased fuel costs and the decreased number of working cycles of dumpers. Open-cast mining, on the other hand, gives the opportunity to fully extract the ore. However, the underground method allows for extracting selectively only the richest sections of the deposit. This is why each case requires the comparison between the two methods in terms of costs per m^3 or t of ore, as well as looking for suitable combination of both methods according to the conditions. Selling prices of the extracted minerals or concentrates are one of the most important factors. Increased prices provide the opportunity of investing more funds for further development of the deposit by transitioning to the underground method or combining underground with open-pit mining. Another significant factor is the development of the mechanization and the mining technology which provide the possibility of mining ore that contains less valuable components. This is especially beneficial for the open-pit mining method due to the larger volume of lower quality ore which could be extracted. Considering the ecological factors, as well as some social aspects of mining, the choice of a suitable method also depends on health and safety factors. Open-cast mining provides a less hazardous environment for the workers, but it has a more significant impact on the environment, while the underground mining method is more environmentally-friendly and gives the opportunity to manage waste more easily. However, it is related to more hazardous working conditions. Combining both methods eliminates some of the drawbacks of each method that would be obvious should those methods be applied separately.

Examples of utilizing both open-pit and underground mining

In this article, some of the world's biggest mines have been reviewed. Predictions are that those mines are going to be the ones to mostly influence the prices of materials in the next 10 years to come (http://www.mining.com/these-10-mines-will-set-the-copper-price-for-the-next-decade/). These mines could also serve as an example for some of the most technologically advanced mines that implement modern technological solutions.

Mines which transitioned or are planning to transition from underground to open-cast mining:

Although transitioning from underground to open-pit mining is not very common, some of the mines of the Freeport-McMoRan company could serve as examples of such transitioning, which took place during the 20th century.

1. Morenci – Arizona, USA – copper – 9.7 billion t of reserves (0.25% copper, 0.002% molybdenum); productivity is 115, 000 t/day – transitioned from underground to open-cast in 1937 (https://www.fcx.com/index.htm).
2. Bagdad – Arizona, USA – copper and molybdenum – productivity is 75, 000 t/day - transitioned from underground to open-cast in 1945 (ibid.)
3. Sieritta – Arizona, USA – copper and molybdenum – productivity is 102, 000 t/day – transitioned from underground to open-cast in 1957 (ibid.)
4. Miami – Arizona, USA – copper – transitioned from underground to open-cast after 1945 (ibid.)
5. Tyrone – Arizona, USA – copper – underground mining stops in 1921; open-pit mining continued in 1967 (ibid.)
6. Kalgoorlie – Australia – gold – from underground to open-cast mining in 1989 (http://superpit.com.au/about/mining/)
7. Cannington – Australia – silver and lead – plans on transitioning from underground to open-cast mining no sooner than 2023 (http://www.townsvillebulletin.com.au/business/bhp-to-shed-up-to-70-jobs-at-cannington-mine/news-story/cc7822ec0dabdf84985c1c229eccc8df)

Mines which transitioned from open-cast to underground mining for further exploitation of the deposit:

These mines follow the traditional technological scheme of transitioning to underground mining after the open-pit mine reaches its project depth.

1. Mir – Russia – diamond – more than 141 Mct of probable reserves; expected production for 2014 was 1 Mt – open-pit mining ceased in 2001; started underground mining in 2009 on the Mir kimberlite pipe (http://www.mining-technology.com/features/feature-the-worlds-top-10-biggest-diamond-mines/)
3. Venetia – South Africa – diamond – open-pit mine reserve is 32.8 Mct (0.975 ct/t diamond); underground reserve is 70 Mct (0.765 ct/t diamond) – production for 2012 was 3.066 Mct of diamonds from 5.618 Mt ore – the forecast is that the open-pit mine will function until 2021, followed by transitioning to underground mining which will function for another 20 years; it has the potential to produce 96 Mct within the period (ibid.)
4. Ernst Henry – Australia – copper – 72 Mt reserves of 1% copper, 0.5 g/t gold and 22% magnetite – transitioned from open-cast to underground mining in 2009 (https://www. australianmining.com.au/features/the-next-age-of-mining/)
5. Kiruna – Sweden – iron – proven reserves 602 Mt of 48.5% iron, probable reserves of 82 Mt grading 46.7% iron – functioned as an open-pit mine until the 1960s, after that transitioned from open-cast to underground mining (http://www.mining-technology.com/projects/kiruna/), (http://www.mining-technology.com/projects/tropicanagoldproject/)
6. Kanowna Belle – Australia – gold – 14.87 Mt ore which is 2.4 Moz recoverable gold (5.1 g/t) – transitioned from open-cast to underground mining in 1998 (http://www.mining-technology.com/projects/kanowna/)
7. DeGrussa – Australia – copper-gold – annual productivity is up to 300, 000 t of high-grade copper concentrate – open-pit mining operations concluded in 2013; currently, production is based on long-term underground development (http://www.sandfire.com.au/operations/degrussa.html)
8. Palabora – South Africa – copper and rare metals – annual production of 80, 000t (0.7% copper) – open-pit mining ended in 2002, due to reaching its economic depth; transitioned to

underground mining and prolonging the life of the mine by at least 20 years (http://www.palabora.com/palabora.asp)

Mines which plan to transition from open-cast to underground mining for a further exploitation of the deposit:

1. Tropicana – Australia – gold – reserves are estimated to be 57.1 Mt (ore grade 2.12g/t) with annual production up to 350, 000 oz; it is rumored to transition from open-pit to underground mining (http://www.mining-technology.com/ projects/tropicanagoldproject/)
2. Mt Keith – Australia – nickel – more than 95 Mt/year; plans to transition to underground mining; currently, the project has not started due to the low price of nickel and the low grades of ore (https://www.thiess.com/projects/mt-keith-mine-alliance/ detail)
3. Rocky's reward – Australia – nickel – plans to transition to underground mining; currently, the project has not started due to the low price of nickel and the low grades of ore (https://www.thiess.com/projects/rockys-reward/detail)
4. Oyu Tolgoi – Mongolia – copper and gold – mined until now by open-cast method; since 2015, the planning stage takes place of transitioning from open-cast to underground mining; development started in 2016 and first production is expected in 2020 with an average copper grade of 1.66% and an annual production of 500, 000 t (http://www.riotinto.com/ copperanddiamonds/oyu-tolgoi-4025.aspx), (http://www. riotinto.com/media/media-releases-237_17323.aspx)
5. Grasberg – Indonesia – copper and gold – 2.8 billion t reserves (1.09% copper, 0.98 g/t gold, 3.87 g/t silver) – combined mining method; since 1990, the ores from the open-pit mine are depleting; the forecast is that the open-pit mine will function until the end of 2017; in planning stage for transitioning from open-cast to underground mining since 2015 (http://www.mining-technology.com/projects/grasbergopenpit/)
6. Los Bronces – Chili – copper and molybdenum – remaining reserves of 2.06 billion t (0.51% copper, 0.014% molybdenum); productivity is 145 Mt/y – transitioning from open-cast to underground mining no sooner than 2020 (http://www.mining.com/these-10-mines-will-set-the-copper-price-for-the-next-decade/)
7. Chuquicamata – Chili – copper and molybdenum – 1.7 billion t reserves (0.7% copper, 552 ppm molybdenum); copper productivity is 336, 000 t/year and molybdenum productivity is 18, 000 t/year – transitioning from open-cast to underground mining no sooner than 2018; the forecast is that this will extend the lifespan of the mine until 2060 (http://www.mining.com/these-10-mines-will-set-the-copper-price-for-the-next-decade/)
8. Udachny – Russia – diamond – reserves estimated to be more than 152 Mct – currently considering the alternative of transitioning from open-cast to underground mining (http://www.mining-technology.com/features/feature-the-worlds-top-10-biggest-diamond-mines/)
9. Bingham Canyon – USA – copper – continues to extract ore using open-pit mining; the forecast is that the open-pit mine will function until 2028; since 2014, the organization considers transitioning from open-cast to underground mining (http://www.mining.com/rio-tinto-heads-underground-at-bingham-canyon-mine/)
10. Grib – Russia – diamond – reserves are estimated to be more than 98 Mct; annual production 4 Mct – transitioning from open-cast to underground mining no sooner than 2030 (http://www.mining-technology.com/features/feature-the-worlds - top-10-biggest-diamond-mines/)

Mines which combine underground and open-cast mining:

1. Andina – Chili – copper and molybdenum – combines open-cast and underground mining in the Rio Blanco deposit (https://mining-atlas.com/operation/Andina-Copper-Molybdenum-Mine.php)
2. Telfer – Australia – copper and gold – reserves are 65 Moz gold, 11 Mt copper, 38 Moz silver; productivity for 2016 was 462, 461oz gold and 18, 940 t copper – the forecast from 2016 is that the open-pit mine will function until 2018 and the underground mine until 2021; since 2002, the underground extraction has a greater priority (http://www.newcrest.com.au/ our-business/operations/telfer-wa/)
3. Diavik – Canada – diamond – 18.1 Mt ore reserve (2.9 ct/t diamond) – transitioned to underground mining in 2012 for further extraction of the deposit; the forecast is that a new open-pit mine will start functioning in 2018 (http://www.riotinto.com/canada/diavik/operations-12110.aspx)
4. Argyle – Australia – diamond – reserve estimated to be 140 Mct (2.1 ct/t diamond) – currently transitioning from open-cast to underground mining; the forecast is that the open-pit mine will function as well after 2020 (http://www.mining-technology.com/features/feature-the-worlds - top-10-biggest-diamond-mines/)
5. Jundee - Australia - gold – ore production is 1 Mt per year – open-pit mining took place from 1995 to 2007; underground mining started in 1997 and currently the mine produces 1 Mt of ore annually using underground extraction (https://www.nsrltd.com/our-assets/jundee/)
6. Olympic Dam – Australia – poly-metallic mine (copper, uranium, gold, silver) – reserves estimated to be 2.95 billion t (1.2% copper, 0.04% uranium, 5 g/t gold, 6 g/t silver) currently mined underground; plans to expand with open-pit mining in the near future (http://www.mining-technology.com/projects/olympic-dam/)
7. Carlin – Nevada, USA – gold – reserves estimated to 33.3 Moz gold – in 2005, the mine operated with 13 open pit mines and 4 underground mines (http://www.mining-technology.com/projects/carlin/)
8. Goldstrike – Nevada, USA – gold – ore body is mined by combined method; Betze-Post is the open-pit mine (94.9 Mt reserve with ore grading 0.128 oz/t), Meikle underground mine (7.42 Mt estimated reserves with ore grading 0.364 oz/t) (http://www.infomine.com/library/publications/docs/Mining.com/Sep2008i.pdf)
9. Raspadskaya – Russia – coal – estimated recoverable reserve 782 Mt; total annual productivity is 13.6 Mt; consisted of 2 underground mines and 1 open-pit mine (http://www.mining-technology.com/features/feature-the-10-biggest-coal-mines-in-the-world/)

Conclusion

The conclusion is drawn that combining the underground and open-cast method is a viable option when extracting ore from deposits of expensive mineral resources which offer a great volume of ore reserves, because it requires a lot of investments. The decision of combining the two methods, as well

as implementing any other mining method, is heavily dependent on the profitability of the selected method. There is a certain tendency that the richest deposits which are close to the surface are gradually depleting. This leads to the future transition of a number of open-pit mines to underground mining technology or to combining underground mining operations with open-cast mining for certain ore bodies. This applies to the deposits of expensive materials such as diamond, copper, gold, etc. The main reason for this choice of transitioning from open-pit to underground mining is the high price of these minerals, as well as the technological innovations in underground mining. According to M. Campbell, a specialist in Sandvik Mining, many open-pit mines are coming to the end of their lifespans because of the enormous volume of burden required to be mined in order to reach the ore in depth (https://www.australianmining.com.au/features/the-next-age-of-mining/). The Rio Tinto company has shared their forecast that, by the year 2025, 40% of the production of copper on a global scale would be done by underground mining, while during the period 2009-2010 it was 26% (ibid.). Although many open-pit mines are planning to combine extraction with underground mining or to transition to underground mining, the viability and potential the open-cast mining method have not diminished. The modernization of the mines, the technological advancements in mining, beneficiation and metallurgic processes all lead to the increased volume of lower quality ore which could be extracted by open-cast mining (http://www. mining.com/web/emerging-trends-in-the-mining-industry/). In addition, the open-pit mining method continues to be leading in the extraction of less expensive materials, such as coal, as well as construction materials. Due to the specific geological conditions in Bulgaria, the combined mining method is not a popular one in this country because of the smaller volume of expensive minerals, as well as to the less valuable content in the ore compared to the mines from the above world review.

References

https://www.fcx.com/index.htm
http://www.townsvillebulletin.com.au/business/bhp-to-shed-up-to-70-jobs-at-cannington-mine/news-story/cc7822ec0dabdf84985c1c229eccc8df
http://superpit.com.au/about/mining/
http://www.riotinto.com/copperanddiamonds/oyu-tolgoi-4025.aspx
http://www.mining-technology.com/projects/grasbergopenpit/
http://www.mining.com/these-10-mines-will-set-the-copper-price-for-the-next-decade/
http://www.mining-technology.com/features/feature-the-worlds-top-10-biggest-diamond-mines/
http://www.mining.com/rio-tinto-heads-underground-at-bingham-canyon-mine/
http://www.mining-technology.com/projects/carlin/
https://www.australianmining.com.au/features/the-next-age-of-mining/
http://www.mining-technology.com/projects/kiruna/
http://www.mining-technology.com/projects/kanowna/
https://mining-atlas.com/operation/Andina-Copper-Molybdenum-Mine.php
http://www.infomine.com/library/publications/docs/Mining.com/Sep2008i.pdf
http://www.newcrest.com.au/our-business/operations/telfer-wa/
http://www.riotinto.com/canada/diavik/operations-12110.aspx
http://www.palabora.com/palabora.asp
http://www.mining.com/web/emerging-trends-in-the-mining-industry/
http://www.mining-technology.com/projects/olympic-dam/
https://www.thiess.com/projects/mt-keith-mine-alliance/detail
https://www.thiess.com/projects/rockys-reward/detail
http://www.sandfire.com.au/operations/degrussa.html
https://www.nsrltd.com/our-assets/jundee/
http://www.riotinto.com/media/media-releases-237_17323.aspx
http://www.mining-technology.com/projects/tropicanagoldproject/
http://www.mining-technology.com/features/feature-the-10-biggest-coal-mines-in-the-world/

All URLs were last accessed on 26th July 2017.

The article is reviewed by Prof. Dr. Marinela Panayotova and Assoc. Prof. Dr. Ilian Djobov.

RATIONAL USE OF HYDRAULIC EXCAVATORS IN IRON ORE PITS

V. K. Slobodyanyuk[1], Yu. Yu. Turchin[2]

Ukraine, [1]Kryvyi Rih, SIHE "KNU", [2]"ME-CENTRE" LLC

Abstract. In the iron ore pits of Kryvyi Rih (Ukraine), only rope shovels were used until recently. Hydraulic excavators have both a number of technical advantages over mechanical shovels and significant drawbacks. Ukraine's regulatory framework for iron ore pit designing does not provide recommendations for their effective use. The question of determining the rational application of hydraulic excavators in deep iron ore pits is a topical issue. The use of hydraulic excavators proves to be the most successful in developing flooded horizons and reactivating temporarily non-mining pit walls. Combined technological schemes involving joint use of rope and hydraulic excavators are also highly efficient.

Keywords: hydraulic excavators, schemes of trenching, reloading platform, counterforce

ОБЛАСТ НА РАЦИОНАЛНОТО ИЗПОЛЗВАНЕ НА ХИДРАВЛИЧНИ ЕКСКАВАТОРИ НА ЖЕЛЕЗОРУДНИ КАРИЕРИ

В. К. Слободянюк[1], Ю. Ю. Турчин[2]

Украйна, гр. Кривой Рог, [1]ДВУЗ „КНУ", [2]"МИ-ЦЕНТЪР" ООД

РЕЗЮМЕ. На железорудните кариери в гр. Кривой Рог (Украйна) доскоро са използвани само кариерни въжени екскаватори. Хидравличните екскаватори имат редица технически предимства пред въжени екскаватори, но също така имат и ред съществени недостатъци. В украинската нормативна уредба, регламентираща проектирането на железорудни кариери, отсъстват препоръки по ефективното им използване. Въпрос за оценка на рационалната област на приложение в дълбоки железорудни кариери на хидравлични екскаватори е актуален. Най-успешен е опита в прилагането на хидравлични екскаватори, свързани с разработването на обводнени хоризонти и минни работи по възобновяване на временно неработещи стени. Висока ефективност ще имат комбинираните технологични схеми, които предвиждат съвместното използване на механични и хидравлични екскаватори.

Ключови думи: хидравлични екскаватори, схема на изкопа, платформа за презареждане, контрафорс

Statement of the problem and its connection with practical tasks

The processes of open-pit mining are influenced by many factors that can be divided into production and non-production ones. Production factors include: availability of mining and transport equipment, efficiency of organization and interaction of related technological processes, formation of working benches and transport berms of the width necessary for the safe and economical operation of the mining equipment, availability of blocked-out reserves, etc. Climatic and hydrological conditions are referred to as non-production factors. The combination of production and non-production factors may create the conditions that will result in poor performance of the main complex of the mining and transport equipment and, thus, in failure to achieve the designed pit performance (Arsent'yev A. I., 2010).

In the recent decade, hydraulic excavators have been used along with traditional mechanical shovels to excavate rock mass in iron ore pits. The question of determining the rational application of hydraulic excavators in deep iron ore pits is a topical issue.

As compared with mechanical shovels, hydraulic excavators have several advantages: lower specific capital costs, higher productivity and travel speed, the smaller weight of the excavator, the smaller body turning radius, the ability to excavate the rock layer below the excavator level (Bules, P., 2016; Poderni, R. Yu., P. Bules, 2015). Among the drawbacks, one should first note the dependence of hydraulic shovels on the quality of drilling and blasting operations.

Analysis of the latest research works and publications

The issues of organization of effective operation of hydraulic excavators in difficult mining conditions have been considered in numerous works since the 1960s. In these works, insufficient attention is paid to the grounding of technological schemes that take into account the design features of hydraulic excavators and the mining and technical conditions of iron ore pits.

In (Seytbayev, Sh. A., 2005), statistical data on the operation of hydraulic and rope excavators in various conditions is analyzed. Technical and economic indicators of rope and hydraulic shovels operation in ore pits are significantly different. Under the conditions of hard rock, there is a rapid wear of the excavator systems, which reduces its technical readiness. The coefficient of technical readiness of hydraulic excavators after operating 30-36 thousand hours is reduced to 80%, while mechanical shovels reach this indicator after 60 thousand hours of operation. After 5-6 years of operation, hydraulic excavators lose their advantage over mechanical shovels (Fig. 1, Fig. 2) (ibid.; Bules, P., 2016).

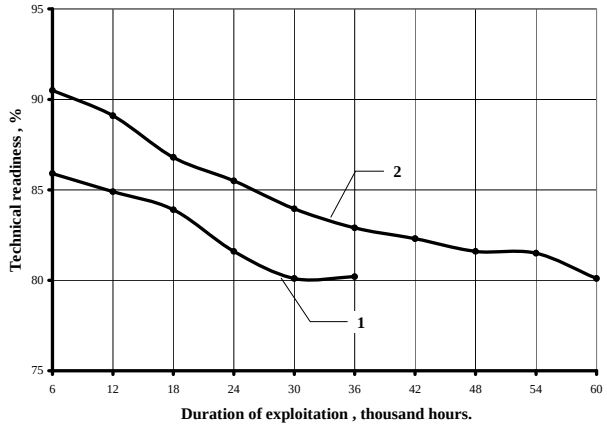

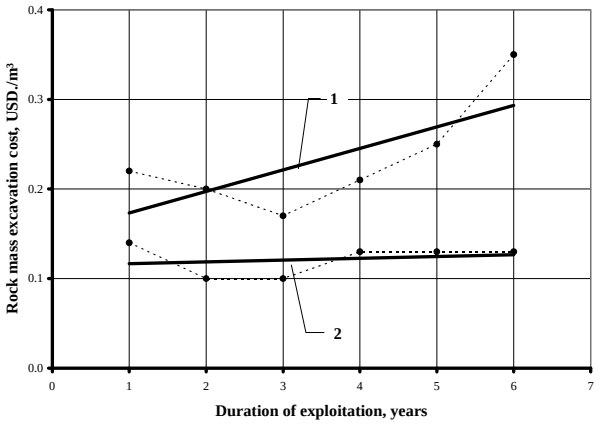

Fig.1. Dependence of technical readiness of hydraulic (1) and rope (2) excavators on the duration of exploitation of the ore pit
Fig.2. Dependence of rock mass excavation cost of hydraulic (1) and rope (2) excavators on the duration of exploitation of the ore pit

Based on the data from the directory "Mine and Mill Equipment Costs" (1995) that summarizes the technical and economic indicators of mining equipment, the diagrams of the dependence of operating and capital costs on the bucket capacity of the excavator are built. Analysis of the diagrams shows that hydraulic excavators, in comparison with mechanical shovels, are characterized by less capital costs, but greater operational costs (Fig. 3).

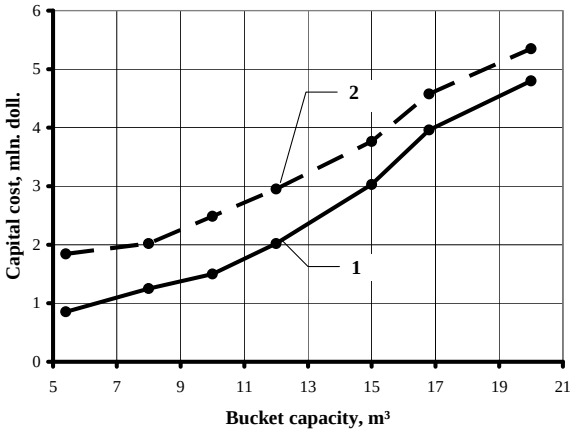

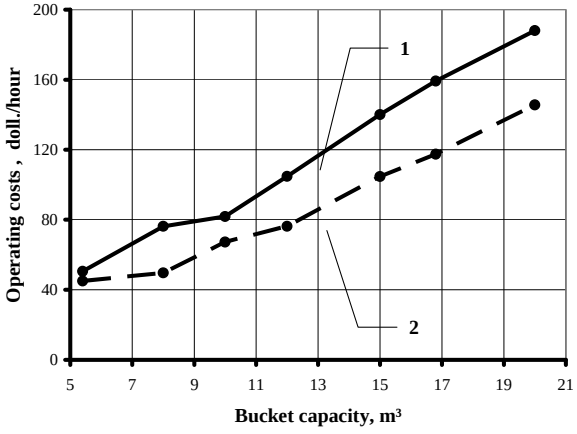

Fig. 3. Dependence of the capital cost of hydraulic (1) and rope (2) excavators on the bucket capacity

An interesting experiment on comparing technical and economic indicators of mechanical and hydraulic excavators was carried out at Muruntau gold ore pit (Uzbekistan) (Shemetov et al., 2005; Seytbayev, Sh. A., 2005). The use of powerful hydraulic excavators of different manufacturers (Caterpillar, Hitachi, O & K, Terex Mining) in the Muruntau mine, combined with heavy-duty dump trucks, made it possible to achieve high mining mass productivity with reduction in the total number of excavators in the first years of their operation. Assessment of the rope excavators' operation has enabled the conclusion that in many respects the differences in the operation indices are insignificant, and in some respects rope excavators outperform hydraulic excavators. Rope excavators are easier in manufacturing and maintaining, and their operation is cheaper considering their 20-30 years of service life. A comparative technical and economic assessment shows that within a period of 6-7 years of operation, the productivity decline rate of hydraulic excavators is substantially higher than that of rope excavators, mainly due to the increase in emergency downtime, leaving aside the fact that average costs of maintaining and repairing one hydraulic excavator are higher than those of a rope excavator. The prime cost of loading rock mass with hydraulic excavators significantly increases and after 6-7 years of operation this figure for rope excavators is exceeded more than twofold. In the course of the industrial experiment, it was established that rational areas for using hydraulic excavators are pit sectors with high concentration and intensity of mining.

Functionality of a straight hydraulic shovel basically corresponds to that of a mechanical shovel. The hydraulic backhoe is designed for working off the face below the excavator level. The digging depth does not usually exceed 7-10 m.

There are three main technological schemes of the independent operation of the hydraulic backhoe (Surface Mining, 1990). The first scheme of excavation is the development of the bench in one pass of the excavator provided that the height of the bench (Hb) does not exceed the maximum digging depth (D) of the excavator. Under the

second scheme of excavation, the bench is worked layer by layer (Nl≥ Hb/D.) The third scheme of excavation is the development of the bench in one pass with the excavator placed on the sub-bench roof by sequential upward and downward digging. There also exist technological schemes of excavation with the use of a backhoe as auxiliary equipment for working off high benches, the excavator being placed on the roof of the bench. The most successful experience of using the hydraulic backhoe is the most efficient in developing flooded horizons, when working off the bench by a hydraulic backhoe can be the only possible option for mining operations. But in general, the independent use of hydraulic excavators complicates mining technology and increases deposit development costs.

Work objective

The main objective is the improvement of mining technology due to grounding the rational areas for using hydraulic backhoes in deep iron ore pits. The main task is to analyze and develop mining technologies, adapted to the deterioration of the hydro-geological and mining conditions of operations on lower horizons of the pits.

Material presentation

The combination of production and non-production factors may create conditions that will result in poor performance of the main complex of the mining and transport equipment and thus in failure to achieve the designed pit performance**.**

One of the solutions to this problem is the differentiation of the used extraction-and-loading equipment by selecting those excavators for which the existing trends of variation of mining and hydro-geological conditions are not unfavorable.

Trenching at the bottom of deep pits is associated with a decrease of the depression cone of ground waters. Here, the trenching time is determined by the hydrogeological conditions of the deposit (the depression cone development rate), not by the geometric volume of the trench and the excavator's productivity. Ukraine's climate is currently characterized by abundant rainfalls. Considering the significant geometric size of pits (the daylight surface area of iron ore pits makes 400-1000 hectares), the risk of rapid rainfall flooding of the pit bottom is rather high. Technological schemes of trenching using only a rope excavator become inefficient due to the impossibility of its efficient operation in flooded conditions. This prevents pits from reaching the designed indicators of the deepening rate and ore productivity, and entails an increase of costs of the stripping of the horizon.

Combined schemes have been developed (Slobodyanyuk and Turchin, 2016) for trenching the bottom horizon of a pit in difficult hydrogeological conditions. The idea of combined schemes is based on the fact that the task of a hydraulic backhoe is to create conditions for the productive operation of a rope excavator. The following order of works on trenching is suggested: The hydraulic excavator forms part of a trench end face to the full height of the bench by advanced heading (Fig. 4).

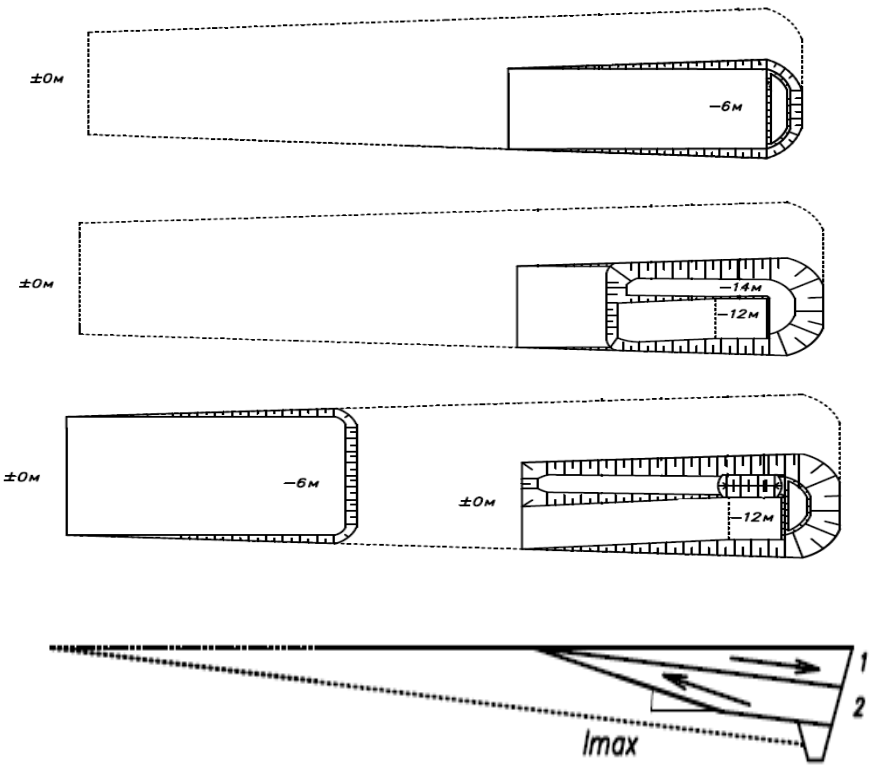

Fig.4. The combined schemes of trenching

The work is done layer by layer; the lower layer is mined by undercutting the base of the overlying layer in the opposite direction. The output slope of the layer bottom is assumed to be the maximum permissible by the condition of normal

operation of crawler machines. Such mining parameters contribute to the concentration of the working area of the hydraulic backhoe and reduce the costs of the horizon stripping. After the decrease of the depression cone, the mechanical shovel performs the longwall driving of the trench along the full height of the bench. It makes technical and economic indicators of the excavator operation closer to those in unflooded conditions.

One of the main types of combined transport in the iron ore pits of Kryvbas is road-rail transport. The bulk of overburden is transported to the dumps by this type of transport. The introduction of deep rail transport in the 1970s-1980s became one of the factors that led to the reduction in the distance of transportation by trucks and the increase in mining efficiency. The excavator reloading platform is a key element of this type of transport. When using a direct mechanical shovel on the reloading platform, it is divided into two equal sectors along its length, which alternately are the places of dump trucks unloading and places of loading on the railway transport. To place the reloading platform, it is necessary to reserve the area on the pit wall (the length of the transfer platform with the sidetrack is 300-400 m, the width – 100-150m). Sometimes the pit productivity is limited due to failure to place the required number of transfer platforms.

A hydraulic backhoe is known to be used at a reloading platform. The excavator is placed on a mound inside the receiving trench and loads the railway transport by digging below the standing level. But this technology has retained a number of shortcomings inherent in technological schemes using mechanical shovels on transfer platforms. To plan the surface of the transfer platform, it is necessary to use a bulldozer; the transfer platform is also divided into two sectors along its length. The division of the reloading platform into the unloading sector and the loading sector increases the length of the receiving trench and the reloading platform area.

The authors propose another way of organizing a reloading platform when using a hydraulic backhoe. The receiving trench is conventionally divided into two sectors across the width: unloading and loading ones. Unloading of dump trucks and loading of railway trains are carried out on the opposite walls of the receiving trench (unloading and loading walls). In general, the unloading one is the trench wall closest to the underlying horizons of the pit, the loading one is the pit wall closest to the upper pit horizons (as a result, the railway and the road do not intersect) (Fig. 5).

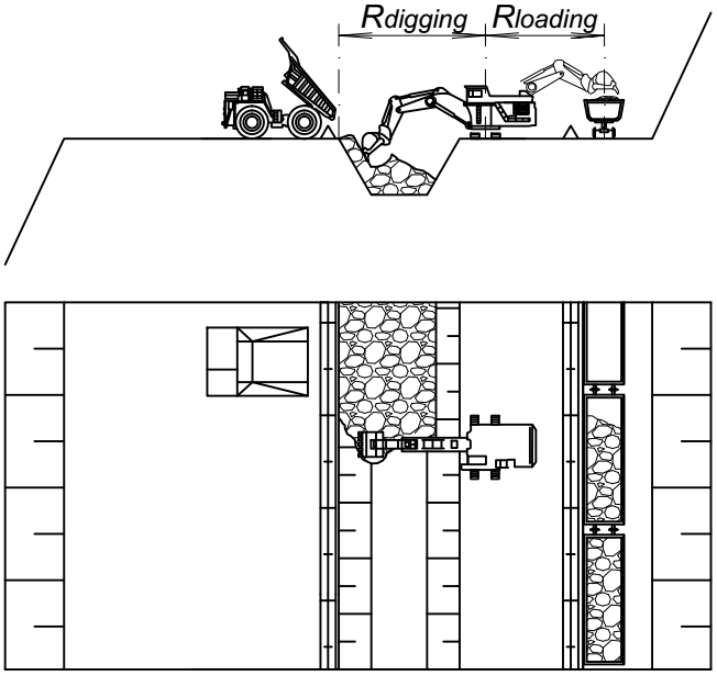

Fig.5. The technological scheme of operating a hydraulic backhoe on a reloading platform

The railway track is laid along the trench loading wall. A hydraulic backhoe is located between the trench loading wall and the railway. The excavator performs frontal digging of the rock mass from the receiving trench and loads it on the railway transport. While loading dump cars, the backhoe moves along the receiving trench wall.

When using a hydraulic backhoe on a reloading platform, there is no need to lift the rock mass one bench above the level of the railway tracks. The transport work economy is determined by the formula:

$$z = VH/i \text{ ; th. km}$$

where
V is the volume of rock transported by road and rail, [t];
H is the height of reload when using mechanical shovels (usually 15 m), [m];
i is the road slope, [thousandths].

The proposed method allows combining, in time and in space, of the unloading of dump trucks on the reloading

platform and the loading of railway dump cars. At the same time, there is no intersection of road and rail transport. Such a way of organizing the reloading platform is characterized by compact dimensions, high safety of mining operations and allows increasing the productivity of the equipment. To increase the receiving capacity of the reloading platform, the excavator re-excavates the rock mass from the unloading side of the trench to its loading side in the period between train exchanges. The receiving capacity of the reloading platform can be increased by forming a trench with larger slope angles.

In the proposed method, the length of the reloading platform is primarily determined by the length of the train. The length of the receiving trench is only determined by the condition of ensuring the minimum level of independence of the performance of the related technological processes.

A number of measures are implemented at pits to prevent landslides and to ensure the safety of mining operations. Constructing rock counterforces and slope filtering cantledges is the simplest of them. According to VIOGEM, the cantledge of slopes by rock mass leads to a redistribution of pressure near slopes and, ultimately, to an increase of the stability margin factor by 20-25%.

The following technology is usually applied to constructing rock cantledge. Dump trucks are unloaded in the mined-out area of the excavator and pass under the lower edge of the formed slope of the bench. Since the bench is composed of weak rocks, the unloading of trucks transporting hard rock mass to the cantledge area is carried out on the lower operating floor of the bench. The unloading of dump trucks is carried out perpendicular to the bench slope. After delivering rock in an amount sufficient to form a bench cantledge with the designed parameters, the excavator transports part of the rock overburden from the bottom of the bench to its slope, forming a retaining prism. Hard rock with a high density is used as a material for constructing counterforces and cantledges. In flooding conditions, to prevent filtration deformations, the cantledge prism is formed immediately, as the face advances. The drawback of the generally accepted technology for constructing cantledges to prevent landslides is that the rope excavator has a relatively small unloading height and it cannot construct a cantledge of the bench height. Counterforces can be created using a technology that is close to the technology of area-based dumping. The main problem is that to place the above-mentioned objects, the area on the lower operating floor of the bench is used, which could have another technological purpose (for example, a transport berm). It is of interest to develop a technology for the formation of anti-landslide structures, which will not reduce the area of the operating floors of pit benches.

The authors propose the following technological scheme for the construction of anti-landslide structures using the hydraulic backhoe. Initially, dump trucks pour off a mound of rock along the front slope of the bench. This mound will be used as an operating floor for a hydraulic excavator, and the rock from this mound will be re-excavated into the body of the counterfort being constructed. If necessary, as rock overburden is re-excavated from the mound, dump trucks will resume pouring it (Fig. 6).

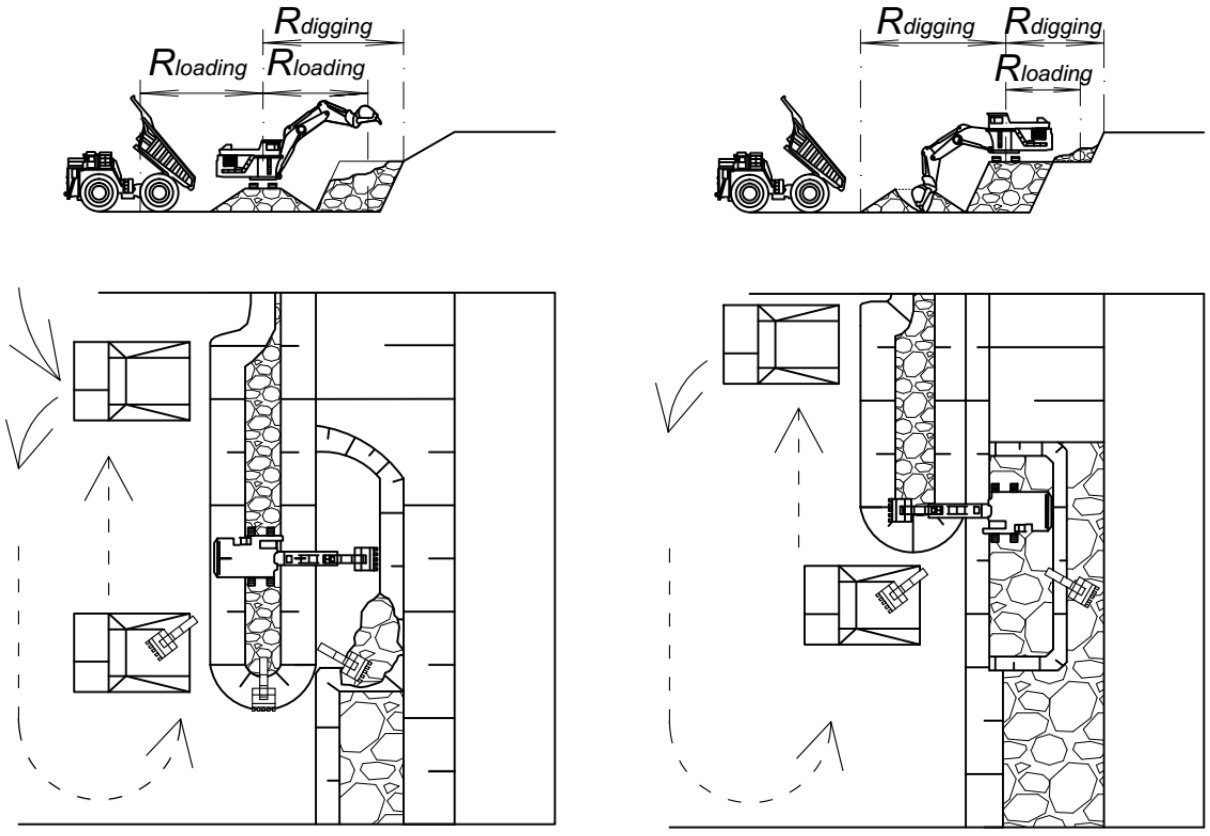

Fig 6. Technology for constructing the counterforce using the hydraulic backhoe

The main idea of the proposed technological scheme is the use of a hydraulic excavator placed on a mound (extended-bench) from the rock overburden, for excavating the loose overburden from a reinforced bench into dump trucks, and for reloading rock overburden from the extended-bench into the mined-out part. If necessary, several stopes can be worked out successively on the loose overburden, the worked-out area will be filled with rock overburden by a hydraulic excavator. This technology enables strengthening all landslide areas of benches along the perimeter of the pit without reducing the area of the operating floors of the benches, which will ensure the formation of the designed transport scheme.

Conclusions and directions for future research

The area of rational use of hydraulic backhoes in the iron ore pits is conditioned by the stable trend for deterioration of mining conditions (tightness of the working zones of the pit, flooding of the lower horizons, development of dangerous geo-mechanical processes) in which extraction-and-loading equipment and mining technology provided for by deposit development designs become inefficient. In a further research, it is planned to analyze the mining and geological conditions of the iron ore pits of Kryvbas for determining the rational area of applying the developed technologies.

References

Арсентьев, А. И. Разработка месторождений твердых полезных ископаемых открытым способом: учебник. СПб. гос. горн. ин-т (техн. ун-т), 2010. – 115 с. (Arsent'yev, A. I. Razrabotka mestorozhdeniy tverdykh poleznykh iskopaemykh otkrytym sposobom. Sankt Pb. gos. gorn. in-t, 2010. - 115 p.).

Шеметов, П. А., С. К. Рубцов, А. Г. Шлыков. Опыт эксплуатации канатных и гидравлических экскаваторов в условиях карьера Мурунтау. - Горная промышленность, 5, 2005. – 46-50 с. (Shemetov, P. A., S. K. Rubtsov, A. G. Shlikov. Opyt ekspluatatsyi kanatnyh i gidravlicheskih ekscavatorov v usloviyah kar'yera Muruntau – Gornaya promishliennost', 5, 2005. – 46-50 p).

Сейтбаев Ш.А. Опыт применения экскаваторов различных модификаций в условиях карьера Мурунтау. - Горный вестник Узбекистана 3, 22, 2005 – 83-86 с. (Seytbayev, Sh. A. Opyt primeneniya ekscavatorov razlichnih modifikatsiy v usloviyah kar'yera Muruntau. – Gorniy vestnik Uzbiekistana 3, 22, 2005 – 83-86 p).

Mine and mill equipment costs. Western Mine Engineering, Inc. Washington, Copyright 1995.

Булес, П. Обеспечение надежности работы карьерных гидравлических экскаваторов при их эксплуатации на открытых разработках России: дис. на соискание ученой степени кандидата технических наук: 05.05.06 М., 2016 – 146 с. (Bules, P. Obespecheniye nadezhnosti rabotiy karyerniyh gidravlicheskih ekscavatorov pri ih ekspluatatsiy na otkrityh razrabotkah Rossii: diss. na soiskaniye uchienoy styepeni kandidata technicheskih nauk: 05.05.06. M., 2016 – 146 p.)

Подэрни, Р. Ю., П. Булес. Сравнительный анализ гидравлических и механических экскаваторов с прямой лопатой. - Горный журнал 1, 2015. – 55–61. (Poderni R. Yu., P. Bules. Sravnitielniy analiz gidravlicheskih i mehanicheskih ekskavatorov s pryamoy lopatoy. – Gorniy zhurnal 1, 2015. – 55-61 p.)

АС 111446U Украины МПК E21C 41/26 (2006/01) Способ вскрытия рабочих горизонтов карьеров в сложных гидрогеологических условиях / Слободянюк В. К., Турчин Ю. Ю.; заявл. 10.04.2015; опубл. 25. 04. 2016 (AS 111446U Ukrainiy MPK E21S 41/26 (2006/01) Sposob vskrytiya rabochih gorizontov karyerov v slozhnyh gidrogeologicheskih usloviyah / Slobodyanyuk V. K., Yu. Yu. Turchin; zayavl. 10.04.2015: opubl. 25.04. 2016).

Surface Mining (2nd edition), Society for Mining, Metallurgy and Exploration, Inc., Littleton, Colorado, 1990.

This article was reviewed by Assoc. Prof. Dr. Ivaylo Koprev and Assoc. Prof. Evgenia Aleksandrova.

ROUND-TRIP HAULAGE AS A MEANS OF INCREASING OPEN PIT MINING EFFICIENCY

Slobodyanyuk Roman[1], Pyzhyk Mykola[2]

[1] Kryvyi Rih National University, Kryvyi Rih, Ukraine, e-mail: slobod.roman@gmail.com
[2] Kryvyi Rih National University, Kryvyi Rih, Ukraine

ABSTRACT. The round-trip concept is well-known in transport logistics. It implies movement of transport, that after unloading of a primary cargo is loaded again with another one on its way to the initial point in order to reduce the empty run in the total run time and thus to increase the time period of efficient operation.

In the early 1990s, this scheme was proposed for open pit mining operations. However, it has not been studied properly yet. We can explain it by limited mining conditions not allowing us to introduce it in industry and also by the conventional one-way orientation of open pit haulage movement. The only case of round-trip haulage introduction concerns internal dumping, it is relatively common and described in literature.

The research aims at developing the methods for wider introduction of round-trip haulage in open pits. The idea of the work is to increase the shovel-truck system efficiency due to such placement of temporary dump in the open pit space, under which the conditions for haul trucks round-trip movement arise.

To substantiate the applied technological schemes implying internal dumping, round-trip haulage accompanied by haul truck passing loading, the preliminary methodology has been developed. Based on its current stage, such internal dump placement is expected to increase the technology efficiency and create a positive impact on the open-pit cargo-flows system. Therefore, the future studies are expected to discover the potential abilities to increase internal dumping efficiency considering such parameters of temporary internal dump as its existence period, location and impact on the haulage system. Also, based on the round-trip haulage dependencies study findings, the active work is being carried out relating to creation of the second scheme type irrespective of internal dumping, that is likely to become a relatively universal technical solution for round-trip haulage introduction in open pit mining.

Keywords: round-trip, internal dumping, shovel-truck system, haulage, open pit mining

ДВУПОСОЧНИЯТ ТРАНСПОРТ КАТО СРЕДСТВО ЗА УВЕЛИЧИВАНЕ ЕФЕКТИВНОСТТА НА РАБОТА В ОТКРИТ РУДНИК

Слободянюк Роман[1], Пужук Мукола[2]

[1] Национален университет Кривой рог, гр. Кривой рог, Украйна, ел.поща: slobod.roman@gmail.com
[2] Национален университет Кривой рог, гр. Кривой рог, Украйна

РЕЗЮМЕ. Двупосочният транспорт е добре познат в транспортната логистика. След разтоварването на първоначалния товар, транспортната машина се зарежда с друг товар по обратния път към началната точка, за да се намали празния ход в общото работно време и по този начин се увеличи времето за ефективна работа. .

В началото на 90-те години на миналия век тази схема е предложена за открити рудници, но все още не е добре изучена. Това може да се обясни с ограниченията на работа в мините, които не ни позвояват да я въведем в промишлеността, както и с конвенционалния еднопосочен транспорт в откритите рудници. Единственото приложение на системата с двупосочен транпорст е при вътрешните насипища, което е сравнително често срещано и е описано в литературата.

Изследването е насочно към разработване на методи за по-широко въвеждане на двупосочния транспорт в открити рудници. Целта е да се повиши ефективността на товарно-транспортната система чрез разполагане на временни насипища в открития рудник, при което се създават условия за двупосочно използване на рудничния транспорт. Разработена е предварителна технология, за да се обоснове прилагането на технологични схеми с вътрешни насипища и двупосочен транспорт с натоварване на самосвалите. На настоящия етап се очаква разполагането на вътрешно насипище да увеличи транспортната ефективност и да повлияе положително върху системата от товарни потоци в откритя рудник. Очаква се бъдещите проучвания да открият потенциални възможности за увеличаване на ефективността на вътрешните насипища като се вземат предвид такива параметри като: период на съществуване на временното вътрешно насипище, местоположение и въздействие върху транспортната система. Въз основа на резултатите от изследването на зависимостите в двупосочния транспорт, се извършва активна работа по създаването на втори вид схема, независима от вътрешното насипище, която има вероятност да се превърне в сравнително универсално техническо решение за въвеждането на двупосочен транспорт в открити рудници.

Ключови думи: двупосочен транспорт, вътрешно насипище, товарно-транспортна система, транспорт, открит добив

Introduction

The current state of haulage systems at deep open pits in Ukraine

The shovel-truck system of a deep open-pit represents a complex that includes excavators, dump trucks and a ramified network of open-pit roads connecting faces and rock mass delivery points located both in the open-pit and on the surface. The network of open-pit roads has a complex topology; the traffic flow varies periodically in its individual sections, reflecting the features of the calendar distribution of the rock mass on the working horizons. The deeper the open pits are, the more complicated the transport communication system is, a significant part of which has a critical width, which leads to deterioration in traffic conditions and is an obstacle to the transition to heavier dump trucks.

The classic way to solve the problems arising when the depth of open-pits increases, is the reconstruction of combined open-pit transport system (Maryev et al., 2006). Two types of combined transport are used in Ukrainian iron ore open-pits,

they are road-rail and haul truck-conveyor ones. However, technical solutions that were effective in the 70-80s of the last century at a depth of 250m of open-pits are already insufficiently effective at a depth of 450-500m (Bahturin Ju.A., 2009). In some areas, this led to the refusal of further use of in-pit crushing and conveying (IPCC) systems (open pit mine No.1 of the CGOK, open pit mine of Poltava GOK), In others it led to rejecting deeper commissioning of the IPCC systems based on the stationary crushers and to revision of the design solutions (Pervomayskiy and Annovsky open-pits of Northern GOK, InGOK open-pit).

Thus, deepening open-pits and imperfection of technical solutions for combined transport use have led to the increase in truck haulage distance in the iron ore open-pits in Ukraine and former Soviet republics (Bahturin Ju.A., 2009, Drizhenko A.Yu., Kozenko G.V et al., 2009;).

Round-trip haulage concept

Application of round-trip haulage (Figure 1) is one of the original solutions for improving the haul trucks efficiency. The possibility of applying it was first regarded when analyzing the haulage systems at the open pit mine №1 of the CGOK in the early 90s of the XX century (Gorjainov A.N., 2006). The round-trip haulage appeared due to the placement of overburden rocks in the mined-out part of the open-pit.

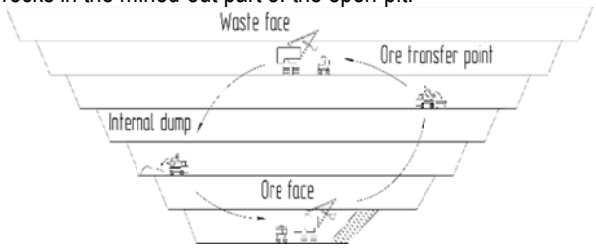

Fig.1. Round-trip haulage in an open pit mine

Round-trip haulage principle is well-known and widely used in transport logistics (Astafiev Yu.P., 1991). It implies movement of transport, which after unloading a primary cargo is loaded again with another one on its way to the initial point in order to reduce the empty run in the total run time and thus to increase the time period of the efficient operation. In some sources, the additional load of transport on its way to the initial point is also called Backhaul [Montague M., 2016; Castendyk D.N.. Eary L.E., 2009).

The same years, the round-trip haulage was organized and described in the Pervomayskiy open pit of the Northern GOK (Malyuta A.D., Belan A.D. et al., 1992).

The works (Gorjainov A.N., 2006; Malyuta A.D., Belan A.D. et al., 1992) do not provide generalization of the regularities describing the possibility of using haul trucks on the round-trip haulage routes in the open pit mine and there were no ideas for the deliberate creation of round-trip haulage conditions.

Subsequent cases of its purposeful application and general theoretical justification were not found in the information sources. The main reason for this is emergency round-trip haulage conditions, which are not very typical for open pit mining. Primarily this is due to the prevailing, in most situations, one-sided orientation of cargo flows in the open pit (Voronov Ju. E. and Bujankin A. V., 2003). The described cases of round-trip haulage are associated with the existence of areas (transport communications) with cargo flows counter direction in the open pit. This is mainly characteristic of a mining situation, when there is existence of an active internal dump inside the open pit (Gorjainov A.N., 2006).

Mining situations with the existence of temporary internal dumps of a relatively small volume, are fairly common for mining practice in the recent decades in Ukraine (Drizhenko A.Yu., Kozenko G.V et al., 2009). However, the possibility of applying the round-trip haulage is not taken into account during the decision-making on internal dumps creation.

Main Exposition

Problem Statement

The main aim of the research is development of methods for wider introduction of round-trip haulage at open pit mines.

The two main hypotheses of the study are:

1. The reason of the current active internal dumping application is caused by transport work variations that are not always considered properly at the mine planning stage.
2. The opportunity to use internal dumps both for fulfilment the needs causing their construction and effective round-trip haulage organization is possible.

Applied methodology and methods

Temporary internal dumping usage

An example of temporary internal dumps (Drizhenko A.Yu., Kozenko G.V et al., 2009; Litvin Ja.O., 2011) use is solving of current, sometimes extremal issues, when the fleet of haul trucks in service is not sufficient to fulfill the planned volumes of mining operations in this case. The shortage of haul trucks is compensated by the necessary and sufficient reduction in the overburden transportation distance. Such temporary dumps are usually placed at open-pit sites where mining operations are not planned for the nearest future. A part of the overburden rocks can also be used for creation or expanding the temporary ramps and for increasing the protection embankment parameters.

The regulation on the designing internal dumps (Shapar A., Kopach P., 2004) is focused on solving the problems, aggravated with the increase of iron ore open pits' depth. Internal dumping is allowed in open-pit (Drizhenko A.Yu., Kozenko G.V et al., 2009; Shapar A., Kopach P., 2004) only if it is envisaged by the project for deposit exploitation. The project is intended to define the lifetime and the order of temporary dumps relocation. The regulation (Shapar A., Kopach P., 2004) is a detailed consideration of the principal technological schemes with the placement of overburden in the section of the open-pit worked out to the final depth. However, in the regulation (Shapar A., Kopach P., 2004) there is no methodological basis for choosing the location of temporary dumps, their volume and useful life.

The annual, quarterly and monthly mining plans are the information basis for assessing the feasibility of using temporary dumps in different mining situations. Analyzing mining plans allows determining the location of recoverable rock volumes, the location of rock mass delivery points and the position of the haul roads system. The position of centers of gravity of mining blocks and haul trucks unloading points allows us to estimate the average distance of the rock mass

haulage for each cargo traffic for the considered planning period.

Nevertheless, taking into account the known length of mining blocks (200-500m and more) and involving mining blocks located on several horizons into simultaneous operation, the combination of mining blocks during different scheduling periods can be different, including one that leads to the emergence of temporary shortage in trucks and the need to create a temporary dump.

Transport work fluctuations analysis

We are studying the influence of relative positions of open-pit faces on transport work using the methods of simulation modeling.

Planning the work of the shovel-truck system is carried out according to the average value of the transportation distance. In the course of mining operations, the actual distance of transportation fluctuates within a certain range relative to the mean value. Due to our hypothesis, in periods when the transportation distance is less than the average or equal to the average value, the available number of dump trucks is sufficient to fulfill the production goal. In periods when the actual distance exceeds the average one, it is necessary to reduce the performance of the excavator or to find another, more closely located rock mass delivery point (temporary internal dump).

We will study the effect of excavator faces movement on the haulage distance and transportation work on condition of unlimited number of haul trucks.

The initial data for carrying out the simulation were collected basing on analysis of annual programs fulfillment by open-pits that used temporary dumps of overburden rocks not specified by the project.

Collecting and processing actual data on the duration of excavator stopes mining allowed us to determine the statistical regularities of the processes. It was established that the process of excavators' work on rock mass loading is described by the normal distribution law. Similar results were obtained in Czaplicki J.M. (2014) work, devoted to the study of statistical regularities in mining.

Setting of the problem. The open-pit has the amount of n excavator stopes. The excavator works on the i-th block with the average rate of face advancing V_i (m/shift) and the standard deviation σ_i. For each face, the width of the excavator stope A_i (m) and the length of the excavator block Lb_i are determined. As the excavators move along the blocks, the distance made by haul trucks to transport the overburden increases with each shift. After the excavator switchover to a new stope, the haulage distance increases by the width of the excavator stope. The open-pit benches (Figure 2) connect the automobile road of L_j length with the delivery point of the rock mass. The simulated open-pit has 8 excavators, 6.7-7.4 m/shift rate of faces advance and the starting overburden transportation distances of 1.1-3.2 km. The stripping site for 120 shifts was simulated in the study.

The results of modeling. In the example considered, the average level of transport work was 15.05 thousand t-km/shift (Figure 3). The range of deviation of the maximum and minimum values of transport work for one shift from the mean value made up ±0.8 thousand t-km/shift. During the simulation period, in 55% of cases the transport work exceeded the average value, in 45% of cases it was less than the average value. The maximum values of transport work per shift are consistent with the situation of mining excavator stopes that are the farthest from the system of automobile ramps. The change of the several excavators' position to the new stopes corresponds to the minimum values.

Consequently, the cases of uneven transport work arise periodically in the open pit mining process. Even in the difficult conditions of haul trucks shortage, peculiar to Ukrainian mining, there are still few methods of transport work regulations. But due to the need of corresponding limitations in mine's productivity, they are rarely used, opposite to the temporary internal dumping.

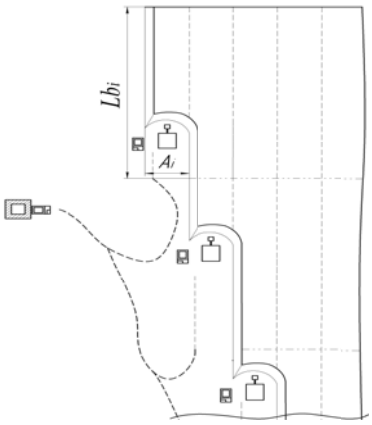

Fig. 2. Provisional diagram of excavator stopes disposition

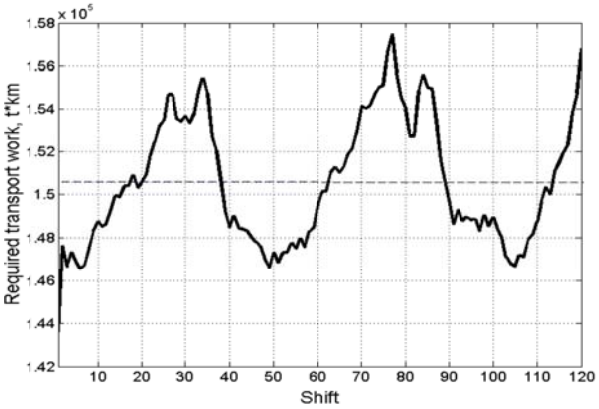

Fig. 3. Transport work fluctuations (modeling results)

Round-trip haulage system analysis

The simplest layouts of shovel-truck system cargo flows

For further study, let us consider a few elementary (the simplest) cases of shovel-truck systems in order to study the basic regularities of the haul trucks round-trip haulage emergence.

In the general case, several variants of the mutual arrangement of faces and unloading points of different types in plan are possible. In the first option loading and unloading points are placed at the tops of the quadrangle (areal disposition); in the second case, the loading and unloading points of the rock mass are arranged along a line (linear disposition).

In the counter direction of different types of cargo traffic (Figure 5), the emergence of concomitant conditions is the most likely to happen. So, first of all let us look at its features):

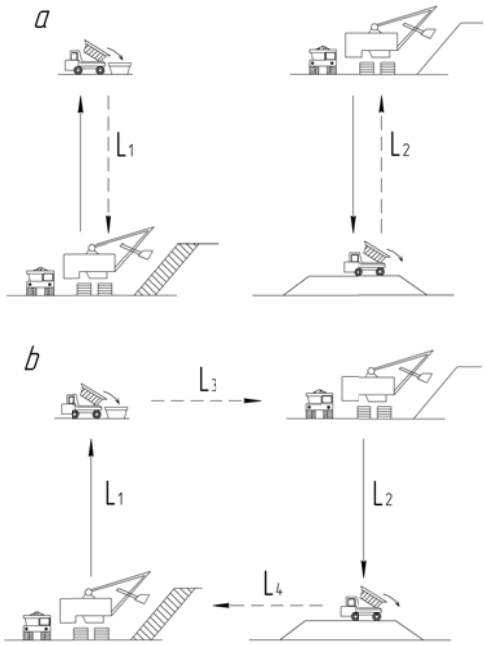

Fig. 5. Areal disposition of shovel-truck system cargo flows with counter direction: a) ordinary haulage b) round-trip haulage

In this case, the distance between the point of unloading of the first cargo flow and the face of the second cargo flow will probably be less than the distance between the face and the point of unloading of the first cargo flow. It is possible to make the following assumption necessary for the emergence of a round-trip haulage scheme for haul trucks movement:

$$L_1 + L_2 + L_3 + L_4 < 2 * (L_1 + L_2) \qquad (2)$$

where: L_1 – the distance between the ore face and the ore unloading point, km;

L_2 – the distance between the stripping face and the unloading point of the overburden, km;

L_3 – the distance between the point of ore unloading and stripping face, km;

L_4 – the distance between the overburden unloading point and the mining face, km.

The loaded mileage proportion (3) is most explicit in describing the efficiency of haul trucks work organization (Voronov Ju. E. and Bujankin A. V., 2003). It is equal to the ratio of the distance traveled with the load to the total length of the run. Let us apply this proportion for evaluating the efficiency of the round-trip haulage.

$$\beta = \frac{L_{loaded}}{L_{total}} = \frac{L_{loaded}}{L_{loaded} + L_{empty}} \qquad (3)$$

where, β – loaded mileage proportion;

L_{loaded} – distance of transport movement in the loaded state, m;

L_{total} – total run's distance, m;

L_{empty} - distance of empty transport movement, m.

The key condition of the round-trip haulage (1) can be simplified to the form $L_3+L_4<L_1+L_2$. This condition will be fulfilled when the transportation distance between points of cargo flows of different types (L_3, L_4) is less than the distance between points of cargo flows of the same type (L_1, L_2). In this case, the loaded mileage proportion for the round-trip haulage will be greater than that for each cargo flow of the same type. To study the dependence of the loaded mileage proportion on the location of excavating faces and rock mass delivery points, let us consider the following simple model of an excavating and haul truck complex. We set the distances L_1, L_2 and L_3, L_4 pairwise equal and gradually reduce the ones between the points of cargo flows of different types.

The result (Figure 6) shows a quadratic dependency of the variables with the expected maximim loaded mileage proportion at the closer located cargo flows points of the different type.

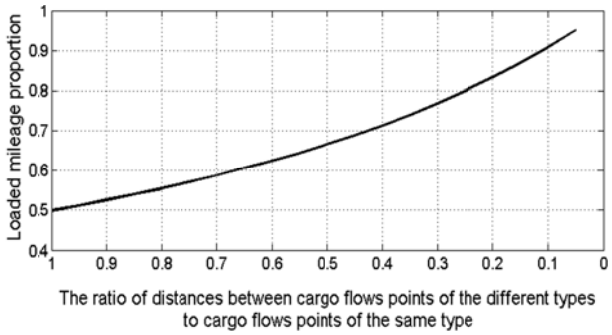

Fig.6. The dependence of the loaded mileage proportion to the ratio of distances between cargo flows points of the different types to cargo flows points of the same type.

However, this kind of cargo flows points location does not belong to open-pits normal conditions of operation [9]. Cargo flows of a passing direction (Fig.7a) are typical for open-pits. It is obvious that their mutual arrangement eliminates the possibility of the round-trip haulage. However, these same conditions lead to decisions to create internal dumps (Fig. 7b) in order to compensate the temporary lack of transport work necessary for attaining the planned objective.

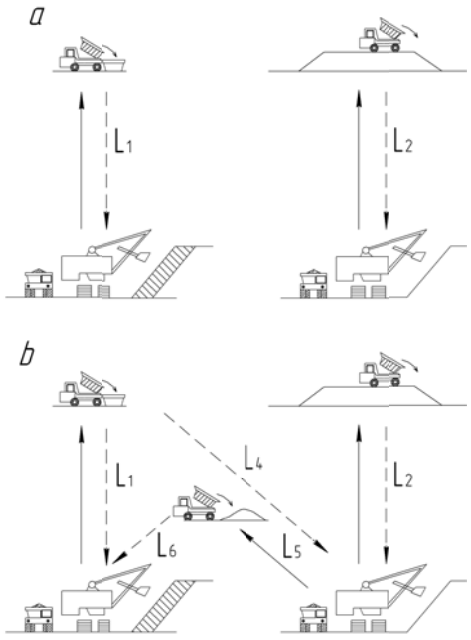

Fig.7. Areal disposition of shovel-truck system cargo flows with passing direction: a) ordinary haulage, b) round-trip and ordinary haulage

To study the influence of the location of internal dump under creation on the haul trucks movement, we will complement the above model with two transportation sections that are: from the stripping face to the internal dump L_5 and from the internal dump to the mining face L_6. By changing the ratio of the distances L_5 and L_6 at the constant distances between the faces and the permanent unloading points L_1, L_2, L_4, we determine the boundary of round-trip haulage route appearance.

It was established that with a decrease in the distance between the internal dump and the ore face, the probability of creating conditions for round-trip haulage and rise in the loaded mileage proportion increases.

At the next stage of the study, an assessment of haul trucks movement with a gradual change in the distances L_1, L_2 and L_4 was made. The presence of the dependence of the possible internal dump locations, which lead to round-trip haulage, from the ratio of the distances between the faces and the permanent unloading points L_1, L_2, L_4 was defined (Figure 8).

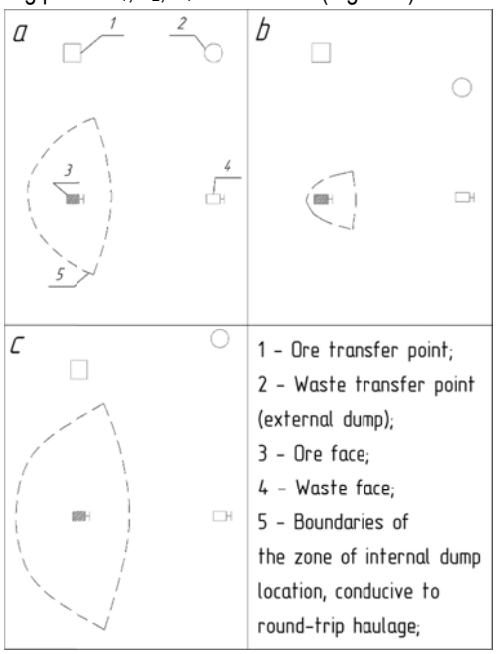

Fig. 8. Zones of internal dump location conducive to round-trip haulage

Areas of rational internal dump location

As mentioned above, the ratio of the distances "ore face – ore unloading point L_1" and "stripping face – overburden unloading point L_2", significantly affects the conditions for round-trip haulage appearance, which can be formed due to the corresponding arrangement of the internal dump. Therefore, if the length of ore haul is greater than the length of the overburden haul, the area of the rational arrangement of the internal dump decreases (Figure 8b). In contrast, if the length of ore haul is less than the length of the overburden haul, the number of places suitable for the location of the temporary internal dump suitable for creation of round-trip haulage increases (Figure 8c).

One of the main tasks of the study is to find an opportunity to carry out the planned volume of rock mass excavation under conditions of insufficient number of haul trucks. We believe that this mining situation has developed as the specific situation of excavating faces and rock mass delivery points' location, that on the whole, have the available number of trucks ensuring the implementation of the annual production program. We divide this task into several stages. At the first stage, using the mentioned above haulage analysis model, we will determine the necessary transport work for rock mass haulage to the planned delivery points and the number of haul trucks required. Knowing data on the existing transport fleet, we determine the shortage of trucks, and the weighted average haul length (4), at which the planned volume of rock mass excavation with the placement of a part of the overburden in the temporary dump can be accomplished.

$$L_{mweighted} = \frac{\sum_{i=1}^{NF}\sum_{j=1}^{NU} P_{ij} L_{ij}}{\sum_{i=1}^{NF}\sum_{j=1}^{NU} P_{ij}} \qquad (4)$$

where: NF – the number of loading points (faces);

NU – the number of unloading points;

P_{ij} – traffic flow intensity on route ij, trucks per min;

L_{ij} – distance between points of loading i and unloading j, m;

Using the method for finding the area of internal dump locations contributing to the introduction of round-trip haulage, it is necessary to determine those of its positions, which ensure the fulfillment of the planned volume of mining operations with the existing mining equipment.

Using known coordinates and distances between the faces and constant unloading points of the rock mass, we analyze the possible locations of the internal dump, in which the distance of the weighted average transportation of the overburden takes the required value. Location options are characterized by the distance to the stripping face and the maximum receiving capacity of the internal dump (in order to control its volume). Displaying all of them on the plan allows us to see the area of the temporary internal dump, designed to compensate the transportation work.

We make a simultaneous comparison of both zones location (Figure 9). The points belonging to parts of both zones are the priorities for the subsequent determining of the optimal location of the internal dump.

Although, the obtained results are only a partial confirmation of the stated hypothesis, it can be used as a part of the future evaluation of the internal dumping location conducive to round-trip haulage. Therefore, the findings create a promising foundation for the consequent studies on the issue.

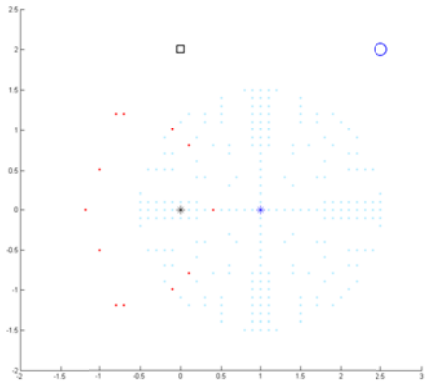

Fig. 9 An example of internal dumping locations: the red points are suitable for round-trip haulage zone edges; the blue points are suitable for the transport shortage compensation; the black star is an ore face; the blue star is a waste face; the black square is an ore transfer point; the blue circle is a waste dump

Conclusions

The study investigates the peculiarities of round-trip haulage in open-pit mining operations. Based on the examples described in the literature, the main concomitant condition which is defined is the existence of counter-directed cargo traffic in the open-pit. It, in turn, is most likely to occur in internal dumping usage.

Mining technical conditions leading to the need of the temporary internal dumps creation were analyzed. The main one is the difference of the current transport work from its average value over the planning period, in which there is a need in reducing the length of haul to ensure a planned excavation of the rock mass.

When searching for a location for the internal dump, it is rational to take into account not only the compensation of temporarily increased transport work, but also the possibility of creating a round-trip haulage. For this purpose, a method taking into account both factors for determining the position of the internal dump are developed. For the known location of the faces and permanent unloading points, the boundaries of the two zones were determined, in which the creation of internal dump leads: in the first one to the possibility of creating a round-trip haulage, in the second one to compensation of the transport work shortage. The points common for these zones are the priority ones for the subsequent calculation of internal dump effective location. The main limitation of the method is its early stage. It needs improvement with regard to its current ability to give the high-accuracy results only for a flat surface between the analysed points that represents only a small area of mining situations.

The more serious issue revealed during the study is that there are not so many open pit mines around the world applying the temporary internal dumping. Moreover, even in case of technology exploitation, mining conditions necessary for the creation of a round-trip haulage will occur rarely in many open-pits. Therefore, an alternative scheme of movement organisation irrespective of internal dumping is being developed to become a relatively universal solution of round-trip haulage application in open-pit mining.

References

Астафьев Ю.П., Модель маршрутизации автосамосвалов во время работы с пунктами перегрузки в карьерах ., Развитие теории открытых горных работ, 1991, С. 98-133. (Astafiev Yu.P., Model of haul trucks routing during the work with the in-pit reloading points, Razvitye teorii otkrytyh gornih rabot, 1991, pp. 98-133)

Бахтурин Ю.А., Современные тенденции развития карьерного транспорта, ГИАБ, №7, 2009., С. 403-414. (Bahturin Ju.A., Sovremennye tendencii razvitija kar'ernogo transporta. GIAB. #7, 2009, pp. 403-414.)

Горяинов А.Н., Виды Маршрутов автотранспортных средств при перевозке грузов в логистической системе Коммунальное хозяйство городов, № 67, Киев: Техника, 2006, С. 304-309. (Gorjainov A.N., Vidy marshrutov avtotransportnyh sredstv pri perevozke gruzov v logisticheskoj sisteme Kommunalnoe hozjajstvo gorodov: NTS. #67, Kyiv: Technika, pp. 304-309. 2006)

Дриженко А.Ю., Козенко Г.В., Рикус А.А. Открытая разработка железных руд Украины: состояние и пути совершенствования. Днепропетровск: НГУ., 452р. 2009 (Drizhenko A.Yu., Kozenko G.V., Rikus A.A., Otkritaya razrabotka zheleznyh rud Ukrainy: sostoyanie i pyti sovershenstvovania. Dnipropetrovs'k: NMU., 2009, p. 452.)

Малюта А., Белан А. Д. и Костянский А. Н., Рациональное использование автосамовалов в глубоких карьерах при комбинированной транспортной схеме, Разработка рудных и нерудных местнорождений, Кривой Рог: НИГРИ, С. 52-55. 1992 (Malyuta A.D., Belan A.D. and Kostyansky A.N., Racional'noe ispol'zovanie avtosamosvalov v glubokih kar'erah pri kombinirovannoj transportnoj sheme. Razrabotka rudnyh i nerudnyh mestorozhdenij, Kryvyi Rih:NIGRI, 1992, pp. 52-55.)

Маруев П.Л., Кулешов А.А., Егоров А.Н., Карьерный автотранспорт стран СНГ в XXI веке, Санкт-Петербург, Наука, 2006. - 387 с. (Maryev P.L., Kuleshov A.A., Egorov A.N. and Zyrianov I.V., Kar'ernyi avtotransport stran SNG v XXI veke. Sankt-Peterburg, Nauka, 2006, - 387p.)

Montague M., Surviving the Buck-A-Mile Backhaul, DAT Truckers Edge® website blog. Available at: http://www.truckersedge.net/trucking-blog/post/Survivingthe-Buck-A-Mile-Backhaul1 (accessed 5 May 2017)

Castendyk D.N.. Eary L.E., Mine pit lakes: characteristics, predictive modeling and sustainability. Littleton, Colo: Society for Mining, Metallurgy & Exploration, 2009, p.303.

Czaplicki J.M., Statistics for Mining Engineering, CRC Press, 2014, p. 288.

Litvin Ja.O. (2011), Obosnovanie uslovij vremennogo otvaloobrazovanija pri pojetapnom peremeshhenii vskryshnyh porod kar'ernymi avtosamosvalami na razrezah Kuzbassa. Justification of temporary dumping conditions at stage-bystage relocation of overburden by haul trucks at strip mines of Kuzbass, p. 29.

Shapar A., Kopach P., Romanenko V. and others (2004), Polozhennya pro proektuvannya vnutrishnogo vidvaloutvorennya ta skladuvannya vidhodiv virobnitstva v zalizorudnih i flyusovih karyerah. Regulations on internal dumping design and storage of waste in iron ore and flux open pits, NASU: In-t problem prirodopolzovaniya i ekologii. Dnipropetrovsk: Mineral, p.15.

Voronov Ju. E. and Bujankin A. V., Obosnovanie pokazatelej kachestva jekspluatacii kar'ernyh avtosamosvalov. A justification of key performance indicators of the haul trucks. Vestnik Kuzbasskogo gosudarstvennogo tehnicheskogo universiteta. #2, 2006

This article was reviewed by Assoc. Prof. Dr. Ivaylo Koprev and Assoc. Prof. Dr. Iliyan Djobov.

ADJUSTMENT OF MINING VENTILATION SOFTWARE FOR CIVIL OBJECTS

Zahari Dinchev[1], Nadezhda Kostadinova[1], Elena Vlasseva[1]

[1]University of Mining and Geology "St. Ivan Rilski", 1700 Sofia
e-mail: dinchev@mgu.bg; nadezhda.kost@gmail.com; elena.vlaseva@mgu.bg

ABSTRACT Due to its complexity and branched structure the ventilation system of underground mining objects is modeled using specialized software products. This paper presents application of two of the most commonly used by the ventilation specialist programs - MfirePro + and Ventsim. Similarities and differences in data input, graphical presentation creation, setting of ventilation facilities and modeling of different modes are analyzed. On the basis of ventilation characteristics of mining objects, an analogy of the ventilation paths for emergency ventilation of a high building is developed. Emergency ventilation is performed by three fans - two supply and one exhaust fans. Air flows are regulated in order to meet safety rescue requirements. Aerodynamic resistances reflect in-situ measurements, but additionally some approximations for pressure drops and air leakage are undertaken. Numerical model and solutions of building emergency ventilation, obtained with MfirePro + and Ventsim, are presented.

Keywords: emergency ventilation, modeling, mining ventilation software

АДАПТИРАНЕ НА МИНЕН ВЕНТИЛАЦИОНЕН СОФТУЕР КЪМ ГРАЖДАНСКИ ОБЕКТИ

Захари Динчев[1], Надежда Костадинова[1], Елена Власева[1]

[1]Минно-геоложки университет "Св. Иван Рилски
e-mail: dinchev@mgu.bg; nadezhda.kost@gmail.com; elena.vlaseva@mgu.bg

РЕЗЮМЕ. Вентилационната система на подземните минни обекти поради своята сложна, разклонена структура се моделира със специализирани софтуерни продукти. Статията представя възможностите на двете най-използвани сред вентилационните специалисти специализирани програми – MfirePro+ и Ventsim. Разгледани са приликите и разликите при въвеждането на данни, създаването на графичен вид на системата, задаване на вентилационни съоръжения и моделиране на различни режими. На основата на вентилационните характеристики на минните обекти е разработена аналогия на вентилационните пътища при аварийна вентилация на висока сграда. Аварийната вентилация се осъществява с три вентилатора – два работещи на нагнетателен режим и един на смукателен. Движението на въздуха се регулира за постигане на изискванията за безопасна евакуация. Аеродинамичните съпротивления са определени с измервания и с допълнителни апроксимационни зависимости. Представен е числениият модел на вентилацията на сградата, получен с програмни системи MfirePro+ и Ventsim.

Ключови думи: аварийна вентилация, моделиране, минен вентилационен софтуер

Introduction

Underground mines as ventilation objects are branched structures with several entrances and exits, developed with levels in depth. Analysis of interaction of ventilation air flows, their distribution, pressure drops and operational modes of regulators and fans is a complex research task, solved successfully with implementation of specialized software products. These programs can find additional applications in other underground objects such as: tunnels – rail- and road (Vlasseva, 2015), underground parking places and garages, metro. There are numerous varieties in type and purposes of underground objects and although there are many similarities with underground mines, some specific features should be taken in consideration. Authors search for possible expansion of application areas of specialized mine ventilation software programs to aspiration systems, industrial ventilation installations with complex topology.

This paper presents emergency ventilation model of a high building, presented as a ventilation object with specialized ventilation programs VnetPc, MineFirePro+ VentSim. Numerical model creation of this object and also operation of emergency ventilation, reflecting fire regulation codes (PSTN, BS EN 12101-6:2005) are discussed in details.

Ventilation systems presentation

Ventilation systems are presented as a network of ventilation paths (branches), where air moves and places where air flows mix (nodes). Important part of their description are regulation devices – passive (producing pressure loses) and active – fans (supply and exhaust) generating pressure. Most common views of ventilation networks representation are graphical or/and tabular. In both variants all parts of the ventilation object, where air flows (branches), should be described. Each branch has a specially evaluated aerodynamic resistance R_i. At a design stage of the project R is calculated by known expressions (Stefanov, 1992), while for objects in operation it can be measured. Aerodynamic resistance depends on geometrical as well as aerodynamic factors. These factors are taken into account for modeling ventilation paths in a high building further in this paper. For one linear section (ventilation branch) the resistance law is valid:

$$W = R.Q^2 \quad (1)$$

where

R - is aerodynamic resistance [N.s^2/m^8];
W - is pressure loss [Pa];
Q - is volumetric flow rate [m^3/s];

Aerodynamic resistance can incorporate friction factor, length, perimeter, area, local loses, pressure drop.

Distribution of ventilation flows in the whole ventilation system obeys two basic network laws - mass conservation in nodes and mechanical energy conservation in independent contours.

Two main approaches in network modeling are applied – incompressible and/or compressible flows. More often stationary problems are solved – no change of parameters in time. But increasing complexity of networks and phenomena occurring there impose additional studies such as: analysis of emergency situations and their reflection on normal ventilation, transition of the system into emergency mode (Vlasseva, 2017). Specialized ventilation software programs can be utilized in modeling of incompressible, thermodynamic and emergency modes. Two of the most applied programs in the world, available for the authors of this paper are:

- Programs of Mine Ventilation Services Inc. - VnetPC (incompressible mode, passive network) and MineFire Pro (transient distribution of fire gases and heat),
- Program of Australian company Chasm Consulting - VentSimTM advance version.

Implementation of two independently developed software products makes possible to compare the results obtained as well as to model various physical phenomena, which are available in one or other program.

Specialized mine ventilation software

Both programs (VentSim and MineFire) incorporate methods described in books such as Subsurface Ventilation and Environmental Engineering by Malcolm J. McPherson (2009). This means, that results obtained by both programs are comparable. The reason for application of two different programs is that both of them have advantages in one or other direction. For instance, VnetPC and MFire Pro+ are text oriented, while VentSim is graphically oriented. Topology of network in VnetPC- MFire Pro+ is uploaded into spread sheet view (Fig. 1). Graphical output is generated after coordinates of nodes are input in a special spread sheet.

Antim-07-07.vdb - Branch Input

Row	Branch ID	From	To	FQi	Type	Resistance (Ns?/m^8)	Description
1	1	182	180		R	1000.00000	ет.18 - просмукване към аварий
2	2	183	182		R	5.30000	ет.18 - коридор - решетка смук. с-
3	3	184	183		R	658.37300	ет. 18 - врата кор. - стълби
4	4	185	184		R	408.00000	ет.18 - през ас.врата
5	5	186	184		R	75.40000	ет. 18 - от нагн. Шахта към стълб
6	6	172	170		R	1000.00000	ет.17 - просмукване към аварийн
7	7	173	172		R	5.30000	ет.17 - коридор - решетка смук. с
8	8	174	173		R	622.25000	ет. 17 - врата кор. - стълби
9	9	175	174		R	408.00000	ет.17 - през ас.врата
10	10	176	174		R	75.40000	ет. 17 - от нагн. Шахта към стълб
11	11	162	160		R	1000.00000	ет.16 - просмукване към аварийн
12	12	163	162		R	5.30000	ет.16 - коридор - решетка смук. с
13	13	164	163		R	642.63100	ет. 16 - врата кор. - стълби
14	14	165	164		R	408.00000	ет.16- през ас.врата
15	15	166	164		R	75.40000	ет. 16 - от нагн. Шахта към стълб
16	16	152	150		R	1000.00000	ет.15 - прросмукване към аварий
17	17	153	152		R	5.30000	ет.15 - коридор - решетка смук. с
18	18	154	153		R	644.04600	ет. 15 - врата кор. - стълби
19	19	155	154		R	408.00000	ет.15 - през ас.врата

Fig. 1

VentSim operate in the opposite way – all branches are introduced either with direct drawing, or by coordinates input (Fig.2). Both programs may import DXF, Autocad DWG, Microstation DGN, Datamine files, which is really useful in the whole process of mine design. Surely, some additional predesign for ventilation purposes is needed after such data transfer. VentSim can even convert a file, prepared by MineFire, for modeling into its environment.

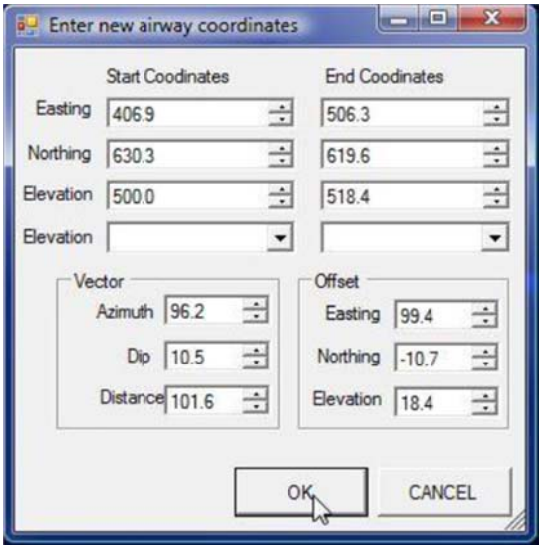

Fig. 2

Both programs have as an outcome airflows distribution along all branches, give fans and regulations regimes. In VentSim some useful for practice problems can be modeled: thermodynamic, diesel particulates, dynamic contaminants, gas, heat and DPM (Fig. 3).

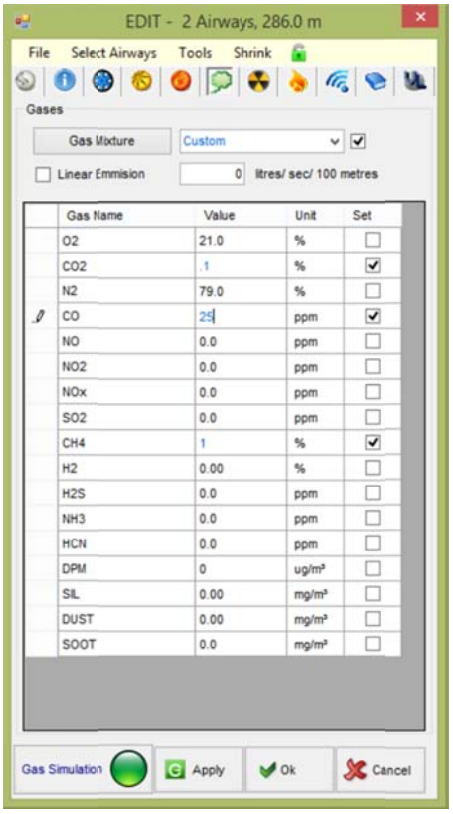

Fig. 3

Heat might come from point sources (such as electric motors), linear sources (such as conveyors), diesel engines, auto-compression of air, refrigeration and spot cooling. A very important feature is taking into account changing densities due to depth and temperature effects, natural ventilation, and moisture from sources such as dust suppression sprays, condensation from over saturated air. It is obvious that all these phenomena exist in other ventilation objects which are more civil oriented. VentSim has well developed visualization in many directions, including real time data from sensors (fig. 4).

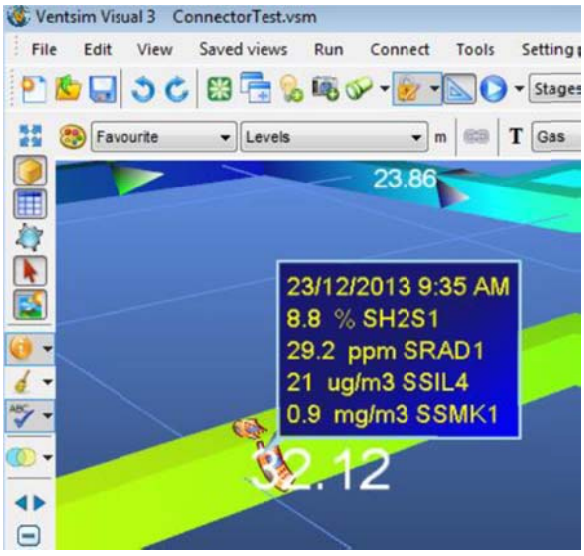

Fig. 4

MineFire Pro+ simulates a system's response to dynamic transient state phenomena such as fire with variable in time parameters, varying outside temperatures, changing ventilation control structures, or development of new mine workings. These features continue the process of full scale modeling of one ventilation system.

Requirements for high building emergency ventilation

Emergency ventilation of a high building should be designed so that to ensure safe evacuation of occupants from any floor through a staircase. It is assumed that fire has started somewhere in the work places. The aim of emergency ventilation is to create fresh air flow towards rescued people (overpressure in a staircase) and to extract fumes from the corridor (Fig. 5a and 5b).

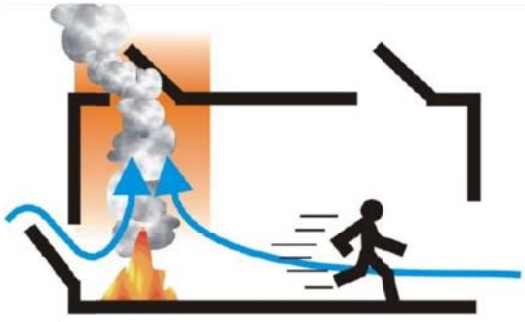

Fig. 5a

Evacuation takes place through the staircases. That means, that no combustible materials should be there as well as the air should remain clean from combustion products during the whole evacuation period.

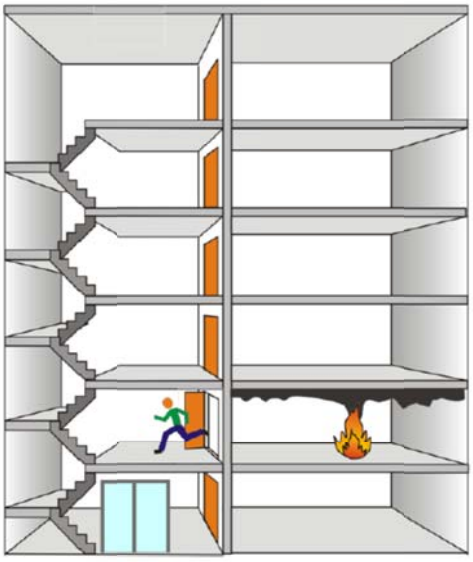

Fig. 5b

Fire safety regulations stated that:

- The staircase is isolated from a corridor with airtight, non combustible, smoke tight, self closing doors. The smoke tightness is secured through the door construction. The gaps should be no bigger than 2 mm with the doorcase, and no bigger than 4 mm with the floor (BS EN 12101, PSTN).
- The minimal pressure difference (overpressure) across a closed door and operating emergency ventilation between the staircase and the corridor shall be not less than 20 Pa.

Ventilation Object

The ventilation object, discussed in this paper, is an 18th floor administrative building. Fig. 6 presents the scheme of each floor of the building. Offices are located along a corridor. It is supposed that fire can occur somewhere there. In case of fire people should leave through the corridor door towards the staircase.

Fig. 6

Smoke extraction is achieved by extracting smoke through an exhaust fan located on the roof. It exhausts fumes from the corridor through a damper, sized 1225 x 225 mm, vertically mounted on the wall, connected to the exhaust fan through a pipeline.

The intake of fresh air is performed via two supply fans:

- Fan V1 supplies air in four lift shafts, creating overpressure to the staircase place; lifts are stopped at the first floor. Air leaks through lift doors and mixes with supply air from fan V2;

• Fan V2 supplies fresh air in staircase platforms through a pipeline and louvers (dampers) sized 425 x 225 mm, each one with 11 lamellas. Air supply is distributed between floors, which presumes different open area of louvers.

In order to fulfill emergency ventilation requirements the amount between supply and extraction flows should be as follows:

$$Q_{extraction} = (1.25 \div 1.4) Q_{supply} \quad (2)$$

A fire scenario, which is closer to the real rescue situation, is the following: the lifts are located on the first floor, all corridor doors are closed, the three fans operate – two supply fresh air in the staircase and in lift shafts, one exhausts from the corridor, all doors at entrance hall are opened.

In-situ measurements

Full scale measurements are published in Michaylov, 2008 and in Project 1856, 2005. Fans' performance, pressure difference (over pressure between potential fire zone and escape route) and other data, required by fire regulations are presented there. In brief, measurements show the following:

Fans:

- fan V1 supplies 13.715 m^3/s fresh air ;
- fan V2 supplies 8.213 m^3/s fresh air;
- fan V3 exhausts 30.69 m3/s fumes and air.

Pressure differences through doors

Fig. 7 presents the results from the measurement of overpressure between the corridor and the staircase. Data show that pressure difference for all floors between rescue section (staircase) and fire place (corridor) is greater than 20 Pa, varying from 55 Pa for 18th floor to 24 Pa for 2nd floor. Requirements of fire regulations are fulfilled.

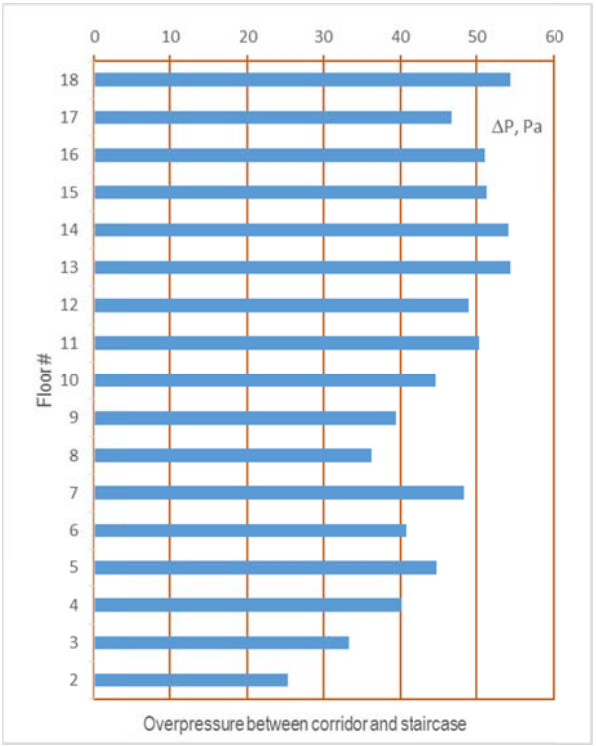

Fig. 7

Emergency ventilation model

Air flow movement is accomplished with the following equipment:

- supply air through lift shaft and air leakage through lift doors;
- supply air through shaft into staircase via air dampers;
- leakage through doors between staircase and corridor;
- exhaust air through shaft via air dampers.

In order to make an adequate model of emergency ventilation air resistances representing air leakage through doors and air supply through dampers, need special attention.

Air leakage through doors

Interesting results for air leakage through doors are presented in (Gross D., 1981 and Gross D., W., Haberman, 1989). Relationship between air flow through small gaps around closed doors and pressure difference between two sides of the door follows the general expression:

$$Q = k A (\Delta P)^n \quad (2)$$

where: Q is volume flow rate of air, m^3/s;

k is a flow factor incorporating the discharge coefficient (Cd,) of the leakage openings;

A is an equivalent area of opening or passage, m^2;

ΔP is pressure difference, Pa;

n is exponent which can vary between 0,5 and 1,0.

When the above variables are expressed in SI units $k = 0{,}827$ *and* $n = 0{,}625$.

Calculation of the area of the opening and further hydraulic diameter of the gab is important in order to ensure type of flow through the closed door. Doors in our ventilation object are 2.05 x 0.92 m. Gaps are 4 mm from the floor and 2 mm from the sides of the door. Then the hydraulic diameter is:

$$D_h = 4\frac{A}{\Pi} = 4\frac{(0.92*0.004+5.02*0.002)}{5.94} = 0.0092 \quad (4)$$

where: Π is perimeter of the gab, m

In order to evaluate resistance R for all branches of a network, representing leakage through doors, Reynolds number should be known. It is expressed in a well-known form, by using of gap flow rate and hydraulic diameter:

$$\mathrm{Re} = \frac{u D_h}{\nu} = \frac{\frac{Q}{L D_h} D_h}{\nu} = \frac{Q}{L\nu} \quad (5)$$

Fig. 8 shows Reynolds numbers vs Q. It is seen that the flow through closed doors is laminar. Using that data, aerodynamic resistance R is calculated (Fig. 9). Depending on measured data for ΔP at each floor, corresponding R is input into the program MineFire.

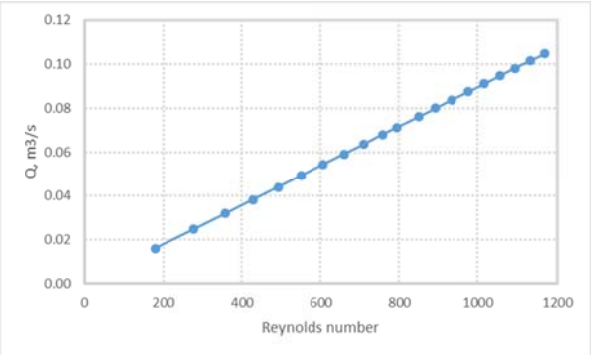

Fig. 8

Air supply through dampers

Air supply dampers, sized 425x225 mm, are with 11 lamellas and with area of 0.08 m2 when fully opened (100%). During measurements lamellas were regulated as follows:

- 1st to 4nd floor – 4 closes lamellas, i.e. 64% open;
- 5th to 8th floor – 3 closed lamellas, i.e. 73% open;
- 9th to 11th floor – 2 lamellas closed, i.e. 82 % open;
- 12th to 18th floor – 100% open.

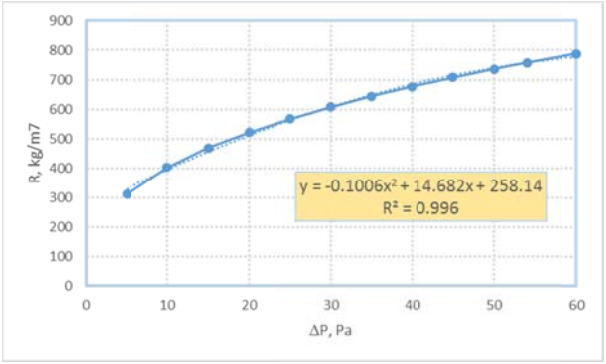

Fig. 9

Assuming regular distribution of air flow through the supply shaft and taking into account reduced area of the dampers at the corresponding floors, air resistances was evaluated. They vary from 149.27 kg/m^7 for 1-4 floors, to 75.4 for 12-18th floors.

The same approach was applied to exhaust shaft and dampers. Their regulation follows percentage of open area same as supply case. Air resistances' of the dampers in the corridors vary from 17.7 to 5.3 kg/m^7.

Numerical model of emergency ventilation

Numerical model of emergency ventilation include all paths, where air moves. Air supply and exhaust for each floor is presented by four similar air branches:

- leakage through lifts doors;
- leakage through corridor doors;
- air supply through dampers;
- air exhaust through fire dampers in the corridor.

In summary – four air branches should be described for each floor. Additionally, three shafts are presented – two supply and one exhaust. They are separated between floors with supply/exhaust dampers and loft doors. Regulation of flows throughout the building is made via adequate air resistances through doors and dampers. In general the ventilation of the building is presented in numerical view with 116 nodes (where air flows interact) and 149 branches (where air flows move through nodes). Initially, a numerical model was created for MFirePro+. Its graphical view is shown on Fig 10. The same model was transferred to Ventsim (Fig. 11). As stated above, it is easier to input a complex ventilation system into MFire Pro+, but Ventsim provides more opportunities for simulation and graphical presentation. Bearing in mind that both programs share the same mathematical models (McPherson, 2009), results are convertible and comparable. The goals of emergency ventilation are fulfilled:

- air is supplied through staircase and lift shafts;
- dampers are regulated so as to supply/exhaust air into required amounts;
- all directions of air flows are according to the purposes of emergency ventilation, i.e. towards rescued people;
- the programs also show fans regimes.

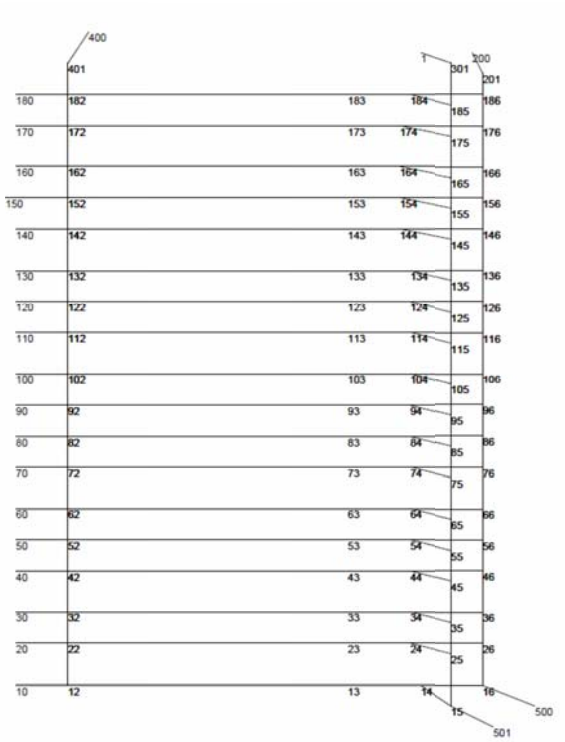

Fig. 10

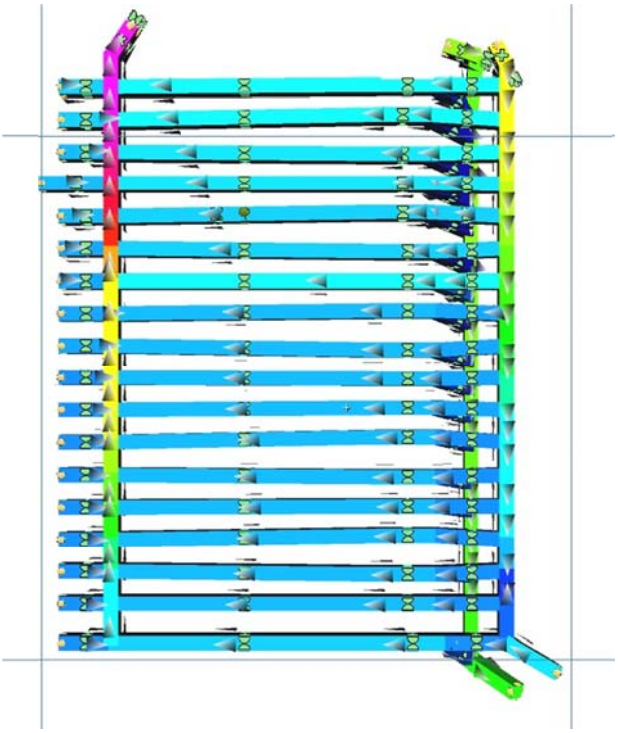

Fig. 11

Fig. 12 presents air reduction through supply shafts:

- starting from 8 m^3/s for the 18th floor for lift shafts and reaching 4 m^3/s at the 1st floor;
- starting from 13 m^3/s for the 18th floor for staircase shaft and reaching 1 m^3/s at the 1st floor.

Fig. 13 presents air extraction rate starting from 1st floor with 1 m³/s and reaching 32 m³/s at the 18th floor.

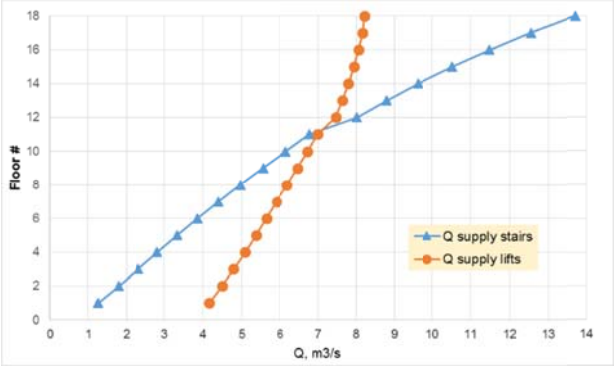

Fig. 12

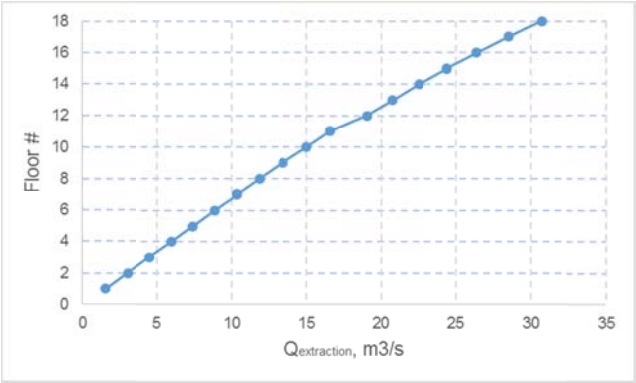

Fig. 13

Fig. 14 shows staircase duct supply fan's operation attributes, generated by VentSim software.

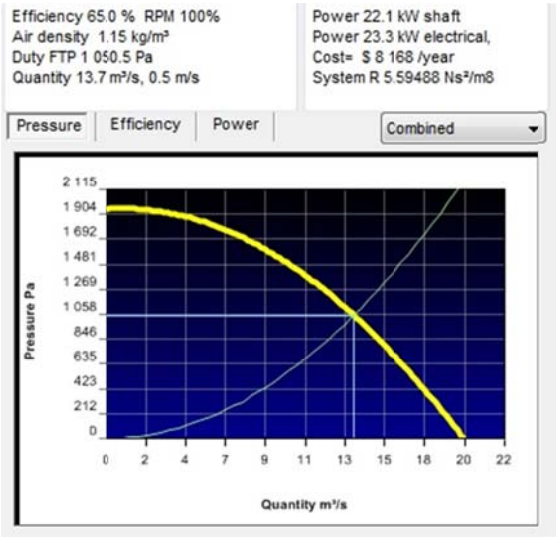

Fig. 14

Conclusion

In the process of transferring high building emergency ventilation system into numerical model a need for additional measurements arose. Pressure difference between air flow in shafts and ambient atmosphere in the staircase is an important parameter, needed to settle air resistance of the dampers. Lack of these values brings about the need for special research on the relationship between velocity through dampers and pressure difference. From the other side, impossibility to measure air leakage through doors also forced some research on air resistance of closed door with air leakage. Additional research in these directions is inevitable.

Application of specialized mine ventilation software towards civil objects gives positive results in several areas:

- better understanding of required air distribution throughout the ventilation system;
- regulation on the model and direct application on real object;
- all possible fire and other accidents modelling, serving as a plan for rescue operation.

Further research and transformation of different civil ventilation objects like underground garages, aspiration systems with several inputs and outputs, road and railway tunnels are appropriate objects for modelling with full scale analyses of thermo-dynamical and air-dynamical phenomena.

Refferences

Michaylov M., Z. Dinchev, El. Vlasseva, 2008, Avarijna ventilatsiya na visoki sgradi, Nauchno-tehnicheski sbornik "Pozharna i avarijna bezopasnost", br.17, Sofia, str. 80 – 93

Dog. 1856, 2005, Depresionna snimka v ANTIM TOWER za opredelyane na depresiyata mezhdu stalbishtnoto otdelenie i koridorite na sgradata, Arhiv na NSI na MGU

BS EN 12101-6:2005, Smoke and heat control systems —Part 6: Specification for pressure differential systems; Part 3 Smoke and heat control systems: Specification for powered smoke and heat exhaust ventilators.

Naredba 2. Protivopozharni stroitelno-tehnicheski normi (PSTN). Dv. br. 33/19.04.94.

AS/NZS 1668 The use of ventilation and air conditioning in buildings.

Vlaseva El., Ventilacija na transportni tuneli, Izd. kasta "Sv. Ivan Rilski", Sofia, 2015, str. 96, ISBN 978-954-353-286-5

Vlaseva El., Matematichesko modelirane v minnata ventilatsiya, Izd. kashta "Sv. Ivan Rilski", Sofia, 2017, 236 str., ISBN 978-954-353-235-1

Gross D., 1981, A Review of Measurements, Calculations and Specifications of Air Leakage Through Interior Door Assemblies, NBS Publications 81-2214

Gross D., W., Haberman, 1989, Analysis and Prediction of Air leakage through Door Assemblies, Fire Safety Science – Proc. of the Second International Symposium, pp. 169-178

HSE Safety Guidelines SG-FS-0-0-2, CERN Safety Code E.

McPherson M., (2009), Subsurface Ventilation and Environmental Engineering, Mine Ventilation Services, Inc., ISBN

Ventsim™ User Guide

MineFire Pro+ A Simulator for Underground Fires, USER'S MANUAL & TUTORIAL, Mine Ventilation Services, Inc., www.mvsengineering.com

This article was reviewed by Prof. Dr. Veliko Kertikov and Prof. Ivan Antonov, DSc.

IMPROVEMENT OF MEASUREMENTS OF 3D AIR FLOWS IN FREE AND SEMI-RESTRICTED SPACE

Zahari Dinchev[1], Yassen Gorbounov[2]

[1] University of Mining and Geology "St. Ivan Rilski", e-mail: dinchev@mgu.bg
[2] University of Mining and Geology "St. Ivan Rilski", e-mail: y.gorbounov@mgu.bg

ABSTRACT. The enhanced requirements for safe, healthy and environmentally friendly workplace and ambience require highly specialized measurements of the air quality in indoor and outdoor workplaces. Many mining work areas have large volumes and in such sites, one-dimensional, directed air flows are rarely observed. It is common that the flows are equally sized in the three directions (x, y, z). In fact this is also the way the harmful particles are spread in the studied areas. Measurement and visualization of the fluid vector field in free and semi-restricted space can be successfully performed with a 3D ultrasonic anemometer. It permits the composition of a real flow speed field by making fast multiple measurements in all the three directions. A microcontroller device is proposed in the paper that enhances the capabilities of the 3D ultrasonic anemometer MODEL 81000 by R.M. YOUNG COMPANY, USA. This is done by reading the data from the standard RS-232 serial interface and logging it on a SD card. A GPS receiver is also added to the system thus making possible the precise capturing of geographic coordinates in open space. All this makes the anemometer much more flexible and portable. A proposal for future development is also presented which will make the anemometer accessible via wireless connection and a mobile platform in the field.

Keywords: ultrasonic anemometer, air quality, data logging

УСЪВЪРШЕНСТВАНЕ НА ИЗМЕРВАНИЯТА НА 3D ВЪЗДУШНИ ТЕЧЕНИЯ В СВОБОДНО И ПОЛУОГРАНИЧЕНО ПРОСТРАНСТВО

Захари Динчев[1], Ясен Горбунов[2]

[1] Минно-геоложки университет "Св. Иван Рилски", 1700 София, e-mail dinchev@mgu.bg
[2] Минно-геоложки университет "Св. Иван Рилски", 1700 София, e-mail y.gorbounov@mgu.bg

РЕЗЮМЕ. Повишените изисквания за безопасна, здравословна и екологична работна и околна среда изискват специализирани измервания за качеството на въздуха в работни места в затворени помещения и на открито. Немалка част от работните зони в минното дело са с големи обеми и при такива обекти едномерни, насочени въздушни течения, рядко се наблюдават. Твърде често теченията са с относително равнопоставени големини в трите направления (по x, y, z). Така се разпространяват и отделените вредности в изследваните зони. Измерване и визуализация на векторното поле на въздушно течение в свободно и полуограничено пространство е възможно да се осъществи с 3D ултразвуков анемометър.Това позволява съставянето на реално скоростно поле чрез бързо многократно измерване в трите направления. В статията е предложено микроконтролерно устройство, което разширява възможностите на 3D ултразвуковия анемометър MODEL 81000 by R.M. YOUNG COMPANY, USA. Това е направено чрез прочитане на данните по стандартен RS-232 интерфейс и тяхното запазване върху SD карта. Освен това към системата е добавен GPS приемник, който позволява прецизно снемане на географски координати на открито. Всичко това прави анемометъра много по-преносим и гъвкав в употреба. Направено е предложение за бъдещо доразвиване на системата, чрез което анемометърът да стане достъпен през безжична мрежа от мобилно устройство в мястото на измерване.

Ключови думи: ултразвуков анемометър, качество на въздуха, регистриране на данни

Introduction

Precise measurements of flow directions and distribution in many industrial areas is crucial for ensuring safe work atmosphere. It is even more important for many mining sites such as open pit mines, face ventilation (Timko, 2005), flows around fans. Other civil objects – tunnels entrances and exits, flows around buildings and typical meteorological measurements (Wilson, 2012) also require 3D velocity field. In such objects one-dimensional, directed air flows are rarely observed. It is common that the flows are sized in the three directions (x, y, z). In fact this is also the way the harmful particles are spread in the studied areas.

The technological development makes possible the utilization of up-to-date devices for flow measurements based on ultrasonic signals. These are ultrasonic anemometers (Fig.1). Their application and measurement results need additional processing for upgrading into a user friendly view. In order to get measured a 3D velocity field one needs a computer linked to the anemometer which is not appropriate in many sites. What is more, after uploading the data it should pass additional treatment, especially in sequencing between positions where the vector and its measured value are taken.

This paper presents one possible way to improve 3D ultrasonic measurements in the following directions: GPS positioning system and transfer of the measured vectors in the specified coordinates to the SD card.

Fig. 1

Technical characteristics of 3D anemometer

The constant increase in computing capabilities enables the creation of ever faster and more powerful computing devices and practical implementation of increasingly sophisticated algorithms. This makes possible the existence of ultrasonic anemometers in which the three-dimensional flow velocity is based on the time of passing ultrasound acoustic signals. This paper is built around the 3D ultrasonic anemometer MODEL 81000 by R.M. YOUNG COMPANY, USA (fig.1).

The YOUNG Model 81000 Ultrasonic Anemometer is a 3-axis, with no-moving-parts, wind sensor (http://www.youngusa.com). The sensor features durable corrosion-resistant construction with 3 opposing pairs of ultrasonic transducers supported by stainless steel members. It measures wind speed in a range from 0 to 40 m/s, with resolution 0.01 m/s in all 360 degrees wind direction. The device has several serial outputs (one user programmable ASCII, RS-232 or RS-485) and 4 voltage outputs (from 0 to 5000 mV).

Serial Output:
- RS232 at 38400 Baud
- ASCII Text Serial String - Wind Speed - 3D (m/s); Direction (Deg); Elevation (Deg); Speed of Sound (m/s); Sonic Temperature (°C)

Analog Voltage Outputs:
- Channel V1: Wind Speed (3D) - 0-5000 mV = 0-50 m/s
- Channel V2: Wind Direction - 0-5000mV = 0-540 Deg
- Channel V3: Elevation - 0-5000mV = -60° to +60°
- Channel V4: Sonic Temperature -0-5000mV = 220K to 320K

Operating principle of ultrasonic anemometer

Operating principle of ultrasonic anemometer can be described briefly in the following way (fig.2).

Fig. 2

The anemometer has 3 arms. The three pairs of transducers are displaced at 120 deg. Redundancy of the measurement is given to each path thus improving the sensor accuracy and reducing aerodynamic turbulence. The time taken for an ultrasonic pulse of sound to travel from one transducer to the diametrically opposite transducer (north to south) is measured, then it is compared with the time for a pulse to travel in the opposite direction (S to N) (Gill Instruments, 2017; Ultrasonic Anemometer, 2017). Simultaneously, times are compared between west and east and vice versa (E to W). If we have preliminary northern wind, then the time taken for the pulse to travel from N to S will be less than from S to N, whereas the W to E, and E to W times will be the same. The wind speed and direction can then be calculated from the differences in the times of flight on each axis. Sonic temperature is derived from the speed of sound which is corrected for crosswind effects. When the wind blows, it increases the time of flight for pulses travelling against it. The time of flight theory principle is illustrated in Fig. 3 with equations (1) to (4).

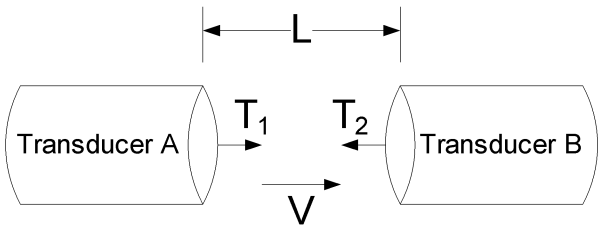

Fig. 3

$$T_1 = \frac{L}{C+V} \quad (1)$$

$$T_2 = \frac{L}{C-V} \quad (2)$$

$$V = \frac{L}{2}\left\{\frac{1}{T_1} - \frac{1}{T_2}\right\} \quad (3)$$

$$C = \frac{L}{2}\left\{\frac{1}{T_1} + \frac{1}{T_2}\right\} \quad (4)$$

where: L is the distance between the transducer faces,
C is the speed of sound,
V is the velocity of the fluid (the air),
T1 and T2 are the propagation times of the ultrasound.

Necessity for measurement improvement

Measurements with ultrasonic anemometer are performed and managed through Command Menu with the following structure:

```
COMMANDS (VERSION 7.0.05)
-------------------------
R) REPORT
S) SETUP
X) EXIT TO OPERATE MODE
```

One can choose consequently positions R), S) or X) in order to set initial parameters according to Model 81000 Instructions. As seen from the passage below, many parameters should be set according to measurements which need to be performed.

```
SET PARAMETERS
--------------------------
A) AVERAGING
B) BAUD
E) ERROR HANDLING
N) SCALING MULT
O) OUTPUT RATE
P) POLL CHARACTER (ADDR)
S) SER OUT FORMAT
T) THRESHOLD
U) UNITS
V) V OUT FORMAT
W) WAKE CORRECTION
X) EXIT TO MAIN MENU
```

Special attention is paid to position R) – report. If 3D speed is selected in order to have 3D vector field, the output file will consist of ASCII string, containing all measured data. This data is in mV for each analog channels outputs.

```
CURRENT SERIAL OUTPUT FORMAT:
5) UVW
6) 2D SPEED
7) 3D SPEED
8) AZIMUTH
9) ELEVATION
A) SOS
B) Ts
C) CHKSUM
E) ERR CODE
V) INTERNAL VOLTAGE
```

Then special conversion should be performed as given below:

```
CONVERSION TO ENGINEERING UNITS
FOR UVW FORMAT:
U,V, OR W
WINDSPEED = [(SCALE X 2 / RANGE) X MV] - SCALE
EXAMPLE:
W CHANNEL OUTPUT VALUE = 2550 MV
 SCALE = 25 M/S
RANGE = 5000 MV
SPEED = [(25 X 2 / 5000) X 2550] -25 = 0.5 M/S
```

What is more, separate coordination of measurement points should be written down during experiments. All these problems need to be overcome in order to put the device in a user friendly mode. One solution is presented hereafter – a modem linked to the anemometer, to the GPS receiver and to the mV converter which transfer measured data in a vector view to a SD card.

Logging device

A NodeMCU ESP12-E is selected as the main controller because of its low price, easy programming and WiFi connectivity capabilities. NodeMCU is an open source IoT platform and includes firmware running on the popular ESP8266 Wi-Fi SoC from Espressif Systems. It can be programmed in the Arduino IDE which provides simplicity and pre-built libraries. A block diagram with all the main components of the controller is shown in Fig. 3.

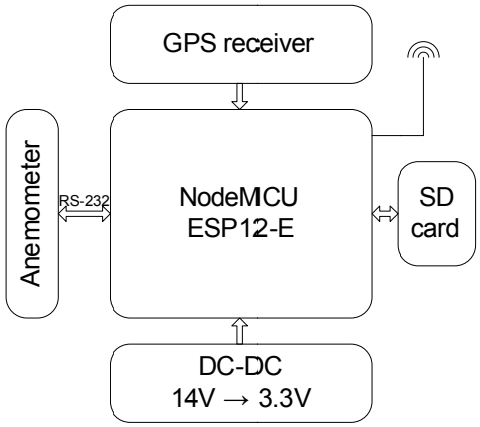

Fig. 4

The anemometer is powered by a 12-24V battery so there is a DC-DC converter to lower the voltage to 3.3V required by the NodeMCU. The anemometer communicates with the controller over a standard RS-232 serial port. The MCU reads the data from the GPS receiver and adds that data to the one from the anemometer and then continuously stores it on a SD card.

Performed measurements with MODEL 8100

Illustration of capabilities and applicability of 3D flow measurements are presented hereafter. Fig. 5a shows schematic view of the stand with wind turbine, while Fig. 5b – the same stand with 3D anemometer (Z. Dinchev, 2014). The purpose of experiments was to measure velocity field flows around wind turbine.

The stand consists of the following elements:
1 – axial fan with regulation;
2 – flexible pipeline;
3 – regulation grid and diffusor;
4 – wind fan in two types (H225 and H150);
5 – anemometer;
6 - 3D supersonic anemometer;
7 – Laptop.

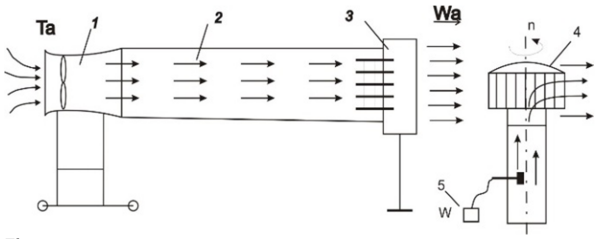

Fig. 5a

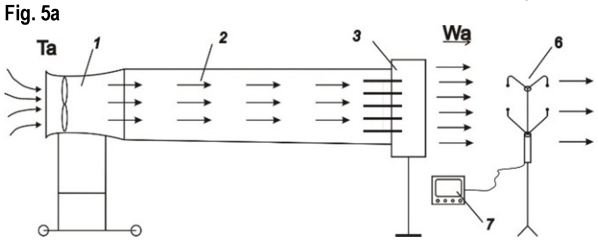

Fig. 5b

Measurement results are summarized in Table 1. They are obtained without a logging device and their final output was achieved with additional treatment of the registered data. As seen from the figures, the velocity field is uniform in plane XY. Very small fluctuations in Z and X direction are seen. That was the purpose of the experimental measurements – well targeted and constant flow towards the wind turbine. Applying such flow, the regime characteristics of the wind turbine were measured (Z. Dinchev, 2014).

Table 1.

U, m/s	V, m/s	W, m/s	3D, m/s	A, Azimuth, deg	E, Elevation, deg
-0.06	6.51	-0.08	6.53	359.4	-0.7
-0.02	6.53	-0.11	6.55	359.8	-1
-0.03	6.54	-0.02	6.56	359.7	-0.2
-0.05	6.48	-0.35	6.51	359.5	-3.1

Future work

The selected NodeMCU ESP12-E main controller gives opportunity for future improvements that can provide additional flexibility. The core of this work includes the use of WebSockets. The WebSocket protocol is a TCP-based protocol. This protocol lowers the overhead in the interaction between a browser and a web server by providing a standardized way for the server to send content to the browser without being solicited by the client. This allows for messages to be exchanged while keeping the connection open.

The basic idea for the proposed improvement is shown in Fig. 6.

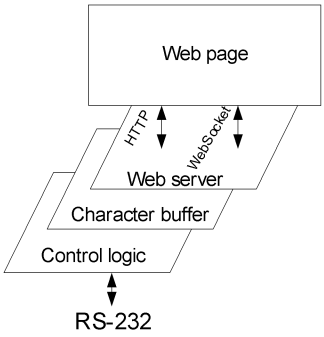

Fig. 6

The implementation of the proposed approach will give the opportunity to build a wireless serial terminal. Thus, a terminal of a convenient computer will be emulated by the NodeMCU via a webpage that can be read on any portable device with a web browser.

Conclusion

Based on general knowledge of 3D measurements and utilization of ultrasonic anemometers one useful improvement of measurement technique is presented. After considering all ideas, researchers will have an intelligent device which can perform all type of three dimensional velocity field in different engineering sites.

References

Gill Instruments Limited, How do Gill Ultrasonic Anemometers Work http://gillinstruments.com/products/anemometer/principleofoperation2.html, 2017

Taylor C., Timko R., Thimons E., Mal T.*Using Ultrasonic Anemometers to Evaluate Factors Affecting Face Ventilation Effectiveness*, Presented at the Society for Mining, Metallurgy, and Exploration (SME) Annual Meeting, Salt Lake City (2005)

Ultrasonic Anemometer MODEL 81000, R.M. YOUNG COMPANY, USA, 2801 AERO PARK DRIVE, TRAVERSE CITY, MICHIGAN 49686, Rev. I102210, 2017

Wilson N., Paldanius J., Hietanen J., *Practical Applications Of Ultrasonic Wind Sensors For Resource Assessment*, EWEA The European Wind Energy Association, Copenhagen, Denmark. April 16th - 19th 2012

Динчев, З., Изследвания върху нетрадиционни методи и конструкции за проветряване на минни и индустриални обекти, докторска дисертация, МГУ „Св.Иван Рилски“, 2014 г. (Dinchev, Z. Izsledvaniya varhu netraditsionni metodi i konstruktsii za provetryavane na minni i industrialni obekti, PhD Thesis, MGU “St. Ivan Rilski”, 2014)

http://www.youngusa.com

ULTRASONIC ANEMOMETER MODEL 81000, Instructions

The results presented in this paper were achieved under project MTF-159/2017.

This article was reviewed by Prof. Dr. Veliko Kertikov and Assoc. Prof. Dr. Elena Vlasseva.

LOCAL VENTILATION SYSTEM'S CONTROL

Zahari Dinchev

University of Mining and Geology "St. Ivan Rilski", 1700 Sofia, dinchev@mgu.bg

ABSTRACT. In the construction and operation of dead-end underground objects local ventilation systems are applied. They diluted liberated waste products and transferred them outside the place. In order to ensure proper ventilation of these objects operation of the system has to be periodically controlled and tested. It includes control measurements of working environment, inspections and control measures and efficiency of auxiliary ventilation. The paper presents whole measurement cycle: inspection of installation, measuring devices, logics in consequence of measurements, results monitoring. Important part of control process is local fan's parameters. Illustration is made on an example of forcing system for local ventilation.

Key words: mine ventilation, local ventilation, control, inspection, auxiliary ventilation, auxiliary fans

КОНТРОЛ НА СИСТЕМИ ЗА МЕСТНО ПРОВЕТРЯВАНЕ

Захари Динчев

Минно-геоложки университет "Св. Иван Рилски", 1700 София; dinchev@mgu.bg

РЕЗЮМЕ. При строежа и експлоатацията на глухи минни изработки за осигуряването на проветряването се използват системи за местна вентилация, които разреждат и изнасят отделените вредности извън тези изработки. За правилното проветряване на изработките и експлоатация на тези системи е необходимо да се извършват периодични проверки и контролни измервания за установяване на режима на проветряване на изработките и ефективността на работа на системите за местна вентилация. В статията са представени методи и необходими уреди за провеждане на контролни измервания при местни вентилационни системи, както и форми за проверка и мониторинг на тези системи. Даден е пример за контрол и мониторинг на нагнетателна система за местно проветряване..

Ключови думи: местно проветряване, минна вентилация, контрол, инспектиране, вентилатори за местно проветряване;

Introduction

Underground facilities at their initial construction phase pass through configuration when fresh and exhaust ventilation air flow/outflow from the same location – dead end pathways. These group include road, railway and metro tunnels, underground parkways and garages, mine workings in development stage. For most of the above mentioned objects these configurations are only temporarily, but still different work phases in their development and exploitation exist while in a real operational process other types of ventilation are applied. In underground mines however such objects – dead end roadways with local ventilation systems operate in the whole work cycle of the mine, being a part of the overall production process. What is more – they remain part of mine ventilation system, influencing at the great extent its efficient work.

This paper presents author's experience in design and control of local ventilation system. Special attention is drawn upon consequence in control operations, methods and means for effectiveness achievement in two directions – ensuring safety work conditions with minimal expenses for ventilation.

Generally used systems for local ventilation

As stated above with application of local ventilation systems normal and safety atmosphere in a face should be guarantee. It serve also to export exhaust air outside the premises according to safety regulations. Since varieties in work conditions exists, different systems for local ventilation are applied. They incorporate exhaust fans and specially constructed pipelines to supply fresh air and to extract exhaust air. Fig. 1 presents one dead end roadway, ventilated by a forced fan, located outside the place. Fan supplies fresh air at the face, diluted the harmful impurities, emitted during the work process Exhaust air is extracted parallel to the pipeline along the length of roadway. Following symbols are marked on fig. 1:

Qv – air flow through the fan, m^3/s,
Qa – air flow of main current, m^3/s,
Qo – air flow, supplied to the face, m^3/s,
Lf – length of face, m.

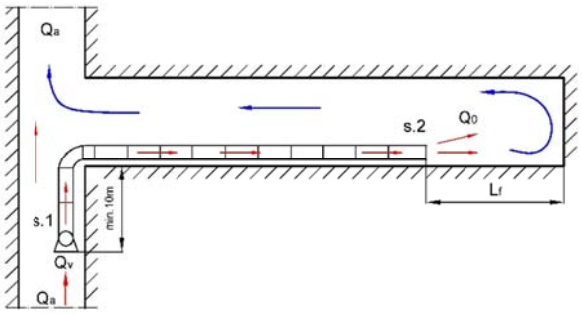

Fig. 1. Forced local ventilation system

Varieties in local ventilation schemes, applied most widely, can be summarized in the following three groups:

- forcing or blowing system for ventilation (fig.1.);
- exhausting system (reversed flow compared to fig.1. – the fan extracts flow from the face and operated at exhaust regime);
- systems with overlaps (fig.2 shows exhausting system with force overlap). Similar scheme can be realized in other way - forcing system with exhaust overlap.

Advantages and disadvantages of the above presented systems for local ventilation are discussed widely and thoroughly in McPherson, 1993 and in Stefanov,1991. Forced systems, due to their advantages, not complicated design and realization, are most widely applied and utilized in practice. By that reason further in the paper given examples are with forced system.

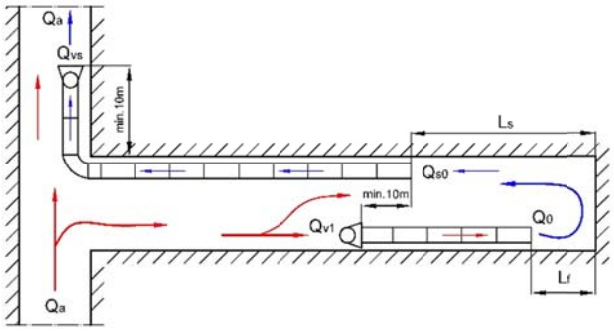

Fig.2. Exhausting system with force overlap

In a big mine during the whole life cycle of the enterprise simultaneously operate several local ventilation systems, together with main ventilation system. Work, requiring local ventilation, include construction of developing workings, chimneys and other facilities. Summing up costs for local ventilation they might equalize or even exceed power of main fans. That is one real reason to control and optimize local systems performance. When these systems are not limited in number, the amount of measurements and regulations increases rapidly in order to maintain ventilation systems in their effective range, closed to the design documentations.

Requirements for local systems control

Control of different systems in a mine, including local and main ventilation systems, is performed upon underground mining regulations (Pravilnik 1992, Pravilnik 1971). As regards to ventilation systems, regulations are restricted mainly to safety requirements (not to technical performance) for main fans and installation. Local ventilation and control of its parameters is discussed in Kertikov, 1996. Again, main attention is drawn upon health and safety work environment factors and their values, rather than clear rules for their achievement.

Passages and texts from BG mine regulations, applied for local ventilation, can be summarized as follows:

- ventilation only by diffusion in a non-gassy mines is restricted to 10m for horizontal pathways and 5m for vertical ones;
- one dead-end facility should be ventilated by its own independent local ventilation system, supplied with fresh air either from the surface or from air flow, delivered by main fan;
- local ventilation systems work uninterruptedly;
- no air recirculation from exhaust flow towards supply one is permitted;
- air recirculation is prevented by the following technical measures: local fan (forced or exhaust) is mounted at least 10 m away from the mouth of dead-end underground workings and 15 m away from ones, having outcome to the surface;
- local fan air flow, supplied to its sucking opening, is restricted to up to 70% of main current flow;
- air flow velocity in developing mine workings is limited into range 0,15 - 4m/s;
- all measurements for ventilation system's performance should be registered in ventilation journal.

Consistent policy for mine ventilation management can bring positive outcomes in several directions – efficiency increase, decrease in electricity consumption but in the same time – ensuring safety work conditions. As stated in De Souza, 2017 establishment of mine ventilation management program, which include local ventilation, will create a basis for achievement of the above given three benefits – effectiveness, costs and safety. Such management program cover purpose, design, measurements and control, analysis, corrections and improvements. This paper is concentrated on measurements and control, without neglecting the other parts of the program.

Local ventilation system's examination

Design of local ventilation system is made by qualified ventilation engineer. The project is then transformed on a real object, as closed as possible to calculations and instructions. Further, maintenance is very important task, which has to be done according to safety regulations, meeting "best practice". In brief – construction of local ventilation system adequate to the project and maintenance in phases, described in it.

All the above mentioned steps in initiation and effective work of local ventilation system, require creation of plan for management, as a part of general management of the whole ventilation in a mine. Such plan include detail examinations of all system's components, air flow and pressure measurements, concentration of contaminants in work environment as well as other parameters, required by safety regulations.

Local ventilation checks should be performed regularly – once for every 24 hours and after increase in length or other change of pipeline. Obtained results is recommended to write and saved into special journal with specially created positions, questions and information. These data should is enough to show ventilation installation's operation status. One example of such check list is presented in table 1. Proposed table is a model and can vary in accordance with type, amount and purpose of ventilation installation and work place of its service.

Table 1.
Examination and control form

Date and time: *10:20*	**Work shift:** *1*	
Work place*: 7th gallery*	**Section:** *II*	
Required air flow, m^3/s: *6.5m^3/s*		
Fan No: *2BM*		
Distance from face to end of pipeline: *12m*		
Gas concentrations:		
Gas	**measured**	**regulation**
Oxygen –O_2, %	*20.3*	**> 20**
Carbon monoxide – CO, ppm	*14*	**32**
Carbon oxide –CO_2 ,%	*0.08*	**0.5**
Nitrogen monoxide – NO ,ppm	*4*	**15**
Nitrogen oxide – NO_2, ppm	*0.5*	**2**
Other: _____		

Check list:	
Parameter	
Fan is correctly mounted and fixed	
Fan's outlet is supplied with safety grid	
Fan has silencer	
Fan's location is at least 10 m away from the mouth of mine working in air flow direction	
Connection between pipeline and fan is correct	
Are there damaged parts of pipeline?	
Is the pipeline safety hanged?	**X**
Pipeline sectors are properly linked	
Pipeline axis is horizontal and strait	**X**
What type of connection between different pipeline diameter and fan's outlet are used and are they properly mounted?	
Is the distance between pipeline end and face is within 20-25 m?	
Gas concentrations are according to regulations	
Required air flow is supplied to the face	
Comment*: Hang safety the pipeline and change the damaged parts of pipeline*	
Check is performed by: *P. Иванов*	Signature: ….

Correctly performed and filled data checks show up-to-date information about local ventilation systems' status and can serve as a basis for corrections, repairments and improvements in them. In case operational personnel can't reach satisfactory results even after measures applied, the problems should be raised to an upper management level – chief engineer, ventilation manager, in order to clear the reasons for bad performance of the system and for adequate measures to be undertaken.

Local ventilation systems' control measurements

Control ventilation measurements, as stated above, should be performed after any change of ventilation installation - lengthen of pipeline, regulators relocation, replacement of pipeline sectors etc. Some changes might arose from regular checks and controls. Ventilation measurements as a first should proof that design parameters are met and if practice require corrections in in the project or its realization (Kertikov, 1995).

Featuring parameters of on local ventilation system are clearly presented and explained in McPherson, 1993 and in Stefanov,1991. One example of forced scheme with one fan are as follows:

- air flow through the fan (Qv),m^3/s;
- air flow, supplied to the face (Qo),m^3/s
- fan static pressure (Ps),Pa
- fan total pressure (Pt),Pa
- system supply coefficient (p=Qo/Qv).

Assessment of the above stated parameters need special knowledge about aerodynamics of flows in local ventilation systems, should be fulfilled by experienced personnel in accordance with requirements for ventilation measurements, as explained in Stefanov,1991. More detailed explanation about consequence in measurements, main links between values, devices used in practice is given in Kertikov, 1995. One very important point is availability of measuring devices, which in minimum should be the following:

- anemometer to measure air flow velocity in a pipeline and in an accompanying flow in mine working;
- manometer to measure total and static pressure in a pipeline and of a fan;
- combine Pito tube to take sample for pressure of a flow in a pipeline and to transfer the information to the manometer. It can be used also for direct evaluation of velocity in a flow;
- psychrometer for air humidity and further density evaluation;
- barometer for barometric pressure measurement;
- combined gas detectors for measuring concentration of gas impurities at a face and along the air flows;
- gas leak detectors for control of air leaks and recirculation in low velocities sectors.

These list of measuring devices is absolutely necessary for required by Pravilnik 1992, Pravilnik 1971 gas, flow and pressure surveys. Measurement devices need calibration and regular examinations in a certified laboratory at least once a year unless stated differently in technical papers of producers. In case units are used more often they underpass calibration every 6-8 months.

Control measurements results should be classified and well presented for further analysis and correct measures when some of parameters are out of order. It is very useful for one enterprise to prepare typical forms for registration of controls for all types of local ventilation systems – forced, exhaust and with overlap. Such forms should include the following data:

- place and time of measurement;
- data for object – dead end part, face, adjacent; gallery;
- data for ventilation system and for fan general description;
- classified information of measurements and post-measurement calculations, where necessary;
- overall system's performance – coefficients, effectiveness, parameters.

One example of control measurements and assessment of forced local ventilation system is given in tables 2 and 3.

Table 2.
Form 1 – general data

Date and time:	*15:40*
Place:	*6 gallery*
Geometrical data:	
Cross section,m^2	*12*
Length,m	*120*
Design length	*260*
Required air flow, m^3/s	*6,5*
Cross section of adjacent working,m^2	*14*
Data for ventilation system:	
Fan type:	*BM-8M*
Fan number:	*3BM*
Motor power, kW:	*55*
Angle of the blades	*+20*
Work wheel diameter, mm	*800*
Pipeline diameter, m	*800*
Length of pipeline, m	*105*
Length of pipeline sectors, m	*10*
Type of connection between sectors	*zip*
Number of connections, number	*10*
Length of pipeline in the adjacent gallery, m:	*10*
Number and type of local resistances: 1. One bend at 90 degree 2. _____	*1*

These forms (table 2 and 3) are models. They might be transformed according to special features of the company and its local systems. The models, presented here, consist only minimal amount of data and any additional information might bring more confidence in presentation of results.

Table 3.
Form 2 - measurements

Ventilation measurements	
Barometric pressure, hPa	*910*
Air temperature at face, ^oC	*24*
Air flow of fan - Qv ,m^3/s	*7,8*
Fan total pressure of P_t,Pa	*2900*
Air velocity in a pipeline, m/s	*15.5*
Air flow at face – Q_0,m^3/s	*6,9*
Air velocity in dead-end working – Uc,m/s	*0.58*
Air flow in dead-end working – Qc,m^3/s	*7*
Air velocity in adjacent gallery – Ua,m/s	*0.9*
Air flow in adjacent gallery – Qa,m^3/s	*12.6*
Air temperature in adjacent gallery – Ta,m^3/s	*21*
System's parameters	
Face supply coefficient p=Q_0/Qv	*0.88*
Dead-end working supply coefficient – z= Qa/Qv z>1.43	*1,6*
Fan's efficiency	*0,45*
Electrical power,kW	*45*
Comment:_____	
Measured by: Ivanov	Signature: +++++

All presented measured results follow methodology given in . McPherson (1993), Stefanov T.,1991 and Kertikov V., Iv. Velchev (1995). The most often mistakes and difficulties exist in measurements of fan air flow (Qv) and air velocity in a pipeline. These are due to close location of measuring points to the fan motor and non-regular profile of velocity there. Other difficulties arose by hardly to reach locations (narrow, high places) where accuracy might be not satisfactory enough. Well designed and built ventilation system should have appropriate holes for portable devices or permanent units for measurement. One example is the diffusor shown on fig. 3. It is mounted on fan's inlet, has safety grid and ring to measure static pressure. Then very easily air flow, inflowing into the system, can be calculated.

Along pipeline length nozzles, orifices and other air-dynamical units might be built in to assist in pressure and flow measurements and controls.

Conclusion

Ideology of local ventilation system's control and required measurements to achieve cost effective and at the same time – ensuring safety work environment, presented in this paper might serve in several directions.

As a first for mine companies it is very important to keep ventilation systems – local and main ones, in correct interaction between them. This means to maintain energy power cost for both systems at such regulation so as to supply required air flows in sufficient amount to the local systems.

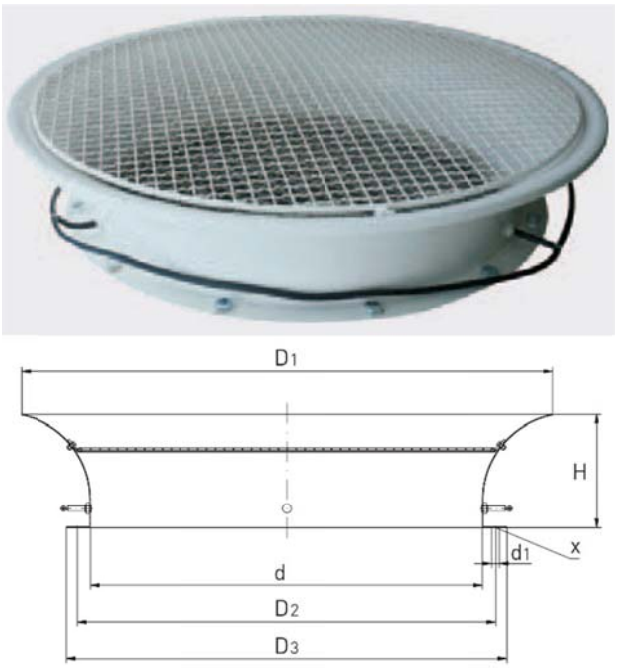

Fig. 3. Diffusor with grid and static pressure ring

As a second – for other underground objects, where dead-end configurations are part of their construction. Requirements, stated in safety regulations for underground coal and metal mines should be taken into account to other underground objects, although it is not explicitly written for them. Reaching great safety standards for all underground objects is task,

which solution should be searched and found. Author's expertise in design and control of mine local ventilation systems can serve as an initial step in that direction.

Results classification in a specially created forms and further systematical analysis of obtained data might be very useful in forecast of future potential problems in the process of this particular local system and even more – in other systems, operating in similar conditions.

References

Malcolm J. McPherson (1993), Subsurface Ventilation and Environmental Engineering, Chapman & Hall, London, 1993, p. 905, ISBN-13- 9780412353000

De Souza E., (2017), "Application of ventilation management programs for improved mine safety," Int. J. Min. Sci. Technol., vol. 27, no. 4, pp. 647–650;

Стефанов Т., 1991, Руднична аерология, София, Техника (Stefanov T., 1991, Rudnichna aerologija, Sofia, Technika).

Кертиков В., Ив. Велчев, 1995. Ръководство за руднични вентилационни измервания, МГУ, София. (Kertikov V., Iv. Velchev, 1995. Rukovodstvo za rudnichni ventilacionni izmervanija, MGU–Sofia).

Кертиков В., 1996. Проектиране и оценка на местни вентилац;ионни системи, сп. Минно дело, бр. 4. (Kertikov V., 1996. Proektirane i ocenka na mestni ventilacionni sistemi, sp. Minno delo, br. 4).

Правилник по безопасността на труда в подземните въглищтни рудници, 1992, В-01-01-01, София. (Pravilnik po bezopasnostta na truda v podzemnite vuglishtni rudnici, 1992. B-01-01-01, Sofia, ISBN 954-8162-03-2).

Правилник по безопасността на труда при разработване на рудни и нерудни находища по подземен начин, 1971. В-01-02-04, Техника, София. (Pravilnik po bezopasnostta na truda pri razrabotvane na rudni I nerudni nahodishta po podzemen nacin, (1971), B-01-02-04, Tehnika, Sofia).

This article was reviewed by Prof. Dr. Veliko Kertikov and Assoc. Prof. Dr. Elena Vlasseva.

AN INNOVATIVE TECHNOLOGY FOR CREATING AN ORTHOPHOTOPLAN

Veselina Gospodinova[1], Petar Georgiev[2]

[1] University of Mining and Geology "St. Ivan Rilski", 1700 Sofia, e-mail: veselina_gospodinova80@abv.bg
[2] University of Mining and Geology "St. Ivan Rilski", 1700 Sofia, e-mail: georgiev.peter1@gmail.com

ABSTRACT. The façade of the building of the Department of Physical Culture and Sports at the University of Mining and Geology "St. Ivan Rilski" was captured with a mobile phone (a smasrtphone using the Android OS). The main aim of the study was to create a model and also an orthophotoplan. The photos were photogrammetrically processed with the Russian software Agisoft Photo Scan. The results obtained were analyzed.

Keywords: close-range photogrammetry, digital photogrammetry, low-cost photogrammetric techniques

ИНОВАТИВНА ТЕХНОЛОГИЯ ЗА СЪЗДАВАНЕ НА ОРТОФОТОПЛАН

Веселина Господинова[1], Петър Георгиев[2]
[1] Минно-геоложки университет "Св. Иван Рилски", 1700 София, E-mail veselina_gospodinova80@abv.bg
[2] Минно-геоложки университет "Св. Иван Рилски", 1700 София, E-mail: georgiev.peter1@gmail.com

РЕЗЮМЕ. Реализирано е заснемане на фасадата на сградата към катедра „Физкултура и спорт" на МГУ „Св. Иван Рилски" чрез мобилен телефон, тип смартфон с операционна система Android. Основната цел беше да се създаде модел, а също и ортофотоплан. Фотограметричната обработка на снимките е извършена в програмната среда на руският софтуер Agisoft Photo Scan. Получените резултати са анализирани.

Ключови думи: близкообхватна фотограметрия, цифрова фотограметрия, ниско струващи фотограметрични техники

1. Introduction

Technologies are evolving every hour, minute and second, and this leads to the appearance of increasingly sophisticated tools, instruments and devices which find usage not only in our lifestyles but in almost all spheres of our life. The creation of more and more simplified processing software allows us to save time and resources. It also provides us with the convenience of working and obtaining final products with the necessary precision and details. These two conditions predetermine the development of contemporary photogrammetry, namely digital photogrammetry.

Digital presentation and archiving of buildings requires simultaneous application of close-range photogrammetry, digital photogrammetry and image processing techniques. The main task that needs to be solved is the photometric and geometric reliability between the object and the model (Marinov, 2008**)**.

Close range photogrammetry is applicable in creating 3D models and object surfaces. Since some aerial and satellite pictures are not readily available, digital cameras are a good alternative. The cheaper equipment and high precision are the basic prerequisites for its development. The high resolution and instant availability of the photos make the method particularly suitable for generating digital models and orthophotomaps of different objects with the required precision. Therefore, it can be concluded that close-range photogrammetry has low cost and is suitable for creating a photorealistic 3D object models. This is evidenced by a number of studies related to the use of digital close-up photogrammetry (Marinov and Hristova, 2001; Marinov, 2008; Draganova et al., 2004; Ramos et al., 2015).

There are also studies aimed at exploring the capabilities of close-range digital photogrammetry compared to other methods. The author Paul Koppel has conducted an experiment to determine whether photogrammetry is an alternative to Earth's laser scanning. It analyzes spatial differences between a test object (a model obtained by capturing a CANON EOS 6D digital camera and processed by Agisoft PhotoScan), and the randomly arranged control points measured with a non-reflex (laser) total station. Analysis of the results of the accuracy assessment is compared with the Cloud Compare software and shows that it is possible to achieve identical accuracy using the Agisoft Photo Scan digital imaging software (http://www.agisoft.com/pdf/articles/Paul_Koppel_Agisoft-PhotoScan_case_study_01.pdf).

Other studies confirm the capabilities of the Agisoft PhotoScan software for photogrammetric applications (Waas and Zell, 2013; G. Plets et al., 2012).

But can we capture with a smartphone and what results will be obtained?

2. Materials and methods

Digital close-range photogrammetry is a method for accurately measuring objects directly from photographs or digital images taken with a camera in a close range of no more than 300m.

The photographic design techniques are based on the basic relationships between the object and its image, i.e. the properties of the central projection. If the projected beam is restored with the inner orientation elements of the image, the construction of the image in perspective can be done using a plan or facade. For this purpose, two coordinate systems are formed (x, z) with the starting point of the image O and a modular spatial coordinate system in which the y-axis is identical to the shooting direction, where X and Y are parallel to the picture coordinates. And there is an S start in the camera's lens on the shooting station (http://w3.uacg.bg/UACEG_ site/fge/Disc/lek_ph_II/pdf/p2_7-8.pdf)

The determination of photogrammetric coordinates is based on the collinearity equation, which states that the point of the object, the center of the projection center of the camera, and the point in the image lie on one line. Determining spatial coordinates (3D) from a certain point is achieved by intersecting two or more straight lines. Therefore, each point should appear in at least two images (Kraus, K., 1992).

The multiple of overlapping images captured by different stations generate measurements that can be used to create accurate 3D object models (Cooper and Robson, 1996).

2.1. Object information and shooting

The study object is the façade (frontage) of the building of the Department of Physical Education and Sports which is part of the University of Mining and Geology "St. Ivan Rilski" in Sofia.

For the present study, we used a smartphone of the brand of Samsung Galaxy S5 SM – G 900F with 16 Mpix, focal length of 4.8 mm, and ISO (the sensitivity of the camera sensor to light) 100 and under 100. The capturing was executed on two levels corresponding to approximately the heights of 1.70m and 4m. The smartphone was attached on a lathe and a program called “Timer Camera” was used, which allows shooting at certain intervals - in this case, 15 seconds - with an approximate base of 1.5 m.

12 control points (for assessing the accuracy of the recovery/ resulting model) and 2 reference points (points 29 and 28 are used for set a reference system) were uniformly distributed and marked onto the object. The positioning scheme of the points can be seen in figure 1.

Fig. 1. Scheme of the distribution of points

All marks are automatically recognized by the software. Figure 2 presents the type of two of the marks that were used for signaling in the present study.

1 2

Fig. 2. The type of two marks used for signaling

The control points were precisely measured with a total station - Trimble S6. The multifunctional and flexible total station is with servodrive, allowing the movable mechanical parts of the tool to move with little resistance. The Trimble DR Plus ™ technology allows an extremely wide range and accuracy of measurement to any surface and requires fewer stations and easier access to hard-to-reach objects, saving time and resources (http://www.solitech.bg/trimble-s6.html).

The capture was executed in a local coordinate system i.e. the total station has random relative coordinates (in this case, X = 2000 m, Y= 1000 m, Z= 500 m). After that they were reduced for convenience. The direction of axis Y was chosen

to start from p.29 as it would be the beginning of the local coordinate system (x29 = y29 = z29 = 0) of the model. The second reference point in case 28 was also carefully selected in order to calculate the rotation angle, in this case **α** = 20ᵍ.0660. Figure 3 shows a scheme of the location of the total station relative to the building façade, and in table 1 – the data from the shooting and calculated rotated local coordinates.

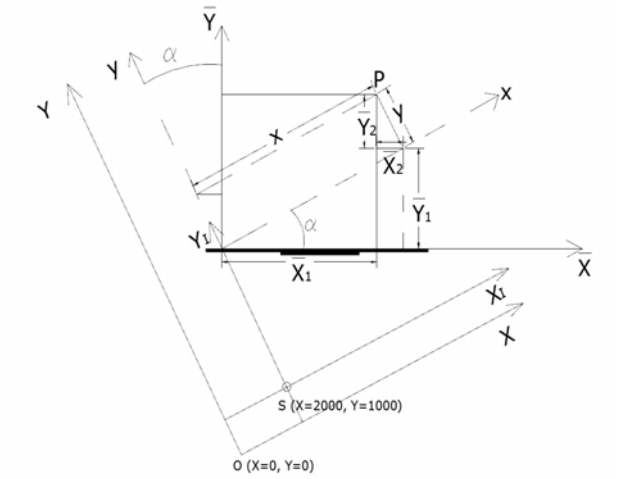

Fig. 3. Scheme of the position and orientation of the total station relative to the building façade

Table 1

Точка №	Относителни координати (m)			Локални координати (m)			20.06600	Завъртени локални координати (m)		
	X	Y	Z	x	y	z	0.310003	x'	y'	z'
29	0.000	26.477	1.890	0	0	0	0.950736	0	0	0
28	34.812	15.126	1.961	34.812	-11.351	0.071		36.616	0.000	0.071
25	-5.523	28.343	1.917	-5.523	1.866	0.027		-5.829	0.062	0.027
27	5.775	25.296	0.315	5.775	-1.181	-1.575		5.857	0.667	-1.575
30	14.608	18.668	2.330	14.608	-7.809	0.440		16.309	-2.896	0.440
31	21.740	16.313	2.133	21.740	-10.164	0.243		23.820	-2.924	0.243
32	18.750	16.860	1.933	18.750	-9.617	0.043		20.808	-3.331	0.043
33	12.626	19.324	1.395	12.626	-7.153	-0.495		14.221	-2.887	-0.495
34	11.062	19.840	3.107	11.062	-6.637	1.217		12.575	-2.881	1.217
35	11.050	19.843	1.382	11.050	-6.634	-0.508		12.562	-2.882	-0.508
100	1.612	26.374	6.895	1.612	-0.103	5.005		1.565	0.402	5.005
101	33.240	16.023	6.930	33.240	-10.454	5.040		34.843	0.366	5.040
102	40.682	13.294	2.703	40.682	-13.183	0.813		42.765	0.078	0.813
103	-5.906	28.544	2.173	-5.906	2.067	0.283		-6.256	0.134	0.283

2.2. Photogrammetric processing

The software "Agisoft – PhotoScan Professional Edition" was used for the photogrammetric image processing. It is a stand-alone software product that performs photogrammetric processing of digital images and generates 3D spatial data. This data can be used in GIS applications, cultural heritage documentation, and visual effects production, as well as for indirect measurements of objects of various scales (http://www.agisoft.com).

2.2.1. Creating a project and generating a block

The project creation involves assigning a project name and the path of the directory where the work files will be stored. For the current experiment, 636 photos were reviewed and those which were redundant or erroneously selected were deleted from the project. 413 photos were used for processing at a maximum distance of 25 m from the subject of shooting. During project creation, the coordinates of the control points were also introduced. A scheme of the block's illustration, in two planes xz and xy, can be seen in Figure 4 and Figure 5.

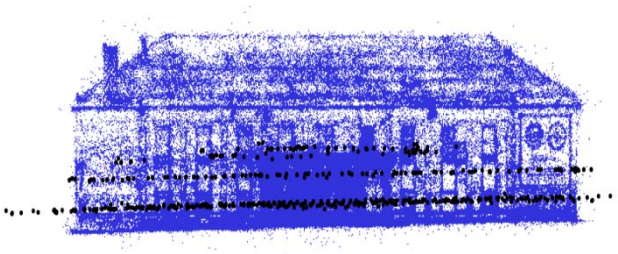

Fig. 4. Scheme of the block in the plane xz

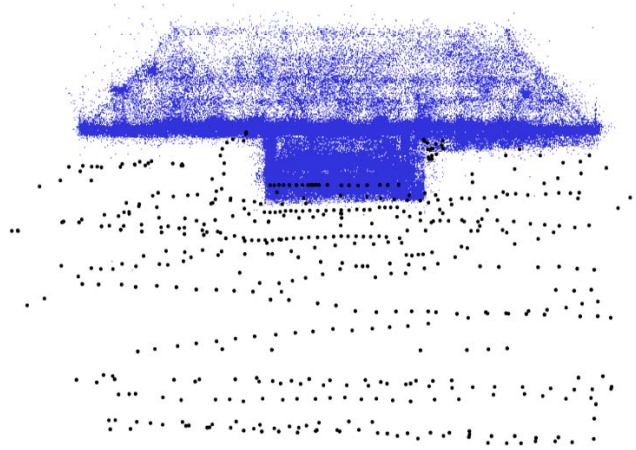

Fig. 5. Scheme of the block in the plane xy

2.2.2. Recognizing control points, performing alignment and then optimization

Once the block was created, each control point was recognized in all the photos where the point existed.. Parameters for the adjustment were set: process precision (the desired accuracy of the alignment) - in this case high, maximum number of points to be compared parallel in each picture - 50, 000, mask usage - a background elimination procedure was applied to some of the photos. Then, processing was performed, followed by optimization. Calibration with this software is done during processing by using the following parameters: fx, fy, cx, cy, skew, k1-k3, p1, p2. For the investigated object, the mean square error (absolute precision of the model) obtained after the alignment was about 1cm (6.7mm), which is shown in Figure 6.

Markers	X (m)	Y (m)	Z (m)	Accuracy (m)	Error (m)	Projections	Error (pix)
point 100	1.565000	0.402000	5.005000	0.005000	0.008065	91	1.170
point 101	34.843000	0.366000	5.040000	0.005000	0.011821	98	1.146
target 34	12.574526	-2.880781	1.217000	0.005000	0.004019	78	1.103
target 27	5.856612	0.667447	-1.575000	0.005000	0.007877	80	0.989
point 102	42.764594	0.077986	0.813000	0.005000	0.006914	76	0.882
target 30	16.309158	-2.895774	0.440000	0.005000	0.004430	106	0.868
target 32	20.807590	-3.330672	0.043000	0.005000	0.005238	111	0.867
target 29	0.000000	0.000000	0.000000	0.005000	0.005274	79	0.858
target 35	12.562187	-2.881649	-0.508000	0.005000	0.004382	76	0.810
target 33	14.221438	-2.886517	-0.495000	0.005000	0.003346	95	0.762
target 31	23.819861	-2.923816	0.243000	0.005000	0.006134	80	0.756
target 28	36.615851	0.000000	0.071000	0.005000	0.006125	55	0.741
point 103	-6.255820	0.134294	0.283000	0.005000	0.005031	47	0.670
target 25	-5.829378	0.061927	0.027000	0.005000	0.009130	37	0.564
Total Error					0.006654		0.911

Fig. 6. The result obtained after the photo alignment

2.3.3. Generation Dense Point Cloud, Triangulated Irregular Network (TIN), Digital Surface Model (DSM), and orthophoto

Generation and visualization of 3D vector points, or the so-called Dense Point Cloud, are used for building a Digital Surface Model and orthophoto and are realized after finishing the Photo Align process. The parameters which were used at this stage of processing were medium quality and mild filtering. In the present study, the generated Dense Point Cloud included 8, 549, 412 points and can be seen in Figure 7.

Fig. 7. The result obtained after the photo alignment

After the cloud of points has been created, it goes to the automated generation of a Triangulated Irregular Network (TIN), from which a digital surface model is obtained later. In the program „PhotoScan", this processing is fully automated by pre-setting the following parameters: surface type - arbitrary, source data for determining an Triangulated Irregular Network - Dense Cloud of Points, maximum number of polygons, which to participate in forming the network – high. A fragment of the network can be seen in figure 8.

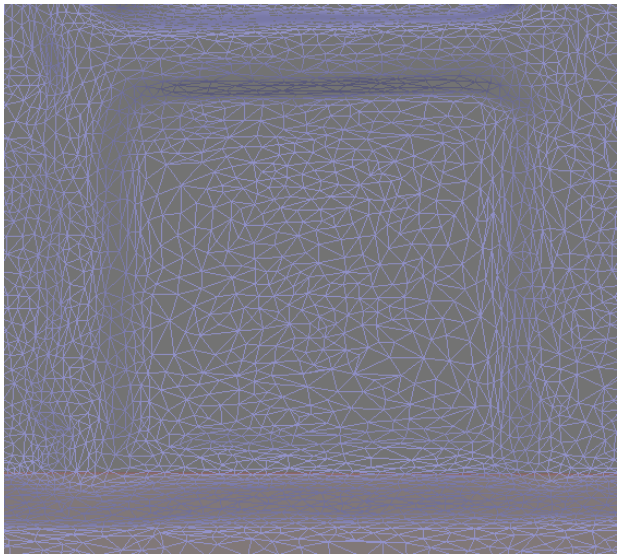

Fig. 8. A fragment of an irregular triangular network

One of the main tasks for photogrammetric software is to generate a digital surface model. It is based on image matching and autocorrelation algorithms. The automatically generated digital surface model can be seen in figure 9. Fig. 10 shows the final product, the orthophotoplan.

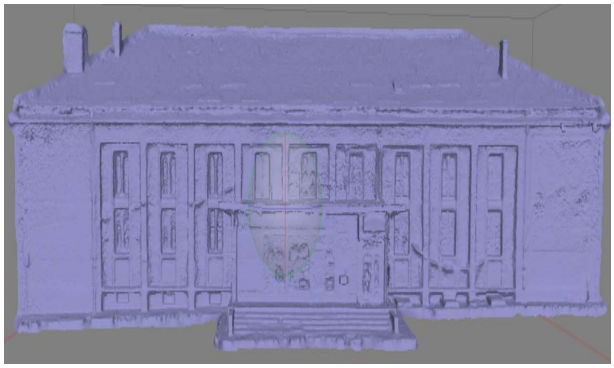

Fig. 9. The generated digital surface model

Fig. 10. The orthophotoplan of the façade of the building of the Department of Physical Education and Sports in M 1: 500

Some areas of the orthophoto plan have lighter areas, due to the use of .jpg, not a row format. In future, efforts should be directed to eliminating such areas by implementing procedures to improve the radiometric and color characteristics of images, and using a higher-class smartphone that not only supports row format, but also good optics and quality matrix.

The average arithmetic error obtained as the difference between the spatial coordinates measured with the total station and the orthophoto plan is in the order of 1 cm.

3. Conclusion

The obtained results suggest that the presented methodology for generating a building façade model and an orthophoto using a mobile smartphone can be used to create digital models, orthophoto plans of buildings and other objects, and to process monitoring. It can also be used to solve tasks of a different nature. The deficiency of the methodology is in the presence of vegetation in front of or close to the objects of capture: plants interfere with visibility and this gives rise to erroneous geometry. Another disadvantage is related to the parameters of the used hardware: high-end systems with a good configuration of the parameters are required for processing such digital images.

The proposed method for capturing different objects and processes, near which there is no vegetation, is a desirable method because it guarantees flexibility, accuracy and safety. The plant obstacle could be avoided if colored RGB sensors are used together with sensing sensors for other ranges of the electromagnetic spectrum, for example the infrared range.

The economic aspect is also one of the leading points because the cost of images taken from satellites and pilot or non-pilot airplanes is significantly higher than the cost of images from mobile devices.

The digital images obtained with the appropriately selected software can be used for creating accurate orthophoto plans and digital models of objects for most engineering and geomorphological projects. They can find their application among all the methods used so far in the practice.

A further sphere of interest for the researchers would be their application in mine surveying and geological purposes related not only to modeling and volume calculation, but also to determining the tectonic crack of rock masses and other tasks, such as underground extraction - why not?

References

Маринов, Б., Г. Христова. Цифрова фотограметрична технология за документиране на архитектурни обекти. Сб. доклади на Международния симпозиум "Геодезически, фотограметрични и спътникови технологии – развитие и интегрирано приложение", София, 2001, - 187-198. (Marinov, B., G. Hristova. Tsifrova fotogrametrichna tehnologiya za dokumentirane na arhitekturni obekti. Sb. dokladi na Mezhdunarodniya Simpozium: "Geodezicheski, fotogrametrichni i sputnikovi tehnologii – razvitie i integrirano prilozhenie", Sofia, 2001, - 187-198.)

Cooper, M., S. Robson, Theory of Close Range Photogrammetry. Close Range Photogrammetry and Machine Vision, 1996, - 9-51.

Draganova, N., G.Hristova, B. Marinov. Digital Photogrammetry at Graduated Study in UACEG. IAPRS (of XX Congress of ISPRS), vol. XXXV, part B6, Istanbul, 2004, - 46-51.

Kraus, K. Photogrammetry, Fundamentals and Standard Processes, Vol. I, Fourth Revised and Enlarged Ed., Dümmler, Bonn. 1992.

Marinov, B. Hierarchical Modelling and Processing of Space Objects in Architectural Photogrammetry. In: International Archives of the Photogrammetry, Remote Sensing and Spatial Information Sciences, Beijing, China, vol. XXXVII, Part B5/WG5-2, ISSN 1682-1750, 2008. - 401-407.

Plets, G., G. Verhoeven, D. Cheremisin, R. Plets, J. Bourgeois, B. Stichelbaut, W. Gheyle, J. De Reu. The deteriorating preservation of the Altai rock art: Assessing three-dimensional image – based modelling in rock art research and management. Rock Art Research, vol 29, Number 2, 2012, - 000-000.

Ramos, A., G. Prieto. 3D virtualization by close range photogrammetry of indoor gothic church apses. The case study of the Church of San Francisco in Betanzos (La Coruña, Spain) In: International Archives of the Photogrammetry, Remote Sensing and Spatial Information Sciences, Avila, Spain vol. XL-5/W4, 2015. - 401-407.

Waas, M., D. Zell. Practical 3D photogrammetry for the conservation and documentation of Cultural Heritage. International Conference on Cultural Heritage and New Technologies, Vienna, 2013.

Agisoft LLC. Official website. Saint Petersbourg, Russia. http://www.agisoft.com (accessed July 2017).

http://www.solitech.bg/trimble-s6.html (accessed July 2017).

http://www.agisoft.com/pdf/articles/Paul_Koppel_Agisoft-PhotoScan_case_study_01.pdf (accessed July 2017).

http://w3.uacg.bg/UACEG_site/fge/Disc/lek_ph_II/pdf/p2_7-8.pdf (accessed July 2017).

This article was reviewed by Prof. Dr. B. Marinov and Assist. Prof. Dr. N. Aleksandrova.

MONITORING OF THE CARBON DIOXIDE CONCENTRATION AND TEMPERATURE OF THE INDOOR ATMOSPHERE IN A LECTURE HALL WITH NATURAL VENTILATION

Kalinka Velichkova[1], Plamen Savov[1], Maya Vatzkitcheva[1]

[1]University of Mining and Geology "St. Ivan Rilski", 1700 Sofia
E-mail: k.velichkova@mgu.bg, psavov@mgu.bg, mayavack@gmail.com

ABSTRACT. One of the main indoor air pollutants and a key parameter in assessing indoor air quality is carbon dioxide (CO_e). Increasing its concentration over time causes discomfort and worsens the quality of the occupants' work. In the particular case of school premises - classrooms and lecture halls, the increased CO_2 content, which is two and sometimes more times than the accepted norm (400 ppm - 1200 ppm), adversely affects the concentration (sharpness) of the attention and mental work of the students and the teacher (lecturer). This, in turn, affects the degree of perception of the content taught and the extent of learning at the moment.
To provide and maintain an acceptable level of CO_2 concentration in the indoor air of the classrooms, it is necessary to ensure continuous or periodical air ventilation.
In our previous research the results of the study of spatial distribution of carbon dioxide concentration and temperature in a lecture hall with a volume of about 300 m^3 with natural ventilation were analyzed and the evolution of the two parameters in dependence on the occupancy of the hall and the intensity of natural ventilation was traced. The experiment was held in late spring (May - June).
The present paper repors the results of the study of the distribution of the air temperature and CO_2 concentration in the same lecture hall but in the heating season(January), when central heating is used.

Keywords: Carbon dioxide, indoor air quality, natural ventilation

МОНИТОРИНГ НА КОНЦЕНТРАЦИЯТА НА ВЪГЛЕРОДНИЯ ДИОКСИД И ТЕМПЕРАТУРАТА В АТМОСФЕРАТА НА ЛЕКЦИОННА ЗАЛА С ЕСТЕСТВЕНА ВЕНТИЛАЦИЯ

Калинка Величкова[1], Пламен Савов[1], Майя Вацкичева[1]

[1]Минно-геоложки университет "Св. Иван Рилски", 1700 София
E-mail: k.velichkova@mgu.bg, psavov@mgu.bg, mayavack@gmail.com

РЕЗЮМЕ. Един от главните замърсители на въздуха в помещение и основен параметър при оценяване на качеството на въздуха е въглеродният диоксид (CO_2). Увеличаването на концентрацията му във времето причинява дискомфорт и влошава качеството на работа на обитателите. В частния случай на учебни помещения - класни стаи и лекционни зали, повишеното съдържание на CO_2 два, а понякога и повече пъти над приетата норма (400 ppm - 1200 ppm), влияе неблагоприятно върху концентрацията (остротата) на вниманието и умствената работа на обучаваните и преподавателя. Това, от своя страна, рефлектира върху степента на възприемане на преподавания материал и дълбочината на усвояването му в момента.
За да се осигури и поддържа приемливо ниво на концентрацията на CO_2 във вътрешния въздух на учебните зали, е необходимо да бъде осъществявана постоянно или периодично вентилация на въздуха.
В предишна наша работа бяха анализирани резултатите от изследването на пространственото разпределение на концентрацията на въглеродния диоксид и температурата в учебна зала с обем около 300 m3 с естествена вентилация. Бе проследена еволюцията на тези параметри в зависимост от заетостта на залата и интензивността на естественото проветряване. Експериментът беше проведен в късна пролет (май - юни).
В настоящата работа са докладвани резултатите от измерването на разпределението на температурата на въздуха и концентрация на CO_2 в същата лекционна зала, но в зимния сезон (месец януари), като за отоплението й се използва парно.

Ключови думи: Въглероден диоксид, качество на въздуха във вътрешна среда, естествена вентилация

Introduction

The main purpose of educational institutions - schools and universities - is the learners to acquire a certain amount of theoretical content to master skills and gain experience to analyze practical problems, make decisions on how to apply their theoretical knowledge and successfully solve them. The prolonged stay in the premises leads to enrichment of the indoor air with carbon dioxide (CO_2). The main reason for the increase in CO_2 is the breathing of the inhabitants themselves (students and people in the hall) during the class hours. CO_2 content in the air exhaled from a human is about 4-5.6%, which is about 100-140 times more than that in the environment – 0.04% (Kapalo et al., 2014).

Indoor air quality is defined as required per person fresh and pleasant air that is not harmful to their health and has a positive impact, stimulates their work and increases their performance and productivity (Fanger, 2006). A number of studies devoted to the indoor air quality on human health have shown a clear connection between polluted air and the quality of activities that workers perform in this environment (Clements-Croome, 2004; Demianiuk et. al., 2010; Satish et al., 2012).

Requirements for energy efficient buildings with a view to reduce energy consumption and associated costs minimize the natural airflow through infiltration. In order to regulate the temperature and cleanliness of the air in the rooms, there

should be a possibility for their additional controlled ventilation. In most educational institutions, this is done by natural ventilation, as the occupants themselves regulate the thermal conditions by periodically opening the windows of the room.

Velichkova et al. (2016) investigated the quality of the indoor atmosphere, predominantly the CO_2 concentration, of a lecture hall at the University of Mining and Geology during the spring-summer season (May, June), where it was found that natural ventilation can provide the necessary conditions for the learning process, as long as the occupant density of the hall does not exceed 0.15 m^{-3}. However, the intensity and duration of natural ventilation under winter conditions, are rather limited due to the need of creation of thermal comfort for the occupants. The question arises whether natural ventilation is a good enough way to ensure the right conditions - temperature and air purity - in the lecture halls during this season.

The aim of this study is to analyze the air quality in a lecture hall during the winter season and to assess the effectiveness of natural ventilation (by means of window operation) in controlling hall thermal conditions and indoor air quality.

Experiment

Lecturer hall

The experiments were carried out in the 346 lecture hall at the Department of Geological Prospecting at the University of Mining and Geology "St. Ivan Rilski". The location of the hall is shown on Fig. 1.

Fig. 1. A view to 346 lecture hall at the department of Geological Prospecting at the University of Mining and Geology "St. Ivan Rilski"

The hall is located on the third floor, it is oriented to the northeast, with its windows facing the courtyard of the University, with forest vegetation.

Its dimensions are: width of 8.20 m, length of 13.50 m, height at the place of the lecturer desk of 3.40 m and height at the opposite edge of the hall of 2.10 m. The floor has a displacement of 1.30 m. The room space is 304 m^3. There are 8 windows, each with an openable area of 1.2x1.2 m^2. The diagram of the room with the points for measuring the temperature (points from 1 to 6) and the concentration of carbon dioxide (point 4 and point 6) is shown in Fig.2.

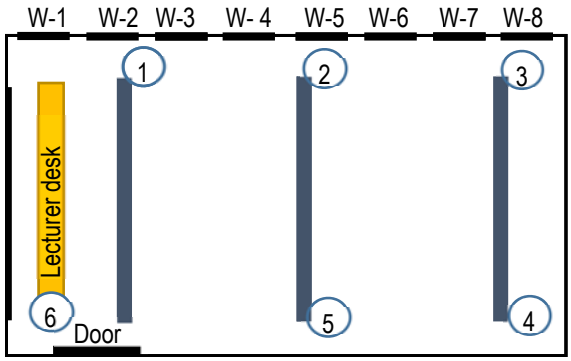

Fig. 2. A scheme of 346 lecture hall: W-1 – W-8 are the windows, 1, 2, 3, 4, 5, 6 are the measurement points. For visibility only the first, medium (the ninth) and the last school decks are shown

Used appliances

The dynamic (time dependence) characteristics of the CO_2 concentration and temperature were determined at p.4 and p.6 (Fig. 2) by a portable air-logger analyzer TROTEC BZ30. The device simultaneously measures and records the CO_2 concentration (0 ÷ 9999 ppm, with accuracy of ± 5 %), the temperature T (-5 ÷+50°C, with accuracy of ±0.1°C) and the relative humidity RH (0.1÷99.9 %, ±0.1%). The concentration of carbon dioxide was obtained by averaging over the measurements, recorded in 1 minute time interval.

The temperature and its behavior over time was also measured in points 1, 2, 3, 5 by Thermo-data logger.

Only in point 6 and when the hall was empty the temperature was measured at three different heights (levels): 0 m - floor level, 1 m and 2 m.

Conditions of the experiments

The measurements were made at a height of 85 cm above the floor of the room (the level of the exhaled air of the present - respiratory zone). The reasons for this choice were described in Velichkova et al. (2016).

The experiments were conducted during the same time interval 14-16:30 h on three dates: on January 26, 2017, during an exam, with 15 occupants in the hall; on January 30, 2017, during a lecture, with 26 occupants and on February 1, 2017 during a lecture, with 13 students in the room. The ambient air temperature was T=-3 ÷1°C.

The experiments were conducted as follows: the hall was ventilated after the previous class, when empty, by opening the eighth window, then the window was closed and the class (lecture or exam) started. The hall was not ventilated for a while. After that, the room was aired again by reopening the eighth window for the experiments on 26th and 30th January and also the door for the experiment on 1st February. For that time interval the dynamic characteristics (i.e. the time dependent changes of these quantities) of the CO_2 concentration and temperature T were recorded in p.4 and p.6.

Students' activity is as follow: on 26th January, an exam (presentations), on 30th January – lecture, and on 1st February - lecture. In all cases, students were unevenly seated in the

room (and took their places) mainly in the front half of the hall, near and slightly below the average desk where were the points of measurements 2 and 5 (Fig. 2). Briefly, the conditions (regimes) of the experiment are as follows:

- Regime M0, the hall was empty and it had been ventilated by opening the last (W-8) window;
- Regime M1, the hall was empty and it had not been ventilated;
- Regime M2, the hall was occupied and it had not been ventilated;
- Regime M3, the hall was occupied and it had been ventilated by opening W-8;
- Regime M4, the hall was occupied and it had been ventilated by opening W-8 and the door;
- Regime M5, the hall was occupied and it had been ventilated by opening W-1 and the door.

Processing the data

To analyze the experimental data, we have accepted that the air in the halls is homogeneous. The equation for the mass balance is

$$V\mathrm{d}C = G\,\mathrm{d}t + QC_{\mathrm{V}}\,\mathrm{d}t - QC\,\mathrm{d}t\,, \qquad (1)$$

where G is the rate of CO_2 generation which is a result of the respiration of the occupants, Q - volumetric airflow rate into (and out of) the space, i.e. it is the airflow exchanged with the outside environment for one second, V – hall space, C_V - the CO_2 concentration in inflow air, and C - the indoor air CO_2 concentration and respectively, CO_2 concentration in the outflow air.

When the hall was occupied and had not been ventilated (Q=0) and if accepted that the generation rate of CO_2 did not change with time depending factors, CO_2 concentration is a linear function of time –

$$C = C_0 + \frac{G}{V}t\,. \qquad (2)$$

C_0 in Eq. (2) is the room CO_2 concentration in the beginning of the experiment.

When the hall has been ventilated ($Q \neq 0$), the carbon dioxide concentration will change exponentially over time

$$C = C_V + \frac{G}{Q} - \left(C_V + \frac{G}{Q} - C_0\right)e^{-\frac{Q}{V}t}\,. \qquad (3)$$

Approximating experimental data in regime M2 with Eq. (2), the rate of CO_2 generation G could be estimated, and in regimes M0, M3, M4 and M5 with Eq. (3) - the airflow rate Q.

Results and discussion

The temperature profile in height (Fig. 3) when a lecture hall is empty (regime M1) indicates that it is stably stratified.

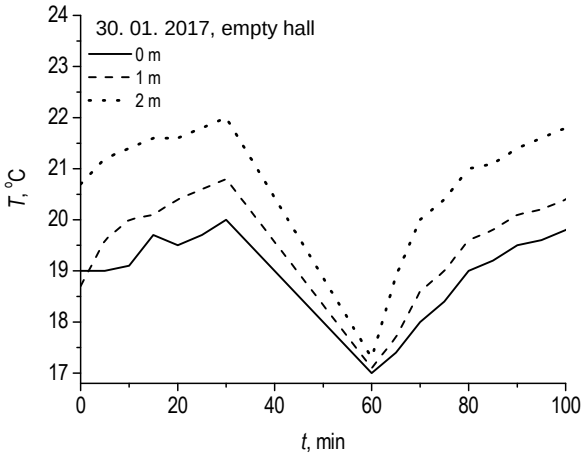

Fig. 3. Stratification of temperature

It can be seen on the figure that in regime M1 the temperature increases with 2.3°C with the increase of the height . Its gradient also grows up with 0.3 K/m. Natural ventilation for 30 minutes by opening W-8 (regime M0) results in a drop of the temperature from about 3°C at the level of the floor to 5°C at 2 m height. At the end of the regime M0 the temperature at the three levels reaches about 17°C, while maintaining its stratification. After shutting down the ventilation (regime M1), the temperature rises twice as fast and 5 minutes later it reaches 2/3 of its maximum value. Then it increases slowly (during 35 minutes) to its previous values still maintaining the stratification

The measurements of the temperature and CO_2 concentration for the three dates show that after the initial ventilation (regime M0), the temperature in the upper inner part of the room (p.4) was higher in comparison with the temperature at the lecturer desk - the lowest inner part of the room (p.6). The difference might range from 0,5–1,5°C depending on the way and the duration of ventilation. When the room was occupied by students located in its front half (as was the case on 26th Jan and 1st Feb), the temperature increase is the same for both points and it is not dependent on the room displacement. On these days the number of students was 13-15 and the respective occupant density of the hall was 0,043 - 0,050 m^{-3}. When the density of occupancy was almost 2 times higher (0,086 m^{-3}, with 26 people on 30th Jan), the temperature in the upper part of the room (p.4) increased by about 1°C, while at its bottom (p.6) it remained almost unchanged.

As expected, the number of students affected the change in CO_2 concentration in the hall as the rate at which it grew was proportional to the number of occupants. Carbon dioxide concentration reached its highest value (1250 ppm) when the number of students in the hall was the biggest (26 students). This fact confirms the result obtained in (Velichkova et al., 2016) that the only source of indoor air pollution with carbon dioxide is the human presence.

The dynamic characteristics of the temperature and CO_2 concentration in p.4 and p.6 were illustrated in Fig. 4 for 30th Jan and in Fig. 5 for 1st Feb. The experimental data for increase and decrease of CO_2 were approximated by Eq.(2) in

regime M2 and Eq.(3) in regimes M0, M3 - M5. The resulting values of CO_2 generation rate *G* and the airflow rate *Q*, are shown in Table 1. In the same table the values of *G* and *Q* obtained from the experiments during the spring-summer season in 2016 are also shown.

The dynamic characteristic of temperature (Fig. 4, left) shows that the changes in temperature in both measuring points in regime M0 are with the same speed, but the magnitude of this change is 1°C greater in the upper inner part of the room. After closing the window (regime M2) the temperature increases relatively slower in p.6 and 50 min later its value is about 1°C lower than the one in p.4. After subsequent ventilation by opening W-8 and the door (regime M4), the temperature decreases, but the rate of its reduction in p.4 now is more than twice as high as the one in p.6. The observed behavior of the temperature could be explained by taking into account the circulation due to the higher temperature of the air exhaled by the students in the respiratory area (around the middle of the room) and the additional circulation that appeared at opening the door, because of the temperature difference between the room and the corridor - about 2 - 3°C.

The described temperature behavior reflects on the dynamic behavior of the CO_2 concentration (Fig. 4, right). It can be seen that the concentration grows up at a higher speed in the upper inner part of the hall p.4, reaching a value of 150 ppm higher than the one in p.6. The air circulation caused by its additional heating in the respiratory area where the CO_2 content is greater might explain such behavior of the dynamic characteristics and respectively the higher value of the generation rate in p.4, although there were no students in this part of the hall.

The fact that the door was also opened at next ventilation resulted in a slightly higher flow rate (see Table 1) and better ventilation, respectively, so that the CO_2 concentration reached the external level - about 400 ppm, (Fig. 4, right).

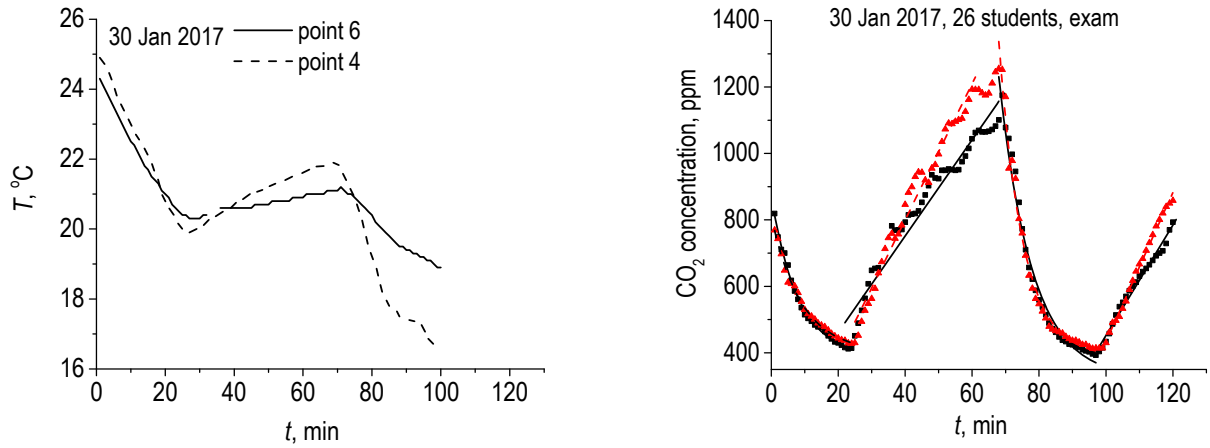

Fig.4.Dynamic characteristics of the temperature (left-hand) and the concentration of CO_2 (right hand), measured at p.4 (▲) and p.6 (■). The lines were obtained by approximation of the experimental data for p.6 (solid line) and p.4 (dashed line) with Eq.(2) for regime M2 and Eq.(3) for regimes M0 and M4

The experiments on 26th Jan and 1st Feb, when the occupants' density of the room is half (0,043-0,050 m^{-3}) compared to 30th Jan (0.086 m^{-3}), show an adequate change in the growth of CO_2 concentration. In both cases, the increase of the temperature in regime M2 (without ventilation) is at approximately the same rate for the two measuring points, and the values of the CO_2 concentration recorded in the upper internal part of the room (p.4) and in the lower internal part of the hall p.6 are practically the same. This fact indicates that as a result of the air circulation when the number of people was smaller, the air temperature and the CO_2 content were uniformly distributed in the hall volume. The temperature in the upper inner part remains higher than in the lower though with only 0.5°C. . This temperature difference observed in all experiments caused the greater amount of fresh air to move around the windows where the temperature gradient is higher.

The lower value of the generation rate derived from the approximation of the data from 26th Jan experiment might be due to the fact that part of the students were leaving the room and there was practically an unpredicted growth of the ventilation when the door was opening. The situation on the 1st Feb experiment was similar, when a little after the beginning of the classes, CO_2 started to increase rapidly, leading to *G* = 173 ml/(min.p) in p.4 and G = 242 ml/ (min.p) in p.6. These values are similar to the ones obtained from the experiments on the other two dates. Shortly after the start of the classes, the door could not be well closed, which reflected the rate of the CO_2 concentration increase. Since we do not have enough data to correctly account for the air flowing through the door (perhaps not very large due to the slight difference between the room and corridor temperatures), we could not calculate correctly the values of *G*. But this could create additional ventilation that might explain the change observed in the increase of CO_2 concentration.

Unlike the initial room airing by W-8 (regime M0, 1st Feb), when the class ends additional ventilation is going through W-1 and the door (regime M5). Then the temperature in p.6, located closest to the source of ventilation, drops by 3°C, while in p.4 - only by 1.2°C. What is interesting is that when the ventilation is done through the W-8 and the door (regime M4), the airflow rate at p.4 (with a higher temperature) was 45 % lower than that in p.6. In regime M5 (airing via W-1 and the door) - the airflow rate in p.4 is 67 % higher than the one in p.6. This difference is only 11-13% for the experiments of 26th and 30th Jan.

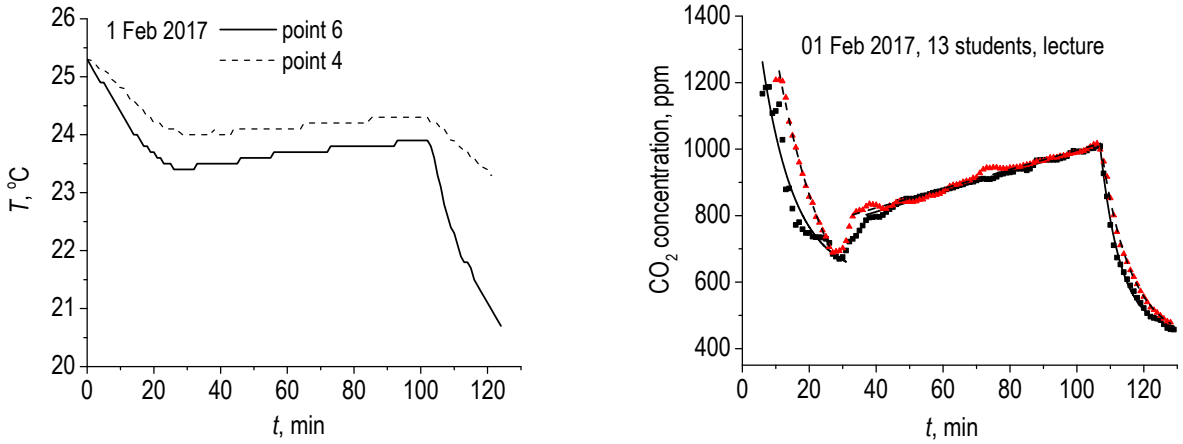

Fig. 5. Dynamic characteristics of the temperature (left-hand) and the concentration of CO_2 (right hand), measured at p.4 (▲) and p.6 (■). The lines were obtained by approximation of the experimental data for p.6 (solid line) and p.4 (dashed line) with Eq. (2) for regime M2 and Eq.(3) for regimes M0 and M5

Table 1

Experimental conditions and calculated by the graph parameters: rate of CO_2 generation G, airflow rate Q and specific airflow rate n, obtained during the summer season experiments 2016 and winter season experiments in 2017

Data		2016 r.		2017 g.					
		18 March	1 June	26 January		30 January		1 February	
activity		lecture	exam	exam		lecture		lecture	
Number of students		16	31	15→3		26		13	
Distribution		Irregular, more students were sitting in the front half of the hall	regular	Irregular, more students were sitting in the front half of the hall					
Occupant density, m^{-3}		0.053	0.103	0.050		0.086		0.043	
G, ml/(min.p), regime M2	point 4	-	-	240	204	232	227	242	
	point 6	153	188	229	78	167	199	173	
Q, ℓ/s	point 4	-	-	646		564	704	312	569
	point 6	417	847	750		626	624	606	340
$n = \frac{Q}{V}, \frac{(m^3/\min)}{m^3}$	point 4	-	-	0.129		0.113	0.141	0.062	0.114
	point 6	0.083	0.169	0.152		0.125	0.125	0.121	0.165
$\Delta C = C_{in} - C_{out}$,ppm		260	380	550		700		600	
				380		890		600	

In all cases it could be clearly seen, that the reduction of carbon dioxide is stronger at the location close to the opening at the lower temperature. This shows that the airflows which are refreshing the air in the process of ventilation depend mainly on the difference between outdoor and indoor temperatures which is almost the same for the three experiments and does not depend on the number of occupants and the CO_2 concentration in the room atmosphere.

Comparing data for 1st Feb and 26th Jan shows that change in CO_2 concentration for the experiments on 1st Feb is less than the one on 26th Jan (Table 1), although the number of students is almost the same (13-15 students). According to Lazović et al., 2015, the speed at which a person generates CO_2 depends on the duration and intensity of physical and mental activities as well as on the stress. In our previous experiment in case of a uniform distribution of the students in the lecture hall, with a high enough density, we received that *G*= 188 mℓ/(min.p). This value is very close to the value given by Dubrovskii, 2002). The *G* values received at data approximation in present experiments exceed those obtained by us in 2016 and also cited for normal mental activity. This is possible, taking in account the fact that during classes, each student presented their own project and after a discussion of their work, the lecturer assessed their knowledge - the way they defended their project and their activity in the discussion of their colleagues' projects. That increases the participants' stress (more possibly its duration).

This situation, similar to an exam, leads to increase of mental activity and undoubtedly causes some degree of stress. Higher *G* values in comparison with experiments in 2016 might also be interpreted as an indicator of more intense mental activity during the winter season than in spring - summer. Underestimation because of the though small ventilation by the opened door could explain the smaller *G* values.

The results from the experiments on all dates show that at given room occupancy and used ventilation regimes each student receives fresh air, much more (2.5-4.5 times) than the required one of 7÷10 ℓ/(s.p), according to the Bulgarian State Standard (BDS/EN 15251, 2007).

Conclusion

A necessary condition for a pleasant and effective work of the students during the learning process is to provide an indoor atmosphere of good quality in educational institutions. Our study shows that the natural ventilation in the considered lecture hall at usual occupancy density is perfectly suitable for this purpose even in winter conditions, as well. For that occupancy of the room and the ventilation regimes employed, each student has received a sufficient amount of fresh air which ensured good conditions for working and training.

It has been found that the way in which ventilation takes place depends on the location of the ventilation source and on the difference between outside and inside temperatures. Therefore, to determine which source of natural ventilation should be used without compromising students' thermal comfort, it should be taken in account which are the preferred seats in the hall.

The existence of a stable temperature stratification in the hall is established.

Having in mind the students' activities during the experiments, the higher values of the generation rate of carbon dioxide might be associated with activating their mental activity and the state of stress.

Acknowledgment

The authors are grateful to the Research Fund for the financial support through a contract SFRE02/19.

References

BDS/EN15251. Indoor environmental input parameters for design and assessment of energy performance of buildings addressing indoor air quality, thermal environment, lighting and acoustics for designing and assessing the energy performance of buildings, Ordinance № 15/28 July 2005 Ministry of Regional Development and Publicity and Ministry of Energy, Part 4, 2007.

Clements-Croome, D. Intelligent Buildings: Design, management and Operation, Thomas Telford, ISBN-10: 0727732668, London, 2004.

Demianiuk, A., Gladyszewska-Fiedoruk K., Gajewski A., Olow A. The changes of carbon dioxide concentration in a cinema auditorium. – Civil and environmental engineering, 1, 2010. – 105-110.

Dubrovskii, V.I. Sports medicine. M., Vlados, 2nd add., 2002. – 512 (in Russian).

Fanger P.O. What is IAQ. - Indoor Air, 16, 2006. - 328-334.

Kapalo, P, S. Vilčeková, F. Domnita, O. Voznyak. Determine a methodology for calculating the needed fresh air. – In: The 9th International Conference "Environmental Engineering". 22–23 May 2014, Vilnius, Lithuania, 2014. – 264. (Selected Papers, Article number: enviro.2014.264).

Lazović I., M. Jovašević-Stoqnović, M. Živković, V. Tasić, Ž. Stefanović. PM and CO_2 variability and relationship in different school environments. - Chem. Ind. Chem. Eng. Q., 21, 1, 2015. – 179-187.

Satish U., M. Mendell, K. Shekhar, T. Hotchi, D. Sullivan, S. Streufert, W. Fisk. Is CO_2 an indoor pollutant? Direct effects of low-to-moderate CO_2 concentrations on human decision-making performance. - Environ. Health Perspect., 120, 2012. – 1671-1677.

Velichkova, K., M. Vatzkitcheva, P. Savov. Indoor Carbon dioxide concentration of a lecture hall with natural ventilation. – Annual of the University of Mining and Geology "St. Ivan Rilski", 59, Part II, Mining and Mineral processing, 2016. – 72-78.

This article was reviewed by Prof. Dr. Stefan Dimovski and Assoc. Prof. Dr. Anatoli Angelov.

ANALYTICAL EXPRESSIONS FOR STRESSES IN A STEEPLY LAYERED ROCK MASS AROUND A CIRCULAR OPENING

Violeta Trifonova – Genova

University of Mining and Geology "St. Ivan Rilski", 1700 Sofia, violeta.trifonova@yahoo.com

ABSTRACT. The article discusses the question of determining stresses in a steeply stratified rock mass around a circular opening. The layers are homogenous, isotropic and parallel to one another and to the axis of the opening. The thickness of layers is significantly smaller than the dimension of the hole. The influence of stresses, due to the working driving, extends into a square area. The specified class of tasks is solved by the theory of elasticity and the mechanics of the layered media. A solution of a vertical shaft, crossing the horizontal layers, is known. The stresses in each layer are expressed by the stresses in a homogenous generalized field. The characteristics of each layer and thickness are included in their expressions.

A horizontal circular opening is driven in a rock, composed of two layers. The boundary between them is inclined towards the horizon. The areas of layers are calculated when the value of the inclination angle changes from zero to ninety degrees. They are compared to their respective values at a horizontal boundary. The deviation is large, when the slope exceeds a certain limit value. This fact requires derivation of new analytical formulas for stresses.

A popular approach for determining the stresses in each layer is applied. Two group relations are used in order to obtain them. The first expresses the condition of continuity of deformations in the plane of contact between the layers. The second group includes the equilibrium of forces, expressed by generalized stresses along the layers' areas. The generalized stresses are obtained using the theory of function of complex variable. New analytical expressions for stresses are obtained. These expressions involve the areas of layers around the opening. The presented solution complements the existing expressions for stresses in horizontal layers.

Keywords: stresses, theory of function of complex variable, opening, layered media

АНАЛИТИЧНИ ИЗРАЗИ ЗА НАПРЕЖЕНИЯТА В СТРЪМНО НАПЛАСТЕН МАСИВ ОКОЛО КРЪГОВА ИЗРАБОТКА

Виолета Трифонова – Генова

Минно-геоложки университет "Св. Иван Рилски", 1700 София, violeta.trifonova@yahoo.com

РЕЗЮМЕ. В статията се разглежда въпросът за определяне на напреженията в стръмно напластен масив около кръгова изработка. Пластовете са хомогенни, изотропни, успоредни помежду си и на оста на изработката. Дебелините на пластовете са значително по-малки от размерите на отвора. Влиянието на напреженията от прокарване на изработката се простира в квадратна област. Указаният клас задачи се решава с методите на теория на еластичността и на механика на напластените среди. Известно е решение за вертикална шахта, пресичаща хоризонтално разположени пластове. Напреженията във всеки пласт се изразяват чрез напреженията в еднородна обобщена среда. В техните изрази участват както характеристиките на всеки пласт така и дебелините.

Хоризонтална кръгова изработка е прокарана в масив, състоящ се от два пласта. Границата между тях е наклонена спрямо хоризонта. Изчислени са площите на пластовете, когато стойността на ъгъла на наклона варира от нула до деветдесет градуса. Те са сравнени със съответната им стойност при хоризонтална граница. Отклонението е голямо, когато наклона надвишава определена гранична стойност. Този факт изисква извеждане на нови изрази за напреженията.

Тук е приложен известен подход за определяне на напреженията във всеки стръмен пласт. За тяхното получаване се използват две групи връзки. Първата изразява условието за непрекъснатост на деформациите в равнината на контакта между пластовете. Втората група включва равновесие на усилията, изразени чрез обобщени напрежения по площите на пластовете. Обобщените напрежения са определени с метода на конформно-изобразителните функции. Получени са нови изрази за напреженията. В тези изрази участват площите на пластовете от разглежданата област. Представеното решение допълва съществуващите изрази за напреженията в хоризонтално разположени пластове.

Ключови думи: напрежения, метода на конформно-изобразителните функции, изработка, напластените среди

Introduction

Analytical and numerical methods are usually used for the calculation of stresses around openings driven in layered rock mass. The stresses around circular, rectangular and semi-circular or "d" cross section openings are examined by the finite element method (Trifonova-Genova, 2012). The rock mass consists of homogeneous layers. They are parallel to each other and to the axis of opening. The theory of elasticity in combination with the theory of layered media is applied to determine stresses around a shaft excavated into a horizontally layered rock mass (Trifonova-Genova, 2012, Sbornik ot dokladi, Varna). Analytical expressions of stresses are used for the thicknesses of layers and their physical and mechanical characteristics. This method is suitable for horizontal and slightly sloping layers.

The current article focuses on extending the scope of application. Therefore, it is necessary to study parallel layers with different inclinations and to summarize the analytical expressions of stresses in them.

Methods

1. Physical and mechanical characteristics of the generalized field

An opening in a circular form is considered. The influence of stresses due to the driving of an opening extends in a square area. It has the dimensions ($12r \times 12r$) shown in Figure 1. The rock consists of layers with thicknesses t_1 and t_2.

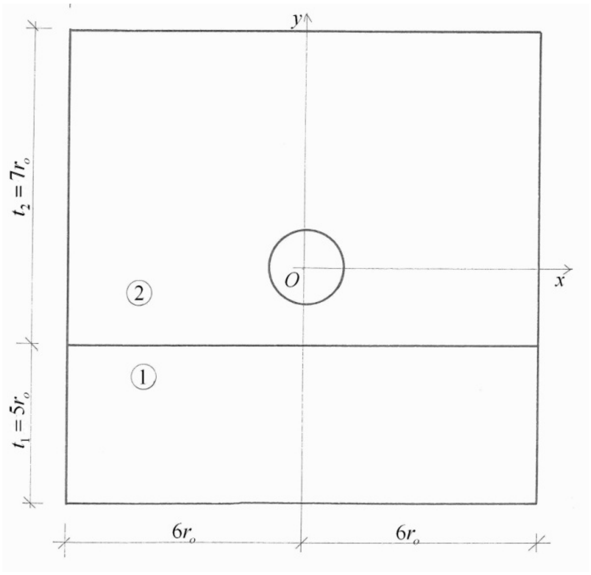

Fig.1. Horizontally layered rock

According to the theory of layered media the stresses in each layer are determined by the stresses in a homogeneous rock with the following physical-mechanical characteristics (Trifonova-Genova, 2012):

$$E^{(o)} = \frac{E^{(1)}t_1 + E^{(2)}t_2}{(t_1 + t_2)}; \quad \mu^{(o)} = \frac{\mu^{(1)}t_1 + \mu^{(2)}t_2}{t_1 + t_2}. \quad (1)$$

Here $E^{(1)}$ and $E^{(2)}$ are Young's modulus for layer 1 and 2, $\mu^{(1)}$ and $\mu^{(2)}$ are Poisson's ratio for corresponding layer.

The areas of two layers are (fig.1):

$$A_1 = 12r.t_1; \quad A_2 = 12r.t_2. \quad (2)$$

Expressions (1) can be summarized and expressed as follows:

$$E^{(o)} = \left[E^{(1)}A_1 + E^{(2)}A_2\right]A^{-1}; \quad A = A_1 + A_2;$$
$$\mu^{(o)} = \left[\mu^{(1)}A_1 + \mu^{(2)}A_2\right]A^{-1}. \quad (3)$$

Introducing Eq. (2) into Eq. (3) gives (1). This result can be summarized for n layers and applied for inclined layers:

$$E^{(o)} = \frac{\sum_{i=1}^{n} E^{(i)}A_i}{\sum_{i=1}^{n} A_i}; \quad \mu^{(o)} = \frac{\sum_{i=1}^{n} \mu^{(i)}A_i}{\sum_{i=1}^{n} A_i}. \quad (4)$$

2. Influence of slope

Rock mass consists by two layers with a boundary conveying angle α to the horizon (fig. 2). This border goes off from the lower points of the circle opening.

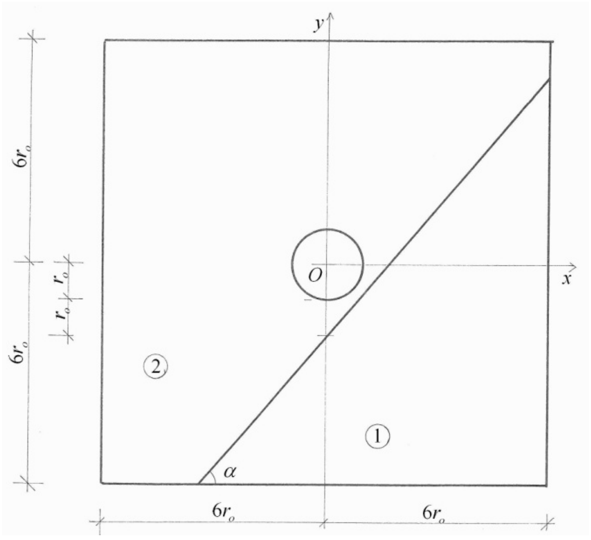

Fig.2. Inclined layered rock

The areas' values $A_{1,i}$ and $A_{2,i}$ of the layers when varying the slope α in $10°$ ($i = 1 \div 10$) are presented in Table 1. The deviations $\Delta A_{1,i}$ and $\Delta A_{2,i}$ from the respective area are obtained. The latter are calculated when the border is horizontal (Fig.1):

$$\Delta A_{1,i} = \frac{\left|A_{1,i} - A_{1,o}\right|.100}{\max\left\{A_{1,i}; A_{1,o}\right\}}[\%];$$
$$\Delta A_{2,i} = \frac{\left|A_{2,i} - A_{2,o}\right|.100}{\max\left\{A_{2,i}; A_{2,o}\right\}}[\%]. \quad (5)$$

The fourth and sixth columns of Table 1 are analyzed. It turns out that the slope's increase leads to a strong increase of indicators ($\Delta A_{1,i}, \Delta A_{2,i}$). To increase the accuracy of stresses it is necessary to apply the method described in (1) (Trifonova-Genova, 2012), but with expressions (4).

Data from Table 1 and Figure 3 show that the gradient slope at which equations (1) are used is over $45°$. Calculating the areas of the layers and applying equations (4) is recommended above this value.

Table 1.
Results

1	2	3	4	5	6
Point $i\downarrow$	α	A_1	$\Delta A_{1,i}$	A_2	$\Delta A_{2,i}$
dimension	$[^\circ]$		$[\%]$		$[\%]$
Multi plier		r^2		r^2	
1	0	60	0	84	0
2	10	60	0	84	0
3	20	60	0	84	0
4	30	60	0	84	0
5	40	60	0	84	0
6	45	60.5	0.826	83.5	0.595
7	50	62	3,17	82,0	2,34
8	60	65	14,15	78,92	6,04
9	70	67.6	11.28	76.37	9.09
10	80	70.0	7.8	74.11	11.77

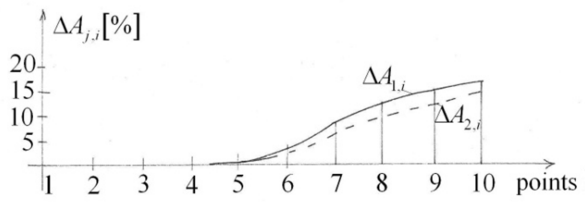

Fig.3. Diagram of deviations $\Delta A_{1,i}$ and $\Delta A_{2,i}$

2. Stresses in steep layers

The stresses at a point in each layer are given in Figure 4. The coordinate system is located along the boundary line between the two layers. The square area is loaded with vertical and horizontal in situ stresses. They are at the center of the circular hole. Vertical stresses are defined by:

$$Q_1 = \gamma_1 H \; ; \; Q_2 = \gamma_2 H \; . \tag{6}$$

In these expressions H is the depth of the opening, γ_1 and γ_2 is the bulk of weights of layers 1 and 2. The coefficients of the lateral pressure for horizontal stresses in the layers is determined by (fig. 4):

$$\lambda_1 = \frac{\mu^{(1)}}{1-\mu^{(1)}}; \quad \lambda_2 = \frac{\mu^{(2)}}{1-\mu^{(2)}}. \tag{7}$$

Stresses in each layer are determined as described in (Trifonova-Genova, 2012) method. They use two groups of links. The first one expresses the conditions for equality of strains of the boundary between the layers. The second group uses the condition of equality of forces, expressed by generalized stresses and area of layers (Lekhnitskii, 1935; Trifonova-Genova, 2012):

$$\begin{aligned} &a_{11}^{(1)}\sigma_{x'}^{(1)} - a_{11}^{(2)}\sigma_{x'}^{(2)} = \left[a_{13}^{(2)} - a_{13}^{(1)}\right]\sigma_{z'}^{(o)}; \\ &A_1\sigma_{x'}^{(1)} + A_2\sigma_{x'}^{(2)} = A\,\sigma_{x'}^{(o)}. \end{aligned} \tag{8}$$

Here $\sigma_{x'}^{(o)}$ and $\sigma_{z'}^{(o)}$ are stresses in the generalized rock, whose expressions are given below.

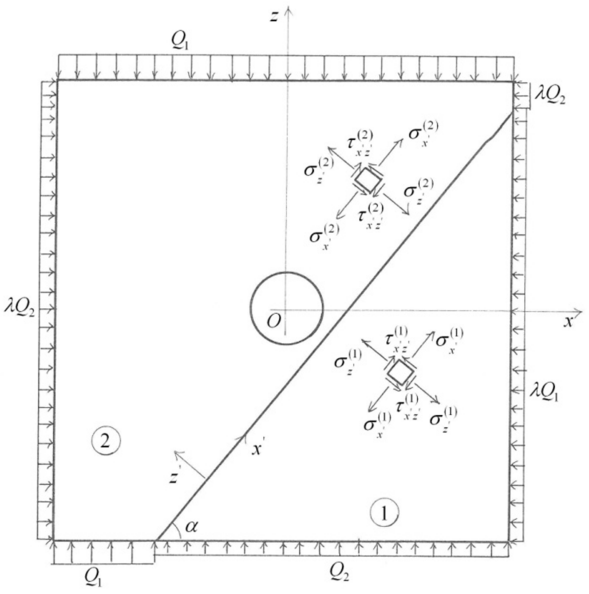

Fig. 4. Stresses in an inclined layered rock

After processing equation (8), the following stresses are obtained:

$$\begin{aligned} \sigma_{x'}^{(1)} &= \frac{A_2\left[a_{13}^{(2)} - a_{13}^{(1)}\right]\sigma_{z'}^{(o)} + a_{11}^{(2)}\sigma_{x'}^{(o)}A}{a_{11}^{(1)}A_2 + a_{11}^{(2)}A_1}; \\ \sigma_{x'}^{(2)} &= \frac{-A_1\left[a_{13}^{(2)} - a_{13}^{(1)}\right]\sigma_{z'}^{(o)} + a_{11}^{(1)}\sigma_{x'}^{(o)}A}{a_{11}^{(1)}A_2 + a_{11}^{(2)}A_1}. \end{aligned} \tag{9}$$

The rest of the stresses can be expressed as:

$$\sigma_{z'}^{(1)} = \sigma_{z'}^{(2)} = \sigma_{z'}^{(o)}; \tau_{xz'}^{(1)} = \tau_{xz'}^{(2)} = \tau_{xz'}^{(o)}. \tag{10}$$

For isotropic rock the coefficients of equations (9) and (10) are expressed as follows (Trifonova-Genova, 2012; Minchev, 1960):

$$\begin{aligned} a_{11}^{(1)} &= \frac{1}{E^{(1)}} \; ; \; a_{11}^{(2)} = \frac{1}{E^{(2)}} \; ; \\ a_{13}^{(1)} &= \frac{-\mu^{(1)}}{E^{(1)}} \; ; \; a_{13}^{(2)} = \frac{-\mu^{(2)}}{E^{(2)}} \; . \end{aligned} \tag{11}$$

The stresses of generalized rock in equations (9) and (10) are expressed by polar coordinates $Or\theta$ (Minchev, 1972):

$$\sigma_x^{(o)} = \sigma_r^{(o)} c^2 + \sigma_\theta^{(o)} s^2 + \tau_{r\theta}^{(o)} s_2;$$
$$\sigma_z^{(o)} = \sigma_r^{(o)} s^2 + \sigma_\theta^{(o)} c^2 - \tau_{r\theta}^{(o)} s_2; \quad (12)$$
$$\tau_{xz}^{(o)} = \tau_{r\theta}^{(o)} c_2^2 + \left[\sigma_r^{(o)} - \sigma_\theta^{(o)}\right] 0{,}5 s_2,$$

where

$$c^2 = \cos^2\beta; \quad s^2 = \sin^2\beta; \quad s_2 = \sin(2\beta);$$
$$c_2^2 = \cos^2(2\beta); \quad \beta = \theta - \alpha; \quad 0 \le \theta \le 90°.$$

In this expression the angle θ is measured from the horizontal axis in counterclockwise direction. The stresses in the rock are given (Bulachev, 1982; Minchev, 1960):

$$\sigma_r^{(o)} = -\gamma^{(o)} H\left(\lambda_1 \sigma_{r2} + \lambda_2 \sigma_{r1} \cos 2\theta\right);$$
$$\sigma_\theta^{(o)} = -\gamma^{(o)} H\left(\lambda_1 \sigma_{\theta 2} - \lambda_2 \sigma_{\theta 1} \cos 2\theta\right); \quad (13)$$
$$\tau_{r\theta}^{(o)} = \gamma^{(o)} H \lambda_2 \tau_{r\theta 1} \sin 2\theta,$$

where

$$\lambda = \frac{\mu^{(o)}}{1-\mu^{(o)}}; \quad \lambda_1 = \frac{1+\lambda}{2}; \quad \lambda_2 = \frac{1-\lambda}{2};$$

$$\sigma_{r2} = 1 - \frac{r_o^2}{r^2}; \qquad \sigma_{r1} = 1 + 3\frac{r_o^4}{r^4} - 4\frac{r_o^2}{r^2};$$

$$\sigma_{\theta 2} = 1 + \frac{r_o^2}{r^2}; \qquad \sigma_{\theta 1} = 1 + 3\frac{r_o^4}{r^4};$$

$$\tau_{r\theta 1} = 1 - 3\frac{r_o^4}{r^4} + 2\frac{r_o^4}{r^2}; \quad \gamma^{(o)} = \frac{\gamma^{(1)} A_1 + \gamma^{(2)} A_2}{A}.$$

Here r_o is the radius of opening (Fig.4). The stresses of equation (13) are obtained by complex variable theory (Muskhelishvili, 1963; Savin, 1961; Bulachev, 1982). The stresses in the contour of opening in generalized rock are of practical interest:

$$\sigma_r^{(o)} = 0; \quad \tau_{r\theta}^{(o)} = 0;$$
$$\sigma_\theta^{(o)} = -2\gamma^{(o)} H\left(\lambda_1 - 2\lambda_2 \cos 2\theta\right). \quad (14)$$

3. Key finding

Analytical expressions of stresses in each layer are applied in layers whose slope is greater than half the right angle.

These expressions are summary of the last expressions of stresses in layers (Trifonova-Genova, 2012). The latter are used in horizontal and parallel layers. The thicknesses of layers are included in them.

Conclusion

The method, described in this article has the following advantages:
-it is very simple to be implemented;
-it can also be used in transversal-isotropic layers (Lekhnitskii, 1935);
-it can be summed up for many layers;
- It can be used in fixed opening, driven at great depth (Minchev, 1960; Bulachev, 1982);
- It can be used taking into account the pitch of the terrain (Li et al., 2008).

The results obtained are applicable in the design of mining works. They are particularly suitable for close physical and-mechanical characteristics. Here we mean the relation between the maximum and minimum values of Young's modulus for layer 1 and 2.

References

Лехницкий С. Г., К расчету на прочность составных балок, Вестник инженеров и техников, 1935, 9. (Lekhnitskii S. G., K raschetu na prochnost sostavnih balok, Vestnik inzhenerov i tehnikov, 1935, 9.)

Минчев И. Тр. Динамична теория на еластичността, Д.И. „Техника", С., 1972, 285с. (Minchev I. Tr., Dinamichna teoriya na elastichnostta, D. I. "Tehnika", S., 1972, 285s.)

Минчев И. Тр., Механика на анизотропното тяло в минното дело, Д.И. „Техника", С., 1960, 126с. (Minchev I. Tr., Mehanika na anizotropnoto tyalo v minnoto delo, D. I. "Tehnika", S., 1962, 126s.)

Трифонова-Генова В.М. Деформирано състояние на разномодулен масив в околността на вертикална изработка, *V-та Международна научна конференция по геомеханика, Сборник от доклади, Варна*, 18 - 20.06.2012, 294-299с. (Trifonova-Genova V. M., Deformirano sastoyanie na raznomodulen masiv v okolnostta na vertikalna izrabotka", *V-ta Mezhdunarodna nauchna konferentsia po geomehanika, Sbornik ot dokladi, Varna,* 18-20.06.2012, 294-299s.)

Трифонова-Генова В. М., Напрегнато състояние в напластен масив около кръгла изработка, София: ИК "Св. Иван Рилски", 2012.-132с. (Trifonova-Genova V. M., Napregnato sastoyanie v naplasten masiv okolo krugla izrabotka, Sofia: I. K. "Sv. Ivan Rilski", 2012.-132s.)

Булычев Н. С., Механика подземных сооружений, М., Недра, 1982, 282с. (Bulachev N. S., Mehanika podzemnih sooruzhenii, M., Nedra, 1982, 282s.)

Lekhnitskii S. G., Theory of elasticity of an anisotropic elastic body. San Francisco: Holden-day; 1963.

Muskhelishvili N. I., Some basic problems of mathematical Theory of elasticity. Groningen: Noordhoff; 1963.

Savin G. N. Stress concentration around holes. London: Pergamon; 1961.

Shu-cai Li, Ming-bin Wang, An elastic stress-displacement solution for lined tunnel at great depth, Int. J. of Rock Mech. & Min. Sci. 45 (2008) 486-494.

This article was reviewed by Prof. Dr. Svetlana Lilkova-Markova and Assoc. Prof. Dr. Chona Koseva.

UPGRADING A SWINGING SCREENING SYSTEM WITH LINEAR MOTIONS IN A HORIZONTAL PLANE

Stefan Pulev

University of Mining and Geology "St. Ivan Rilski", 1700 Sofia, E-mail: st_pulev@yahoo.com

ABSTRACT. This research proposes and proves a method of upgrading swinging screening systems with linear motions in the horizontal plane – namely, replacing the rigid link between the housing and the vibration exciter with an elastic one. This can be achieved with the introduction of an elastic connecting rod. With the help of methods from analytical mechanics and the mechano-mathematical models of the initial and improved constructions we prove that this leads to reduced dynamic bearing reaction forces and significantly improved vibroisolation.

Keywords: swinging screening systems, elastic connecting rod, upgrading

МОДЕРНИЗАЦИЯ НА ЛЮЛКОВА ПРЕСЕВНА УРЕДБА С ПРАВОЛИНЕЙНИ ДВИЖЕНИЯ В ХОРИЗОНТАЛНА РАВНИНА

Стефан Пулев

Минно-геоложки университет "Св. Иван Рилски", 1700 София, e-mail: st_pulev@yahoo.com

РЕЗЮМЕ. В настоящата работа се предлага и обосновава един начин за модернизация на люлковите пресевни уредби с праволинейни движения в хоризонтална равнина – замяна на твърдата връзка между корпуса и вибровъзбудителя с еластична. Това може да се осъществи с въвеждането на еластична мотовилка. С помощта на изградените механо-математични модели на съществуващата и на модернизираната конструкции, с методите на аналитичната механика се доказва, че по този начин се намаляват стойностите на динамичните опорни реакции и значително се подобрява виброизолираността.

Ключови думи: люлкови пресевни уредби, еластична мотовилка, модернизация

Introduction

The main advantages of swinging screening systems with linear motions in the horizontal plane are:

- simple construction;
- easy maintenance;
- small magnitude of the friction forces;
- insignificant operating costs.

Because of them, such systems continue to be used today despite their serious disadvantage, namely the large unbalanced forces transmitted to supporting structures and surrounding facilities.

This work proposes and proves an easy method for upgrading swinging screening systems with linear motions in the horizontal plane – namely, replacing the rigid link between the housing and the vibration exciter. This can be done by installing an elastic connecting rod. With the help of the established mechanometric models and the methods of the analytical mechanics, it is proved that in this way the values of the dynamic bearing reaction forces are reduced and the vibro-isolation and working conditions in the mining enterprises are significantly improved.

Description of existing swinging screening systems with linear motions in the horizontal plane

Representatives of this type of screening system are characterized by constant kinematic parameters at all points of the screening surface because of the rigid connection between the drive and the housing, as well as the inelastic attachment of the housing to the foundation. Fig. 1 shows the schematic diagram of a swinging screening systems with linear motions in the horizontal plane (Denev 1964; Tsvetkov 1988). The housing together with the screening surfaces is secured by the cylindrical joints A and B and levers AB. It moves translationally. The distance $AB = b$ from the support A to the housing is much larger than the eccentricity e of the vibrator, and therefore it can be assumed that the sieve surface moves in a horizontal line instead of a circle. The source of oscillation is the eccentric shaft OD that rotates with a constant angular velocity ω. Movement is transmitted to the screening surfaces with the help of the connecting rod BD.

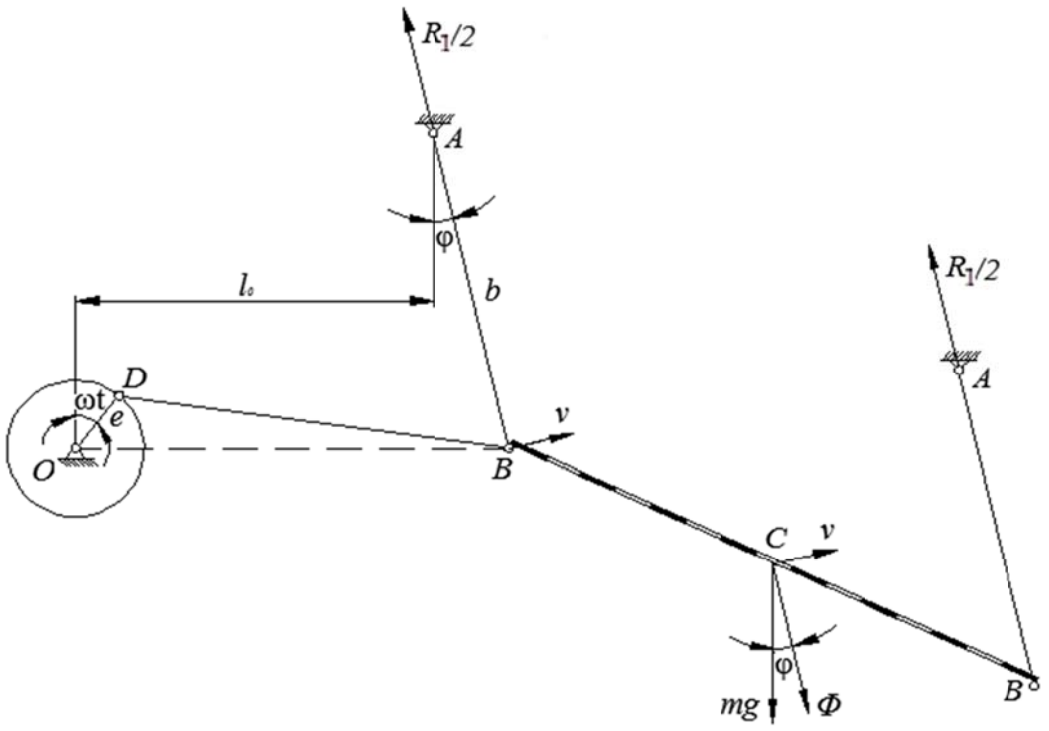

Fig. 1. A swinging screening systems with linear motions in the horizontal plane

The described screening system is considered to be a one-mass swinging system with one degree of freedom. For the coordinate φ, the angle of rotation of the levers AB relative to the vertical is selected. The mass of the housing and the screening surfaces is m. The distance from the axis O of the eccentric shaft to the joint B in the position of static equilibrium is indicated by l_0. The levers AB, the connecting rod BD and the eccentric are considered lean, due to the fact that their weight is hundreds of times smaller than that of the screen housing. Friction in the cylindrical joints is disregarded.

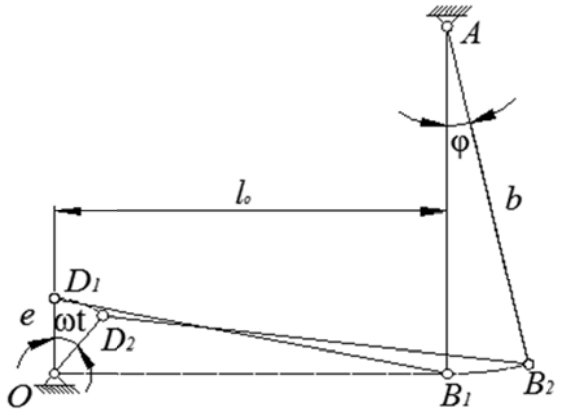

Fig. 2. Determining the relationships between kinematic parameters

Fig. 2 presents a scheme for determining the relationships between kinematic parameters. At the initial moment of motion, the crank of the vibrator and the housing suspension lever are respectively OD_1 and AB_1. At any point in the movement they occupy positions OD_2 and AB_2. On the one hand, point B can be viewed as part of the vibrator and its motion will be represented as $e.sin\omega t$. On the other hand, the same point belongs to the lever AB and moves along the arc

$$B_1B_2 = l.\varphi .$$

Therefore, the following equality applies (Pulev, 2014)

$$b.\varphi = e.sin\omega t \text{, or } \varphi = \frac{e}{b}sin\omega t .$$

The speed of the housing and the screening surfaces at any point in time is

$$v = b\dot{\varphi} = e\omega\cos\omega t .$$

The centrifugal inertial force acting on the screen body is

$$\Phi = \frac{mv^2}{b} = \frac{m}{b}\left(e\omega\cos\omega t\right)^2 .$$

The dynamic bearing reaction force R_1 is

$$R_1 = mg\cos\varphi + \Phi = m\left[g\cos\varphi + \frac{\left(e\omega\cos\omega t\right)^2}{b}\right]. \quad (1)$$

Description of the upgraded swinging screening system

Fig. 3 shows a dynamic model of the upgraded swinging screening system with linear motions in the horizontal plane.

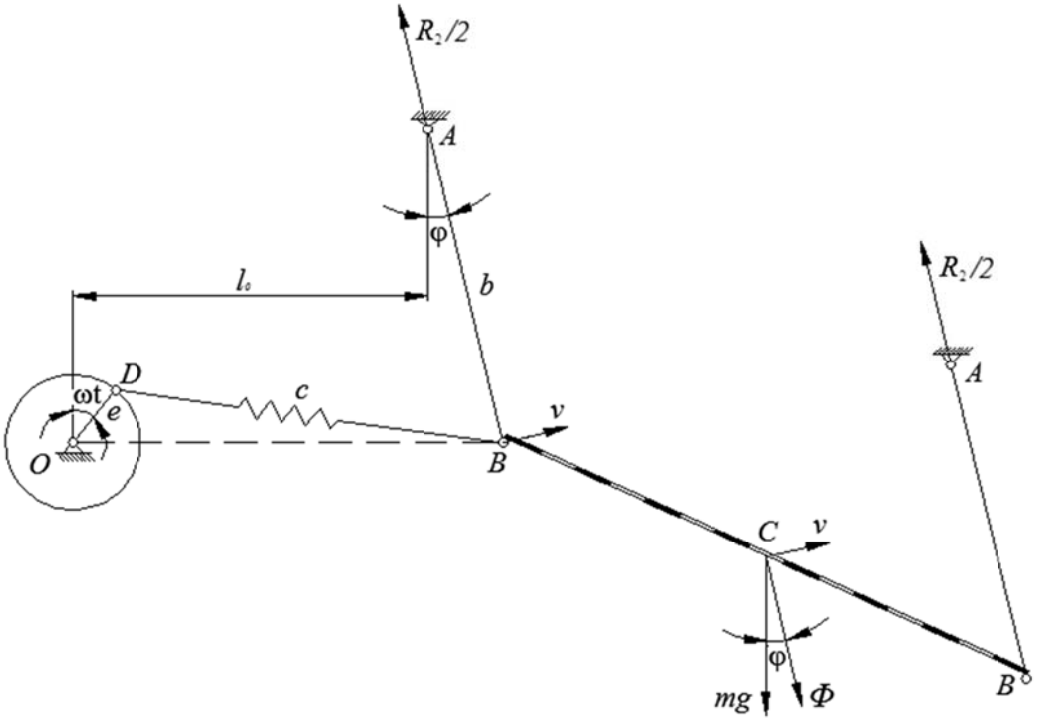

Fig. 3. Schematic diagram of the upgraded swinging screening system with linear motions in the horizontal plane

The elasticity of the newly installed connecting rod is characterized by the coefficient c.

An analysis of this model has been carried out with the methods of analytical mechanics (Pulev, 2016). The approximate differential equation of movement is

$$\ddot{\varphi} + k^2\varphi = \frac{ce}{mb}\sin\omega t\ .$$

The law of motion of the screening surfaces is

$$\varphi = \frac{ce}{\left(k^2-\omega^2\right)mb}\left(\sin\omega t - \frac{\omega}{k}\sin kt\right), \qquad (2)$$

and the expression for the variation in the speed is

$$\dot{\varphi} = \frac{ce\omega}{\left(k^2-\omega^2\right)mb}\left(\cos\omega t - \cos kt\right), \qquad (3)$$

where

$$k = \sqrt{\frac{mg+cb}{mb}}$$

is the system´s circular frequency of vibration.

With the help of the deduced expressions (2) and (3), the centrifugal inertial force $\Phi = mb\dot{\varphi}^2$, acting on the screen body, can be determined, as well as the dynamic bearing reaction force R_2 of the support A, namely

$$R_2 = mg\cos\varphi + \Phi = m\left(g\cos\varphi + b\dot{\varphi}^2\right). \qquad (4)$$

Numerical experiment

To prove the positive effect of the upgade, a numerical experiment is carried out with the help of MATLAB. The aim of the experiment is to compare the values of the dynamic bearing reaction force between the initial and upgraded swinging screening system. The values of the parameter are

$$c = 200\,000\ N/m$$
$$m = 2000\,kg$$
$$\omega = 600\ s^{-1}$$
$$l_0 = 0{,}7\ m$$
$$b = 0{,}8\ m$$
$$e = 0{,}03\,m$$

Fig. 4 presents the graph of time-varying values of the bearing reaction force R_1 in the initial system. Formula (1) is used. A maximum value of 24804 N is recognized.

Fig. 5 shows the variation of the bearing reaction force R_2 in the upgraded version by applying formulas (2), (3) and (4). Values do not exceed 19663 N. Difference between the

minimum values of the two systems is not observed. After comparing the data in Fig. 4 and 5, a reduction in the maximal value of the dynamic backlash was observed by 5141 N or by 20.73% in favor of the upgraded version.

The results of the numerical experiment clearly demonstrate the benefits of installing an elastic connecting rod. The upgrade costs are low, but the the vibrations are significantly reduced.

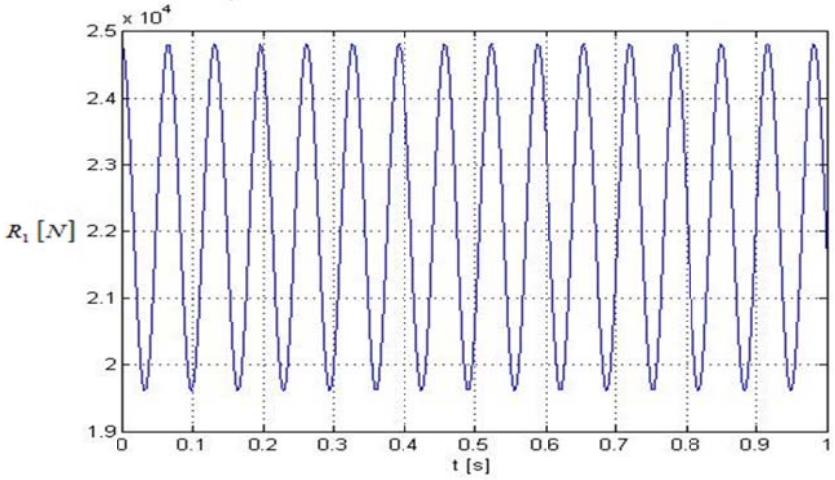

Fig. 4. Variation of the dynamic bearing reaction force in a conventional swinging screening system

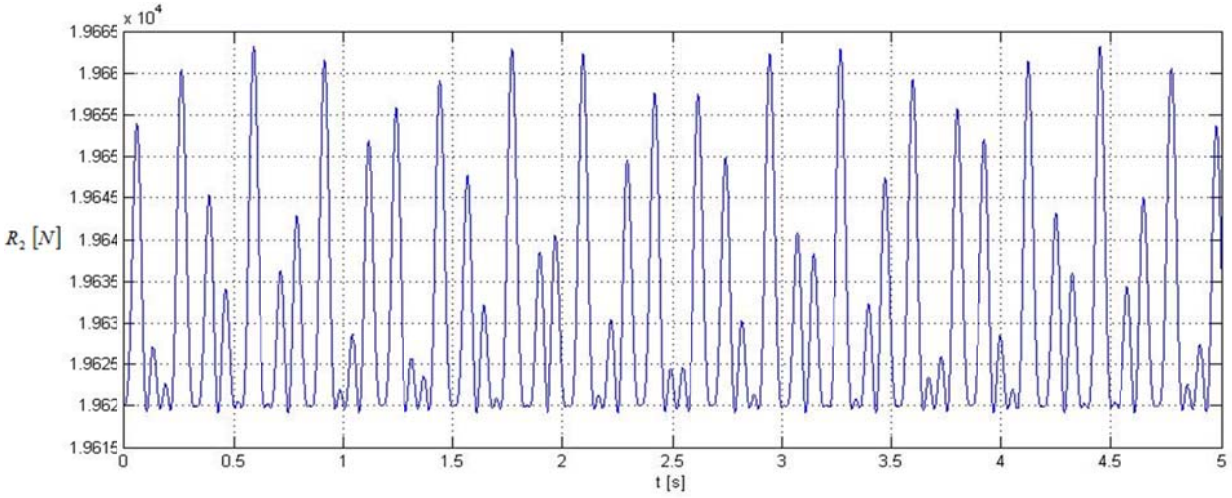

Fig. 5. Variation of the dynamic bearing reaction force in the upgraded swinging screening system

References

Денев С. И. Трошене, смилане и пресяване на полезни изкопаеми. С., Техника, 1964. (Denev S. I. Troshene, smilane i presyavane na polezni izkopaemi. Sofia, Tehnika, 1964.)

Пулев, Ст. Динамика на вибрационни машини с ексцентриков вибровъзбудител. Годшник на МГУ, том 57, 2014, № 3, с. 92-95. (Pulev St. Dinamika na vibratsionni mashini s ekstsentrikov vibrovuzbuditel. Godishnik na MGU, tom 57, 2014, № 3, p. 92-95.)

Пулев Ст., Динамика на люлкова пресевна уредба с праволинейни движения в хоризонтална равнина, XVI международна научна конференция ВСУ'2016, 9-10 юни 2016, София, Доклади том II, с. 356-361. (Pulev St. Dinamika na lyulkova presevna uredba s pravolineini dvizhenia v horizontalna ravnina, XVI mezhdunarodna nauchna konferentsia VSU'2016, 9-10 june 2016, Sofia, Dokladi tom II, p. 356-361.)

Цветков Х. Ц. Обогатителни машини. Техника, С.,1988. (Tsvetkov H. Ts. Obogatitelni mashini. Sofia, Tehnika, 1988.)

This article was reviewed by Prof. Dr. Michail Valkov and Assoc. Prof. Dr. Violeta Trifonova-Genova.

COLUMN FLOTATION MACHINES - TRENDS AND APPLICATIONS

Tsvetelina Ivanova[1], Marin Ranchev[1], Ivan Nishkov[1]

[1]University of Mining and Geology "St. Ivan Rilski"; 1700 Sofia, Department of Mineral Processing and Recycling
E-mail: inishkov@gmail.com

ABSTRACT. The rapid development of the flotation technique, which began in the first quarter of the twentieth century, led to the development of a large number of flotation machineryconstructions, a small number of which had come into practice. In the middle of the previous century, great attention was paid to hydrodynamic processes in the flotation machines design and operation. Column flotation is a physical improvement in the flotation separation process. Due to the excellent results, column flotation was studied on raw materials containing fluorite, manganese, platinum, palladium, titanium and other minerals. The paper presents the trends of column flotation machines use according to the model, processed raw material and distribution area.

Keywords: column flotation machines

КОЛОННИ ФЛОТАЦИОННИ МАШИНИ – ТЕНДЕНЦИИ И ПРИЛОЖЕНИЯ

Цветелина Иванова[1], Марин Ранчев[1], Иван Нишков[1]

[1]Минно-геоложки университет "Св. Иван Рилски", 1700 София, катедра "Обогатяване и рециклиране на суровини"
E-mail: inishkov@gmail.com

РЕЗЮМЕ. Бурното развитие на флотационната техника, започнало през първата четвърт на XX век, довежда до разработването на голям брой конструкции флотационни машини, малка част от които са навлезли в практиката. В средата на предходното столетие при конструирането и оперирането с флотационните машини е обърнато голямо внимание на хидродинамичните процеси в тях. Колонната флотация се явява физическо усъвършенстване в процеса на флотационно разделяне. Поради постигнатите отлични резултати колонната флотация е изследвана на суровини съдържащи флуорит, манган, платина, паладий, титан и др. минерали. В настоящата работа е направен преглед на тенденциите в използването на колонните флотационни машини според техния модел, преработвана суровина и област на разпространение.

Ключови думи: колонни флотационни машини

Introduction

In 1980s the column flotation was patented for first time. This led to numerous studies and subsequent publication of the obtained results in specialized scientific literature. Originally, the column flotation machines have been developed for application in flotation cleaning stage and expected to be adopted in both rougher and scavenger flotation operations, as well as completely displace the mechanical cells. (Willis, 2010).

According to a number of authors, the column ("columns") flotation machines represent a non-mechanical or non-sub aeration flotation cells, a definition popularized during the 1990s (Rubinstein, 1995; Sastry, 1988; Agar et al., 1991; Gomez and Finch, 1996; Finch, 1995). The term ''tall columns" refer to counter current columns, with a height generally greater than twice the diameter, and they are often referred to as ''conventional" columns. Short ''columns" refer to other non-mechanical flotation cells, variously referred to as novel columns, pneumatic cells and high intensity cells (Harbort, Clarke, 2017).

Development of column flotation

The development of column flotation machines can be divided into six stages:

- **Early columns (1905-1925)**

This period covers the time from the initial stage of the development of the flotation process by 1905 to 1925. The majority of the installations were what are now referred to as short columns, the most popular being the Callow machine, the MacIntosh machine and the Forrester machine. Tall columns were also tested, with a notable installation being that of Inspiration (Lynch et al., 2010).

- **The long decline (1926-1960)**

In 1926 the Minerals Separation Company launched its subaeration mechanical flotation cell, which was considered to have significant advantages over the non-mechanical short and tall columns. This was to start a long decline in the popularity of flotation columns that continued to 1960 (Harbort, Clarke, 2017).

- **Revival of Colonial Flotation (1960-1980)**

This period lasted between 1960 and 1980. In the 1960s it was driven by developments in China (Hu and Liu, 1988), the Soviet Union and Australia. Notable events included the first column installed in metalliferous flotation in China by the China MolybdenumCompany (Ananthan, 2013), as well as the Chinese free jet cell (Wu and Ma, 1998), the development of the Multisectional Column in the Soviet Union (Rubinstein and Badenicov, 1995) and the Davcra cell in Australia (Cusack and Oley, 1971). The 1970s were to see an increased emphasis on tall flotation column development with the Diester Flotaire Column (Zipperian and Svensson, 1988), the Canadian Flotation Column (Wheeler, 1986) and the Cominco/CESL Column (Murdock, 1991).

- **The first wave of column flotation (1980-1994)**

This period represents 15 years of sustained growth in flotation column capacity installed from 1980 to 1994, followed by four years of declining installations, to 1999. Major flotation column development occurred, with 14 new significant models of flotation column installed around the world. Many of these would not survive the period of decline, but those that continue in manufacture today include the Jameson Cell (Harbort et al.,1994), the Microcel (Luttrell et al., 1991) and the Pneuflot Cell (Markworth et al., 2007).

- **The second wave of column flotation (1999-2004)**

The period includes an ascending period of application of flotation columns between 1999 and 2004. The major impetus was refurbishment and growth in the Chinese coal industry, initially through refitting of mechanical cells with free jet aerators, and later via new greenfield installations. The end of the period approximately coincides with the Global Financial Crisis. Once again it represented a time of extensive development with nine new significant models of flotation column installed around the world. These included the FCSMC (Zhou et al., 2008) and BGRIMM tall columns in China (Hu, 2015), modifications to earlier Chinese jet aeration machines to make to the FJC free jet machine (Wu et al., 2010), development of the Prequip Column in South Africa (PreQuip, 2009) and the Imhoflot short column. Also during this period the CESL Column would become part of Canadian Process Technologies and by the end of the period part of the Eriez Flotation Division, with a number of new column designs (Kohmuench et al., 2007; Kiser et al., 2012).

- **The third wave of column flotation (2005-2012)**

This period represents another period of rapid column flotation growth to 2012, driven by high commodity prices, followed by a spectacular decline in installations to 2014, as commodity prices plummeted. A significant event to arise from this period was the increased installation of Chinese flotation columns in other countries and the development and installation of the Staged Flotation Reactor (Kosick, 2015).

Fig. 1 provides a timeline of the various types of flotation column installed between 1961 and 2016s.

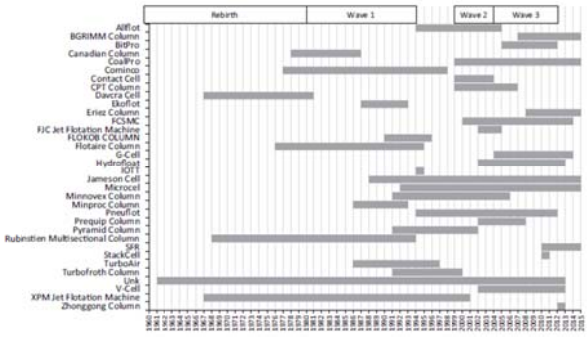

Fig. 1. Application of the different types of flotation columns for the period 1961 – 2016.

Spreading of column flotation capacity

According to the data from Amec Foster Wheeler (Harbort, Clarke, 2017) with details for the number of individual columns installed per year, three peaks, followed by a period of decline in the column flotation timeline, could be distinguished (fig. 2).

- 1994 – Wave 1, with 118 flotation columns installed.
- 2004 – Wave 2, with 521 flotation columns installed.
- 2012 – Wave 3, with 199 flotation columns installed.

Each peak is matched by a subsequent trough,

- 1998 – installed flotation columns decreased to 39.
- 2011 – installed flotation columns decreased to 96.
- 2014 – installed flotation columns decreased to 62.

Of note is the year 2015, which witnessed a rebound in the number of flotation columns installed to 90.

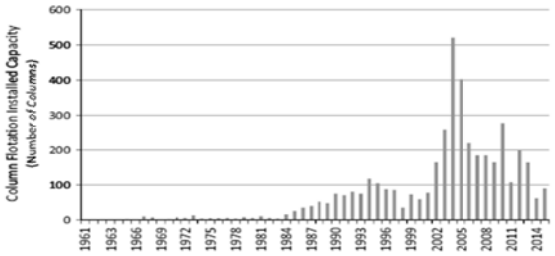

Fig. 2. Number of columns installed. (Harbort, Clarke, 2017)

Determining the flotation column capacity by the number of flotation columns installed can be misleading, as differing throughputs, differing duties and commodities which are being treated, require different flotation column diameters. For example, a molybdenum cleaner column could be 0.5 m in diameter, compared to a coal flotation column of 6.0 m in diameter (Harbort, Clarke, 2017).

Figure 3 presents some details about the average yearly column flotation diameter across all column types, commodities and duties. Many of the early tall flotation columns were in small, base metals cleaning duties. The short flotation column Davcra Cells were also initially lower capacity and cross section area machines, although by the early 1970s they had achieved substantial increases in unit capacity and resulted in a net increase in average column flotation diameter 2.5 m). This was maintained by installation of Flotaire Columns in larger capacity phosphate and coal duties in the late 1979s

and early 1980s. The increased use of flotation columns in base metals cleaning roles (specifically molybdenum) resulted in a decrease in average column flotation diameter to 1.5 m by 1986 (Harbort, Clarke, 2017).

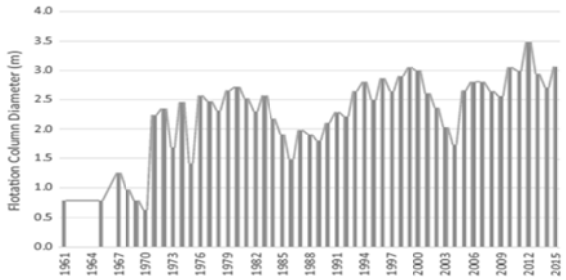

Fig. 3. Column flotation cells – average diameter

The advent of short columns such as the Jameson Cell, Ekoflot, Allflot, and Pneufloat heralded a new age where their cell diameters increased rapidly. This, coupled with increased flotation column use in coal in Australia (Murphy et al., 2000) and the USA (Luttrell et al., 1999), phosphate and iron ore in Brazil (Araújo et al., 2005), larger porphyry copper cleaning roles in Chile (Schena and Casali, 1994) and a number of significant rougher applications for the Jameson Cell (Harbort et al., 1997) witnessed a net increase in average column flotation diameter to 3.0 m by the year 2000. By 2012 the average yearly column flotation diameter had peaked at 3.5 m.

The trend of installed flotation column capacity expressed in terms of flotation area is similar to that of the number of columns installed. A significant change occurred in 2012, when the installed flotation column flotation area increased to 3000 m^2. The Amec Foster Wheeler database indicates that since 1961, 34,742 m^2 of column flotation area has been installed. This would represent approximately 3600 columns of 3.5 m diameter. (Harbort, Clarke, 2017).

Fig. 4 indicates the flotation column mechanical cell equivalent volume. It shows that, approximately 210,000 m^3 (mechanical cell equivalent) has been installed since 1961. The peak year was 2012 when approximately 19,000 m^3 (mechanical cell equivalent) was installed (Harbort, Clarke, 2017).

Fig. 5 presents the number of different varieties of flotation columns installed in industry per year, across all commodity groups. The graph clearly shows the proliferation of flotation column designs that occurred in the first wave of column flotation from 1980 to 1994. (Harbort, Clarke, 2017).

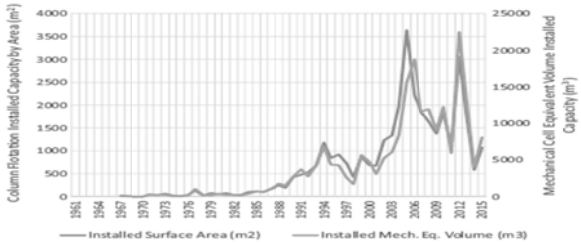

Fig. 4. Column and mechanical flotation machines installed capacity

Different typesof flotation columns installed included the Cominco/CESL Column, XPM Jet Flotation, Machine Multisectional Column, Flotaire Column, ‘‘Canadian Column”, Bahr Cell (Cordes, 1997; Ventert and van Loggerenbergt, 1992), KenFlote (Peters and Parekh, 1992), TurboAir Column (McKay and Foot Jr, 1990), Ekoflot (Heintges et al., 1984; Alizadeh and Simonis, 1985), Microcel, MinnovEX Column (Shaw, 1992), Minproc Column (Newell et al., 1988), Pyramid Column (Foot Jr et al., 1993), Jameson Cell, FLOKOB Column (Brzezina and Sablik, 1995), Allflot (Jungmann and Reilard, 1988), Pneuflot, Turbofroth Column (Arnold and Terblanche, 2001) and IOTT Column (Rubinstein,1995).

Many of the flotation columns manufactured during the first wave of column flotation would not maintain popularity by the time the second wave commenced in 1999. Those that appear to have disappeared from installation lists include the Multisectional Column, Flotaire Column, ‘‘Canadian Column”, Bahr Cell, KenFlote, TurboAir Column, Ekoflot, Minproc Column, FLOKOB Column, Turbofroth Column and IOTT Column (Rubenstein, 1995; Harbort, Clarke, 2017).

The second wave of column flotation between 1999 and 2009 would once again see a significant number of different types of flotation columns being installed. New varieties of flotation columns included the BGRIMM Column, BitPro, CoalPro, CPT Column, Dual Extraction Column (maxFLOT, 2008), Eriez Column, FCSMC Column (Zhou et al., 2008), FJC Jet Flotation Machine, Hydrofloat, Imhoflot G-Cell (Imhof et al., 2007) and V-Cell (Imhof et al., 2005), MultiCell (Opperman et al., 2002), Packed Column (Yang, 1991; Kawatra and Eisele, 1994), Prequip Column and Contact Cell (Amelunxen, 1993).

Flotation columns that successfully survived the first wave to enter the second wave of column flotation included the Microcel, MinnovEX Column, Pyramid Column, Jameson Cell, XPM Jet Flotation Machine, Allflot and Pneuflot cells. Attrition during the period resulted in a decrease in the production of flotation columns before the third wave of column flotation commenced in 2009. This would include the Dual Extraction Column, FJC Jet Flotation Machine, MultiCell, Packed Column, Contact Cell, MinnovEX Column, Pyramid Column, XPM Jet Flotation Machine and Allflot Cell. Flotation columns that appear to have achieved longevity and year on year installations include the Cominco/CESL/CPT/ Eriez columns, the Microcell, Chinese free jet machines and the Jameson Cell (Harbort, Clarke, 2017).

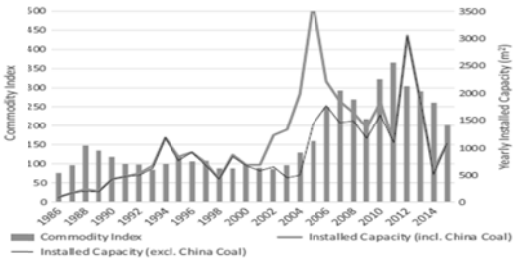

Fig. 5. Number of different varieties of flotation columns installed in industry per year

Figure 6 provides a snapshot of the total number of flotation columns installed per country, as at the end of 2015. It is evident that column flotation is widespread around the world, with northern Africa the only region without registered installations. Considering that all installations are not recorded in the database on Amec Foster Wheeler this figure may underestimate the number of flotation columns installed.(Rubenstein, 1995; Harbort, Clarke, 2017).

Most flotation columns are situated in China, Australia, Canada, USA, Chile, Peru and Brazil. Column flotation also plays a significant role in Mexico, South Africa and Russia.

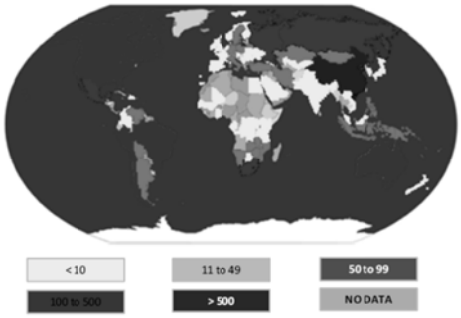

Fig. 6 Total number of flotation columns installed per country

The popularity of flotation columns has fluctuated in geographic regions over the last five decades. Fig. 7 provides (a) details of changes in the distribution of installed flotation column area per decade per major geographical area, and (b) the cumulative distribution of installed flotation column area per geographical region since 1961s (Harbort, Clarke, 2017).

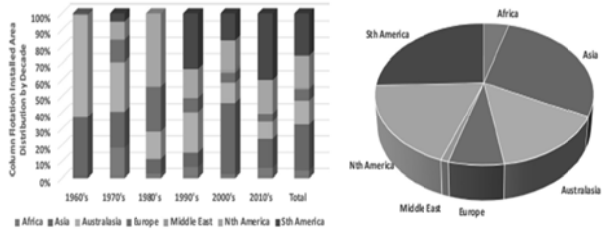

Fig. 7. Flotation columns installed per geographical region

During the 1960s flotation columns use dominated in Australasia, through the installation of the Davcra Cell in the Zinc Corporation's Broken Hill operations. Approximately 30% of flotation column capacity was installed in China in a variety of duties. The 1970s were again dominated by Australasia, with ongoing Davrca Cell installations including the Bougainville copper mine, PNG and the Coal Cliffs mine. The late 1970s also witnessed the introduction of the Cominco/CESL column to Australasia. As a proportion their share in Asia decreased during the decade, with a limited number of XPM Jet Flotation Machines installed. European flotation column capacity increased significantly, largely due to the installation of Multisectional Columns in sites such as Kafansky and Kuznetsk. During the decade Africa also represented a significant proportion of installed flotation capacity with several Davcra Cell installations. The initial growth of column flotation in North America also commenced with the installations of the Flotaire Column, Cominco/CESL column and Canadian Column. (Harbort, Clarke, 2017).

In the 1980s a quantum shift in the geographical regions using column flotation occurred, with North America dominating column flotation capacity. By proportion Europe had the second largest installed capacity with the spread of the Multisectional Column in Russia and other countries of the Soviet Union. The distribution of flotation in Africa, Asia and Australasia decreased dramatically. In Australia and Africa this was largely due to the removal of the high capacity Davcra Cell from the flotation market (Harbort., Clarke, 2017).

In the 1990s South America was to overtake North America as the dominant region for flotation column installations, driven by the large porphyry copper mines of Chile and numerous installations across multiple commodities in Brazil. Australasia witnessed a surge in column flotation popularity, primarily due to installations of the Jameson Cell and Microcel in coal operations (Araújo and Peres, 1995).

The 2000s were dominated by the China growth phenomenon, which witnessed nearly half of all column flotation capacity installed in Asia. By the 2010 a change had commenced and North and South America both accounted for 60% of the decade's flotation column installations (Harbort, Clarke, 2017).

Flotation columns installed by raw materials type

One reason for the fluctuating fortunes of flotation columns has been their varying acceptance in treatment of different commodities. Fig. 8 provides (a) details of changes in the distribution of installed flotation column area per decade per commodity, and (b) the cumulative distribution of installed flotation column area per commodity since 1961. (Harbort, Clarke, 2017).

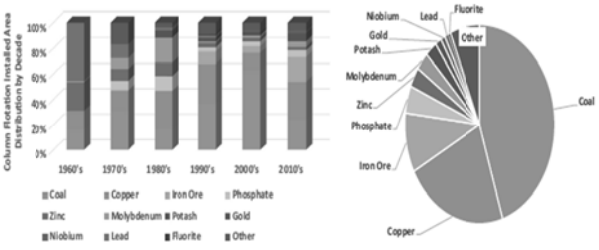

Fig. 8. Installed flotation columns by raw materials type

Overall, coal easily represents the commodity in which most flotation column capacity is installed (42%). The reasons for this are multiple and include the dilute nature and high volume of coal feeds, changing mining methods that generate more fines and the increased need for flotation, stringent contaminant requirements for coking coal and increasingly stringent product specifications in thermal coal for environmental reasons. Copper also makes a major contribution, with 21% of column flotation capacity which has been installed since 1961 being in this commodity. Primarily these installations occur in the large porphyry operations of Chile, Peru and the USA (Harbort, Clarke, 2017).

Flotation column capacity in iron ore is also significant, representing 9% of the installed total. The majority of this is in Brazil (67% of installed iron ore column flotation capacity), with other countries utilizing columns for iron ore flotation including, at various times, China, Peru, USA, Russia, India, Mexico, South Africa, Venezuela and Chile. Rounding out the top four column flotation commodities is phosphate, representing 4% of total installed column flotation capacity. An assortment of commodities including zinc, molybdenum, potash, gold, niobium, lead and fluorite represent a further 10% of installed capacity. The remainder of column flotation capacity includes more than sixty other commodities. Flotation columns installed in the 1960s were overwhelmingly in base metals, with 45% in lead, 25% in zinc operations and 20% in copper operations. The remaining 10% of flotation columns were installed in coal operations (Harbort, Clarke, 2017).

During the 1970s there was a major transition away from column flotation use in both zinc and lead, and a minor increase in use in copper. Flotation column use in coal operations increased dramatically during the decade, representing 30% of the capacity of those installed. Increased use in both phosphate and molybdenum is also apparent, with each amounting to approximately 5% of the decade total. During the 1980s the popularity of flotation columns in North America witnessed major increases in the use for copper and molybdenum (to 30% and 20% of the decade total, respectively). Phosphate use also increased to approximately 10% due to the use of flotation columns in both the USA and Brazil phosphate operations. A significant rationalization of the flotation columns distribution capacity occurred in the 1990s with coal increasing to 35%, due to increased use in Australia, USA and China. Copper maintained its proportion, due largely to use in the South American porphyry copper mines. This decade also represented the first significant use of column flotation in the iron ore industry, for the removal of silica. Largely in Brazil, iron ore composed approximately 10% of flotation used installed flotation column capacity. In comparison with the 1980s the distribution of column use in other commodities decreased significantly, with the most apparent decline being in molybdenum. Phenomenal growth in the use of column flotation in China's coal industry during the 2000s distorts the distribution for this entire decade, with coal representing 60% of capacity. During the last six years the trends have returned to more normal levels, with coal and copper representing the two most popular commodities for column flotation use (20% and 30% of installed capacity respectively). Considering the current market price of iron ore, this commodity with 20% of installed capacity is surprising. (Harbort, Clarke, 2017).

Conclusion

Over the years, flotation column machines have undergone various modifications. Since 1961, the flotation column machines have passed through three development and implementation periods, largely related to the variations in commodity prices. In addition, the following secondary causes for the growing interest in flotation column machines development and implementation could be mentioned: specific raw materials requirements, market needs, spare parts, auxiliary equipment, etc. Flotation column machines are widely used in Australia, China and the United States for coal production, as well as for iron ore processing in the United States and Brazil. In the world practice of non-ferrous metals treatment, the flotation columns are mainly used in the cleaning flotation stage. Furthermore, column flotation machines have been successfully implemented in Bulgaria. Examples are Dundee Precious Metals Chelopech and Rudmethal JSC, Rudozem. The interest in column flotation machines has been growing quickly and over the years different modifications for various raw material processing have been installed.

References

Agar, G.E., Huls, B.J., Hyma, D.B. (Eds.). Column '91. Proceedings of an International Symposium on Column Flotation, Sudbury, Ontario, Canada, 1991 - June 2–6.

Amelunxen, R.L. The contact cell – a future generation of flotation machines. Eng. Min. J. 194, 1993 - 36–37 p.

Ananthan, M.M. China Molybdenum Co Ltd Factsheet. <www.chinamoly.com/en/06invest/doc/CMOC%20Factsheet.pdf (accessed 2013).

Barry Willis. Did column flotation cells ever realise their potential? MEI Blog (May) 2010.

Alizadeh, A., Simonis, W. Flotation of finest and ultra-finest size coal particles. Aufbereitungs-Technik, No. 6/1985, 363–366 p.

Araújo, A.C., Peres, A.E.C. Froth flotation: relevant facts and the Brazilian case. CEMET/CNPq, Rio de Janeiro, 1995.

Araújo, A.C, Viana, P.R.M., Peres, A.E.C. Flotation machines in Brazil—columns versus mechanical cells. In: Centenary of Flotation Symposium Brisbane, QLD, 6–9 June 2005. AusIMM, Melbourne, 187–192 p.

Arnold, B.J., Terblanche, N. Froth flotation with the Turbo Froth flotation column. SME Annual Meeting, Denver, Colorado, 2001 - Feb. 26–28.

Brzezina, R., Sablik, J. The FLOKOB column flotation machine. In: Blaschke, W. S. (Ed.), Proceedings of XII International Coal Preparation Congress (ICPC), 1995.

Cordes, H. Development of pneumatic flotation cells to their present day status. Miner. Process. J. 2, 1997 - 69–82 p.

Cusack, B.L., Oley, M.W. Operation of large DAVCRA cells in production and test circuits. In: The AusIMM Regional Conference, Adelaide, 1971.

Finch, J.A. Column flotation: a selected review. Part IV – Novel flotation devices. Miner. Eng. 8 (6), 1995 - 587–602 p.

Finch, J.A., Dobby, G.S. Column Flotation. Pergamon Press. Foot Jr, D.G., McKay, J.D., Keyser, P.M., 1993. In: Malhotra, D. (Ed.), New Uses of Flotation Columns, Flotation Plants. Are They Optimized. AIME, 1990 - 159–163 p., (Chapter 23).

Gomez, C.O., Finch, J.A. (Eds.). Column '96. Proceedings of an International Symposium on Column Flotation, Montreal, Quebec, Canada, Met. Soc. CIM, 1996, August 26–28 p.

Harbort, G.J., Jackson, B.R., Manlapig, E.V. Recent advances in Jameson flotation technology. Miner. Eng. 7 (2/3),1994 - 319–332 p.

Harbort, G.J., Murphy, A.S., Budod, A. Jameson cell developments at Philex Mining Corporation. In: Proceedings of 6th Mill Operators Conference, Madang. AusIMM, 1997.

Hardort, G.J., D. Clarke. Fluctuations in the popularity and usage of flotation columns – An overview. Minerals Engineering, 2017 – 17-30 p.

Heintges, S., Alizadeh, A. and Simonis, W. German Patent No. 3140966 A1: Process and flotation cell for flotation of coal and ore (translation from German), 1984.

Hu, H. Amec Foster Wheeler Shanghai Procurement Hub. Personal communication, 2015.

Hu, W., Liu, O. Design and operating experiences with flotation columns in China. In: Sastry, K.V.S. (Ed.), Column Flotation'88 – Proceedings of an International Symposium on Column Flotation, SME Annual Meeting, Phoenix, Arizona, Jan 25–28, 1988. SME, Littleton, Colorado, 35–42 p.

Imhof, R., Fletcher, M., Vathavooran, A., Singh, A. Application of IMHOFLOT G-Cell centrifugal flotation technology. J. SAIMM 107 (October), 2007 - 623-631 p.

Imhof, R., Battersby, M., Parra, F., Sanchez-Pino, S. The successful application of pneumatic flotation technology for the removal of silica by reverse flotation at the iron ore pellet plant of Compañía Minera Huasco, Chile. Proceedings of the AusIMM Centenary of Flotation Symposium, Brisbane 2005, 861–867 p.

Jungmann, A., Reilard, U.A. Investigations into pneumatic flotation of various raw and waste materials using the Allflot system. Aufbereitungs-Technik, 1988 - 363–366p.

Kawatra, S.K., Eisele, T.C. Use of horizontal baffles to reduce axial mixing in column flotation. In: Proceedings of the 12th International Coal Preparation Congress, Cracow, Poland, 1994 - 1241–1249 p.

Kiser, M., Bratton, R., Luttrell, G., Kohmuench, J., Christodoulou, L., Davis, V., Stanley, F. StackCell flotation – a new technology for fine coal recovery. In: Klima, M.S., Arnold, B.J., Bethell, P.J. (Eds.), Challenges in Fine Coal Processing, Dewatering and Disposal. SME, 2012 - 81–98 p.

Kohmuench, J.N., Mankosa, M.J., Kennedy, D.G., Yasalonis, J.L., Guy, B., Taylor, G.B., Luttrell, G.H. Implementation of the HydroFloat technology at the South Fort Meade mine. SME Annual Meeting & Exhibit. Preprint 07-072, 2007.

Kosick, G. Woodgrove Technology. Personal communication, 2015.

Luttrell, G.H., Mankosa, M.J., Yoon, R.-H. In-plant testing of microbubble column flotation. Presented at SME Annual Meeting, Denver, Colorado –February 1991, 25–28 p.

Luttrell, G.H., Kohmuench, J.N., Stanley, F.L., Davis, V.L. Technical and economic considerations in the design of column flotation circuits for the coal industry. SME Annual Meeting and Exhibit, Symposium Honoring M.C. Fuerstenau, Denver, Colorado, March 1–3, 1999. Preprint No. 99–166 p.

Lynch, A.J., Harbort, G.H., Nelson, M.G. History of Flotation, Chapter 4 –Flotation Machines, AusIMM, Melbournepp, 2010 - 93–104 p.

Markworth, L., Jaspers, W., Kottmann, J. PNEUFLOT®-Modern Flotation Technology in the 21st Century. In: SAIMM Conference, South Africa, 2007.

maxFLOT. Dual extraction column. maxFLOT promotional brochure, 2008.

McKay, Foot Jr. Recent column flotation advances. SME Annual Meeting, Salt Lake City, Utah – February 26–March 1, 1990.

Murdock, D.J. Technology development – an overview of column flotation. J. SAIMM (March), i–iii, 1991.

Murphy, A.S., Honaker, R., Manlapig, E.S.V., Lee, D.J., Harbort, G.J. Breaking the boundaries of Jameson Cell capacity. In: Membrey, W.B. (Ed.), Proceedings Eighth Australian Coal Preparation Conference. ACPS: Nelson Bay, New South Wales, 2000.

Newell, A., Gray, D., Alford, R. The application of flotation columns to gold recovery at Paddington Gold Mine, WA. In: Presented at the 13th International Precious Metals Institute Conference, Montreal, Canada, 1988.

Opperman, S.N., Nebbe, D., Power, D. Flotation at goedehoop colliery. J. SAIMM (October), 2002 - 405–409 p.

Peters, W.J., Parekh, P.K. Column Flotation Results at Powell Mountain Coal Company, ENERGEIA, vol. 3, no. 2, 1992, CAER – University of Kentucky, Centre for Applied Energy Research.

PreQuip. Promotional brochure, 2009.

Rubinstein, J.B. Column Flotation: Processes, Designs, and Practices. Gordon and Breach Science Publishers, Langhorne, PA, Basel, Switzerland, 1995.

Rubinstein, J., Badenicov, V. New aspects in the theory and practice of column flotation. In: Proc. of XIX Mineral Processing Congress, San Francisco, 23–25 October, 1995, 113–116 p.

Sastry, K.V.S. (Ed.), 1988. Column Flotation '88. In: Proceedings of an International Symposium on Column Flotation. SME Meeting. Phoenix. AZ: SMEAIME, 1988 Jan. 25–28.

Schena, G., Casali, A. Column flotation circuits in Chilean copper concentrators. Miner. Eng. 7 (12), 1994 - 1473–1486 p.

Shaw, J.M. Progress through innovation: three companies show how it's done. Can. Chem. News 1 (July), 1992.

Ventert, P.E., van Loggerenbergt, C. Modifications to the coal-preparation circuit at the Grootegeuk coal mine to improve its efficiency. J. S. Afr. Inst. Min. Metal 1992 (2), 53–61 p.

Wheeler, D.A. Column flotation – the original flotation column. Presented at the 87th Annual General Meeting of CIM, 24th April, 1985.

Wu, D., Ma, L. XPM-Series Jet Flotation Machine. XIII International Coal Preparation Congress, Brisbane, Australia, 1998 - 737–745 p.

Wu, D., Yu, Y., Zhou, G., Zhu, J., Jiang, M. A novel type of jet coal flotation machine. In: Honaker, R.Q. (Ed.), International Coal Preparation Congress 2010 Conference Proceedings, 456–465 p.

Yang, D C. Technical advantages of packed flotation columns. Column '91. CIMM, Sunbury, Ontario, 1991 - 631–643 p.

Zhou, X., Liu, J., Zhao, C., Li, X., Wang, Y. Cyclonic separation mechanism of cyclonic static micro-bubble column flotation and its application. SME Annual Meeting, Salt Lake City, Utah, Feb 24–27, 2008.

Zipperian, D.E., Svensson, U. Plant practice of the FLOTAIRE column flotation machine for metallic, non-metallic and coal flotation. In: The International Symposium on Column Flotation, AIME, Phoenix, Arizona, Jan 25–28, 1988.

This article was reviewed by Assoc. Prof. Irena Grigorova, DSc and Prof. Metodi Metodiev, DSc.

SURFACE CHEMISTRY INVESTIGATIONS OF PYRITE BEFORE AND AFTER TREATMENT BY DIFFERENT REAGENTS

Stanislav Dzhamyarov[1], Margarita Vassileva[1], Ivalina Avramova[2], Tsvetelina Ivanova[1]

[1]University of Mining and Geology" St. Ivan Rilski", 1700 Sofia, miravas@abv.bg
[2]Institute of General and Inorganic Chemistry, BAS, 1113 Sofia, iva@svr.igic.bas.bg

ABSTRACT. In order to produce high-grade copper concentrates, the depression of pyrite, accompanying the copper sulfide minerals has a significant role. In the practice of the processing plants, it is most often performed in an alkaline media, using CaO. The subsequent activation of pyrite is usually accomplished by H_2SO_4, which adversely affects the processing equipment. After its treatment with CaO; after subsequent activation by H2SO4, and after mechanical treatment of the depressed pyrite, X-ray photoelectron spectroscopy (XPS) for the purpose of studying the surface chemistry of pyrite in its natural state, was performed. Positive results were obtained for the possible application of mechanical activation of depressed by CaO pyrite, as a substitute for the aggressive sulfuric acid.

Keywords: surface chemistry, depressed pyrite, activated pyrite, H_2SO_4, mechanical treatment

ИЗСЛЕДВАНИЯ ВЪРХУ ПОВЪРХНОСТНАТА ХИМИЯ НА ПИРИТ ПРЕДИ И СЛЕД ОБРАБОТКАТА МУ С РАЗЛИЧНИ РЕАГЕНТИ

Станислав Джамяров[1], Маргарита Василева[1], Ивалина Аврамова[2], Цветелина Иванова[1]
[1]Минно-геоложки университет „Св. Иван Рилски", 1700 София, miravas@abv.bg
[2] Институт по обща и неорганична химия, БАН, 1113 София, iva@svr.igic.bas.bg

РЕЗЮМЕ. Съществено значение за получаването на висококачествени медни концентрати има депресията на пирита, съпътстващ медните сулфидни минерали. В практиката на ОФ тя най-често се извършва в алкална среда, с помощта на CaO. При последващата активация на пирита обикновено се използва H_2SO_4, което оказва неблагоприятно въздействие върху съоръженията. Проведена е рентгенова фотоелектронна спектроскопия РФС (x-ray photoelectron spectroscopy – XPS), за изучаване на повърхностната химия на пирита в естествено състояние; след третирането му с CaO; след последваща активация с H_2SO_4 и след механична обработка на депресирания пирит. Получени са положителни резултати за възможното прилагане на механична активация на депресиран с CaO пирит, като заместител на агресивната сярна киселина.

Ключови думи: повърхностна химия, депресиран пирит, активиран пирит, H_2SO_4, механична обработка.

Introduction

In order to produce a high-grade copper concentrate, the depression of pyrite, accompanying the copper sulfide minerals has a significant role. In the processing plants practice, the depression is most often performed in an alkaline medium, using lime (CaO). In many cases, a subsequent activation of the depressed pyrite is necessary, with the purpose of further processing and usually H_2SO_4 is used as an activator. Application of H_2SO_4 as an activator of the pyrite, has an adversely effect on both equipment in the processing plants and on the environment.

In order to optimize the processes of pyrite processing and recovery, one of the main ore minerals in the Chelopech Cu-Au deposit, investigations were carried out to determine the chemical composition on the surface of the mineral in its natural state and after treatment by CaO, subsequent activation by H_2SO_4, and after mechanical treatment of the depressed pyrite. The study of surface chemistry of pyrite before and after treatment with different reagents and subsequent mechanical activation was performed using X-ray photoelectron spectroscopy (XPS). Furthermore, the possibilities of applying the mechanical desorption as an activator of depressed by CaO pyrite, as a substitute for the aggressive sulfuric acid used in practice, was investigated.

Materials and methods

For the purpose of the conducted examinations, two polished square sections (plate), with size 1x1x0.5 cm, cut out of massive pyrite ore from the Chelopech Cu-Au deposit were prepared. Pyrite plates have the identical mineral composition, fine-grained and microporous structure. Optical microscopy in reflected light and quantitative X-ray microanalysis was performed to determine the chemical composition of the mineral and the content of impurities.

The optical studies of the pyrite polished plates were performed using MEIJI MT 9430 polarizing microscope, equipped with a DK 3000 digital camera. Quantitative electron microprobe analyses were performed to determine the chemical composition of pyrite and its inclusions from gangue minerals. The analyses were performed using a scanning

electron microscope (SEM) JSM-6010 Plus/LA, with an EDS spectrometer, at the UMG "St. Ivan Rilski". The accuracy of X-ray spectral analyses is in the range of ± 1%.

The laboratory experiments were conducted to study the surface chemistry of pyrite after treatment with different reagents - treatment with an alkaline solution of lime (CaO); activation with H_2SO_4 of lime-depressed pyrite (CaO + H_2SO_4); mechanical activation of CaO-treated pyrite. The experiments were performed according to the following sequence and procedure:

- A solution of 1000 ml of distilled water and 0.98 g of CaO is prepared in a beaker. The pyrite was carefully placed at the bottom of the container.
- The solution is agitated for 20 minutes with a mechanical stirrer at 300 rpm until a pH of about 12 (12.3-12.5) is reached.
- The pH of the solution was determined with the laboratory pH meter, the pyrite plate was removed and analyzed with XPS.
- H_2SO_4 is added dropwise to the CaO alkaline solution (pH of about 12), containing the depressed pyrite plate in it, , and then the solution is agitated to a pH of about 9, the plate is removed and studied by XPS.
- The pyrite plate is again treated with an alkaline solution of CaO in the manner described above.
- A mechanical activation of the pyrite plate depressed by CaO was performed and subjected to XPS.

X-ray photoelectron spectroscopy (XPS) was conducted in order to determine the surface chemistry of pyrite in its natural state and after its sequential treatment by different reagents - treatment with alkaline solution of CaO; activation with H_2SO_4 of pyrite treated by CaO; mechanical desorption of CaO-depressed pyrite.

The XPS analyses were performed on a Kratos Axis Supra spectrometer with a monochromatic AlKα source. Each analysis started with a survey scan from 0 to 1200 eV pass energy of 160 eV at steps of 1 eV with 1 sweep. For the high resolution analysis the number of sweeps was increased, the pass energy was lowered to 20 eV at steps of 100 meV.

The C1s, O1s, Fe2p, Cu2p, S2p, Ca2p photoelectron lines were recorded and the obtained spectra were discussed. The C1s photoelectron line at 284.6eV was used for calibration of recorded spectra.

All data were recorded at 90° take-off angle. High resolution spectra were collected with pass energy of 20 eV.

The obtained spectrum of the Ca2p photoelectron line was deconvoluted into components using the XPSPEAK 4.1 program.

In order to reduce the possibility of mineral oxidation in air or liquid medium, all studies were carried out on pyrite plates, but not on pyrite fractions.

Results and Disscusion

Optical microscopy investigations

Optical observations show that pyrite plates have an identical mineral composition and are made of pyrite aggregates with grainy and microporous structure. In reflected light under a microscope, in some parts of the pyrite aggregates, pyrite grains with fine zonal structure, with an alternation of light and dark zones were observed. Zonal structure of the pyrite is related to variation in the Cu content, incorporated into the pyrite structure.

Pyrite aggregates are microporous, the size of the pores and cavities varies from several μm to about 500 μm, and in some parts of the polished sections reaches even more (Fig. 1, 2). In some places in the cavities and pores in the matrix of grained, microporous pyrite fine inclusions of copper sulfosalt minerals are found such as enargite (Cu_3AsS_4) (Fig. 2) and tennantite ($Cu_{12}As_4S_{13}$). Gangue non-metallic minerals in the form of inclusions in the pyrite are represented by kaolinite and barite, filling some pores, voids or cracks in the pyrite aggregates (Fig. 2).

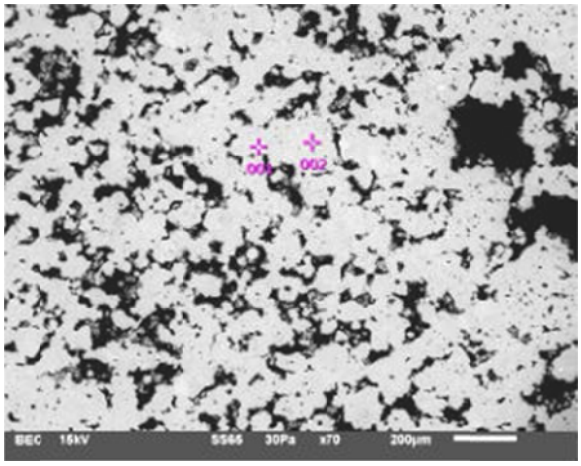

Fig. 1. Pyrite (pale grey), microporous aggregates. Backscattered electron image, SEM, Scale bar - 200 μm

The performed quantitative X-ray microanalyses showed, that pyrite composition is close to the theoretical one (Fe - 46.55%, S - 53.45%). Most of the analyzed pyrite grains contain an isomorphic impurity of Cu, which content varies and reaches 1.4% (Table 1).

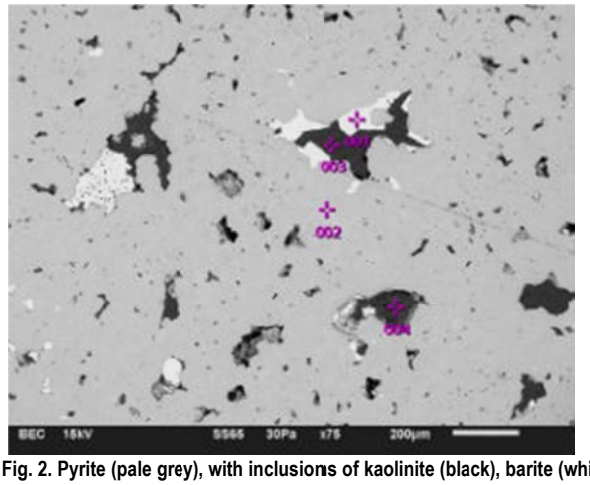

Fig. 2. Pyrite (pale grey), with inclusions of kaolinite (black), barite (white, microporous), enargite (white). Backscattered electron image, SEM, Scale bar - 200 μm

Table 1.
Electron probe microanalyses of pyrite

Analysis №	Element (wt %)			
	Fe	Cu	S	∑
1	47.05	-	52.95	100.00
2	46.44	0.73	52.83	100.00
3	45.93	1.23	52.85	100.01
4	45.46	1.40	53.14	100.00
5	46.33	0.32	53.34	99.99

Crystallo-chemical formulas of pyrite:
1. $Fe_{1.01}S_{1.99}$; **2.** $(Fe_{1.00}Cu_{0.01})_{1.01}S_{1.99}$;
3. $(Fe_{0.99}Cu_{0.02})_{1.01}S_{1.99}$; **4.** $(Fe_{0.98}Cu_{0.03})_{1.01}S_{1.99}$;
5. $(Fe_{1.00}Cu_{0.01})_{1.01}S_{1.00}$

X-ray photoelectron spectroscopy (XPS)

X-ray photoelectron spectroscopy is an extremely sensitive and non-destructive method for studying the surface chemistry of solids, because it allows obtaining information for the chemical composition and states from the surface layer with a thickness up to 5 nanometers.

X-ray photoelectron spectroscopy was performed on untreated pyrite plate in its natural state and after its subsequent treatment with different reagents.

The registered Fe2p XPS spectra of untreated pyrite and after subsequent treatment (Fig. 3) are typical for the mineral pyrite (FeS_2). The Fe2p spectra has a very strong peak at 707 eV that is typical for Fe^{2+} in the crystal lattice of pyrite (Fig. 3) (Eggleston et al., 1996; Nesbitt et al., 1998; Derycke et al., 2013). The S2p peak is located at 162.5 eV and corresponds to the disulfide ion (S_2^{2-}) in the pyrite (FeS_2) crystal lattice (Chatuverdi et al., 1996; Nesbitt et al., 1998). Some amount of isomorphic impurity from Cu, which replaces Fe^{2+} in the crystal lattice of the mineral, is present due to a low presence of Cu2p spectra. These results coincide with the data from the performed quantitative electron probe microanalysis of pyrite showing the content of structural impurities of Cu, reaching to 1.4% (Table 1).

On the surface of the pyrite there is a small amount of iron hydroxides – $Fe^{3+}OOH$ (goethite) (a peak with binding energy of 531.5 eV in the O1s spectrum) and iron oxides. The presences of sulfate or sulfur have not been found.

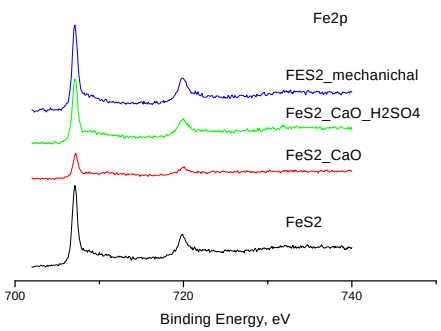

Fig. 3. Fe (2p) XPS spectra of the pyrite surface before and after treatment by CaO, CaO + H_2SO_4, and after treatment by CaO + subsequent mechanical activation

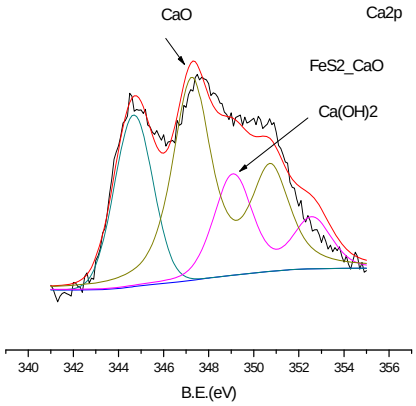

Fig. 4. Ca (2p) XPS spectrum of the pyrite surface after treatment by CaO

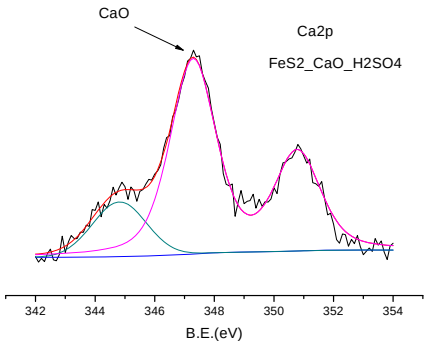

Fig. 5. Ca (2p) XPS spectrum of the pyrite surface after treatment by CaO + H_2SO_4.

Figures 4 and 5 show the spectra of Ca2p photoelectron line of pyrite after CaO treatment as well as subsequent activation of the depressed pyrite by H_2SO_4, respectively. The same spectra were compared to the XPS spectrum recorded after mechanical activation of CaO depressed pyrite (Fig. 6).

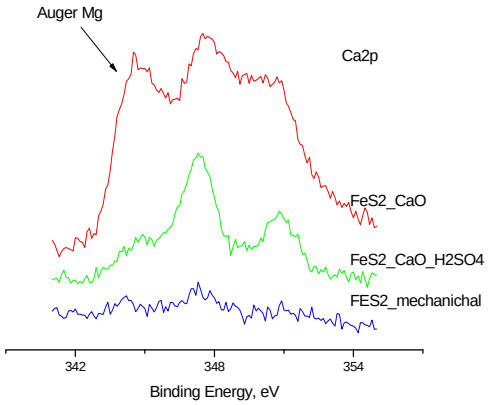

Fig. 6. Ca (2p) XPS spectra of the pyrite surface after treatment by CaO, CaO + H_2SO_4, and after treatment by CaO + subsequent mechanical activation

The obtained spectra show that after treatment of pyrite with alkaline solution of CaO, a fine coating of CaO and a subordinate amount of $Ca(OH)_2$ is found on the surface of the mineral (Fig. 4). The presence of $CaSO_4$ is not observed. The addition of H_2SO_4 leads to the dissolution and complete removal of $Ca(OH)_2$, leaving a certain amount of CaO,

probably in the voids and pores of the pyrite aggregates. (Fig. 5). After treatment of pyrite by CaO and subsequent mechanical activation by attrition, a clean pyrite surface from hydrophilic phases is achieved, and only traces of CaO have been detected (Fig. 6).

It should be noted, that after pyrite treatment with an alkaline CaO solution, the presence of Mg contained as an impurity in the lime used, is observed over the pyrite surface, so for a better interpretation of the results, the obtained spectra are subjected to deconvolution.

Surface chemistry of pyrite

The surface chemistry of pyrite is affected by a number factors such as oxidation in air or water, temperature, presence of bacteria, concentration of ferric ions Fe^{3+}, particle size, trace element content, mechanical activation when milling, etc. (Paneva et al., 2007).

According to Chatuverdi et al. (1996), the surface properties of the naturally occurring, cube face of pyrite (100) differ from the pyrite surfaces, obtained through mechanical action such as mechanical cutting, crushing, grinding. The crystallographic orientation of the pyrite cuttings it is also very important.

It was found that natural pyrite exhibits structural sensitivity to oxidation, and the octahedral crystal face (111) show greater oxidation potential than pyrite cube crystal face (100) (Guevremont et al., 1998).

Pyrite can be mechanochemically oxidized by intensive grinding, since the mechanical activation during milling leads to an increase in the specific surface area of the pyrite particles and contributes to the formation of hydrophilic phases such iron sulfates, iron oxides and hydroxides.

During the mechanical activation of the pyrite in the initial stage, transformation of the mineral into ferrous sulfate monohydrate is performed, according to the reaction: $FeS_2 \rightarrow FeSO_4.H_2O$ (szmolnokite) (Paneva et al., 2007).

Initially, in the first minutes of grinding, ferrous sulfate nuclei are formed, which subsequently form a fine layer on the activated pyrite surfaces. During long-term grinding, the amount of iron sulfate monohydrate formed is increased, as for 36 minutes about 7.1% $FeSO_4.H_2O$ is formed (Paneva et al., 2007). The oxidation of the pyrite in the initial phase is carried out by oxidation of the sulfur - S^{2-} to $S^{6.+}$.

In natural environment, pyrite exposed to air and in the presence of water is readily oxidized to ferric hydroxide $Fe(OH)_3$, according to the following scheme:

$FeS_2 + nO_2 + mH_2O \rightarrow FeSO_4 \rightarrow Fe_2(SO_4)_3 \rightarrow Fe(OH)_3 + H_2SO_4$.

The ferric hydroxide $Fe(OH)_3$ is deposited as a gel which is dehydrated and converted to FeOOH (goethite) and/or other iron oxides.

According to Cai et al., (2009) pyrite oxidized easily in air and aqueous media. The oxidized productsthat are formed on the pyrite surfaces are different, depending on the pH of the medium, and under alkaline conditions Fe^{3+}oxyhydroxides the only oxidizing product, which is formed on the pyrite surface.

The chemical nature of the phases, deposited on the pyrite surface during the processes of depression, reactivation and flotation of the pyrite, is dependent on a number of factors such as: the type of ore grinding (dry or wet), grain size, reagent type, pH of the medium, dissolved oxygen content, chemical composition and presence of impurities in the pyrite, etc.

In the processing and flotation of copper ores in the processing plants, such as pyrite depressant in alkaline conditions, predominantly lime (CaO) is used. It has been widely accepted that in alkaline conditions pyrite surfaces are mainly covered with hydrophilic species – iron oxides and hydroxides – $Fe(OH)_3$, $Fe(OH)_2$ or α-$Fe^{3+}OOH$ (goethite). However, studies by some authors show, that in alkaline environments on the pyrite surfaces sulfates are often deposited - $Fe_2^{3+}(SO_4)_3$ or $Fe_2^{3+}(SO_4)_3.9H_2O$ (coquimbite) and $Fe^{2+}SO_4$ or $Fe^{2+}SO_4.7H_2O$ (melanterite) (Mermillod-Blondin et al., 2005). The ratio Fe^{2+}/Fe^{3+} on the pyrite surface, depends mainly on the pH of the medium and the particle size, respectively variations in surface chemistry of the mineral particles are observed at different pyrite particle sizes.

It was found that after dry grinding the spatial distribution of oxidation products on the pyrite surfaces is non-uniform. Slightly oxidized zones of several nanometers (nm), located between zones with a higher degree of oxidation with thickness of several tens of nanometers (nm), forming pillar shaped aggregates, are observed. Oxidation products with pillar structure show heterogeneous composition and are built by iron sulfates, hydroxides and hydrated iron oxides (De Donato et al., 1993, 1998; Mermillod-Blondin et al., 2005). Hydrated ferrous sulfates predominate at the base of the pillars, at the top part ferric sulfates dominate, and in the central part there is a skeleton of iron hydroxides and hydrated iron oxides. Many observations on various oxidized pyrite surfaces have confirmed the presence of pillar shaped oxidation products of different thickness amid a quasi un-oxidized pyrite surface.

The published data in the literature for the Ca-bearing species, adsorbed onto lime-depressed pyrite surfaces are contradictory. The phases $Ca(OH)_2$, CaO, $CaCO_3$, $CaSO_4$ have been established by the different authors (Mermillod-Blondin et al., 2005).

According to Xiaojun and Kelebek (2000), the hydrophilic phases on the pyrite surfaces after treatment with lime are predominantly CaO, $CaSO_4$ and $Ca(OH)_2$, but may also include $Fe(OH)_3$. The same authors carried out studies on a pyrite fraction of 100-200 mesh (149-74 μm). It was observed that on the surface of lime depressed pyrite particles, besides the Ca oxide and hydroxide, a certain amount of $CaSO_4$ is deposited as a result of the reaction of Ca^{2+} from the solution with SO_4^{2-} ions from the oxidized pyrite surfaces. The pyrite is easily oxidized, with the smaller size of the analyzed pyrite particles favoring the oxidation processes. On the other hand, at a higher pH of the medium, as a result of oxidation of pyrite the deposition of ferric hydroxide Fe $(OH)_3$ is easily achievable.

The presence of a fine hydrophilic coating on the pyrite reduces the flotation kinetics of the mineral.

The results of the present studies applying XPS, show a fine CaO and Ca $(OH)_2$ coatings on the pyrite surface during the treatment of a pyrite plate by CaO (Figure 4). Presence of $CaSO_4$ and Fe $(OH)_3$ was not observed. With the mechanical activation by attrition, removal of hydrophilic phases on pyrite surface could be achieved, and barely traces of CaO being recorded.

The presented studies on pyrite surface chemistry, before and after treatment by different reagents, were carried out on polished pyrite plates, to limit the possibility of oxidation of the mineral in air and liquid media. In real conditions during the processing and flotation of copper ores in the processing plants, the much smaller size of the pyrite particles and their greater specific surface area will contribute to the formation of oxidation products on the pyrite particles. The obtained positive results related to the use of mechanical treatment as activator of depressed by CaO pyrite, can be confirmed by conducting semi-industrial experiments, with the aim of applying the mechanical activation as a substitute of the commonly used sulfuric acid.

References

Cai, Y., Y. Pan, J. Xue, G. Su. Surficial phase-identification and structural profiles from weathered natural pyrites: A grazing-incidence X-ray diffraction study.- Applied Surface Science, 255, 2009. - 4066-4073.

Chaturvedi, S., R. Katz, J. Guevremont, M. A. A. Schoonen, D. R. Strongin. XPS and LEED study of a single-crystal surface of pyrite. – American Mineralogist, 81, 1996. - 261-264.

Derycke, V., M. Kongolo, M. Benzaazoua, M. Mallet, O. Barres, P. De Donato, B. Bussiere, R. Mermillod-Blondin. Surface chemical characterization of different pyrite size fractions for flotation purposes. – International Journal of Mineral Processing, 118, 2013. - 1-14.

De Donato, P., C. Mustin, R. Benoit, R. Erre. Spatial distribution of iron and sulphur species on the surface of pyrite. - Applied Surface Science, 68, 1993. - 81-93.

De Donato, P., M. Kongolo, J. Yvon, O. Barres, J. M. Cases, R. Benoit. Effect of mechanical fragmentation on surface composition of sulfides. – Industrie Minerale Mines et CarriPres – les techniques, September, 1998. -27-31.

Eggleston, C. M., J. J. Ehrhardt, W. Stumm. Surface structural controls on pyrite oxidation kinetics: An XPS-UPS, STM, and modelling study. – American Mineralogist, 81, 1996. - 1036-1056.

Guevremont, J. M., A. R. Elsetinow, D. R. Strongin, J. Bebie, M. A. A. Schoonen. Structure sensitivity of pyrite oxidation: Comparison of the (100) and (111) planes. – American Mineralogist, 83, 1998. – 1353-1356.

Mermillod-Blondin, R., M. Kongolo, P. De Donato, M. Benzaazoua, O. Barres, B. Bussiere, M. Aubertin. Pyrite flotation with xanthate under alkaline conditions – application to environmental desulfurisation. – Centenary of Flotation Symposium, Brisbane, QLD, 6-9 June, 2005.- 683-692.

Nesbitt, H. W., G. M. Bancroft, A. R. Pratt, M. J. Scaini. Sulfur and iron surface states on fractured pyrite surfaces. - American Mineralogist, 83, 1998. -1067-1076.

Paneva, D., D. Mitova, E. Manova, H. Kolev, B. Kunev, I. Mitov. Study of initial stage of mechanochemical transformation in pyrite. – Journal of Mining and Metallurgy, 43B, 2007. - 57-70.

Xiaojun, X., S. Kelebek. Activation of xanthate flotation of pyrite by ammonium salts following its depression by lime. – In: Proceedings of the XXI International Mineral Processing Congress (ed: P. Massacci), Elsevier, Rome, 2000. - C8b 43-C8b50.

This article was reviewed by Assoc. Prof. Dr. Ivan Nishkov and Prof. Metodi Metodiev, DSc.

GYPSUM SCALE FORMATION IN HYDROMETALLURGICAL OPERATIONS AND FLOTATION

Stanislav Dzhamyarov

University of Mining and Geology "St. Ivan Rilski", 1700 Sofia, Department of Mineral Processing and Recycling
E-mail: inishkov@gmail.com

ABSTRACT. The presence of gypsum scale formations on the technological equipment surfaces is a common problem in industrial technological processes. The scale formations contaminate equipment surfaces, reducing the processes' effectiveness and cause higher maintenance costs. The paper presents the results of a study on the scale formation in machinery and equipment, used in hydrometallurgical operations and flotation, as well as technological possibilities for their elimination.

Key words: scale formations, hydrometallurgical operations, flotation

ОБРАЗУВАНЕ НА ГИПСОВИ ОТЛАГАНИЯ ПРИ ХИДРОМЕТАЛУРГИЧНИ ОПЕРАЦИИ И ФЛОТАЦИЯ НА РУДИ

Станислав Джамяров
Минно-геоложки университет "Св. Иван Рилски", 1700 София, катедра „Обогатяване и рециклиране на суровини"
E-mail: inishkov@gmail.com

РЕЗЮМЕ. Наличието на гипсови отлагания върху повърхности на технологично оборудване е често срещан проблем при промишлени технологични процеси. Гипсовите отлагания замърсяват повърхностите на оборудването, намаляват ефективността на процесите и са причина за повишаване разходите за поддръжка. В доклада е представено извършеното проучване на формирането на гипсови отлагания в машини и съоръжения, използвани при хидрометалургични операции и флотация на руди, както и технологични възможности за елиминирането им.

Ключови думи: гипсови отлагания, хидрометалургични операции, флотация на руди

Introduction

Scale formation or deposition of inorganic salts from aqueous solutions onto surfaces is a widespread problem in many industrial processes. These formations can be hard, crystalline and strongly adherent deposits, or soft porous, loosely held sludge (Hasson, 1981). Scale formation is an issue because it fouls equipment surfaces, reducing process efficiency and increasing maintenance costs. Industries and processes where scale formation is most common include oil and gas production, geothermal energy production, desalination operations, steam generation, heat transfer systems, water supply systems as well as hydrometallurgical and flotation operations.

The main objective of the paper is to review the gypsum scale formation in machinery and equipment, used in hydrometallurgical and flotation operations, as well as to identify possible technological approaches for the elimination of these formations.

Gypsum scale formation in hydrometallurgical operations

In hydrometallurgical operations, a wide variety of scale formations are commonly encountered. High temperatures and high ionic strengths make their formation unavoidable .One example is the formation of hematite and alunite scales on autoclave walls during high temperature leaching of nickeliferous laterites. (Perdikis, 1996). Another example from the field of hydrometallurgy is the formation of calcium sulfate scales, mostly dihydrate ($CaSO_4.2H_2O$), but also semihydrates ($CaSO_4.1/2H_2O$) and anhydrite ($CaSO_4$), depending on the temperature and operating conditions.

Due to the very low solubility of the calcium sulfate hydrates, the scales are deposited almost anywhere where calcium and sulfate are present in aqueous solutions. The result is fouled reactor walls, impellers and pumps, as well as clogged pipes. Gypsum scales are formed even at low pH and can only be removed mechanically (Nulty, 1991)

The largest occurrence of gypsum scale formations in hydrometallurgical operations is during the partial or total neutralization of acidic leach solutions with limestone ($CaCO_3$) and lime (CaO).The reactions are:

$$H_2SO_4 + CaCO_{3(S)} + H_2O \rightarrow CaSO_4.2H_2O_{(S)} + CO_{2(G)} \uparrow \quad (1)$$

$$H_2SO_4 + CaO_{(S)} + H_2O \rightarrow CaSO_4.2H_2O_{(S)} \quad (2)$$

Since the reactors operate at atmospheric pressure and temperature below 90°C, gypsum ($CaSO_4.2H_2O$) is the primary reaction product. Under these conditions, gypsum is the precipitating phase. (Hand, 1997; Ostroff, 1964; Posnjak, 1938).

In the treatment of nickeliferous laterite ore both partial and total neutralization stages are required. A simplified process flowsheet of the process is given in Figure 1.

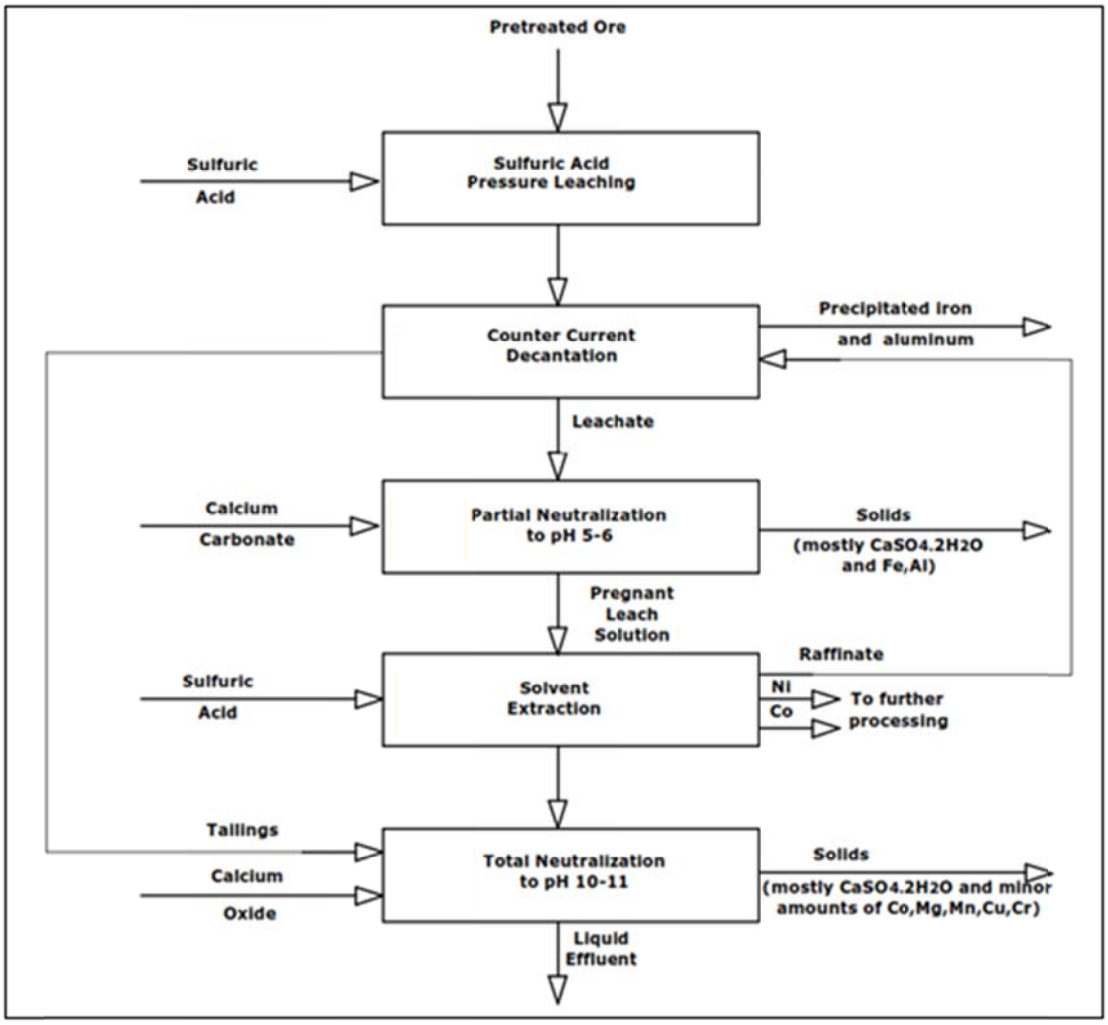

Fig. 1. Simplified process flowsheet of nickeliferous laterite ore treatment

The neutralization (reaction 1) takes place right after the high-temperature laterite leaching. The autoclave effluent is in the form of slurry and contains precipitated iron and aluminium, as well as dissolved iron, aluminium, nickel, minor amounts of cobalt, magnesium, manganese, chromium, copper, some trace impurities and free sulfuric acid. The leach slurry temperature and pressure are first reduced and then it is subjected to the counter current decantation (CCD) stage (Perdikis, 1996). Further, the liquid phase leaving the CCD is partially neutralized to a pH of 5-6 with limestone (reaction 1) to precipitate the remaining in solution iron, aluminium and sulfate, and to adjust the pH for subsequent nickel/cobalt treatment steps.

From the partial neutralization step, the resulting slurry is again separated and the pregnant leach solution continues to a solvent extraction operation, while the residue containing solid gypsum, iron, and aluminium is sent to waste impoundment.

The recovered leach solution, containing target nickel and cobalt metals is directed to the solvent extraction stage. The metals are extracted using an appropriate solvent extractant followed by stripping with sulfuric acid and further processing for nickel and cobalt recovery. The solvent extraction raffinate is sent to a final total neutralization stage (reaction 2) to neutralize the sulfuric acid and to precipitate out all of the remaining metal ions.

The issue of gypsum scale formation occurs in both neutralization stages. It leads not only to gypsum precipitation in the bulk solution, but also to scale deposition on reactor surfaces and in pipes around the reactors.

Gypsum scale formation in flotation

In the flotation of polymetallic sulfide minerals, especially complex sulfide ores the pyrite can only be depressed at very high additions of lime. The best pH range for pyrite depression is between 10 and 12.The high pH and oxidizing atmosphere leads to formation of calcium hydroxide and calcium sulfate at the pyrite surface. At high pH formation of iron (III) hydroxide also occurs. These hydrophilic species account for the complete depression of pyrite by lime treatment. The activation flotation of the lime depressed pyrite is to remove these hydrophilic coatings. Sulfuric acid is the main activator for the flotation of depressed pyrite, however it causes environmental and scale formations problems due to the large additions of sulfuric acid required.

Figure 2 shows the addition points of slaked lime and sulfuric acid in DPM Chelopech flotation plant and Figure 3 – gypsum scale formations in the DPM Chelopech flotation plant equipment.

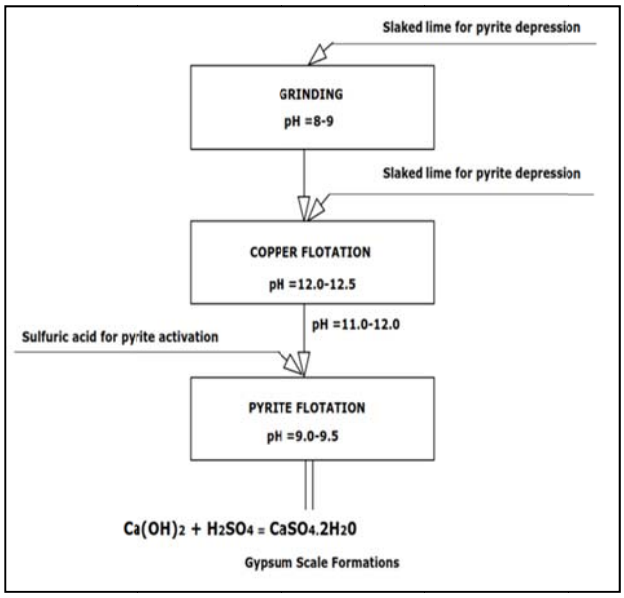

Fig. 2. Addition points of slaked lime and sulfuric acid in DPM Chelopech flotation plant

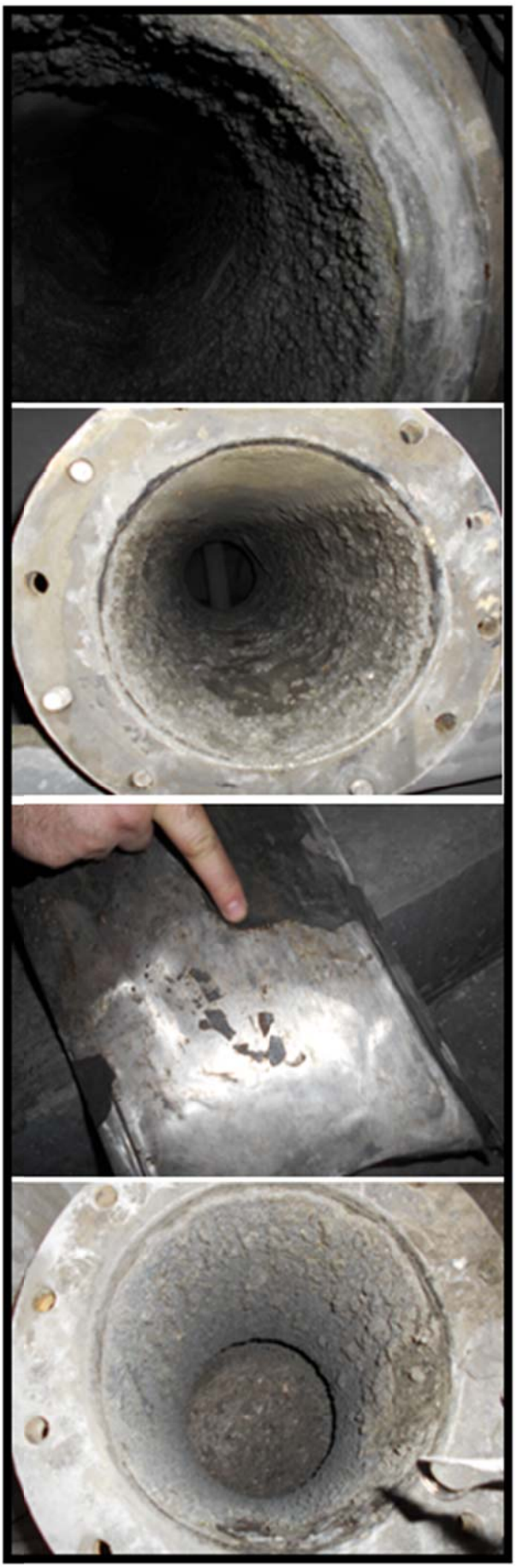

Fig. 3.Gypsum scale formations in the DPM Chelopech flotation plant equipment

Gypsum scale formation mechanism

In order to understand the mechanism of gypsum scales formation, it is necessary to review the fundamental crystal theory, which includes crystal precipitation, nucleation, and growth theory.

Crystal precipitation

Precipitation is defined "as reactive crystallization, i.e. the production of a solid compound out of a solution via a chemical reaction"(Dirksen, 1991).

Nucleation

If the saturation ratio S is above 1, the first stage of crystal formation commences. This stage is called nucleation and it has three main categories: (1) primary homogeneous, (2) primary heterogeneous and (3) secondary heterogeneous.

Primary homogeneous nucleation occurs in bulk solution, in the absence of a solid interface (Dirksen, 1991). This is done through solute molecules combining to form nuclei. These nuclei either reach a critical size above which they are stable, or dissolve back into solution. Homogeneous nucleation occurs at relatively high values of S, because the interfacial energy between the crystal and the solution is relatively high, and therefore a substantial driving force is necessary for it to occur (Stumrn, 1992)

Primary heterogeneous nucleation occurs in the presence of an external surface. Nuclei form on a solid surface such as grime, reactor or pipe walls, colloidal particles, etc. In this case, the interfacial energy between the crystal and the solid is less than the interfacial energy between the crystal and solution. Thus, primary heterogeneous nucleation occurs at lower values of S than primary homogeneous nucleation. (Dirksen, 1991; Stumrn, 1992).

Secondary heterogeneous nucleation occurs on seed particles of the same composition and phase as the precipitating ones. When these seed particles are purposefully added to the solution to induce precipitation, it is called apparent secondary nucleation. When the seed consists of fragments of crystals that are already present in the solution, it is called true secondary nucleation. And when the seed is formed from crystals breaking due to collisions with other crystals, reactor walls, or impellers, it is called contact secondary nucleation (Perdikis, 1996). The interfacial energy between particles of the same composition and phase is generally relatively low, so the secondary heterogeneous nucleation occurs even at low values of S. (Hasson, 1981; Perdikis, 1996).

The nucleation can arise via several different mechanisms, depending on the degree of saturation and operating conditions. Primary homogeneous nucleation occurs only at higher levels of the saturation ratio, primary heterogeneous nucleation occurs at lower values of the saturation ratio, and secondary heterogeneous nucleation at even the lowest values of saturation ratio if there is seed present. This is presented in Figure 4, which shows a general plot of normalized nucleation rate vs. saturation ratio S (Perdikis, 1996).

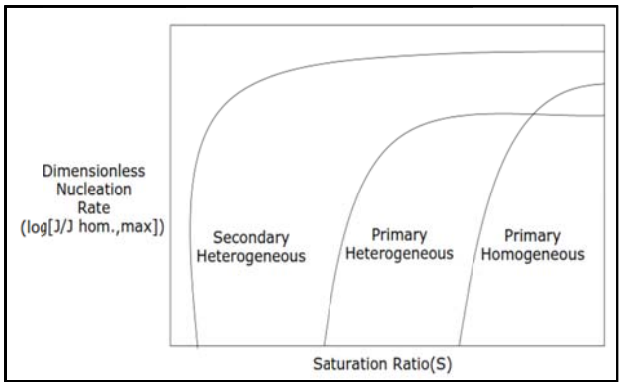

Fig. 4. Nucleation rate vs. saturation ratio S

As a result, it can be expected that primary heterogeneous nucleation would occur on the equipment surfaces, followed by secondary heterogeneous nucleation which would lead to a scale growth.

Crystal Growth

Crystal growth is critical to scale formation. It occurs via the incorporation of solvated solute molecules called growth nits, into step or bend sites on the crystal surface (Dirksen, 1991).The growth is accomplished by the eight-step process given in Figure 5:

1) Transport of the growth unit from the bulk solution to the crystal surface.
2) Adsorption on the crystal surface.
3) Lateral diffusion over the surface.
4) Attachment to a step.
5) Diffusion along a step.
6) Integration into the crystal at a bend site.
7) Diffusion of solvent molecules away from the crystal surface.
8) Release of heat of crystallization and its transport away from the crystal.

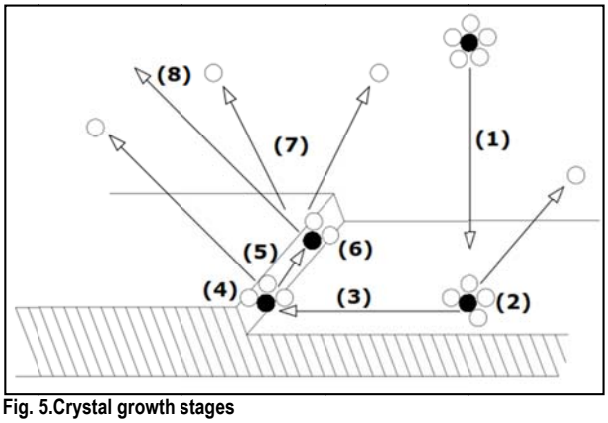

Fig. 5.Crystal growth stages

Besides the saturation ratio, there are some other factors that can affect crystal growth and thus, scale formation. These factors include temperature, matrix anion effects, impurity effects, presence of seed crystals and surfactants.

Conclusion

Based on the research studies carried out, it was found that as soon as formed on the industrial equipment surfaces, gypsum scale formations can only be effectively removed mechanically.

Regardless of the fact that the scale formation mechanism and the factors that affect it are identified, gypsum scale formation is inevitable when calcium-containing bases such as quicklime and slaked lime, and sulfuric acid are mixed.

Once the scale formation is deposited on the equipment surface, it becomes extremely impervious to chemical removal and is only removable by most established mechanical methods, which in general are labor-intensive and costly.

In order to find viable technological approaches for the elimination of gypsum scale formation during the pyrite flotation a comprehensive research study has been initiated. The study surveys both mechanical and chemical techniques for activation of depressed pyrite.

References

Dirksen, J.A., T.A. Ring. Fundamentals of Crystallization: Kinetic Effects on Particle Size Distributions and Morphology. - Chemical Engineering Science, 46, 1, 1991. - 2389-2427.

Hand, R.J. Calcium sulphate hydrates: A review. - British Ceramic Transactions, 96, 3, 1997. -16- 120.

Hasson, D. Precipitation Fouling, Fouling of Heat Transfer Equipment, Hemisphere Publishing Corp., Washington, 1981.- 527-568.

Nulty, J.H., B.Grace, D.Cunningharn. Control of Calcium Based Scales In Australian Mineral Processing, Australian Institute of Mining and Metallurgy, Pub 1, Sec. 2, 1991. - 185-188.

Ostroff, A.G. Conversion of Gypsum to Anhydrite in Aqueous Salt Solutions. - Geochimica et Cosmochimica Acta, 28, 1964. -1363-1372.

Perdikis, P. Scale Formation in Batch Reactor under Pressure Acid Leaching of a Limonitic Laterite, M.A.Sc. Thesis, Department of Chemical Engineering and Applied Chemistry, University of Toronto, 1996.

Posnjak, E. The System $CaSO_4.2H_2O$. - American Journal of Science, 35-A, 1938. - 247-272.

Stumrn, W. Chemistry of the Solid-Water Interface, John Wiley & Sons, Inc., New York, 1992. - 211-241.

This article was reviewed by Prof. Metodi Metodiev, DSc. and Assist. Prof. Dr. Todor Angelov.

WASTE MANAGEMENT – CURRENT TRENDS

Irena Grigorova[1], Marin Ranchev[1], Teodora Yankova[1]

[1]University of Mining and Geology "St. Ivan Rilski", 1700 Sofia, Department of Mineral Processing and Recycling
E-mail: irena_mt@abv.bg

ABSTRACT. Solid industrial and municipal waste, besides an environmental problem, can also be a source of a number of valuable ingredients, in relation to which they have to be analysed in two aspects: as a sustainable development problem and as alternative raw materials. The solution of problems in solid industrial and municipal waste processing is of particular importance due to the gradual natural mineral resources depletion and the need of the full use of all waste types as useful products. In a number of countries, such as the USA, Japan, Germany, UK, Sweden, etc., most of the tasks related to the solid industrial and household waste processing have been successfully solved. This paper presents and analyses the most promising technologies for waste recovery or re-use. Numerous good practices for their implementation are known worldwide.

Keywords: solid industrial and household waste, technologies, recycling

СЪВРЕМЕННИ ТЕНДЕНЦИИ В УПРАВЛЕНИЕТО НА ОТПАДЪЦИ

Ирена Григорова[1], Марин Ранчев[1], Теодора Янкова[1]

[1]Минно-геоложки университет „Св. Иван Рилски", Катедра „Обогатяване и рециклиране на суровини", 1700 София
E-mail: irena_mt@abv.bg

РЕЗЮМЕ. Твърдите промишлени и битови отпадъци, освен екологичен проблем, могат да бъдат и източник на редица ценни съставки, във връзка с което те трябва да се анализират в два аспекта: като проблем на устойчивото развитие и като алтернативни суровини. Решението на проблемите при преработката на твърдите промишлени и битови отпадъци придобива особена значимост, поради постепенното изтощаване на природните минерални суровини и необходимостта от пълноценното използване на всички видове отпадъци, като полезни продукти. В редица държави, като САЩ, Япония, Германия, Великобритания, Швеция и др., успешно са решени повечето задачи, свързани с преработката на твърдите промишлени и битови отпадъци. Настоящата разработка представя и анализира най-обещаващите технологии за оползотворяване на отпадъци или тяхната повторна употреба. В световен мащаб са известни множество добри практики за тяхното прилагане.

Ключови думи: твърди промишлени и битови отпадъци, технологии, рециклиране.

Introduction

Urban density is rapidly increasing in line with an expanding global population. The importance of creating a sustainable legacy is now widely recognized throughout the world at every level of society – from those responsible for designing the developments of tomorrow to those who will ultimately inhabit them. Waste management has never before been such a crucial factor in achieving this legacy and is now an essential component of any long-term sustainability strategy.

Currently, world cities generate about 1.3 billion tonnes of solid waste per year. This volume is expected to increase to 2.2 billion tonnes by 2025. Waste generation rates will more than double over the next twenty years in lower income countries (Hoornweg, Bhada-Tata, 2012).

Solid wastes arise from unusable residue in raw materials, leftovers, rejects and scrap from process operations, used or scrap packaging materials and even saleable products themselves when they are finally discarded (Tchobanoglous et al., 1993).

According to the Pan-American Health Organization (2005) solid or semi-solid waste generated in population centers including domestic and commercial wastes, as well as those originated by the small-scale industries and institutions (including hospitals and clinics); market street sweeping, and from public cleansing.

Solid waste management includes control of generation, storage, collection, transport or transfer, processing and disposal of solid waste materials in a way that best addresses the range of public health, conservation, economics, aesthetic, engineering and other environmental considerations (LeBlanc, 2017).

The selection of treatment technology and disposal of solid waste vary from one country to another and depends on the types of waste, composition, infrastructure, land availability, labour, economic aspects, recycling strategy, public awareness, calorific value of waste, energy availability and demand, and environmental impact (Agamuthu, 2001; Samah et al., 2005). The ecological merits of resource conservation and recycling became an area of growing interest.

New technologies are continuously developing in the urban infrastructure and improving the environment. Yet the principal of waste management has remained unchanged since the 19th century.

The last two decades have brought a new challenge for waste management: the growing vagaries of global secondary materials markets.

Rogoff (2014) reports that over the past several decades, the variety of technologies, and their ability to recover more of the incoming waste stream than ever before, has been a significant improvement in recycling management. This trend has enabled recycling coordinators to help implement programmes with the objective of increasing the diversion of potentially recyclable materials from landfills and waste-to-energy facilities. Better designs of materials recovery facilities and the addition of specialized equipment are improved recovery of fiber, plastics, and metals, thereby improving the overall economics and reducing the residues for plant operators (Rogoff, 2014).

This paper provides a summary of the priorities technologies for solid waste processing. A large number of research papers are reported in solid waste recycling area. The main focus of this paper is to survey the state of the art techniques for solid waste management.

Waste management

Waste treatment and disposal methods

Waste treatment and disposal methods are selected and used, based on the form, composition, and quantity of waste materials (LeBlanc, 2017). Table 1 briefly summarizes and presents the major methods.

Table 1.
Waste treatment and disposal methods (adapted from LeBlanc, 2017)

Methods	*Waste treatment process*	*In brief*
Thermal waste treatment (refers to the processes that use heat to treat waste materials)	Incineration	One of the most common waste treatments. Involves the combustion of waste material in the presence of oxygen. Used as a means of recovering energy for electricity or heating. *Advantages:* quickly reduces waste volume, lessens transportation costs and decreases harmful greenhouse gas emissions.
	Gasification and pyrolysis	Two similar methods, both of which decompose organic waste materials by exposing waste to low amounts of oxygen and very high temperature.
	Open burning	Environmentally harmful.
Dumps and landfills	Sanitary landfills	The most commonly used waste disposal solution.
	Controlled dumps	More or less the same as sanitary landfills.
	Bioreactor landfills	The result of recent technological research. These landfills use superior microbiological processes to speed up waste decomposition.
Biological waste treatment	Composting	Frequently used waste disposal or treatment method, which is the controlled aerobic decomposition of organic waste materials by the action of small invertebrates and microorganisms. The most common techniques include *static pile composting, vermin-composting, windrow composting and in-vessel composting*.
	Anaerobic digestion	Also uses biological processes to decompose organic materials, however, uses an oxygen and bacteria-free environment to decompose the waste material where composting must have air to enable the growth of microbes.

Waste technologies

Saleem et al. (2016) reviewed latest technologies of waste management from storage, collection, recycling, processing, energy recovery and final disposal. The following Table 2 summarizes information based on Saleem et al. (2016) research.

Table 2.
Waste management technologies

Management system	*Technology*
Collection and transport	Underground collection system
	Web based on geographic information system technology
	Waste bin monitoring technology using Global System of Mobile
	Compact garbage collection trucks
Segregation and sorting	Multi-compartment bins
	Optical sorting
	Automatic Bottle Sorting

	System
	Automated Sorting
	Mechanical Biological Treatment (MBT)
Recycling	Deinking Technology for paper recycling
	Biodegradable and degradable plastic
	Cullet remanufacturing
Processing	Autoclaving
	Fluffing
	Melting technology
	Incineration
	Vermicomposting
Energy recovery	Thermal Conversion: *Plasma Gasification and plasma pyrolysis; Refuse Derived Fuel (RDF); Fluidized Bed Technology.*
	Bio-conversion: Dry Anaerobic Composting
Disposal	Sanitary Landfill
	Bioreactor Technology
	Landfill gas recovery technologies (*Microturbine and Fuel cell Technologies)*

Serious environmental degradation occurs due to open, uncontrolled and poorly managed waste dumping in many cities of developing countries. Municipal solid waste sustainable management can reduce the short and long term environmental and human health hazards. The proper implementation of latest technologies in the sector of MSW management can play a very important role in providing pollution free and sustainable environment (Saleem et al., 2016).

Waste-to-energy (WTE) technologies

Seltenrich (2016) observes that three thermal waste-to-energy (WTE) technologies seek to turn municipal solid waste from a burden to an asset. Adherents of these technologies (gasification, plasma gasification, and pyrolysis) they produce fewer toxic emissions and virtually eliminate landfilling. Today, 70 mass-burn plants in 21 states consume about 13% of the USA waste, down from a peak of 14.5% in 1990. Cumulatively they offer roughly 2.5 gigawatts of power in return, less than a tenth of what the U.S. solar industry produces (EPA, 2014, 2015).

Waste gasification technology is recognized as an alternative thermal treatment technology. Gasification, plasma gasification, and pyrolysis involve the super-heating of a feedstock - be it municipal solid waste, coal, or agricultural residues - in an oxygen-controlled environment to avoid combustion. The primary differences among them relate to heat source, oxygen level, and temperature, from as low as about 300°C for pyrolysis to as high as 11 000°C for plasma gasification. In these low-oxygen environments the production of dioxins and furans from waste can be significantly reduced compared with incineration, with emissions potentially falling even below detection limits (Stringfellow, 2014).

Conversion technologies are further distinguished from conventional solid waste incineration by the production of synthesis gas composed mainly of hydrogen and carbon monoxide, a product of the thermal reactions that take place during the processes. The synthesis gas can then be burned in a boiler system to generate electricity. It can also be processed into fuel for an efficient, low-emissions natural gas generator or refined into other valuable products.

Incinerators produce significant amounts of a waste called bottom ash, of which about 40% must be landfilled. The remaining 60% can be further treated to separate metals, which are sold, from inert materials, which are often used as road base. The newer technologies, by contrast, offer immediate recovery of metals and inert slags, with smaller volumes of landfill. This explains why conversion technologies have caught on in regions where landfill space is extremely tight or available at a premium (Arena, 2015; Arena, Gregorio, 2013; Seltenrich, 2016)

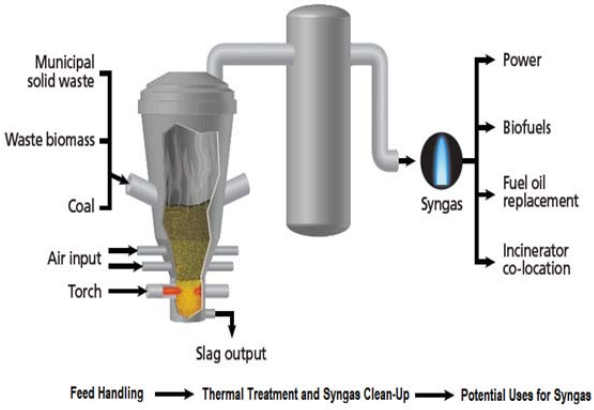

Fig. 1. Technologies work scheme (Stringfellow, 2014)

Municipal solid waste (MSW) is a mix of all kinds of materials: not just combustible carbon-based materials but also glass, metals, and more. Proponents of a decades-old philosophy called “zero waste” contend that at least 80% of the typical MSW stream can be recycled or composted (e.g. through anaerobic digestion), and that reuse and waste prevention can reduce the remaining portion - if not all the way to zero (Stringfellow, 2014).

Waste sorting innovations

Gundupalli, Hait and Thakur (2017) reviewed recent advances in physical processes, sensors, and actuators used as well as control and autonomy related issues in the area of automated sorting and recycling of source-separated municipality solid waste.

The authors (Gundupalli et al., 2017) observed that most of the research advances in the area of automated waste sorting systems have taken place in developed countries. In developed countries, source segregation of waste into recyclables is very common. Therefore, most of the automated

waste sorting systems have been designed and are suitable only for the automated sorting of source-segregated waste. In contrast to this, source segregation is usually not implemented in developing countries due to very limited door-to-door collection and lack of motivation. As a result, the collected waste is in mixed form and is later dumped in landfill sites. After this, waste sorting is performed manually and exposes involved workers to toxic and pathogenic work environment. Therefore, a need exists to facilitate the workers involved in mixed waste sorting with automated tools to improve safety and efficiency (Paulraj et al., 2016; Takemura et al., 2006).

Plastic solid waste (PSW) recycling

Years of research, study and testing have resulted in a number of treatment, recycling and recovery methods for PSW that can be economically and environmentally viable (Howard, 2002).

PSW treatment and recycling processes could be allocated to four major categories (Mastellone, 1999): re-extrusion (primary), mechanical (secondary), chemical (tertiary) and energy recovery (quaternary). Each method provides a unique set of advantages that make it particularly beneficial for specific locations, applications or requirements. Mechanical recycling (i.e. secondary or material recycling) involves physical treatment, whilst chemical recycling and treatment (i.e. tertiary encompassing feedstock recycling) produces feedstock chemicals for the chemical industry. Energy recovery involves complete or partial oxidation of the material (Troitsch, 1990), producing heat, power and/or gaseous fuels, oils and chars besides by-products that must be disposed of, such as ash (Al-Salem et al., 2009).

Integrated solid waste management (ISWM)

LeBlanc (2016) published a comprehensive review on ISWM. An efficient ISWM system considers how to reduce, reuse, recycle, and manage waste to protect human health and the natural environment. ISWM is based on the hierarchy of waste management: reduce, reuse, and recycle. ISWM represents a contemporary and systematic approach to solid waste management. The functional elements of ISWM include source reduction, recycling and composting, waste transportation and landfilling (LeBlanc, 2016).

Actually, Bulgaria is also putting its waste management system up to best practice standards. The European Investment Bank has helped the capital city of Sofia successfully develop an integrated waste management system that turns waste into a resource. Today, about 60% of the waste in Sofia is composted, recycled or energetically recovered. By diverting the biodegradable materials away from landfills, these facilities help to limit greenhouse gas emissions that contribute to climate change. In addition, the waste management system also re-injects valuable materials back into the economy; thus contributing to the circular economy, saving energy, and avoiding the production of greenhouse gases.

The key components of the Sofia Municipality ISWM are landfill for non-hazardous waste "Sadinata", mechanical and biological treatment plant for Refuse Derived Fuel (RDF) production, placed also on "Sadinata" landfill, "Han Bogrov" installation for biological treatment and installation for anaerobic digestion of biowaste, part of the installation for biological treatment "Han Bogrov".

The treatment process incorporates state of the art technologies making the mechanical and biological treatment plant (MBT) one of the most modern MSW facilities in Europe. MSW are received and treated through process lines which are fully automated and optimized according to the special characteristics of the input waste and are designed for residue minimization and product maximization.
The products are recyclable materials, high quality Refused Derived Fuel (RDF) and non-standard compost (CLO) while residue is material suitable for sanitary landfilling.

The construction and operation of the MBT Facilities is in full compliance with the European legislation regarding waste management and environmental regulations. The technical solution applied achieves minimization of the residues that needs to be diverted to landfill, production of useful by-products, avoidance of hazardous residuals, minimization of CO_2 emissions and positive carbon footprint.

Urban waste management underground solutions

Kaliampakos and Benardos (2013) note that the utilization of subsurface space is nowadays a key issue towards attaining an environmental friendly and sustainable development, especially in urban areas. Thus, activities or infrastructures that are difficult, impossible, environmentally undesirable or even less profitable to be installed above ground can be relocated underground releasing valuable surface space for other uses and enhancing urban living conditions. Hence, the management of waste through underground developed infrastructure can be looked as an important evolution which would allow for the efficient and cost-effective tackling of one of the more pressing needs of modern society.

Rising waste volumes, increased hygienic and amenity demands as well as environmental considerations impose additional requirements to the waste management system that traditional management schemes are either unable to meet or come across with increased operating cost figures. The utilization of the subsurface space can provide the setting for the development of infrastructure which is capable of addressing in a more efficient manner the limitations of existing waste management schemes (Kaliampakos, Benardos, 2013).

Automated vacuum (pneumatic) waste collection systems (AVAC) provide an integrated framework for the tackling of the waste handling problem. Table 3 presented the major advantages and disadvantages of the underground AVAC system.

Table 3.
Underground AVAC system advantages and disadvantages (Kaliampakos, Benardos, 2013)

Advantages	*Disadvantages*
Minimized operation cost and long term savings	Heavy construction operations needed requiring high investment costs
Ability to collect apparently all waste streams	Cannot collect large items, bulky wastes, WEEE and has difficulties with glass wastes
Flexible system with the ability to easily adopts to changes	After installation the flexibility of the system is reduced
Minimized usage of garbage collection trucks in urban areas	Truck transportation is not eliminated
Minimized noise, aesthetic pollution and odour problems	Risk of problems related to pipe blockages
Release of surface space for community needs or development	Public willingness and training to proper disposal required
Enhanced safety for collection workers (hygiene, accidents, etc.)	Experienced workforce is required

Table 4 provides some examples of cities that utilize underground waste collection systems.

Table 4.
Cities that utilize underground AVAC systems

Country/City	*Comments*
Roosevelt Island (NY, USA)	AVAC was commissioned in 1975 and since then it has handled 10 tons of waste on a daily basis from the island's 16 apartment complexes.
Disney World (FL, USA)	Was put into operation in the early 1970's and was the first underground waste collection scheme ever employed in the United States. The systems operate on a 24 hour basis and transport the waste from all points around the park to a central location where they are processed and recycled.
Wembley city (Great Britain)	The automated waste collection system has been operating there since 2008, handling 160 tons of waste per week.
Yas Island (UAE)	Consisting of 43 inlet points, installed around walkways or in buildings and a total of 5.3 km of pipes with a handling waste capacity of about 40 tons per day.
Abu Dhabi (UAE)	The installation of the AVAC is expected to be operational by the end of 2017.
Barcelona (Spain)	The first automated underground vacuum collection system was developed in the Olympic city (Villa Olympica) in 1992, as part of the city's renovation for the 1992 Olympic Games.
Leon (Spain)	The system handles two waste types organic waste and paper / cardboard.
Romainville (France)	The system consists of 179 inlet points and of 4.1 km of transport pipes placed 2 m below ground level.
Hammarby Sjöstad (Sweden)	One of the results of the vacuum system is that the traffic with heavy waste collection vehicles has been reduced by 60%. At the same time, residents benefit from reduced waste collection fees.
Porimao – Algarve (Portugal)	An underground collection point was introduced to the town's waste management system in 2010.
Mecca - Masjid al-Haram (Saudi Arabia)	The largest facility of its kind in the world, with a capacity of 600 tons per day, or 4,500 m^3 of waste.

According to an increasing number of experts the automated vacuum (pneumatic) waste collection systems (AVAC) provide an integrated framework for the tackling of the waste handling problem.

Conclusions

The development of many new industries has led to a sharp increase of the waste products quantities with varied origin. The proper management of these waste products by applying suitable processing technology is appropriate in terms of effective economic development. A necessary condition for achieving sustainable development and minimize environmental pollution is the technological efficiency of processing technology. The problems of economic development and environmental protection are inextricably connected, and the current and future generations life quality depends on their resolution. To protect the public health and the environment from potentially harmful effects of waste is a primary objective of waste management.

The disposal methods such as landfilling were insufficient to the waste problems tackle. The modern municipal solid waste processing plants are complexes of technologies and installations for the separation, disposal, recycling and waste conversion into target products. In order to increase the plants' efficiency and reduce the impact on human health and the environment, it is necessary to achieve the most complete raw materials processing and to use proven systems of waste stream treatment.

The analysis of key trends that may determine waste management future indicated that in recent years, rapid development has shown waste-to-energy technologies with energy recovery and the waste products processing in alternative fuels replacing natural gas, oil and coal.

Our survey demonstrated that the main waste management and recycling trends are as follows:

- Energy production from waste is the biggest trend.
- Some of the new ways through which wastes are being transformed into energy with no harm to the environment are incineration, gasification and anaerobic digestion. Newly designed incinerator

models are being used to trap methane from decomposing waste and turning it into renewable energy.

- Carrying out prior planning to reduce the amount of waste generated per activity. A lot of waste comes from using more than the required amounts of raw materials.
- Waste sorting technological advancements, where machines can separate the different recyclable materials at recycling plants.

There is no doubt that the waste management and recycling requires global efforts. The easier method of waste management is to reduce waste materials creation.

References

Al-Salem, S.M., P. Lettieri, J. Baeyens, Recycling and Recovery routes of plastic solid waste (PSW): A review, Waste management, 29, 10, 2009. - 2625-2643.

Arena, U., et al., A life cycle assessment of environmental performances of two combustion- and gasification-based waste-to- energy technologies. Waste Manage, 41, 60 - 74, DOI:10.1016/j. wasman. 2015.03.041.

Arena, U., D. Gregorio, Element partitioning in combustion- and gasification-based waste-to-energy units. Waste Manage 33, 5, 1142–1150 (2013), doi:10.1016/j.wasman.2013.01.035.

EPA. Advancing Sustainable Materials Management: Facts and Figures 2013. EPA530-R-15-002 Washington, DC:U.S. Environmental Protection Agency (2015). available at: https://www.epa.gov/smm/advancing-sustainable-materials-management-facts-and-figures-report (accessed 20 May 2016).

EPA. Municipal Solid Waste Generation, Recycling, and Disposal in the United States: Facts and Figures for 2012. Washington, DC:U.S. Environmental Protection Agency (February 2014). Available: https:// www.epa.gov/sites/production/files/2015-09/documents/2012_ msw_fs.pdf (accessed 20 May 2016).

GSTC Technology: Downstream Conversion Processes (website). Arlington, VA: Gasification & Syngas Technologies Council (2016). available at: http://www.gasification-syngas.org/technology/ downstream-conversion-processes/ (accessed on 20 May 2016).

Gundupalli, S., S. Hait, A. Thakur, A review on automated sorting of source-separated municipal solid waste for recycling, Waste management, Vol. 60, 2017. - 56-74.

Howard, G.T. Biodegredation of polyurethane: a review, International Biodeterioration and Biodegradation, 49, 1, 2002. - 245-252.

Hoornweg, D., Bhada-Tata, P., What a waste. A Global Review of Solid Waste Management, The World Bank, Urban Development and Local Government Unit, March 2012, 15.

Kaseva, M. E.; Mbuligwe, S.E., Appraisal of solid waste collection following private sector involvement in Dar es Salaam city, Tanzania. Habitat International, 29, 2005. - 353-366.

Kaliampakos, D., A. Benardos, Underground Solutions for Urban Waste Management: Status and Perspectives, ISWA Report, 2013.

LeBlanc, R., Integrated Solid Waste Management (ISWM) – An Overview, 2016, available: www.thebalance.com (accessed 08 June 2016).

LeBlanc, R., An Introduction to Solid Waste Management, 2017, available: www.thebalance.com (accessed 01 July 2017).

Mastellone, M.L. Thermal treatments of plastic wastes by means of fluidized bed reactors. Ph.D. Thesis, Department of Chemical Engineering, Second University of Naples, 1999, Italy.

PAHO. Report on the Regional Evaluation of Municipal Solid Waste Management Services in Latin America and the Caribbean. Pan American Health Organization, 2005.

Paulraj, S., S. Hait, A. Thakur, Automated municipal solid waste sorting for recycling using a mobile manipulator, 40th Mechanisms and Robotics Conference (MR) at ASME Conference on International Design Engineering Technical Conferences and Computers and Information in Engineering Conference (IDETC/CIE), 2016.

Rogoff, M., Solid Waste Recycling and Processing, Second Edition, Elsevier. 2014.

Samah, M., Manaf, L., Aris, A., Sulaiman, W. Solid Waste Management: Analytical Hierarchy Process (AHP) Plication of Selecting Treatment Technology in Sepang Municipal Council, Malaysia, Current World Environment, Vol. 6, 1, 2011. -1-16.

Seltenrich, N., Emerging Waste-to-Energy Technologies, Environmental Health Perspectives, Vol. 124, 6, 2016.

Stringfellow, T. An independent engineering evaluation of waste-to-energy technologies. Renewable Energy World.com (13 January 2014). available: http://www.renewableenergyworld. com/articles/2014/01/an-independent-engineering-evaluation-of-waste-to-energy-technologies.html (accessed 20 May 2016).

Saleem, W., A. Zulfiqar, M. Tahir, F. Asif, G. Yaqub, Latest technologies of municipal solid waste management in developed and developing countries: A review, International Journal of Advanced Science and Research, Vol. 1, 10, 2016. - 22-29.

Tchobanoglous, G., Thiesen. H., Vigil S.A. Integrated solid waste management, Engineering principles and management issues. Mc Graw-Hill International Edition. California, 1993. - 193-245.

Takemura, Y., Y. Fuchikawa, S. Kurogi, S. Ito, M. Obata, N. Hir atsuka, H.Miyagawa, Y. Watanabe, T. Suehiro, Y. Kawamu ra, F. Ohkawa, Development of a sensor system for outdoor service robot, SICE-ICASE, International Joint Conference, 2006. - 2687-2691.

Troitsch, J., International Plastics Flammability Handbook Hanser Publishers, Munich, 1990.

This article was reviewed by Prof. Dr. Ivan Nishkov and Prof. Dr. Marinela Panayotova.

PRESSURE LEACHING OF SMELTER FLUE DUST: AN EXPERIMENTAL INVESTIGATION

Todor Angelov[1], Ivanka Valchanova[2], Alexander Tsekov[2]

[1]University of Mining and Geology "St. Ivan Rilski", 1700 Sofia, Department of Mineral Processing and Recycling
[2]Iontech 2000 JSC, Sofia, e-mail: ivanka.valchanova@gmail.com

ABSTRACT. The investigation reported in this paper has been the initial phase of an experimental program to study the application of hydrometallurgical techniques to the recovery of copper and zinc from copper smelter flue dust. Flue dust is generated as a by-product of copper smelting operations and contains metals such as copper, zinc, iron, arsenic, cadmium, and lead. Characterization of the flue dust has been performed by means of chemical and X-ray diffraction analysis. The principal aim has been to evaluate pressure leaching kinetics of the material, under a range of experimental conditions that might have process potential. The parameters such as pressure, temperature, acid concentration, liquid/solid ratio and leaching time have been used to identify the optimum acid leaching of flue dust with highest copper and zinc leaching efficiency. Pressure acid leaching tests have been performed in a laboratory scale autoclave. The autoclave had a total volume of 2 l and it was loaded with 1.6 l of solution as the recommended batch size for such autoclaves is 80% of the capacity. Pregnant leach solutions, wash waters and residues have been analyzed for their copper, zinc and acid constituents to allow for stricter mass balances in each of the tests. The experimental results obtained show that using a solid/liquid ratio of 1/10, it was possible to leach more than 90% of copper and zinc after 2 hours, with a solution of 35 g/l H_2SO_4 at 110ºC temperature and 8 atm oxygen pressure.

Keywords: flue dusts, pressure leaching, copper, zinc

ИЗЛУЖВАНЕ ПОД НАЛЯГАНЕ НА ПРАХ ОТ ОЧИСТВАНЕ НА ДИМНИ ГАЗОВЕ: ЕКСПЕРИМЕНТАЛНО ИЗСЛЕДВАНЕ

Тодор Ангелов[1], Иванка Вълчанова[2], Александър Цеков[2]

[1]Минно-геоложки университет „Св. Иван Рилски“, 1700 София, Катедра „Обогатяване и рециклиране на суровини”
[2]Йонтех 2000 АД, София, e-mail: ivanka.valchanova@gmail.com

РЕЗЮМЕ. Представеното изследване е начална фаза на експериментална програма за определяне на възможността за използване на хидрометалургични техники при извличане на мед и цинк от прах, получен при очистката на димни газове. Димният прах се генерира като вторичен продукт при топенето на медни концентрати и съдържа основно метали като мед, цинк, желязо, арсен, кадмий и олово. Охарактеризирането на димния прах е извършено чрез химичен и рентгенов дифракционен анализ. Основната цел на изследването е да се оцени киселинното излужване под налягане при редица експериментални параметри като налягане, температура, концентрация на киселина, отношение твърдо/течно и време на излужване, и да се определят оптималните условия за достигане на най-високо извличане на медта и цинка. Киселинното излужване под налягане е проведено в лабораторен автоклав с ефективен обем 1,6 l, което е 80% от общия. Набогатените разтвори от излужването, промивните води и кековете са анализирани за мед, цинк и концентрация на сярна киселина, за да се направи пълен материален баланс на всеки експеримент. Резултатите от изследването показват, че е възможно да се излужат над 90% от медта и цинка при следните условия: отношение твърдо/течно 1/10, 35 g/l H_2SO_4, температура 110ºC, налягане на O_2 8 atm и контактно време 2 часа.

Ключови думи: димни прахове, излужване под налягане, мед, цинк

Introduction

Secondary sources can be considered as raw materials which have potentially high grade but also high complexity. Recovery of materials from secondary sources can be more difficult because the feed is less constant and homogeneous than in primary production. Several pyrometallurgical processes have been implemented for the treatment of secondary materials, however, these are generally only efficient for a constant composition feed and need to have a high production capacity to be economically viable.

Alternative hydrometallurgical routes to treating metallurgical wastes are therefore required (Liew, 2008). Pressure oxidation has been developed as a viable technology. It has found extensive commercial applications in mineral industry. Numerous pressure processing plants have been constructed worldwide for production of nickel, cobalt, copper and zinc from ores, concentrates and other metallurgical intermediates or secondary materials (Ozberk et al., 1995; Dreisinger, 1999; Evans, 1999; Collins et al., 2000).

Devnya Waste Treatment Plant (DWTP) will use a hydrometallurgical process route to treat a wide variety of metal-containing wastes. The investigation reported in this paper has been the initial phase of an experimental program to study the application of hydrometallurgical techniques to the recovery of copper and zinc from copper smelter flue dust. Flue dust is generated as a by-product of copper smelting operations and contains metals such as copper, zinc, iron, arsenic, cadmium, and lead. The composition of these dusts varies for different operations. The composition depends on

the mineralogy of the concentrates, fluxes and circulating material (slag, dust, etc.), and their respective proportions.

The key unit operation envisaged in the Devnya Waste Treatment Plant (DWTP) is pressure oxidation leaching in autoclaves, where the copper and zinc are extracted into solution, lead is precipitate as lead sulfate and the precious metals are liberated conceivably for subsequent recovery. Before starting experiments on the pressure oxidation, a series of atmospheric leach tests with flue dust were performed to evaluate whether there was a response in copper and zinc extraction. Since the atmospheric leaching did not yield good results – very low copper and zinc recoveries, pressure leaching was initiated.

The amenability of the flue dust to the pressure oxidation process was evaluated in process development study, comprising batch tests, to assess the effects of parameters such as oxygen pressure, temperature, acid concentration, liquid/solid ratio and leaching time and to identify the optimum acid leaching conditions with highest copper and zinc leaching efficiency.

Materials and methods

The dust sample was collected during the smelting operation. The as-received sample was mixed thoroughly. Representative samples were subjected to chemical analysis, particle size analysis and X-ray diffraction (XRD).

Elemental composition

The composition of the sample was determined by Inductively Coupled Plasma Atomic Optical Emission Spectroscopy (ICP-OES) after the sample were digested in aqua regia. Table 1 presents the elemental analysis of the sample.

Table 1.
Elemental analysis of the flue dust

Element, unit	Value	Element, unit	Value
Au, g/t	5.40	Ni, g/t	227
Ag, g/t	205	Pb, %	15.07
As, %	1.03	Sb, g/t	798
Bi, %	2.05	Se, g/t	542
Cd, g/t	11100	Sn, g/t	2753.15
Co, g/t	18.3	Ta, g/t	0.10
Cu, %	27.4	Te, g/t	56.6
Fe, %	1.63	Zn, %	3.52
Ga, g/t	0.6	S, %	13.88

The analysis shows that the major metal constituents in the sample are copper, lead and zinc.

Particle size analysis

Screen analysis was conducted on the sample to assess the particle size distribution of the material. Results of the analysis show that the greatest percent of the sample was in the -0.5 +0.25 mm size fraction (Table 2).

Table 2.
Screen analysis of the flue dust

Sieve size, mm	Weight, g	Wt.% Ret.	Cum. Wt % Ret.	Cum. Wt % Pass
+1.0	34.54	6.9	6.9	93.1
-1.0 +0.5	52.76	10.6	17.5	82.5
-0.5 +0.25	376.6	75.5	93.0	7.0
-0.25+0.16	0.98	0.2	93.2	6.8
-0.16+0.09	24.2	4.9	98.1	1.9
-0.09+0.071	0.58	0.12	98.22	1.78
-0.071	8.95	1.8	100	
Total	**498.61**	**100**		

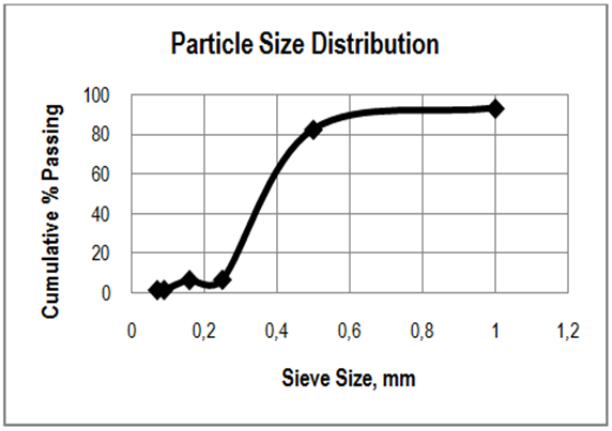

Fig. 1. Particle size distribution curve

From the cumulative curve (Figure 1), it can be seen that about 80% of the material was smaller than 0.5 mm.

X-ray diffraction (XRD) analysis

The mineralogy of the sample was determined by X-ray powder diffraction (XRD) with a Topas 4.2 (Bruker) software and PDF-2(2009) ICDD database. The diffraction pattern is shown on Figure 2. It can be seen that the main phases are poitevinite $(Cu,Fe)SO_4.H_2O$ – 30% and anglesite $PbSO_4$ – 30%. The other phases are bonattite $CuSO_4.3H_2O$ – 13%, cuprite Cu_2O – 2%, copper sulfate pentahydrate $CuSO_4.5H_2O$ – 9%, arsenolite As_2O_3 – 1% and moganite SiO_2 – 15%. Single phases of zinc, cadmium and bismuth were not identified. Cadmium and bismuth and certain amount of copper may be present in the anglesite.

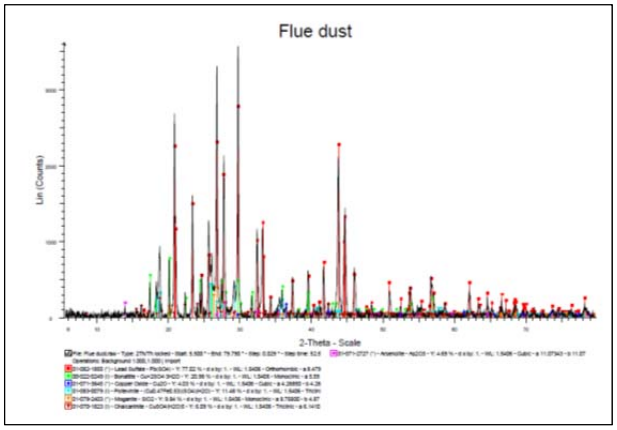

Fig. 2. X-ray diffraction (XRD) analysis of the flue dust

Pressure oxidation leaching

Batch pressure acid leaching tests with the flue dust have been performed in a laboratory scale autoclave. Experimental set-up is given in Figure 3. The autoclave had a total volume of 2 l and it was loaded with 1.6 l of solution as the recommended batch size for such autoclaves is 80% of the capacity. Pressure leaching examinations were performed using oxygen as an oxidant. At the end of the experiment, the pressure was relieved, the heater and the agitator switched off, and the flow of oxygen stopped. The reaction vessel was taken out and cooled rapidly by plunging it in cold water. The solution when cooled was filtered. The filtrate was collected, the residue was washed well with distilled water, and the wash water collected and analyzed. The residue was dried, weighed and a portion was analyzed. Chemical analyses were carried out by atomic absorption spectrometer (AAS), inductively coupled plasma optical emission spectrometry (ICP-OES) as well as by titration.

Results and Discussion

The experimental program was designed to investigate the influence on the flue dust sulfuric acid leaching of the following parameters - acid concentration, temperature, oxygen pressure and time of leaching. With this in mind, the experimental conditions were chosen so as to give the optimum results. The solid:liquid ratio was maintained at 1:10 and agitation speed - 650 rpm. The temperature of the process is dictated by the behaviour of sulfur during leaching. Temperatures of 90,100 and 110°C were chosen to maintain the temperature of reaction below the melting point of sulfur (119°C). Oxygen pressures of 6 and 8 atm were selected as being the optimum values from the data of other investigators. The initial sulfuric acid concentration was fixed at low value (35 g/l) in all of the experiments. The acid concentration was chosen to give a minimum required free acid of approximately 5 g/l of sulfuric acid in the autoclave discharge. Time of leaching was varied from 90 to120 minutes to give maximum extraction. Copper (Cu, %) and zinc (Zn, %) recovery results, calculated and based on chemical analysis of solutions and leach residue, are shown in Table 3 and Figure 4.

Table 3.
Experimental conditions and results of pressure leaching

Exp #	Temp, °C	pO_2, atm	Time, min	Cu, %	Zn, %
1	90	6	90	82.2	97.6
2	100	6	90	85.6	97.7
3	110	6	90	91.2	98.0
4	90	8	90	85.4	97.9
5	100	8	90	89.8	97.9
6	110	8	90	92.8	98.1
7	90	6	120	84.7	98.2
8	100	6	120	93.1	98.0
9	110	6	120	95.3	98.2
10	90	8	120	89.8	98.5
11	100	8	120	94.2	98.5
12	110	8	120	96.8	98.6

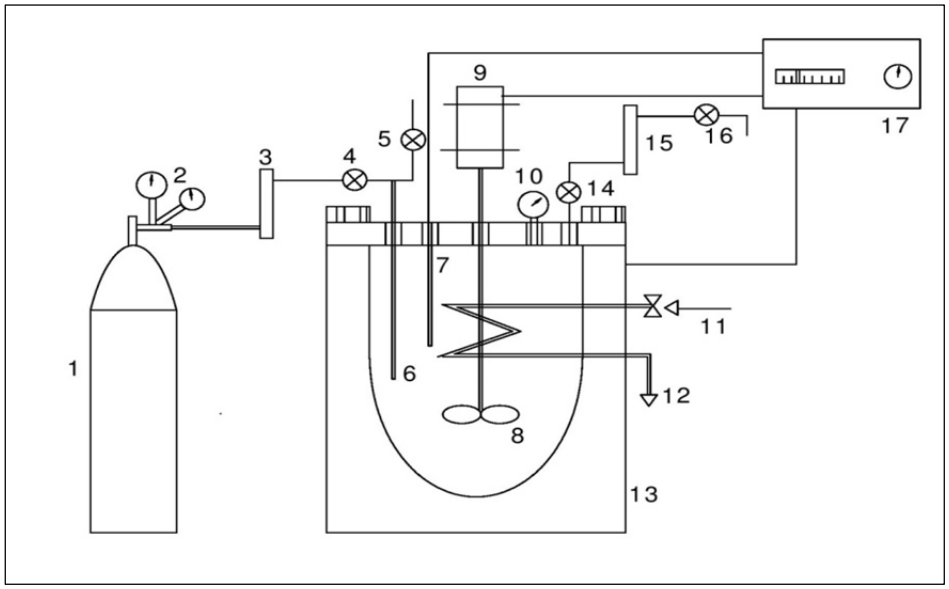

Fig. 3. Experimental set-up
1- Oxygen Gas Cylinder; 2 - Pressure Regulator; 3 - Gas Inlet Rotameter; 4 - Gas Inlet Valve; 5 - Sampling Valve; 6 - Gas Inlet; 7 - Temperature Sensor; 8 – Stirrer; 9 - Stir Motor; 10 - Pressure Gauge; 11 - Cooling Water; 12 - Water Drain; 13 - Heating Jacket; 14 - Gas Outlet Valve; 15 - Gas Outlet Rotameter; 16 - Pressure Control Valve; 17 – Controller.

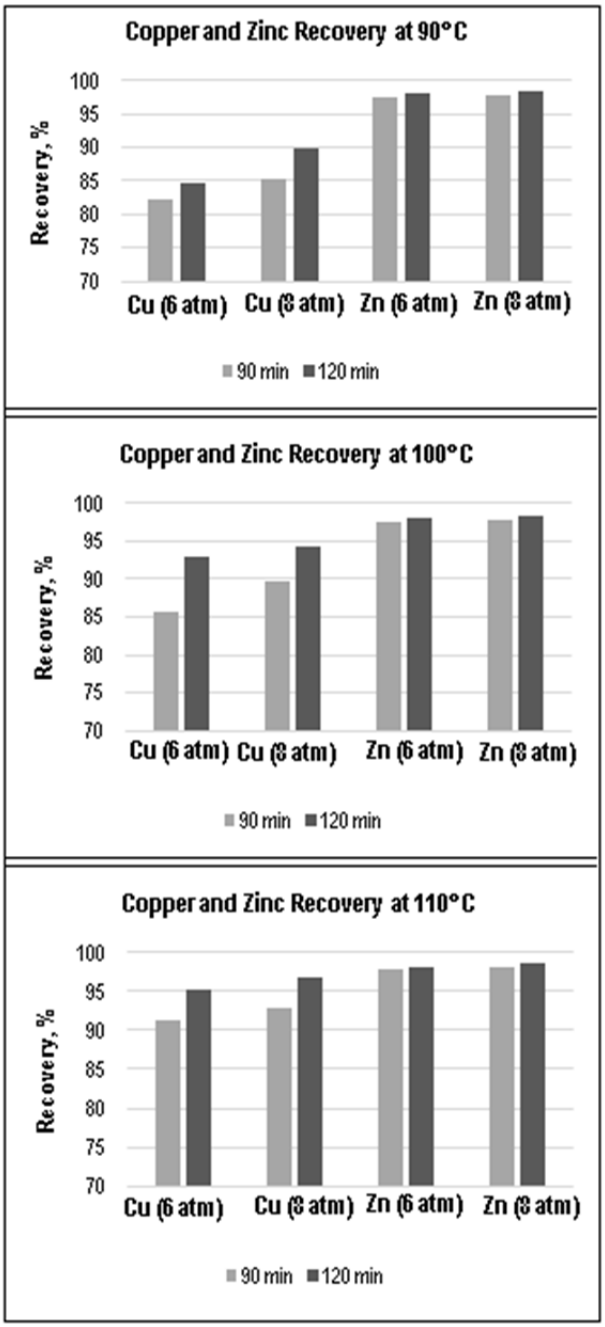

Fig. 4. Copper and zinc recoveries

As can be seen from the results, the pressure leach tests produce high copper and zinc recoveries at relatively low temperatures, medium oxygen pressures and short leaching times. The copper recoveries range from 82.2% to 96.8%, while the zinc recoveries range from 97.6% to 98.6%. The increase of temperature, oxygen pressure and leaching time leads to an increase in percent recovery of the two metals, particularly for copper. Copper and zinc recoveries reach their maximum of 96.8% and 98.6%, respectively at the temperature of 110°C, oxygen pressure of 8 atm and leaching time of 120 min.

Conclusions

The following conclusions, drawn from the results obtained from the experimental investigation, can be made:

- The recovery of copper and zinc from a flue dust, in an oxidative pressure-acid medium, is definitely viable with recoveries, higher than 95% in a leach time of 120 minutes.
- The rate of leaching, particularly for copper, increases with increasing temperature, oxygen pressure and leach time, with optimum conditions found to be at a temperature of 110°C, 8 atm oxygen pressure and a 120 minutes leach time.
- The recovery of the copper from the flue dust is much more dependent on the operating conditions than the recovery of the zinc.
- A solid:liquid ratio of 1:10 ensures fast leaching rate for the recovery of copper and zinc.
- An agitation rate of 650 rpm appeared to be adequate for oxygen dispersion, in order to ensure a fast reaction rate.
- An initial sulfuric acid concentration of 35 g/l produced low in acid base metals solution, is suitable for direct solvent extraction of copper.

References

Collins, M., Stiksma, J., Buban, K., Masters, I. Pressure acid leaching of zinc and copper concentrates by Dynatech, In Proceedings of EPD congress, 2000. - 597-605.

Dreisinger, D. The total pressure oxidation process, TMS Copper Hydrometallurgy Short Course (Copper 99), October 1999.

Evans, H. The Activox copper process, TMS Copper Hydrometallurgy Short Course (Copper 99), October 1999.

Liew, F.C., TES-AMM Analysis. Pyrometallurgy versus hydrometallurgy, April 2008.

Ozberk, E., Chalkley, E., Collins, M. J., Masters, I. M. Commercial Applications of the Sherritt Zinc Pressure Leach Process and Iron Disposal, Mineral Processing and Extractive Metallurgy Review, 15, 1995.- 115-13.

This article was reviewed by Assoc. Prof. Irena Grigorova, DSc. and Prof. Dr. Metodi Metodiev.

EQUIPMENT FOR THE CLASSIFICATION AND CRUSHING SECTION IN FERTILIZER PRODUCTION

A. Norov[1], D. Pagaleshkin[2], A. Gribkov[3], Y. Dimitrienko[4], M. Zlatev[5]

[1] PHOSAGRO GROUP, Research Institute for Mineral Fertilizers (NIUIF), 162622 Russia, Cherepovets, ANorov@phosagro.ru
[2] PHOSAGRO GROUP, Research Institute for Mineral Fertilizers (NIUIF), 162622 Russia, Cherepovets, DPagaleshkin@phosagro.ru
[3] Apatit; Russia, Saratov district, Balakovski region, AGribkov@phosagro.ru
[4] MAVEG Industrieausruestungen GmbH Moscow 123610, Russia, dimitrienko@matrading.ru
[5] Head of the Sales & Project department, m.zlatev@haverniagara.com

ABSTRACT. The paper includes an analysis of the most common grain-size raw material preparation schemes applicable in the mineral processing. Factors influencing the optimal management of the crushing process are clarified and authors' and other installations to regulate this process are presented. Based on this, a variant for equipment for the crushing and sieving sections, tested in practice, is presented.

Keywords: sieving, crushing, fertilizer production

ОБОРУДВАНЕ ЗА ВЪЗЛИТЕ ЗА КЛАСИФИЦИРАНЕ И РАЗДРОБЯВАНЕ ПРИ ПРОИЗВОДСТВОТО НА ТОРОВЕ

Андрей Норов[1], Денис Пагалешкин[2], Алексей Грибков[3], Юрий Димитриенко[4], Методи Златев[5]
[1] ГРУППА «ФОСАГРО», АО «НИУИФ», 162622 Россия, г.Череповец, ANorov@phosagro.ru
[2] ГРУППА «ФОСАГРО», АО «НИУИФ», 162622 Россия, г.Череповец, DPagaleshkin@phosagro.ru
[3] АО «Апатит»; Русия, Саратовская область, Балаковский район, AGribkov@phosagro.ru
[4] МАВЕГ ГмбХ Москва 123610, Русия, dimitrienko@matrading.ru
[5] Head of the Sales & Project department, m.zlatev@haverniagara.com

РЕЗЮМЕ. В статията е направен анализ на най-често срещаните схеми за зърнометрична подготовка на суровини, приложими при обработката на минерални суровини. Изяснени са влияещите фактори за оптимално управление на процеса на раздробяване и са представени авторски и други инсталации за регулиране на този процес. На тази основа е разработен вариант на апаратурно оборудване на възлите за раздробяване и пресяване, който е проверен в практиката.

Ключови думи: пресяване, раздробяване, производство на торове

Nowadays, the granulation methods, used at modern large-scale fertilizer production plants, cannot guarantee the obtaining of a product with narrow particle size distribution range, conforming to strict requirements of standards. Thus, any fertilizer production incorporates the classification and crushing section. In spite of that this section is often considered as a mechanical unit, the operation of granulation unit and product qualitative parameters depend significantly on it [1, 2]. Not only particle size distribution depends on it, but, also physical and chemical properties of fertilizers, primarily, caking and dust formation. The more fines in commercial product, the higher value of these parameters. In paper [3], it is specified that caking of DAP granules with size less than 2 mm is higher by 1.8-4.4 times than caking of granules with size of 2-5 mm.

In the fertilizer industry, the following granulation processes are the most prevailing:

1. Process with ammonizer-granulator (AG) and drying drum (DD). In this process, after the granulation and drying, the material is classified into three fractions in four or six double-sieve screens (1st stage of classification). Further, fines and oversized fraction (after crushing) are returned to recycle, and product fraction is additionally classified in single or two double-sieve screens (control classification). The part of product fraction, conforming to load, is discharged as a final product, another part is fed to recycle. Usually, these processes have larger recycle ratio – from 2.5-3.0 and more. Accordingly, the classification unit shall be suitable for such amount of material:

$M = (1 + P) \times B$, where

M – amount of material, which should be classified, t/h;

P – recycle ratio (ratio of recycled material flow and final product);

B – final product yield (determined by load), t/h.

2. Process with drum granulator-dryer (DGD) or spherodizer. In these units, slurry is sprayed onto granules curtain, formed by special lifting flight. The DGD unit and spherodizer are different, DGD has a screw for moving of internal recycle. Usually, the processes with DGD have lower external recycle ratio (not more than 3). Thus, in these processes, the material

is classified in less number of screens – usually, in two screens at one stage (without control classification), but there are some exclusions.

3. Process with granulation tower. This is the process with the lowest recycle ratio. Here, the recycled material is determined by removal of off-spec fractions (fines and oversize fraction) only, i.e. granulation uniformity. Therefore, lower classification capacity is required.

The most typical classification processes were shown, actually, the processes are more various. For example, for the production of flexible products like urea-based NPK, some companies like Jacobs propose the removal of fine fraction from the material after drying in single-sieve screens (hot screens), further oversieved product is cooled and classified again in double-sieve screens (cold screens) [4]. At WMC Fertilizers factory (Australia), at DAP production plant (capacity 123-145 t/h), the three stage material classification after DD is used: at first, in three double-sieve screens, then in four single-sieve screens, further, after cooling, in two control double-sieve screens.

In paper [5], the screening process is proposed, in which the material from DD is divided into two flows: one is classified in standard way, and second flow is classified firstly in single-sieve screens with particle size limit of 4 mm; oversieved product is fed for crushing and to recycle, and undersieved product is fed partially to recycle and partially into single-sieve screen and final product. Advantages: recycle is not classified by lower size limit, the upper limit is artificially understated; simultaneously, the recycled material particle size becomes lower. Jacobs proposes the different ways of development of classification systems for optimization of fertilizer quality [6].

The authors of paper [7] propose the perspective process of classification and crushing, which helps to regulate the granulation process for changing of granules size. In this process, material after DGD or drying drum (DD) is fed by elevator onto two vibrating distributors, which help to distribute the material uniformly onto vibrating screens meshes, on which it is classified into fractions. Fine fraction from lower sieves is fed to recycle directly – product fraction is divided into two parts by gates with remote control: one part is fed to final product conveyer and further, it is fed for cooling etc., another part is fed to recycle.

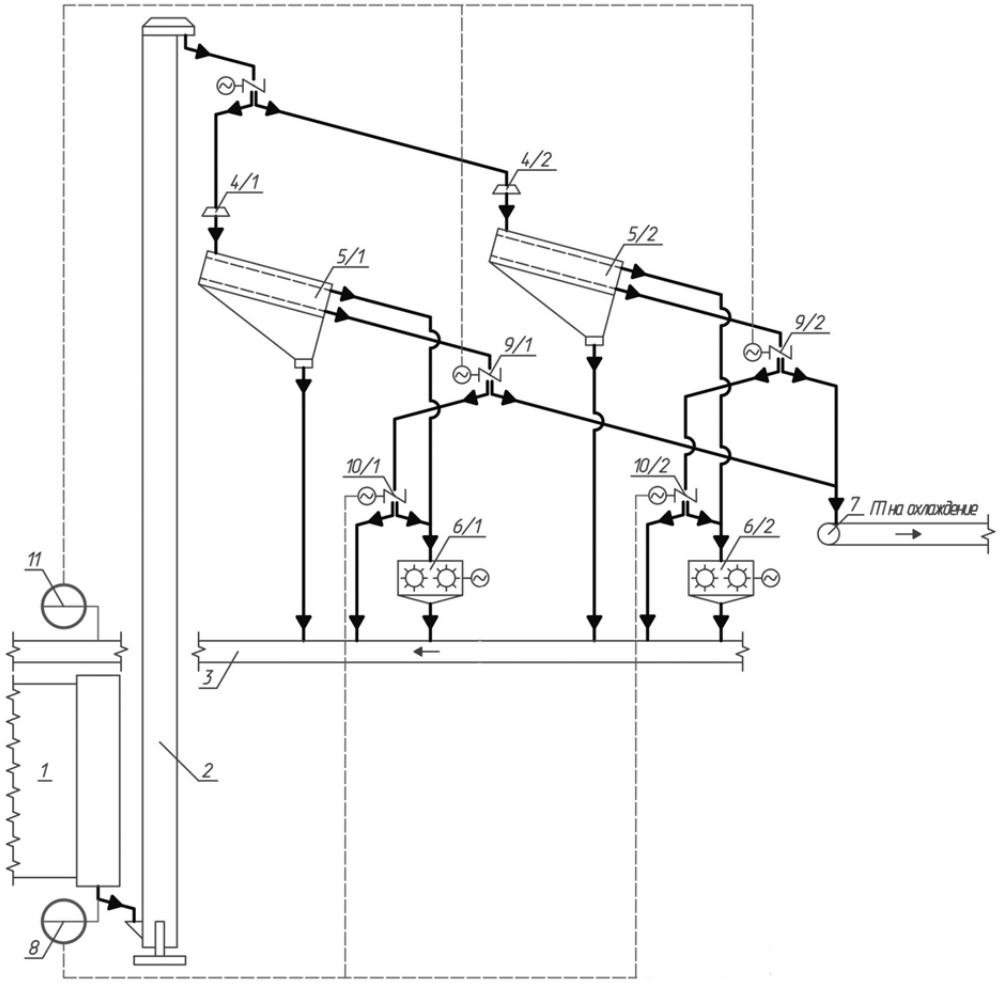

Fig. 1 – Principal diagram of classification and crushing unit, allowing to regulate the granulation process
1 – DGD; **2** – elevator; **3** – recycled material belt conveyor; **4/1**, **4/2** – vibrating distributor; **5/1**, **5/2** – vibrating screen; **6/1**, **6/2** – chain crusher; **7** – final product belt conveyor; **8** – particle size automatic analyzer; **9/1**, **9/2**, **10/1**, **10/2** – gate with remote control; **11** – recycled material scales.

The part of product fraction, fed to recycle, is divided in two flows by gates with remote control, one flow is fed directly to recycled material conveyor, and second flow is crushed in chain crushers before being fed to recycle also. The oversize fraction from upper sieves of screens is also fed to these chain crushers, after crushing it is fed to recycle. The rotary speed of chain crushers rotors (i.e. crushing intensity) and amount of product fraction, fed for crushing, is automatically controlled by frequency regulators and regulated gates, depending on values of automatic particle size analyzer and based on tendency of oversizing or fining of fraction. (Fig.1).

Such classification and crushing process allow to regulate and stabilize the particle size of fertilizers without interference in general process parameters. But, for implementation of such flexible process, it is needed to have the certain crushing capacity reserve, i.e. it is necessary to implement the above-proposed method: 1 screen – 1 crusher.

The general equipment of classification and crushing section is screens and crushers. More often, the inertial screens are used in fertilizer industry. They differ by number of sieves, methods of their tension, fixing, cleaning, sealing design of device for material distribution, sieve width etc. The significant improvement of screen operation is achieved at usage of material vibrating distributors.

Screens are selected on the basis of following requirements:

1 Provision of required capacity;
2 Provision of required quality of classification;
3 Operation reliability;
4 Easy to maintain;
5 Tightness.

In accordance with these parameters, the screens should be selected. Screen reliability is related to its long-term operation without repair. Easiness of maintenance – firstly, it is the accessibility of sieves for cleaning and replacing. Tightness – the screens should not form dust.

It is impossible to calculate precisely the performance of inertial screens, this value is a test value. It is proportional to sieve width, material layer height and its motion rate. It is considered that the layer height, equal to two or three fraction sizes, is the most preferable for classification. Vibration frequency of inclined screen [5]:

$$f = 44\sqrt{\frac{l}{a}}, \text{ where:} \quad (1)$$

l – opening size;
a – vibration amplitude.

Roughly, the screen performance may be determined by the following methodology [10]:

at sieve vibration per minute n, the motion rate of particle on sieve will be:

$$v = \frac{a \times \tan\alpha \times n}{60} \text{ (м/с), where:} \quad (2)$$

a – amplitude;
α – sieve inclination angle.

At sieve length L (m), the retention time on it will be:

$$\tau = \frac{L}{v} \text{ (c)} \quad (3)$$

At known classification time, it is possible to calculate the sieve length L at given capacity Q (kg/s):

$$Q = B \times h \times v \times \rho_{\text{н}}, \text{ where:} \quad (4)$$

B – sieve width, m;
h – material layer height, m;
$\rho_{\text{н}}$ – material bulk density, kg/m^3.

Using the value v, the following will be obtained:

$$Q = \frac{B \times h \times a \times \tan\alpha \times n \times \rho_{\text{н}}}{60} \quad (5)$$

Screen specific capacity q (kg/(m^2×s)):

$$q = \frac{Q}{S} = \frac{h \times \rho_{\text{н}}}{\tau} \quad (6)$$

This formula shows that, under this methodology, screen capacity is not connected with classification quality, the general parameter for calculation – classification time – may be determined from experiment only.

Specific load also depends on required efficiency of segregation. As a result of processing of experimental data, the following relation has been obtained [4]:

$$q = q_0^{1-n\times\eta}, \text{ where:} \quad (7)$$

q_0 – specific load, at which the efficiency is 0, depending on design, operation mode of screen and size of material;
n – empiric coefficient, depending on flowing and adhesive properties of product;
η – total screening efficiency.

$$\eta = \frac{(\beta-\alpha)\times(\alpha-\theta)}{\alpha\times(1-\alpha)\times(\beta-\theta)}, \text{ where:} \quad (8)$$

α, β and θ – content of any fraction in initial, undersieved and oversieved product, respectively. Classification efficiency decreases with increasing of specific load onto sieve.

For optimal classification process, the correct selection of amplitude and frequency of screen vibration is needed. In vibrating screens, the effect of vibrational motions of sieve surfaces is used for material distribution on sieve, its transferring and loosening of caked material.

There is a certain relation between amplitude, vibration frequency and granule size (fraction size). The higher the fraction size is, the higher amplitude and lower frequency are. And vice-versa, the lower the fraction size is, the lower amplitude and higher frequency are. The relation of sieve vibration amplitude and fraction size is shown on Figure 2.

On the figure it is seen that the relative low vibration amplitude is applied for screens with direct excitation, the fraction size of 5 mm is located at the extreme bound of their operation.

As written above, the most preferable height of a layer on sieve is the height, equal to two-three fraction sizes [8]. But, this requires a certain screen vibration amplitude.

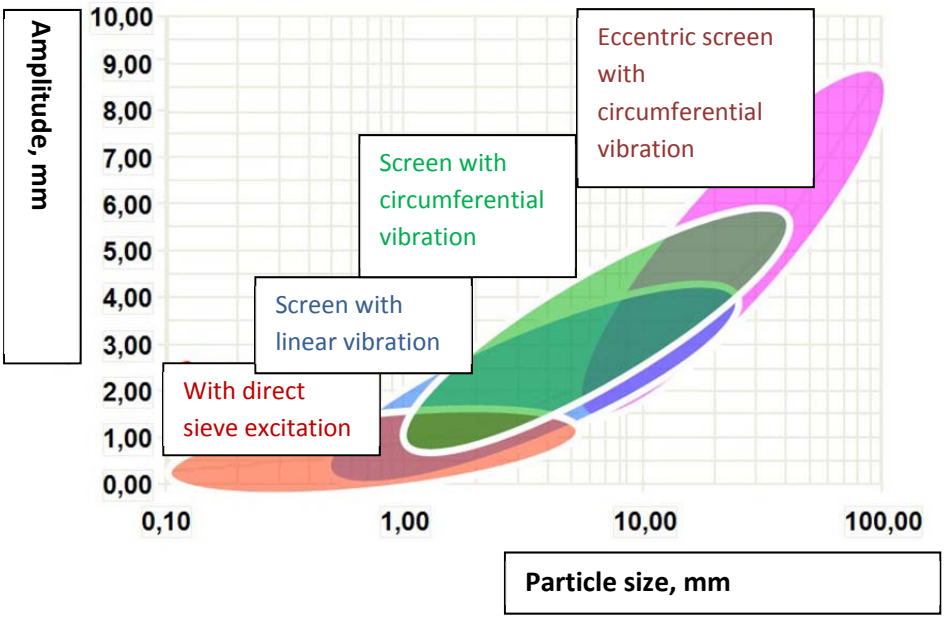

Fig. 2 – Diagram of relation of amplitude and fraction size

At high temperatures, the intensive tossing, loosening of material layer occur, the large lumps of caked and adhered material are broken. At the same time, at overrated amplitudes, fine granules fly over the mesh and don't pass through the sieve. At low amplitude, the screen capacity decreases because of insufficient shaking of material. Also, the possibility of fouling of sieve meshes increases because the particles, stuck in mesh, don't get the sufficient acceleration for fly out from mesh. It is experimentally determined that screen operates effectively, and at this the self-cleaning from hard-to-remove particles at height of material tossing [8, 10, 11]:

$h \geq 0{,}4 \times l$, where: (9)

h – material tossing height;
l – sixe of sieve mesh.

Also, it should be considered that at constant amplitude, the frequency cannot be increased infinitely, because, in this case, this will result in screen wearing and decreasing of its life-time. If the frequency is underrated, the screen capacity will decrease.

Now, if we, with taking into account the above-mentioned, again look at Figure 1, we will understand that screens with direct sieve excitation are not suitable for fertilizer classification at fraction size of 5 mm, because they have insufficient amplitude. Also, it is seen that the most optimal parameters for required product conform to the screens with circumferential vibration. They are suitable for increasing of capacity of existing and revamp requiring plants, and have the good capacity reserve.

It is experimentally determined that for the screens of this type, the specific capacity of classification at 5-mm fraction size is 12-15 t/(m^2×h); at 2-mm fraction size – 3,0-4,5 t/(m^2×h).

The following may be said about certain models of screens, used in fertilizer industry. Within the course of about ten years, within a special program, proposed to us by the German company MavegIndustrieausrüstungen GmbH (MAVEG), our specialists had visited plants and studied the experience of leading fertilizers producers in Germany, Poland, Spain, Bulgaria, Morocco, Turkey, Jordan, Australia etc. The meetings and consultations with leading developers of fertilizers production technologies, like INCRO and Jacobs, were carried out.

On the basis of this work results, the following conclusions can be made.

According to our data, screens with direct sieve excitation (direct transferring of vibration onto classifying surface) are reliable enough, they have high overhaul run, they doesn't require the monolithic platforms from reinforced concrete for their installation (because the vibration doesn't transfer onto steel construction structures). However, they have certain disadvantages. The access to lower sieves for repair and maintenance is difficult. Also, the large screen inclination angle decreases the classification quality. In our opinion, screens with direct vibration transfer onto sieve surface are better for classification of finer products (for example, feed phosphates) than granulated fertilizers (see Figure 2).

This type of screens has no sufficient reserve of capacity. At relatively not high loads, screen with direct sieves excitation may be able to solve its tasks in full manner; but, at load increasing, the dramatic decreasing of capacity by target product and decreasing of classification quality may happen.

From our point of view, other types of sieves are less suitable for fertilizer production.

In our opinion, units with vibration at horizontal plane are not effective and inefficient and not suitable for fertilizers production. They are rather for flour-grinding industry.

Also, there is a doubt about the effectiveness of screens with top axial arrangement of vibrating motors, because the vibration from them transferred to sieve center with the help of special closure dams (Figure 3).

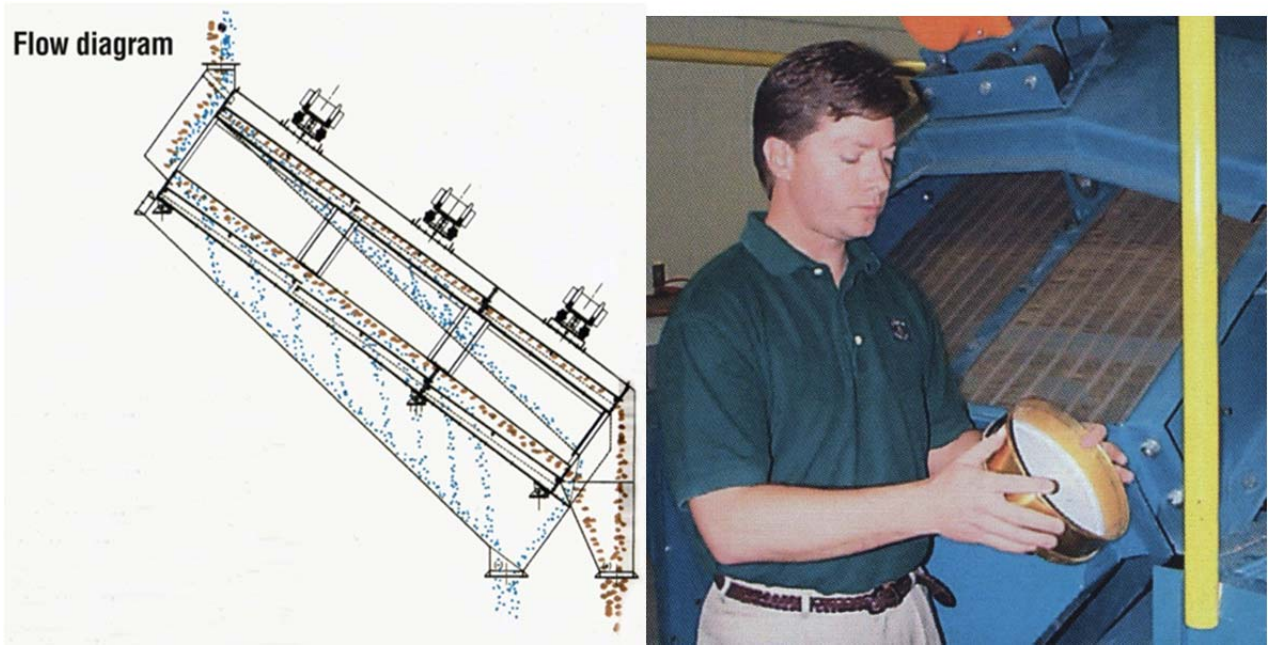

Fig. 3 – Screen with top arrangement of vibrators

As a result, the sieve central part has the high vibration amplitude, which decreases practically down to «0» at edges of sieve surface, this leads to non-uniformity of fertilizer distribution along sieve width and decreases dramatically the capacity and effectiveness of classification, and therefore, this leads to faster wearing of sieve itself. Producers of such screens try to compensate this disadvantage by increasing of screens size, but, this also creates the problems with their arrangement, layout and creates the additional loads on construction structures. Although these screens are quite cheap, we can't recommend them as equipment for classification and crushing sections of fertilizer production plant.

The most suitable screens for fertilizers production are vibrating screens with circumferential vibrations, because they have the optimal parameters, particularly, sufficient amplitude (see Figure 2). In spite of this type of vibrating screens requiring platforms from reinforced concrete for suppression of vibration or special additional frames for vibration suppression at installation, these units have high capacity and effectiveness. As we mentioned above, on the basis of our operational data, the specific capacity of this type of vibrating screens (at presence of high effectiveness of classification and provision of qualitative particle size distribution of commercial product) is 12-15 t/(m^2×h) at 5-mm fraction size, at 2-mm fraction size – 3,0-4,5 t/(m^2×h).

Theoretic calculations and studying of equipment operation experience at similar plants, impressive reference list – more than 110 units of installed similar equipment in more than 40 countries around the world, give us the right to recommend the equipment of Haver Niagara GmbH company for these specified purposes.

The familiarization with Haver Niagara GmbH screens at foreign and Russian fertilizer production plants convinced us in their high reliability and efficiency, even at operation in severe conditions, during long period of time (more than 20 years).

At revamp of phosphorous-containing fertilizers production plant at one of the largest factory for production of this product, JSC NIUIF specialists in the factory and MAVEG engineering company specialists made a selection of vibrating screens for replacement of existed old-fashioned screens GIL-52. The Haver Niagara screens with the size of sieving surface of 2000x6000 mm (Figure 4), selected by us, were supplied to the factory by MAVEG company, which is an authorized representative of Haver Niagara GmbH. After replacement of screens, the classification capacity increased significantly (up to values 0.949 at 2 mm interface and up to 0.933 at 5 mm interface, at DAP production), and also, this allowed (with other measures) to increase significantly the capacity of process lines [2, 13, 14]. This equipment proved its value, and it has already been used for 5 years. The single disadvantage of these screens is their insufficient tightness due to presence of soft inserts, which requires the periodic replacement due to their breakages during operation.

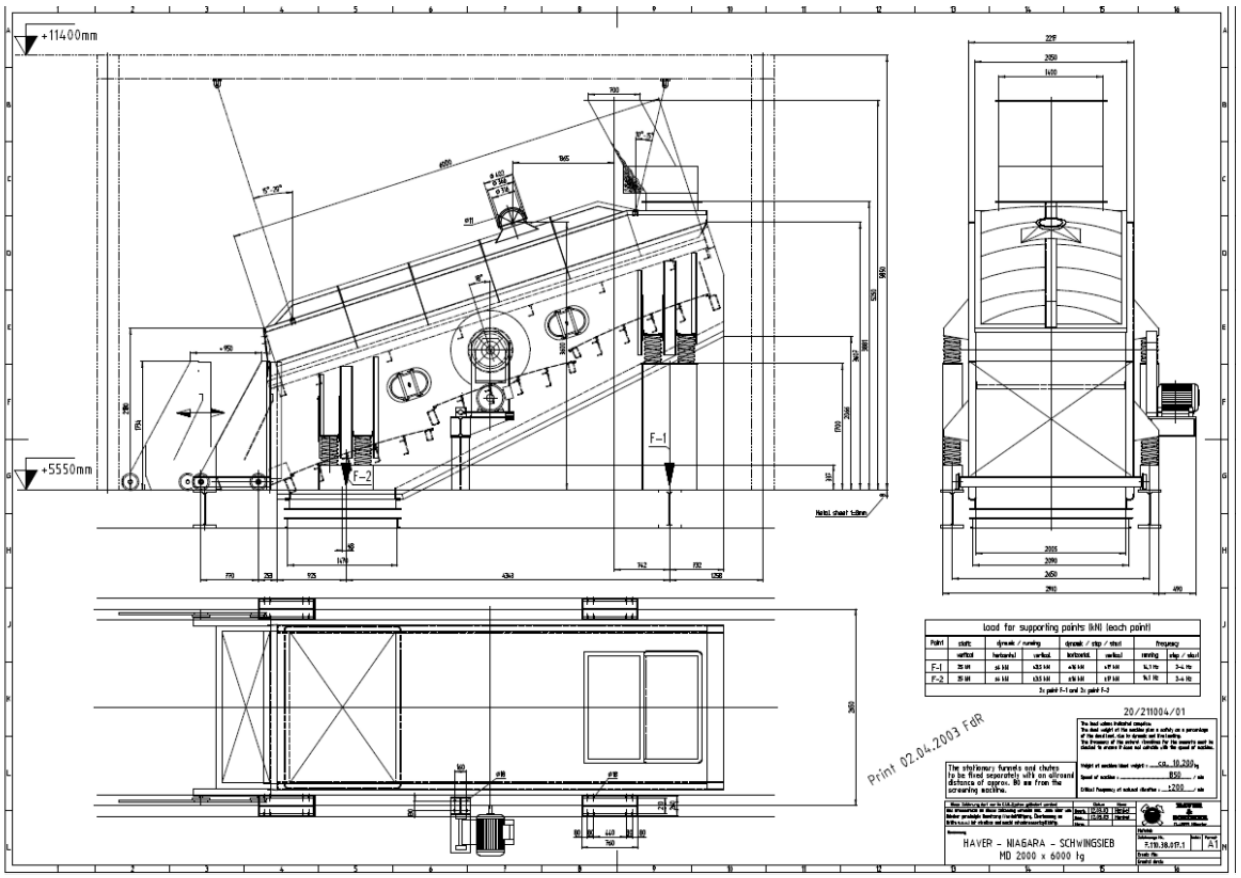

Fig. 4 – Haver Niagara 2000×6000 screen

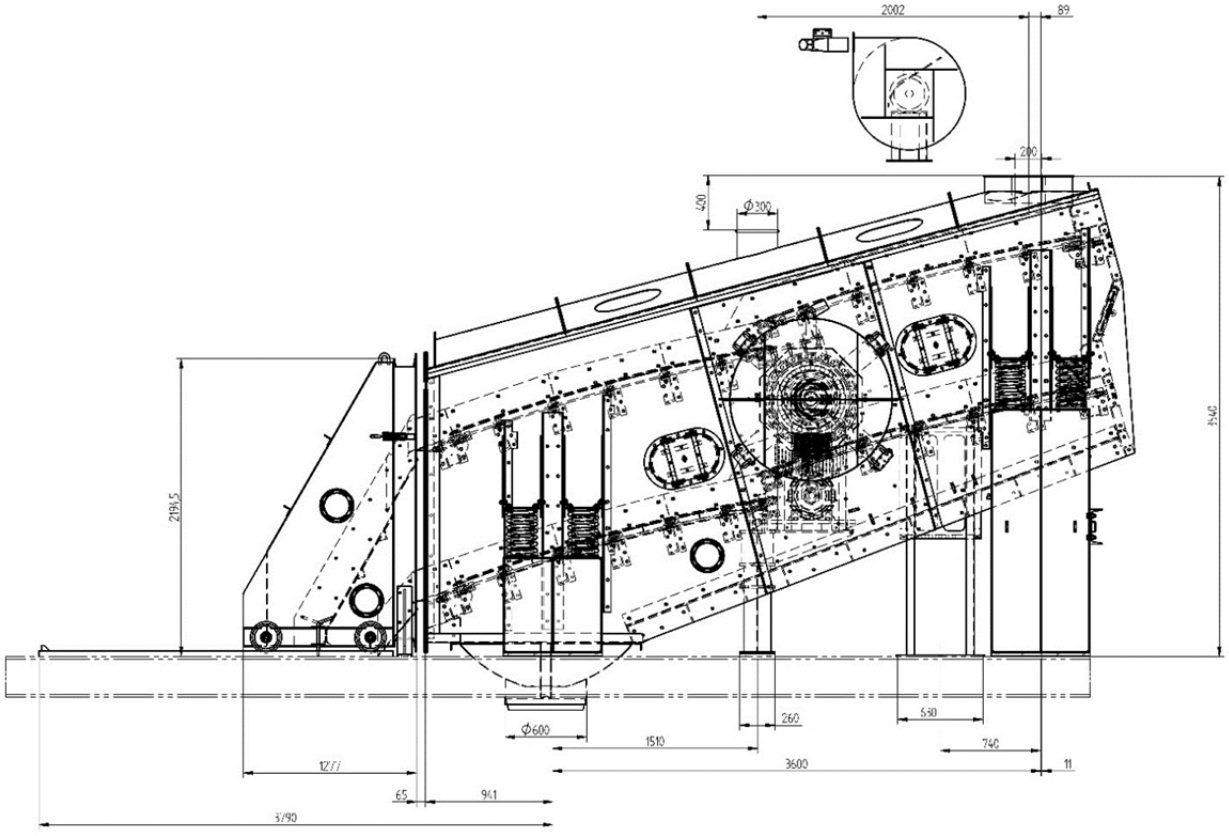

Fig. 5 – Haver Niagara 1800×5000 screen

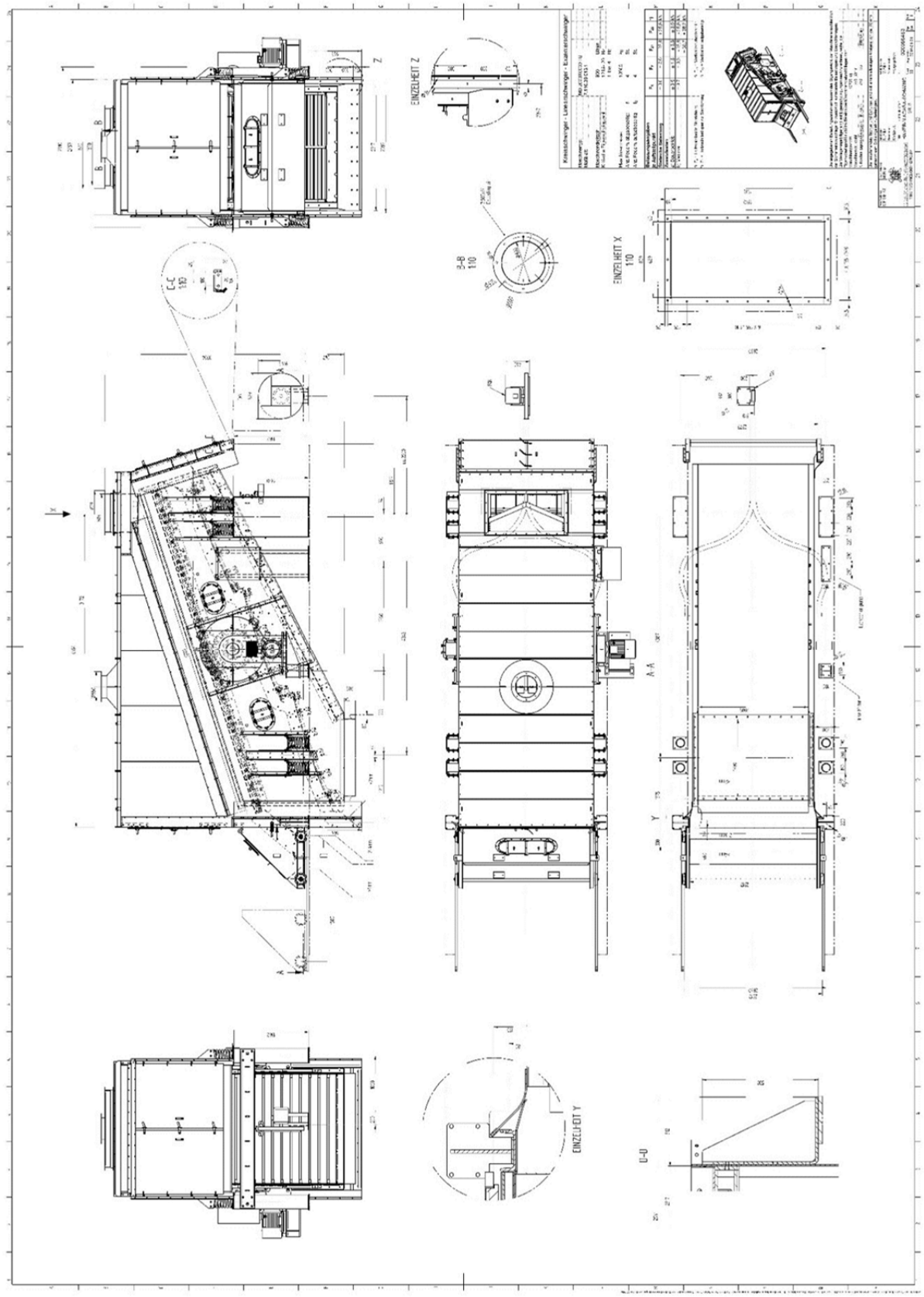

Fig. 6 – Haver Niagara 1800×6000 screen

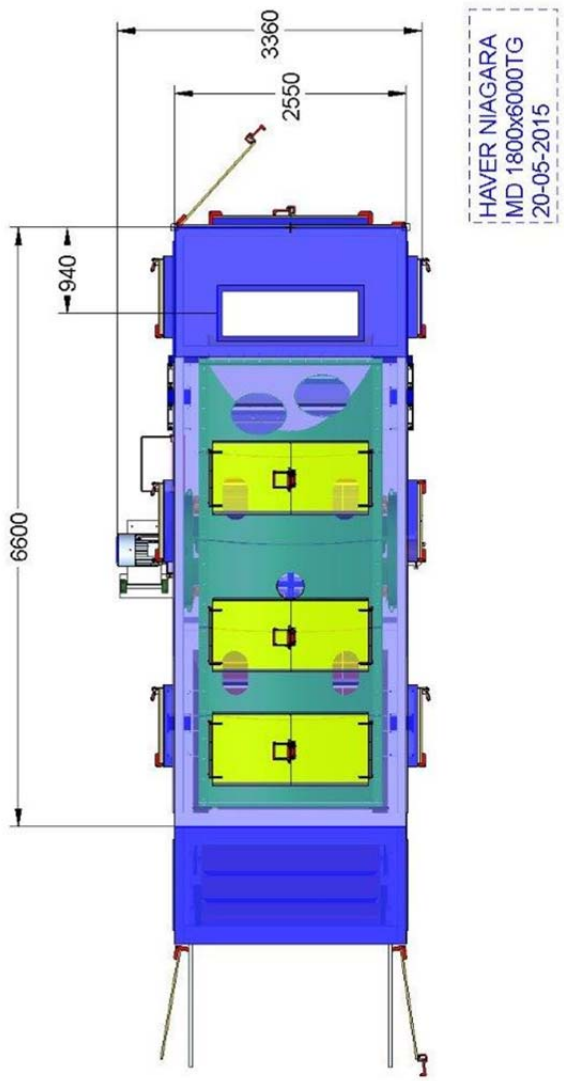

Fig. 7 – Fully closed modification of Haver Niagara 1800×6000 screen (top view)

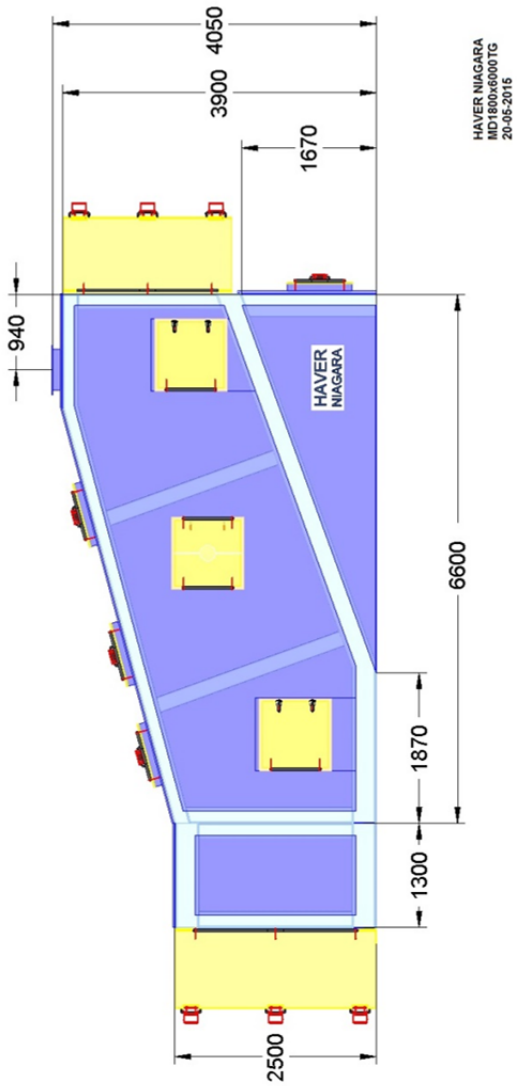

Fig. 8 – Fully closed modification of Haver Niagara 1800×6000 screen (side view)

In our point of view, the vibrating screens Haver Niagara 1800×6000 mm, proposed by MAVEG, as screens at first classification stage, and screens 1800×5000 mm for control classification, have the following advantages:

– They provide the required classification quality, including at higher capacities;

– They are reliable in operation – for several years, such units have operated successfully at fertilizer production plants in Balakovo and Kingisepp, and also at many other plants;

– They are easy to maintain;

– They are tight.

The important, and most critical criterion, for the selection of equipment for revamp of existing plant were the capabilities of MAVEG engineering company and the manufacturer, Haver Niagara GmbH, for adaptation of the new equipment with significantly higher capacity to certain conditions at the Customer's plant, designed earlier under the parameters of previously used equipment with less capacity.

The capabilities of the mentioned companies allowed to convert the serial equipment into equipment of individual design with taking into account all features of the Customer's production areas, this allowed to reduce significantly the possible costs for capital construction.

It is necessary to point out that it is rationally to install the modern vibrating screens only with proper vibrating distributors (vibrating feeders). This gives the following advantages:

– The screen sieves surface is used more fully, the material is distributed more uniformly along mesh width, as a result of this, the capacity and effectiveness of segregation onto fractions increase;

– As a result of more uniform product distribution along the whole width of the sieve, the wearing of its surface is more uniform; therefore, the life time increases;

– The impact load onto screen (firstly, onto vibrating frame) decreases, as a result of this, its life time increases, and idles decrease.

Also, the necessity of usage of vibrating feeders before screens is proved by the specialists from fertilizer production processes developing companies, such as Jacobs Engineering and INCRO [12].

We analyzed the operation of vibrating feeders of different companies. It was determined that many of them are plugged periodically by lumps of adhered product during operation, this happened due to their design features. This leads to failures in feeder and screen operation, non-uniform distribution of material onto sieves, and further, to decreasing of capacity and effectiveness of classification. This issue may be solved by installation of additional device for lumps removal from vibrating feeders, as was done at one of the foreign plants (Figure 9).

Fig. 9 – Device for lumps removal from vibrating feeder

But, it is more rational to equip the screens with vibrating feeders of Haver Niagara company, which do not have these disadvantages due to their original and reliable design (Figures 10 and 11).

Practical usage of vibrating feeders shows that, for provision of stable operation of classification unit, it is needed to provide some reserve of vibrating distributors capacity: for a screen with classification capacity of 150 t/h at 5-mm fraction size, the vibrating distributor shall have capacity of 200 t/h, for a vibrating screen with capacity of 100 t/h – 150 t/h.

Particular attention shall be paid to crushing equipment at classification unit arrangement. The detailed study of usage of different equipment for these purposes at many plants around the world allowed us to give preference to the proposed by MAVEG chain crushers with capacity of 50 t/h, made by Sulta company, with taking into account the solved tasks on increasing of production capacities (Figure 12). Some years ago, together with the specialists from a large plant and MAVEG company, which is the authorized representative of Sulta company, we selected this equipment for phosphorous-containing fertilizer production plant. Since then, more than 5 years have been passed, and they have been operating at all process lines. The main advantages of equipment of this type are:

- operational reliability;
- efficiency;
- easiness in maintenance and repair;
- this type of crushers gives the highest yield of grain fraction from 0.5 up to 2,0 mm (it is the germs for granules formation) and less dust fraction at crushing;
- with the frequency regulators, it is easy and convenient to change intensity and thinness of crushing;
- at shut-down, the crushers are not overfilled by product, therefore, they doesn't require the by-pass chutes and dampers.

During the selection of equipment, we had familiarized ourselves with the operation of chain and chain-hammer crushers at foreign facilities (in Lithuania, Turkey, Jordan, Morocco, Spain etc.), and the best references were obtained from everywhere. Also, the preference to chain crushers, as more reliable in operation and having higher capacity, is given by lead developers of fertilizer production plants, such as Jacobs Engineering [12] and INCRO.

Below, the Sulta comparative data on particle size distribution of product, obtained after crushing in chain and chain-hammer crushers, is specified. The company provides the possible content of fractions, critical for production, more than 3 mm and less than 1 and 3 mm (Table 1).

For fertilizer production, Sulta company recommends the use of chain crushers, for feed phosphates – chain-hammer crushers.

During crushing of fertilizer large-size fraction, it is rational to obtain «grains» – particles of size from 0,5 up to 2,0 mm, which are the "germs" of granules at granulation process in AG or DGD. Finer, dusty fraction is of significantly less interest for granules obtaining, the most part of it flows to the gas scrubbing system, increasing the density of absorbing liquid and mole ratio NH_4/H_3PO_4 in it, complicating water balance; this results in decreasing the capacity of the process line and worsening of the gas scrubbing.

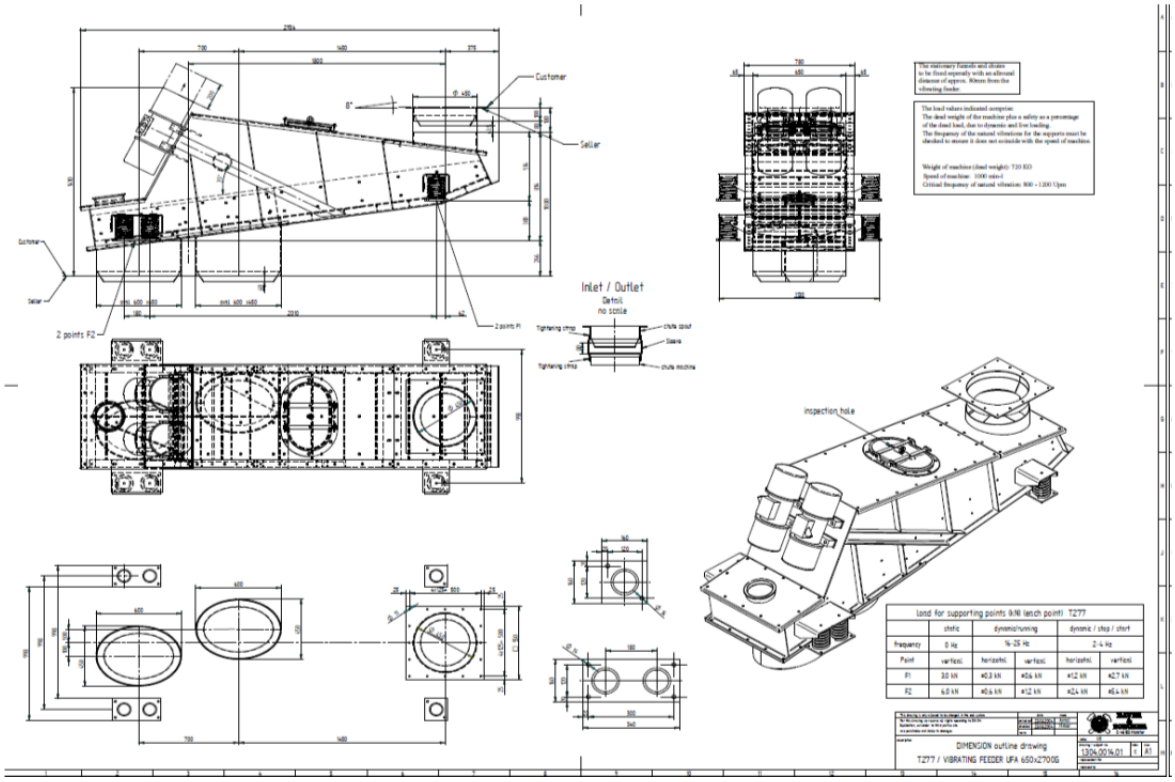

Fig. 10 – Vibrating distributor «Haver&Boecker»

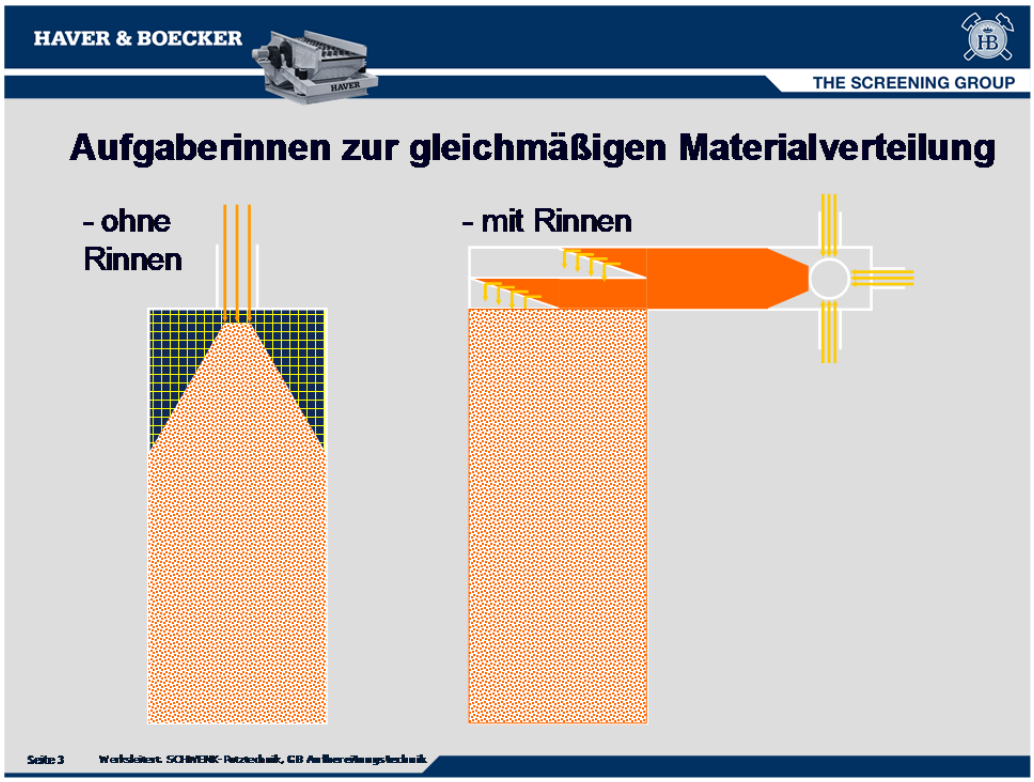

Fig. 11 – Diagram of flows in feeder «Haver&Boecker»

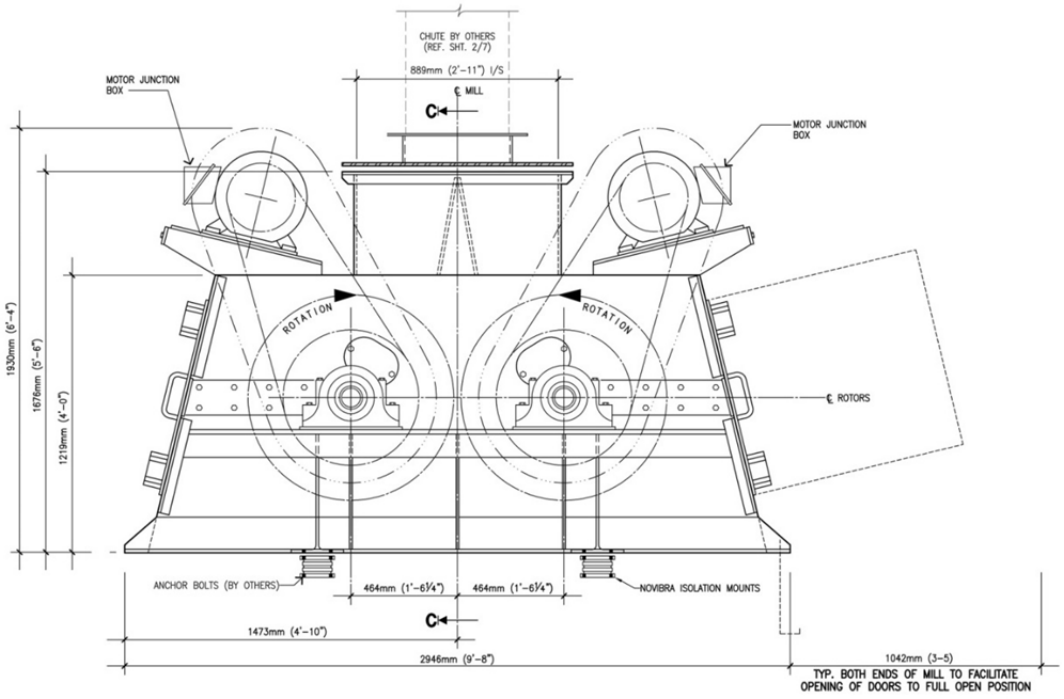

Fig. 12 – Sulta chain crusher with capacity of 50 t/h

Table 1.
Characteristics of chain and chain-hammer crushers of Sulta company

Item No.	Parameter	Crusher MODEL 604-W36-C			
		Chain		Chain-hammer	
1	Particle size distribution of loaded product, %				
	>20 mm (max.)	10		10	
	>10 mm (max.)	20		20	
	>4 mm	100		100	
2	Particle size distribution of unloaded product, %	MAP/DAP	NPK	MAP/DAP	NPK
	>3 mm	20-35	30-45	15-30	25-40
	<3 mm	80-65	70-75	85-70	75-60
	<1 mm (max.)	10	5	12	8
3	Design capacity, t/h	50		50	

Examination, made after phosphorous-containing fertilizer production plant revamp at one of the largest facilities in Russia [2, 13, 14], showed that particle size distribution values at crushers outlets were close to the shown in Table 1. The content of fractions less than 0.5 mm and less than 1.0 mm decreased more than 2 times as a result of usage of the mentioned crushers. Other types of crushers give worse results.

After crushing, the hammer crushers give the significant amount of fine fraction (dust) and non-crushed product lumps, passed through the crusher.

Three-roll crushers also form mush dust at crushing; and in case of using of more flexible products, they may even form the plates (“cakes”) of pressed fertilizers.

The examination also proved the possibility of crushing process regulation with frequency regulators: at changing the rotating speed, the intensity and thinness of crushing change.

We can conclude that our proposed option of equipment for classification and crushing sections at fertilizer production plants has been proved in practice and is worth serious attention.

References

1 I.G. Grishaev. New developments in equipment and process of phosphorous-containing fertilizers production //NIUIF proceedings. – M., 2014. p. 375-382;

2 A.M. Norov, A.S. Malyavin, M.N. Tcikin. Modernization and development of complex phosphorous-containing fertilizers production. In collection "Modern trends in production and usage of phosphorous-containing fertilizers and non-organic acids". Materials of International scientific and practical conference, May, 26, 2015, Moscow //JSC NIUIF. – M., 2015. p. 12-25;

3 A.M. Norov, A.S. Malyavin, K.N. Ovchinnikova., V.V. Sokolov and others. Development of norms of optimal process mode for production of granulated diammonium phosphate from non-concentrated wet phosphoric acid // Chemical technology. 2012. No.11. vol. 13. p. 641-647;

4 D.M. Ivell. Method of production of urea-based NPK-fertilizers. Paper of IFA Technical Conference. April, 2004, Beijing, China.

5 I.G. Grishaev, A.A. Gordin. Improvement of classification and crushing unit at ammonium phosphates production with usage the process with ammonizer-granulator. Bulletin "World of sulphur, N, P and K", M., OJSC NIUIF, issue 4, 2008.

6 Van Nguyen. The evolution of screening systems for optimum fertilizer product quality. SYMPHOS Conference 2013.

7 Patent of Russian Federation No. RU2545328. The method of regulation of phosphorous-containing fertilizers granulation process/B.V. Levin, I.G. Grishaev, A.M. Norov, D.A. Pagaleshkin, A.S. Malyavin, A.B. Gribkov, published in 27.03.2017.

8 P.V. Klassen, I.G. Grishaev. General fertilizers production processes // Khimiya. – M., 1990;

9 M.B. Generalov and others. Design of equipment for fertilizers granulation //Mashinostroyenie. – M., 1984;

10 P.V. Klassen, I.G. Grishaev, I.P. Shomin. Granulation // Khimiya – M., 1991;

11 P.M. Sidenko. Crushing in chemical industry // Khimiya. – M., 1977;

12 M.J. Bowness and D.M. Ivell, Jacobs Engineering, USA. Granulation plant revamps – methodology and design options. IFA Technical Conference. Chennai, India, September 24-27, 2002;

13 V.V. Davydenko, A.M. Norov, I.G. Grishaev, A.S. Malyavin and others. Experience of technical re-equipment of fertilizing ammonium phosphates production plant at OOO Balakovo Mineral Fertilizers. Bulletin "World of sulphur, N, P and K". M., OJSC NIUIF, issue No. 2, 2011.

14 Y.D. Chernenko, A.M. Norov., I.G. Grishaev, A.S. Malyavin and others. Possibilities of intensification of complex phosphorous-containing fertilizers. Chemical technics, No. 10, 2011.

This article was reviewed by Assoc. Prof. Dr. Pavel Pavlov and Prof. Dr. Nikolay Jechev.

NANOTECHNOLOGIES FOR PURIFICATION OF CONTAMINATED WATER

Petya Gencheva[1], Ivan Kanazirski[1]

[1]University of Mining and Geology "St. Ivan Rilski", 1700 Sofia, E-mail: p.gench@gmail.com

ABSTRACT. An overview is made of the nanotechnologies and nanomaterials that are consistent with traditional water purification methods. The possible nanomaterials that can be applied through traditional water purification technologies are discussed. The adsorption of impurities is possible through the introduction of nanoparticles that have a highly developed specific surface, which, in turn, determines the discovery of new sorption layers that accelerate diffusion and chemical processes. Membrane processes whereby nanomaterials are employed make it possible to manage nano-level properties. Thus, not only a large area for purification processes is provided, but also permeability is improved, as well as the mechanical and the thermal stability, the decomposition of the deposits built up in the process of membrane operation, and the self-cleaning of the membranes. Nanomaterials are also used in the treatment of industrial waste water from toxic heavy metals by the application of modified zeolites. The creation of systems of nanomaterials for possible re-use is a key element in the implementation of nanotechnology, the outcome of which will be easy applicability, low costs, and last but not least, the protection of human health.

Keywords: Nanotechnology, nanomaterials, water purification, re-use of water, membrane processes.

НАНОТЕХНОЛОГИИ ЗА ПРЕЧИСТВАНЕ НА ЗАМЪРСЕНИ ВОДИ

Петя Генчева[1], Иван Каназирски[1]

[1]Минно-геоложки университет "Св. Иван Рилски", 1700 София, E-mail: p.gench@gmail.com

РЕЗЮМЕ. Направен е обзор на нанотехнологиите и наноматериалите, съвместими с традиционните методите за пречистване на води. Обсъдени са възможните нанаматериали, които могат да бъдат приложени чрез традициониte технологии за пречистване на води. Адсорбцията на онечиствания е възможна чрез внедряване на наночастиците, които притежават силно развита специфична повърхност, което от своя страна обуславя откриване на нови сорбционни слоеве центрове, ускоряващи дифузията и химичните процеси. Мембранните процеси при които се използват наноматериали дават възможност за управление на свойства на нано-ниво, при което се осигурява не само голяма площ за протичане на процеси по пречистване, но и подобряване на пропускливостта, механичната, термичната стабилност, разграждането на налепите, формирани в процеса на работа на мембраната и самопочистването на мембраните. Наноматериали се използват и при пречистването на промишлени отпадъчни води от токсични тежки метали, чрез прилагането на модифицирани зеолити. Създаването на системи от наноматериали с възможна повторна употреба е ключов елемент при внедряването на нанотехнологиите, което да включва лесна приложимост, нисък разход на средства и не на последно място - опазване на човешкото здраве.

Ключови думи: Нанотехнология, наноматериали, пречистване на води, повторно използване на вода, мембранни процеси

Introduction

Water is the most valuable element on the Earth. In many parts of the world, access to pure water is a luxury that few could afford. Water purification and the full and rational use of water is a challenge for both water supply companies and industry. On a world scale, access to clean sources of water is a problem that is on the agenda in each country. This problem is related to global climatic changes, the still rapidly developing industries, and the population growth. This requires the need for technological innovations to create opportunities for an integrated water management policy.

The accelerated consumption of water supplies leads to the use of unconventional sources such as rain water, polluted freshwater, sewage and waste water, and sea water. Current purification technologies have reached the limit for providing adequate supplies of water so vital for human needs.

Nanotechnologies have the potential to contribute to the sensible management of water resources and to create the conditions for the efficient use of every drop of water. Progress in the field of nanotechnology offers opportunities for the development of next-generation water supply systems. This review aims at presenting the new highly efficient, modular and multifunctional nanotechnology-based processes that ensure high-performance water treatment at affordable pricess without being linked to major infrastructure projects (Qu et al, 2013).

Nanotechnologies are focused on the production of nanomaterials based on manipulation, control and integration of atoms and molecules of nanometric size, whereby the change in size leads to a change of properties. In the metric system, the prefix "nano" refers to one billionth (0.000 000 001 = 10^{-9}). In nanoparticles, at least one particle size should be less than 100 nm. At this level, both chemical activity due to reduced particle size and physical properties change. Owing to the increase in the surface-to-volume ratio at the nano level, the properties of the material become highly dependent on the surface of the materials. Nanomaterials can be classified in terms of particle size, surface morphology, crystalline forms, chemical nature, chemical composition, magnetic behavior, functional properties. They exist in hybrid compilations of these classifications.

Adsorption

Nanoparticles have an extremely high specific surface, which in turn leads to the discovery of new sorption centers that give opportunities for diffusion and chemical processes. A study of the adsorption of various organic substances (Pan and Xing, 2008) shows higher performance of carbon nanotubes (CNT's) compared to monolithic particles of activated carbon. The high adsorption capacity is mainly due to the large specific surface area and the possibility of interaction between carbon nanotubes and the polluting agent. According to Pan and co-authors (Pan et al., 2008), activated carbon has a lower adsorption affinity for polar organic compounds with low molecular weight than CNT's (carbon nanotubes) that easily adsorb polar organic compounds. Carbon nanotubes have been found to interact hydrophobically with the pollutant, whereby interaction between π-π-electrons is observed, as well as hydrogen, covalent bonding, and electrostatic interactions (Yang and Xing, 2010). Organic compounds with -COOH, -OH, -NH_2 can form a hydrogen bond to the surface of nano-sized carbon tubes, yielding electrons (Yang et al., 2008).

The effective adsorbents for heavy metals are iron oxide, titanium dioxide and alumina (dialuminium trioxide), where sorption occurs through complexation between dissolved metals and oxygen in the metal oxide (Koeppenkastrop and Decarlo, 1993). Theoretically, surface diffusivities can be predicted from site activation theory, which is based on the random walk model where atoms or molecules vibrate at localized sites along the surface. And for given oxide, the associated activation energy was observed to be equivalent for all three oxides, and for each oxide, the Polanyi constant (α) That relates adsorption enthalpy and activation energy was equivalent to the transition metals studied (Trivedi and Ax, 2000). Compounds with higher adsorption capacity have a higher rate of adsorption reaction, as well as a shorter diffusion process due to a higher number of surface reaction centers (Yean et al., 2005). Auffan and co-authors (Auffan et al., 2009) report that when the particle size drops below 20 nm, the specific surface thus formed accelerates the adsorption process due to the new adsorption sites created and the change in the surface structure.

Membranes

The main purpose of water purification is to remove undesirable organic, inorganic and biological pollutants. Membranes provide a physical barrier for these substances, allowing them to be used for purification of water from unregulated sources. In the design of membranes, the material from which they will be built is of great importance. Nanomaterial deployment makes it possible to manage nano-level properties, providing not only a large surface area for purification processes but also improved permeability, mechanical stability, thermal stability, as well as decomposition and self-cleaning of membranes (XiaoleiQu at all, 2013).

Electrospinning is an effective way of producing superfine fibers of different materials (e.g. polymers, ceramics, or even metals) (Cloete et al., 2010). The resulting nanofibers have a high specific surface and porosity. Membranes made of nanofibres can remove particle the size of up to a micron (Ramakrishna et al., 2006). Managing functional properties on the nano level can be achieved at the stage of electrospinning or during the final processing with impregnating solutions to supplement the purifying properties of matter (Li and Xia, 2004). Recently, many research groups have focused on creating multifunctional polymer and/or inorganic membranes to reduce contamination by increasing membrane hydrophilicity. The addition of nanoparticulate metal oxides Al_2O_3 (Maximus et al., 2010), silicon nanoparticles (Bottino et al., 2001), zeolite (Pendergast et al., 2010), and TiO_2 (Bae and Tak, 2005) to polymer ultrafiltration membranes increases the resistance of the membranes themselves to contamination. (Ebert et al., 2004; Pendergast et al., 2010).

The development of TFN (thin-film composite nanomembers) mainly focuses on the inclusion of nanomaterials in the active layer of thin-film composite (TFC) membranes by adding substances that modify the surface. Nanomaterials that have been tested for such applications include nano-zeolites, nano-Ag, nano-TiO_2, and CNTs. Membrane permeability and selectivity depends on the type, size and amount of added nanoparticles (XiaoleiQu at all, 2013).

Removal of heavy metals

Heavy metals are dangerous to living organisms, because due to their stability, toxicity, and persistent compounds formed, they easily accumulate in the environment. With the rapid development of such industrial activites as galvanising, exploitation of mines, tanning, manufacturing of batteries and pesticides, heavy metals in the industrial wastewater that is released into the environment are a threat to every living creature (F. Fu, Q. Wang, 2011, W. Yang et al., 2013). The heavy metals that recognised as bioaccumulative in the food chain are Pb, Hg and Cd. The removal of toxic heavy metals, such as Zn, Cu, Ni, Hg, Cd, Pb, and Cr, is of particular importance in the treatment of industrial waste water. Water purification usually involves mechanical purification, coagulation and flocculation, chemical precipitation, adsorption, solvent extraction, ultrafiltration, and ion exchange. Nanoparticles display unique characteristics due to their small sizes and large surface area compared to monolithic materials. A wide range of nanoparticles obtained by various methods have been investigated for the purposes of the removal of metallic contaminants, such as Cr (VI), Cu (II), Co (II), Cd (II), As (V), As (III), and Hg (II). Sharma and co-authors (Sharma et al., 2009) found that in most cases nanoparticles show better efficiency for removing these metallic contaminants. Separation from aqueous solutions is possible by specific methods depending on the selected nano-adsorbent.Their small size and large surface area compared to the monolithic ones. A wide range of nanoparticles obtained by various methods have been investigated for the removal of metallic contaminants such as Cr (VI), Cu (II), Co (II), Cd (II), As (V) And Hg (II), Sharma and co-authors (Sharma et al., 2009) have established that, in most cases, nanoparticles show better

effectiveness in the removal of these metallic contaminants. The latter are removed from aqueous solutions by specific methods that depend on the selected nano-adsorbent.

Research by Hristovski and co-authors (Hristovski et al., 2009) found that nanoparticles of metal (hydro-) oxides could be incorporated into the micropores of activated charcoal or other porous materials. The nanocomposites thus produced can simultaneously remove organic pollutants and arsenic.

Zeolites are natural materials with a highly selective capacity and cation exchange activity. The most common among the natural zeolites, as well as the one that is used most often, is clinoptilolite. Replaceable cations in the zeolite structure, such as K, Na, Ca, Mg, are not toxic, so zeolite is particularly suitable for final treatment in sewage treatment (M. Trgo et al., 2006).

Milan Kragovića and associates (Kragovića et all, 2013) conducted studies with zeolite modified with Fe (III). The results of their research have shown that significantly higher sorption of lead is achieved by modifying the natural zeolite with Fe (III) ions under normal conditions. The characterisation of the sorption processes in both natural zeolite and Fe (III)-zeolite before and after the sorption of lead confirms a complex lead sorption mechanism involving ion exchange, as well as hemisorption and precipitation of lead on the zeolite surface. Researchers have confirmed that in zeolite modified with Fe (III) ions there is an increased sorption of lead, which makes it a reliable water purifier.

Lv Guocheng and co-authors (Lv Guocheng. et all, 2014), reported that they used zeolite modified with Fe (II) with a concentration of 55 mmol/kg or 0.3% Fe in their research work. The zeolite employed by them showed good Cr (VI) sorption. Immobilization of Cr (VI) was increased by decreasing the pH of the solution and increasing the ionic strength. In an input sample with a Cr (VI) content and a concentration of 100 mg/l, Fe (II) modified zeolite removes Cr (VI) more efficiently than unmodified zeolite. Greater particle size and well-maintained conductivity of the modified zeolite make it an appropriate permeable barrier material for restoring groundwater.

Chromium and its compounds are widely used in many industries such as metallurgy, metal finishing, and production of chemicals. Wastewater from these industries contains hexavalent chromium, Cr(VI), at concentrations ranging from tens to hundreds of mg/l. Zeolites are an appropriate material for removing heavy metal ions from wastewater because of their relatively low price coupled with the harmlessness of their exchangeable ions. Natural Bulgarian zeolite and zeolite modified with metal, Cu (II), Fe (II), Fe (III), and Pb(II), i.e. Bulgarian clinoptilolite from the region of the East Rhodopes, have been studied for their ability to remove chromium oxyanions from model wastewater. It has been found that natural and Cu (II)-modified zeolite display negligible ability to uptake Cr (VI) from soft neutral model industrial wastewater. The modification of zeolite, by its pre-treatment with Fe (II), Fe (III) and Pb (II) solutions, increases its uptake capacity. Pb-modified zeolite removes over 95 % of the available Cr(VI) in one step for 30 min at initial Cr (VI) concentration of 30 mg/l and pH=6. Over 45 % of the available Cr (VI) was removed in one step for 30 min at initial Cr (VI) concentration of 10 mg/l and pH=6 by Fe (III)-modified zeolite. These facts could be a basis for using this natural clinoptilolitic rock to remove in consecutive steps firstly Pb (II) or Fe (III) ions, and then Cr (VI) can be removed by the already loaded zeolite. Panayotova (Marinella Panayotova, 2015) establishes, that chromium removal decreases with the increase of the pH value of the wastewater subjected to treatment. The zeolite uptake capacity increases with the increase in the pollutant's initial concentration. The kinetics of Cr uptake by Fe (II) and Fe (III)-modified zeolite obeys the pseudo-first order kinetic equation for adsorption. This fact, together with the correlation that was found between Cr uptake and Na+ and K+ release into the solution, shows the importance of ion-exchange processes in Cr immobilisation by iron-modified zeolite.The kinetics of Cr uptake by Pb-modified zeolite is described by the equation for the first order irreversible reactions. The findings support the idea for the mechanism of the surface chemical precipitation of $PbCrO_4$. (Marinela Panayotova, 2015).

Osmosis

Osmosis is the process of purification by means of fine-pored membranes that permeate water molecules and retain the larger molecules of dissolved substances. Permeable membranes retain all dissolved salts, organic substances, viruses and bacteria. Liu and associates (Liu et al., 2011) describe a pollutant removal system by "destabilization" using superparamagnetic nanoparticles, thereby removing drinking water without hydraulic pressure or heat. The process of producing drinking water is environmentally sustainable and without any waste.

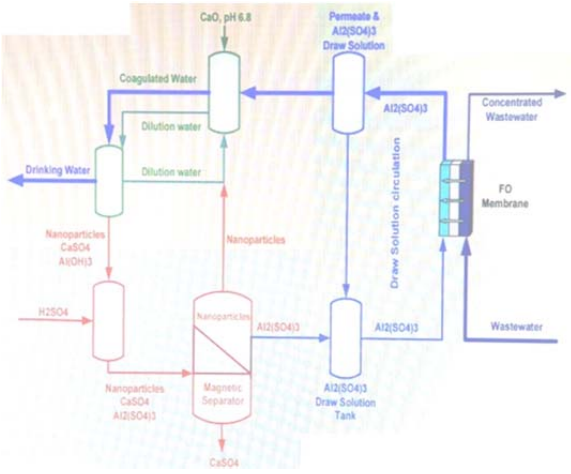

Fig.1. A detailed diagram of the release process through a $Al_2(SO_4)_3$ solution and using nanoparticles (Liu et all, 2011).

Figure 1 shows a multistage process comprising controlled osmosis, whereby a solution of 250 ml, 0.5 M $Al_2(SO_4)_3$ diffuses through the semipermeable membrane, then passes through a separating portion to separate the dissolved $Al_2(SO_4)_3$, and to produce drinking water. The $Al_2(SO_4)_3$ solution is diluted with de-ionized water and can be used repeatedly during the process. The addition of CaO to the diluted solution results in the formation of a gel-like mixture containing gel and $CaSO_4$ crystals which are stably suspended

in the solution and can not be precipitated from the solution. Negatively charged nanoparticles of Fe_3O_4@SiO_2 are added to the solution. Upon application of an external magnetic field, the particles of the solution are separated within minutes, leaving clean water behind. The separated particles of $Al(OH)_3$, $CaCO_4$, and $Fe_3O_3SiO_2$ nanoparticles are sent for re-use by adding sulfuric acid (H_2SO_4), whereby Fe_3O_4@SiO_2 nanoparticles are collected by an external magnetic field and $CaSO_4$ precipitates to the bottom and is removed. The regenerated $Al_2(SO_4)_3$ solution is returned back to the process of controlled osmosis.

In the process of osmosis, it is necessary to create a hydrophilic coating on the permeable membranes, which helps dissolve the impurities that have been formed on the membrane during the process.

Conclusion

Nanotechnology for water purification is a topic that affects the entire world community. The unique properties of nanomaterials and their implementation in the familiar water purification technologies is a challenge for many researchers. Nanotechnologies for water purification are important, but it should be pointed out that not all of those could be used in modern purification systems, because, in addition to technical hurdles and high cost, there is also the risk of potential threat to the environment and human health.

Creating systems of nanomaterials with possible re-use is a key element in the implementation of nanotechnology, which includes easy applicability, low costs, and, last but not least, the protection of human health. The introduction of nanoparticles into a single monolith system would result in better property management and control over matter. It is necessary to combine technologies that allow nanoparticles to manifest their specific properties, while at the same time firmly seizing the nanoparticles in a reinforced matrix to prevent further separation of the particles from the matrix. Nanomaterials that release metal ions should be carefully controlled by laying a coating or by optimising the size and shape. The detection and release of the nanomaterial is a challenge and a major technical barrier to risk assessment (B.F. da Silva, 2011; Tiede et al., 2008).

The adoption of innovative technologies strongly depends on work efficiency, on cost, and on the management of potential risk. The production of nanomaterials and the creation of nanotechnologies that manage to purify water without allowing the nano particles involved in the purification process to leave the system is a challenge for many researchers. The use of nanofilters to capture the particles that have escapedis a possible solution to this problem but is also bound to the high value of the end product. The use of nanosystems designed to prevent potential hazards associated with the use of nanomaterials in water and in waste water treatment will lead to a wider public support, which is crucial for the spread of new technologies.

References

Auffan M., Rose J., Bottero J.Y., Lowry G.V., Jolivet J.P., Wiesner M.R., Towards a definition of inorganic nanoparticles from an environmental, health and safety perspectiveNature Nanotechnology, 4 (10) (2009), pp. 634-641.

Bae T.H., Tak T.M., Effect of TiO_2 nanoparticles on fouling mitigation of ultrafiltration membranes for activated sludge filtration, Journal of Membrane Science, 249 (1–2) (2005), pp. 1-8.

Bottino A., Capannelli G., D'Asti V., Piaggio P., Preparation and properties of novel organic-inorganic porous membranesSeparation and Purification Technology, 22–23 (1–3) (2001), pp. 269-275.

Cloete T.E., Kwaadsteniet M.d., Botes M., Lopez-Romero J.M., Nanotechnology in Water Treatment ApplicationsCaister Academic Press (2010).

Ebert K., Fritsch D., Koll J., Tjahjawiguna C., Influence of inorganic fillers on the compaction behaviour of porous polymer based membranesJournal of Membrane Science, 233 (1–2) (2004), pp. 71-78.

Fu F. , Wang Q. , Removal of heavy metal ions from wastewaters: a review, Journal of Environmental Management, 92(2011), pp. 407-418.

Hristovski K.D., Nguyen H., WesterhoffP.K., Removal of arsenate and 17-ethinyl estradiol (EE2) by iron (hydr)oxide modified activated carbon fibersJournal of Environmental Science and Health Part A - Toxic / Hazardous Substances & Environmental Engineering, 44 (4) (2009), pp. 354-361.

Jeong.H. B, Hoek E.M.V. , Yan Y.S. , Subramani A., Huang X.F. , Hurwitz G. , Ghosh A.K., Jawor A. , Interfacial polymerization of thin film nanocomposites: a new concept for reverse osmosis membranes, Journal of Membrane Science, 294 (1–2)(2007), pp. 1-7.

Koeppenkastrop D., Decarlo E.H., Uptake of rare-earth elements from solution by metal-oxidesEnvironmental Science and Technology, 27 (9) (1993), pp. 1796-1802.

Kragovića Milan, Dakovića Aleksandra, Markovića Marija, Krstićb Jugoslav, Gattac G. Diego, Rotirotic Nicola, Characterization of lead sorption by the natural and Fe(III)-modified zeolite, Applied Surface Science, Volume 283, 15 October 2013, Pages 764-774.

Liu Z.Y. , Bai H.W. , Lee J. , SunD.D. , A low-energy forward osmosis process to produce drinking water, Energy & Environmental Science, 4 (7)(2011), pp. 2582-2585

Li D., Xia Y.N., Electrospinning of nanofibers: reinventing the wheel, Advanced Materials, 16 (14) (2004), pp. 1151-1170.

Lv Guocheng, Li Zhaohui, Jiang Wei-Teh, Ackley Caren, Fenske Nancy, Demarco Nick, Removal of Cr(VI) from water using Fe(II)-modified natural zeolite, Chemical Engineering Research and Design, 2014, pp. 384 - 390.

Marinela Panayotova, Possible use of metal - modified clinoptilolite for chromium removal from wastewater, Annual Univ. Mining and Geology", 58, Part II, 2015, 163-167.

Maximous N., Nakhla G., Wong K., Wan W., Optimization of $Al_{(2)}O_{(3)}$/PES membranes for wastewater filtration, Separation and Purification Technology, 73 (2) (2010), pp. 294-301.

Pan B., Xing B.S., Adsorption mechanisms of organic chemicals on carbon nanotubesEnvironmental Science and Technology, 42 (24) (2008), pp. 9005-9013

Pan B., Lin D.H., Mashayekh H. i, Xing B.S., Adsorption and hysteresis of bisphenol A and 17 alpha-ethinyl estradiol on carbon nanomaterialsEnvironmental Science and Technology, 42 (15) (2008), pp. 5480-5485

Pendergast M.T.M. , Nygaard J.M. , Ghosh A.K., Hoek E.M.V. , Using nanocomposite materials technology to understand and control reverse osmosis membrane compaction, Desalination, 261 (3) (2010), pp. 255-263

Qu. X.L., Brame J., Li.Q., Alvarez J.J.P., Nanotechnology for a safe and sustainable water supply: enabling integrated water treatment and reuse, Accounts of Chemical Research, 46 (3) (2013), pp. 834-843

Ramakrishna S., Fujihara K., Teo W.E., Yong T., Ma Z.W., Ramaseshan R., Electrospun nanofibers: solving global issuesMaterials Today, 9 (3) (2006), pp. 40-50

Silva B.F.da, Perez S. , Gardinalli P. , Singhal R.K., Mozeto A.A. , Barcelo D. , Analytical chemistry of metallic nanoparticles in natural environments, Tr Ac Trends in Analytical Chemistry, 30 (3)(2011), pp. 528-540

Sharma Y.C., Srivastava V., Singh V.K., Kaul S.N., Weng C.H., Nano-adsorbents for the removal of metallic pollutants from water and wastewaterEnvironmental Technology, 30 (6) (2009), pp. 583-609

Tiede K. , A. Boxall B.A. , Tear S.P. , J Lewis. , David H. , Hassellov M. , Detection and characterization of engineered nanoparticles in food and the environment, Food Additives and Contaminants, 25 (7)(2008), pp. 795-821

Trivedi P., Axe L., Modeling Cd and Zn sorption to hydrous metal oxidesEnvironmental Science and Technology, 34 (11) (2000), pp. 2215-2223

Trgo M. , Perić J. , Vukojević-Medvidović N. , A comparative study of ion exchange kinetics in zinc/lead-modified zeolite–clinoptilolite systems, Journal of Hazardous Materials, 136 (2006), pp. 938-945

Xiaolei Qu., Alvarez Pedro J.J., Li Qilin, Applications of nanotechnology in water and wastewater treatment, Water Research, Volume 47, Issue 12, 1 August 2013, Pages 3931-3946.

Yang K., Xing B.S., Adsorption of organic compounds by carbon nanomaterials in aqueous phase: Polanyi theory and its applicationChemical Reviews, 110 (10) (2010), pp. 5989-6008

Yang K., Wu W.H., Jing Q.F., Zhu L.Z., Aqueous adsorption of aniline, phenol, and their substitutes by multi-walled carbon manotubesEnvironmental Science and Technology, 42 (21) (2008), pp. 7931-7936

Yang W. , Ding P. , Zhou L. , Yu J. , Chen X. , Jiao F. , Preparation of diamine modified mesoporous silica on multi walled carbon nanotubes for the adsorption of heavy metals in aqueous solution, Applied Surface Science (2013), 10.1016 / j.apsusc.2013.05.028

This article was reviewed by Prof. Dr. Marinela Panayotova and Assoc. Prof. Nely Mincheva.

LIQUID PHASE OXIDATION AS A POSSIBILITY FOR THE REMOVAL OF OIL COMPOUNDS FROM PRODUCED WATER

Marinela Panayotova[1], Gospodinka Gicheva[1], Lyubomir Dzherahov[1], Neli Mincheva[1]

[1]University of Mining and Geology "St. Ivan Rilski", Sofia 1700, Bulgaria, marichim@mgu.bg

ABSTRACT. The extraction of oil is accompanied by the generation of a large amount of wastewater polluted with various organic compounds. In order to be discharged into natural water bodies or re-injected into the wells, the wastewater must be treated to meet the requirements laid down in the relevant legislation. This work presents: (a) the results of the analysis of real water samples produced in the course of oil production – discharged or re-injected; (b) the results of laboratory experiments carried out with real water samples that explore the potential of two liquid phase oxidation methods (using hydrogen peroxide and hypochlorite solution) to remove organic pollutants. Data from the hydrogen peroxide oxidation study at different concentrations of the added reagents are provided. Information on the effect of the added hypochlorite concentration and treatment time on the oil compounds and COD removal efficiency is presented. The kinetics of the process of decreasing the concentration of pollutants from both types of water (discharged and re-injected) has been monitored at the optimum concentration of the added hypochlorite.

Keywords: oilfield produced water treatment, oily wastewater purification, liquid phase oxidation

ОКИСЛЕНИЕ В ТЕЧНА ФАЗА КАТО ВЪЗМОЖНОСТ ЗА ОТСТРАНЯВАНЕ НА НЕФТОПРОДУКТИ ОТ ПРОДУКЦИОННА ВОДА

Маринела Панайотова[1], Господинка Гичева[1], Любомир Джерахов[1], Нели Минчева[1]

[1]Минно-геоложки университет "Св. Иван Рилски", 1700 София, marichim@mgu.bg

РЕЗЮМЕ. Добивът на нефт е съпроводен с генериране на огромно количество отпадъчна вода, замърсена с различни органични съединения. За да бъдат заустени в естествени водосборни басейни или реинжектирани, отпадъчните води трябва да бъдат третирани, за да отговарят на изискванията, предвидени в съответното законодателство. Настоящата работа представя: (а) резултатите от анализа на заустваните или използвани за реинжекция реални водни проби от добив на нефт; (б) резултатите от лабораторни експерименти, проведени с реалните водни проби и изследващи възможностите на два метода за окисление в течна фаза (с водороден пероксид и с разтвор на хипохлорит) с цел отстраняване на органичните замърсители. Предоставят се данни от изследване на окислението с водороден пероксид, при различни концентрации на добавения реагент. Дава се информация за влиянието на концентрацията на добавения хипохлорит и времето за третиране върху ефективността на отстраняване на нефтопродукти и ХПК. Проследена е кинетиката на процеса на намаляване на концентрацията на замърсителите в двата вида води (заустваните и използвани за реинжекция) при оптимална концентрация на добавения реагент.

Ключови думи: третиране на отпадъчна вода от добив на суров нефт; пречистване на отпадъчна вода, замърсена с нефтопродукти; окисление в течна фаза

Introduction

Oil well production fluid usually consists of oil and water that is generally separated by physical techniques. The water stream is referred to as "produced water" or in broader sense – "oily wastewater". The composition of the produced water depends mainly on the oilfield geological conditions, the recovery method, and the age of the production wells. Although concentrations of different pollutants can vary by order of magnitude, the contaminants in the produced water can be divided into the following groups: dissolved and dispersed oils, dissolved formation minerals, production chemicals, production solids, and dissolved gases (Ahmadun et al., 2009). Oil is a natural mixture of hydrocarbons, such as benzene, toluene, ethylbenzene and xylenes (BTEX), naphthalene, phenantherene, dibenzothiophene (NPD), polyaromatic hydrocarbons (PAHs), and phenols. The polar constituents distributed between the low and medium carbon ranges are water-soluble. BTEX and phenols are the most soluble compounds in produced water. Organic acids (formic and propionic) are typically found in produced water. Aliphatic hydrocarbons, phenols, carboxylic acid, and low molecular weight aromatic compounds are most often included as soluble oil compounds in produced water. Usually, PAHs and some of the heavier alkyl phenols (C6–C9 alkylated phenols) are less soluble in produced water and less present as dispersed oil. The dissolution of the formation minerals leads to the availability of inorganic anions and cations, and radioactive materials in produced water. Salt concentration can vary in very wide ranges. Production chemicals are added to treat or prevent operational problems. However, their concentration in produced water is usually as low as 0.1 mg/L (Veil et al., 2004). Production solids are a wide range of materials (formation solids, corrosion and scale products, bacteria, waxes, and asphaltenes). In anoxic produced water, sulfides (polysulfides and hydrogen sulfide) are generated by sulfate reducing bacteria (Neff, 2002).

Produced water is the largest waste stream generated in oil industry (Hosny et al., 2015). Table 1 summarizes the range of produced water characteristics in different oilfields in the world (Tibbetts et al., 1992; Bessa et al, 2001; Li et al, 2006; Lu et al., 2006; Ahmadun et al., 2009; Li et al, 2010; Hosny et al., 2015).

Table 1.
Range of produced water characteristics in different oilfields in the world

Parameter	Value	Parameter	Value
pH	4.3 – 10.0[1]	Phenols, mg/L	0.009-23
COD, mg/L	274-2,517	Chlorides, mg/L	274-2,517
BOD_5, mg/L	11-21[2]	Sulfates, mg/L	2-1,650
TOC, mg/L	0-1,500	Bicarbonates, mg/L	77-3,990
TSS, mg/L	1.2-1,000	Sulfides, mg/L	0.14[4]
TDS, mg/L	675-141,522	Sodium, mg/L	132-97,300
O&G, mg/L	31-275	Potassium, mg/L	24-4,300
TPH[3], mg/L	49-64	Calcium, mg/L	13-25,800
Total polar, mg/L	9.7-600	Magnesium, mg/L	8-6,000
Higher acids, mg/L	<1-63	Barium, mg/L	0.25-650
Volatile, BTEX, mg/L	0.39-35	Strontium, mg/L	0.02-1,000
Total oil (IR), mg/L	2-565	Heavy metals[5], mg/L	0.068-48.38

[1] Most often: 6.7 – 7.4
[2] Only Li et al., 2010
[3] Total petroleum hydrocarbons
[4] Only Lu et al., 2006
[5] Considered elements in this case are: Sb, As, Be, Cd, Cr, Cu, Pb, Hg, Ni, Ag, V, and Zn

Produced water is considered an oilfield waste which has to be managed before being discharged into natural water bodies or re-injected into the wells. Different methods have been proposed for produced water treatment: physical (such as the use of sand filters and cyclones, evaporation, freeze–thaw / evaporation), chemical (such as liquid phase oxidation with hydrogen peroxide - H_2O_2, Fenton reagent, hypochlorite, ozonation, supercritical water oxidation), physicochemical (such as adsorption on activated carbon, coagulation and flocculation, flotation, the use of electrochemical processes, the use of membrane processes), photocatalytic, and biological. The methods mentioned are used alone or in combination (Ahmadun et al., 2009; Yu et al., 2013; Jamaly et al., 2015; Seyed et al., 2016).

Chemical oxidation relies on the oxidation half-reaction, whereby a substance loses electrons, and a reduction half-reaction, whereby a substance accepts electrons. Both half-reactions always occur together since free electrons cannot exist in a solution and electrons must be conserved (RPSEA, 2012). Oxidants commonly studied in produced water treatment applications include hydrogen peroxide, ozone and calcium hypochlorite. The appropriate oxidant for a given application depends on many factors such as raw water composition, specific contaminants present in the water, and local chemical and power costs. Chemical oxidation is a well-established technology for treating wastewater. Generally, it requires minimum equipment. Oxidation can be employed to remove organics and some inorganic compounds, like iron and manganese, from produced water. The degree of removal or oxidation rate may be controlled by applied chemical dose and contact time between oxidants and water. No pre-treatment is required for oxidation.

Within 30 min, Wenhu and co-authors (2013) achieved up to 70 % COD removal from oily wastewater in batch experiments using wet hydrogen peroxide oxidation. Chemical oxidation of produced water separated from the gas stream of a gas refinery in Iran has been attempted by using hydrogen peroxide, ozone, and calcium hypochlorite (Shokrollahzadeh et al., 2012). The stoichiometric amount of hydrogen peroxide for the complete COD removal from produced water achieved 15% degradation of organic materials. Ozonation of produced water for 1 hour ended at 12% COD removal. Increasing the pH of the water to 10 improved treated water quality which indicated higher ozonation efficiency of the produced water at higher pH values. Maximum COD removal was achieved by using calcium hypochlorite as an oxidant - in the range of 36-70% depending on the hypochlorite concentration. The reaction was completed within 30 minutes.

Some authors find H_2O_2 as a proper oxidizing reagent, while others claim it is inefficient and report high oxidation efficiency when calcium hypochlorite is used; therefore, we have decided to test both reagents for the treatment of wastewater from a Bulgarian oilfield plant.

Methods and materials

Two water samples (noted as No 1 and No 2) were collected from two points where the produced water is discharged into a surface water body. Another two samples (noted as No 3 and No 4) were picked up from produced water re-injected into wells. Temperature, pH value, ΔpH value (index of water saturation with respect to $CaCO_3$), Eh value, and specific conductance were measured on site by using electrometric methods (with combined electrodes and WTW Multi 340i/SET device). Collected samples were preserved following the standard procedures and were transported in a cooling bag to the laboratories where other parameters were measured.

Dissolved oxygen was determined by the Winkler method. Hardness, respectively concentration of calcium and magnesium ions, was found by titration with EDTA. Concentration of chloride and bicarbonate ions were determined by titrimetric methods - titration against silver nitrate (Mohr's method) and hydrochloric acid solution (methyl orange method), correspondingly. The turbidimetric method was applied to determine the concentration of sulfates. The concentration of sodium and of potassium was determined by ICP-AES. Oil hydrocarbons concentrations were determined by the spectrophotometric method in the UV range, after their separation by extraction with CCl_4 (ASTM, 1979; BDS, 1989;

APHA, 1992; Krawczyk, 1996; UNEP/WHO, 1996). Sulfide concentration was determined spectrophotometrically. The method is based on the fact that sulfide ions and hydrogen sulfide form a sulfur-containing compound with dimethyl para-phenylenediamine in an acidic medium, which, upon oxidation with iron (III) chloride passes into methylene blue (BDS, 1989). Phenol concentration was determined spectrophotometrically by using Spectroquant NOVA 60 and Spectroquant phenol test. The method is analogous to EPA 420.1, APHA 5530 C+D, and ASTM D 1783-01. Chemical oxygen demand (COD) was determined spectrophotometrically by using Spectroquant NOVA 60, a Merck COD cell test, after chloride depletion and sample digestion in a Spectroquant TR420 device. The method corresponds to DIN38409-41-2, DIN ISO 1575 and is analogous to EPA410.4, APHA 5220 D, and ASTM D 1252-06 B. The concentration of residual active chlorine was determined by using Chlorine Test (free chlorine) in freshwater and seawater of Merck (1.14670.0001). The determination of chlorine is based on the reaction between tetramethylbenzidine (TMB) and free chlorine.

Water treatment with H_2O_2 was conducted at initial reagent concentrations of 25 mg/L and 200 mg/L of H_2O_2 for 30 min reaction time. Experiments with calcium hypochlorite [$Ca(ClO)_2$] were carried out at different initial concentrations (50, 200 and 400 mg/L) for 30 min of treatment time. In each experiment, 700 mL of the corresponding wastewater sample was used. All samples were stirred with a magnetic stirrer at a speed of 400 rpm. The presented data are average from two parallel trials.

Results and discussion

Data on integral physicochemical parameters of the studied samples are presented in Table 2. The values of concentration of macro-components are summarized in Table 3.

Table 2.
Integral physicochemical parameters of the studied water samples

No	t °C	pH	Eh mV	rH	χ mS/cm	ΔpH	Diss.O_2 mg/L
1	20.2	7.46	-14	14.45	5.76	+0.07	<0.08
2	19.0	7.42	-16	14.30	3.45	-0.01	<0.08
3	25.2	7.23	-86	11.55	4.43	-0.01	<0.08
4	30.3	7.67	-141	10.57	5.74	-0.07	<0.08

Table 3.
*Concentration of macro- and meso-components of the studied water samples, mg/L**

No	1	2	3	4
Ca^{2+}	101	73	83	100
Mg^{2+}	54	40	47	56
Na^{+}	1052	624	900	1050
K^{+}	17	16	15	16
Cl^{-}	1782	980	1312	1780
HCO_3^{-}	433	500	567	580
SO_4^{2-}	18	18	22	28
S^{2-}	2.40	1.96	3.42	9.76
Hardness	4.74	3.47	4.0	4.8

*Hardness – in mmol/L

Table 4 shows some integral chemical parameters of the analyzed water samples.

Table 4.
Some integral parameters of the studied water samples

No	COD, mg/L	Oil compounds, mg/L	Phenols, mg/L
1	46	52	0.11
2	39	262	0.18
3	39	47	0.07
4	58	184	0.21

By comparing the values presented in Tables 1 and 2, it may be stated that the pH value of the studied water is in the range of the typical values. Having in mind the existing relation between salt concentration and specific conductance, it is clear that the produced water under consideration is practically in the lower edge of the worldwide reported salt concentrations of produced water. The measured Eh values are indicative for anaerobic conditions. This is in accordance with the very low concentrations of dissolved oxygen and concentrations of sulfides determined in most samples (Table 3). Considering the calculated rH values, we can conclude that all tested waters possess slightly reducing properties and those are more pronounced for re-injected waters. The quick ΔpH test showed that waters are practically in equilibrium with respect to calcium carbonate.

As expected for the produced oilfield water, Na^+ is the major cation and Cl^- is the major anion found in studied waters (Table 3). Concentrations of all other macro-components are in the lower edge of the worldwide reported concentrations in produced water (Tables 1 and 3).

Requirements toward the oil-drilling companies for discharging produced water are given by Decree 6 (Bulgarian Council of Ministers, 2000). The limits which must not be exceeded are given in Table 5.

Table 5.
Maximum permissible concentrations / levels of some water pollutants subjected to observation in oilfield production water intended for discharge (Bulgarian Council of Ministers, 2000)

Parameter	Threshold value
pH	6 - 9
Oil hydrocarbons	20 (40[1]) mg/L
Phenols	1.0 mg/L
Sulfides	1.0 mg/L

[1] - at production capacity of less than 10, 000 t/day

The comparison between the limits given in Table 5 and the values found and presented in Tables 2, 3 and 4 shows that the water samples meet the legislation criteria with respect to pH values and concentration of phenols, while higher concentrations of sulfides and oil compounds were observed. The measured COD values are below those reported for non-treated produced water by other authors (compare with Table 1). The data for COD point out that all studied samples show low concentration of chemically oxidizable compounds by dichromate ions. Usually, this is the case when heavy organic compounds are present in the wastewater as tiny droplets. We

have determined the density of the extracted crude oil of 0.952 g/cm^3. The oil can be classified as heavy crude oil - with density in the range of 0.88 – 1.00 g/cm^3 (Fingas, 2015). This finding is supported also by the gas chromatography that shows availability in the produced water not only of typical low molecular weight hydrocarbons but also of compounds having a molar mass that is higher than 300 g/mol and corresponds to polycyclic aromatic hydrocarbons (Marvin, 1999). According to Fingas (2015), heavy crude oil is rich in tri- to pentacyclic terpenes and aromatic steranes.

Treatment of all samples with 25 mg/L of H_2O_2 led to the removal of oil compounds by less than 3 %. Increasing the H_2O_2 concentration up to 200 mg/L did not cause significant chemical oxidation of organics and the determined removal was no more than 5 %. Therefore, the wet oxidation with H_2O_2 is not suitable for the studied type of produced water and further experiments with this oxidizing reagent were aborted.

Results on oil compounds removal by oxidation with calcium hypochlorite are presented in Table 6.

Table 6.
Oil compounds removal (%) by hypochlorite treatment at different concentrations for 30 min

No	Oil Removal, %		
	50 mg/L	200 mg/L	400 mg/L
1	18	77	78
2	77	84	86
3	3	42	81
4	3	11	55

The results presented in Table 6 show: (a) Increasing the reagent concentration from 200 to 400 mg/l does not improve the results significantly for samples 1 and 2; (b) For samples 3 and 4 only the highest concentration of the oxidant results in good oil removal. Such behavior corresponds to the two types of studied waters – discharged (1 and 2) and re-injected (3 and 4).

The only significant difference between these two types of water samples can be found in the concentrations of sulfides, the Eh and rH values, which reveals different reductive properties of the media. The oxidizability of the oil compounds present in the water depends not only on the oxidizing agent but also on the solution properties and results in a different degree of decomposition of organics.

A reported drawback of using calcium hypochlorite is the high concentration of residual active chlorine in the treated water (Shokrollahzadeh et al., 2012). In our case, such disadvantage was not observed and the measured residual chlorine concentration was less than 0.3 mg/L, which is within the limits for drinking water (Bulgarian Council of Ministers, 2001).

It is worth mentioning that a lower removal for samples 1 and 4 was determined and it may have been due to a short reaction time. In order to study the kinetics of the reaction, we chose these two samples (1 and 4) for further experiment. Our preliminary experiments showed that a concentration 200 mg/L of $Ca(ClO)_2$ causes good oil removal for sample 1 and would allow us to study the kinetics of the oxidation process for 60 min. Sample 4 requires higher oxidant concentration to achieve a moderate removal, and the kinetic study was performed with 400 mg/L of $Ca(ClO)_2$ for 60 min.

The kinetic curves for samples 1 and 4 are presented in Figure 1.

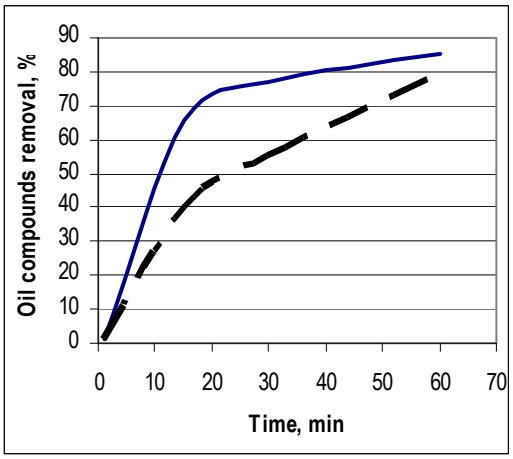

Fig. 1. Kinetic curves of oil compounds removal by oxidation with $Ca(ClO)_2$: sample 1 —, sample 4 - - -

As can be seen in Figure 1, increasing the treatment time leads to higher oil removal for both samples. We can relate that to the more complete oxidation for a longer time. Kinetic curves reveal that the reaction consists of two stages – 1st "fast" and 2nd "slow". Generally, it shows that different processes take place and limit the oxidation reaction rate during the fast and slow step. Despite of lower oxidant concentration for sample 1, its initial reaction rate for the first 20 minutes is higher than that for sample 4. Most probably, the oil contaminants in water 4 are compounds that are more stable to oxidation. After this period, the reaction rate for both samples decreases, but the rate for sample 1 drastically lowers due to the consumption of oxidant. The rate for sample 4 seems to become higher than that of sample 1, which may relate to the oxidation of organic compounds with lower molecular weighs produced during the first stage of the reaction. In the end of the reaction time, the removal for sample 1 is 85% and for sample 4 is 79%. We cannot assume that complete oxidation will be achieved, unless a large excess of the oxidant is used, because the whole amount of oxidant added in wastewater may not be available for the oxidation of organic matter only. Some amount of oxidant is expected to react and oxidize inorganic pollutants present in the wastewater (for example, heavy metals and sulfides).

Chemical oxygen demand is another parameter that was controlled during the treatment of produced water. Taking into consideration the kinetic study results, we applied $Ca(ClO)_2$ in concentration 200 mg/L for sample 1 and treated it for 30 and 60 min, while for sample 4 we have used higher concentration of $Ca(ClO)_2$, 400 mg/L. Results on COD removal for samples 1 and 4 by oxidation with hypochlorite are presented in Table 7.

It seems that (Table 7) the increase in treatment duration leads to an increase in the COD removal. The impact of the reaction time on COD removal was more pronounced for sample 4, which contained more organics that were stable to oxidation and was treated with higher concentration of the oxidizing reagent.

Table 7.
COD removal for samples 1 and 4 by hypochlorite treatment for 30 and 60 min reaction time

No	Treatment conditions	COD removal, %
1	30 min, 200 mg/L $Ca(ClO)_2$	14.6
1	60 min, 200 mg/L $Ca(ClO)_2$	18.2
4	30 min, 400 mg/L $Ca(ClO)_2$	17.5
4	60 min, 400 mg/L $Ca(ClO)_2$	36.6

Such finding is in accordance with the data observed for the oil removal parameter (Table 6 and Fig. 1). Similar percentage of the COD removal, at similar concentrations of the $Ca(ClO)_2$ used, were reported by other authors as well (Shokrollahzadeh et al., 2012). It is worth to mention that in many cases, the COD removal is considerably lower in comparison with the oil removal. It can be considered as an indirect evidence for the transformation of oil compounds with big molecular weight to smaller molecules upon treatment with oxidant, and then low-carbon-chain organics are easily oxidized by dichromate, which cause a higher analytical result for COD. Further studies are needed to clarify the mechanism of chemical oxidation of various oily compounds.

Conclusions

In this study, we explored the possibility for chemical oxidation treatment of oilfield produced water, generated after gravitational separation of heavy crude oil from the extraction fluid. We found that the wet oxidation with H_2O_2 is not suitable a method for the produced water polluted with high molecular and polycyclic oil compounds.

Oxidation with calcium hypochlorite is a promising technology for removing heavy oil compounds and decreasing the water COD. Chemical properties of the oil compounds, treatment time and oxidant dose are important factors that influence the oil removal efficiency. Generally, the increase of oxidant concentration and treatment time increase the oil compounds and COD removal efficiency.

References

Ahmadun, F. R., A. Pendashteh, L. C. Abdullah, D. R. A. Biak, S. S. Madaeni, Z. Z. Abidin. Review of technologies for oil and gas produced water treatment. - Journal of Hazardous Materials, 170, 2009. - 530–551.

APHA, Standard Methods for the Examination of Water and Wastewater, 18th edition. American Public Health Association (APHA), American Water Works Association (AWWA), Water Pollution Control Federation (WPCF), Washington, DC., 1992.

ASTM, Methods for ChemIcal AnalysIs of Water and Wastes, EP*AI600f4-79f020,* U S. EnvIronmental Protection Agency; Cincinnati, OH., 1979.

Bessa, E., Jr. G. Sant'Anna, L. M. Dezotti. Photocatalytic/H_2O_2 treatment of oil field produced waters. Applied Catalysis B: Environmental, 29, 2001. - 125–134.

BDS, Bulgarski durzhaven standart, Zashtita na okolnata sreda, t.1, Standartizatsia, Sofia, 1989.

Bulgarian Council of Ministers**,** 2000. Decree 6 / 9.11.2000 on emission standards for permissible content of harmful and dangerous substances in wastewater discharged into water bodies, Bulgarian State Gazette No. 97 / 28.11.2000 and No. 24 / 23.03.2004.

Bulgarian Council of Ministers, 2000. Decree 9 / 16.03.2001 on the quality of water intended for drinking and household purposes, Bulgarian State Gazette No. 30 / 28.03.2001 and No 102 /12.12.2014.

Fingas, M. Handbook of oil spill science and technology, John Willey&Sons, 2015, - 728 p.

Hosny, R., M. Fathy, M. Ramzi, Th. Abdel Moghny, S.E.M. Desouky, S.A. Shama. Treatment of the oily produced water (OPW) using coagulant mixtures. - Egypt. J. Petrol, 2015. available at: http://dx.doi.org/10.1016/j.ejpe. 2015.09.006.

Jamaly, S., A..Giwa, S. W. Hasan. Recent improvements in oily wastewater treatment: Progress, challenges, and future opportunities. J. Env. Sci., 37, 2015. - 15-30.

Krawczyk, W. E. Manual for karst water analysis, University of Silesia, Poland, 1996.

Li, G., T. An, J. Chen, G. Sheng, J. Fu, F. Chen, S. Zhang, H. Zhao. Photo-electro-catalytic decontamination of oilfield produced wastewater containing refractory organic pollutants in the presence of high concentration of chloride ions. J. Hazard. Mater. B138, 2006. - 392–400.

Li, G., S. Guo, F. Li. Treatment of oilfield produced water by anaerobic process coupled with micro-electrolysis. *Journal of Environmental Sciences,* 22(12), 2010. - 1875–1882.

Lu, J., X. Wang, B. Shan, X. Li, W. Wang. Analysis of chemical compositions contributable to chemical oxygen demand (COD) of oilfield produced water. Chemosphere, 62, 2006. - 322–331.

Marvin, C. H., R.W Smith., D.W.Bryant, B.E. McCarry. Analysis of high-molecular-mass polycyclic aromatic hydrocarbons in environmental samples using liquid chromatography-atmospheric pressure chemical ionization mass spectrometry. J. Chromatogr. A, 863, 1999. - 13-24.

Neff, J. M., Bioaccumulation in Marine Organisms: Effect of Contaminants from Oil Well Produced Water. Elsevier, The Netherlands, 2002.

RPSEA, *Assessment of produced water treatment technologies,* 1st Ed., November 2009 Colorado School of mines, 2012**.**

Seyed, A., C. Knutson, Y. Yang, H. H. S. Dastgheib. Treatment of produced water from an oilfield and selected coal mines in the Illinois Basin. Int. J. Greenhouse Gas Control, 2016. (http://dx.doi.org/10.1016/j.ijggc.2016.05.002).

Shokrollahzadeh, S., F. Golmohammad, N. Naseri, H. Shokouhi, M. Arman-mehr. Chemical oxidation for removal of hydrocarbons from gasfield produced water. Procedia Eng 42, 2012. - 942 – 947.

Tibbetts, P.J.C., I.T. Buchanan, L.J. Gawel, R. Large. A comprehensive determination of produced water

composition. In: J. P. Ray, F. R. Engelhardt (Eds.), Produced Water: Technological/Environmental Issues and Solutions, Plenum Publishing Corp., New York, 1992. - 97–113.

UNEP/WHO, Water Quality Monitoring – A Practical Guide to the Design and Implementation of Freshwater Quality Studies and Monitoring Programmes, (Eds. Bartram J. and Ballance R.), Published on behalf of United Nations Environment Programme and the World Health Organization, 1996.

Veil, J., M. G. Puder, D. Elcock, R.J.J. Redweik. A White Paper Describing Produced Water from Production of Crude Oil, Natural Gas and Coal Bed Methane, 2004. available at: http://www.netl.doe.gov/publications/oilpubs/prodwaterpaper.pdf.

Wenhu, Z., W. Wang Dejin, F. F. Ruoyu, L. Feng. Studies on affecting factors and mechanism of oily wastewater by wet hydrogen peroxide oxidation. Arabian Journal of Chemistry. 2013. (http://dx.doi.org/10.1016/j.arabjc.2013.08.022).

Yu, L., M. Han, F. He. A review of treating oily wastewater Arabian J. of Chemistry, 2013, (http://dx.doi.org/10.1016/j.arabjc.2013.07.020)

Acknowledgements

This work was supported by the MTF158/2017 project “Investigation of methods for oilfield produced water treatment” at the University of Mining and Geology under the Regulation for Scientific and Research Projects.

This article was reviewed by Prof. Dr. Ivan Nishkov and Assoc. Prof. Dr. Ivan Kanazirski.

COPPER IONS REMOVAL FROM AQUEOUS MEDIUM THROUGH EMERALDINE

Grigor Hlebarov[1], Silviya Lavrova[1], Bogdana Koumanova[1]

[1]University of Chemical Technology and Metallurgy, 8 Kliment Ohridski Blvd., 1756 Sofia, Bulgaria, e-mail engeco2001@uctm.edu

ABSTRACT. *In situ* synthesized emeraldine salt and emeraldine base were used for copper ions removal from aqueous medium. Physicochemical parameters such as initial copper ion concentration, polymer dosage and contact time between the emeraldine and the metal ions in aqueous solution were studied. Removal efficiency of copper using the obtained emeraldine forms was estimated. It was found that the emeraldine base extracts the Cu^{2+} from aqueous solutions better than emeraldine salt. The binding process between the metal ions and the polymer occurs immediately after their mixing and the main process occurs within 15 minutes in all the experiments. For this period of time and 50 mg/l initial copper ions concentration, removal efficiency of 76.8 % was achieved using 1.5 g emeraldine base. The maximal removal efficiency (98.3 %) of the ions was achieved for 1440 min.

Keywords: *In situ* polymerization; polyaniline; emeraldine; copper ions removal

ОТСТРАНЯВАНЕ НА МЕДНИ ЙОНИ ОТ ВОДНА СРЕДА ЧРЕЗ ЕМЕРАЛДИН

Григор Хлебаров[1], Силвия Лаврова[1], Богдана Куманова[1]

[1]Химикотехнологичен и металургичен университет, София 1756, бул. Климент Охридски 8, e-mail: engeco2001@uctm.edu

РЕЗЮМЕ. За отстраняването на медни йони от водна среда са използвани емералдин сол и емералдин база, синтезирани чрез in situ полимеризация. Изследвани са физико-химични параметри като начална концентрация на медните йони, доза на полимера и време на контакт между емералдина и металните йони във водния разтвор. Изчислен е ефектът на пречистване на водната среда от медните йони чрез получените емералдинови форми. Установено е, че емералдин база извлича Cu^{2+} йони от водния разтвор по-добре от емералдин сол. Процесът на свързване между металните йони и полимера се случва веднага след смесването им, а основния процес протича в рамките на 15 минути при всички експерименти. За този период от време и 50 mg/l начална концентрация на медните йони, ефектът на пречистване, който се постига при използването на 1.5 g емералдин база е 76,8 %. Максималният ефект на отстраняване (98.3 %) на тези йони се постига за 1440 минути.

Ключови думи: In situ полимеризация; полианилин; емералдин; отстраняване на медни йони

Introduction

Because of the toxic effect of heavy metals they have to be removed from the wastewater before discharge in the aquatic environment. Among the most dangerous heavy metal ions are Cu, Cd, Cr, As, Pb, Ni, etc. During the production of copper from copper ores, manufacturing of printed circuit board, electronics plating, plating, printing operations, wire drawing, copper polishing, paint manufacturing and wood preservatives production, large amounts of wastewaters with high concentrations of copper ions are produced. Copper ions are very toxic for living organisms and therefore should not be released into the environment. Adsorption is a basic process for metal ions removal from wastewater and the scientists are looking for new materials which are alternative to the conventional sorbents, such as Polyaniline, Polypyrrole, Polythioamide, Chitosan, etc. [Hutchison et al., 2008; Henneberry et al., 2011; Wiatrowski et al., 2009; Urgun-Demirtas et al., 2012; Hamissa et al., 2010; Blázquez et al., 2011; Schiewer and Balaria, 2009; Yu et al., 2011]. Some of these materials have polymeric nature [Gupta et al., 2004; Li et al., 2009; Balarama et al., 2005; Kumar et al., 2008; Zhang et al., 2010; Wang et al., 2009; Chandra and Kim, 2011; Bhaumik et al., 2012; Vieira and Beppu, 2006; Kagaya et al, 2010; Qu et al., 2010], The usage of such substances is significant because of their high stability, selectivity, low cost, easy polymerization and effectiveness. It is well-known that the nitrogen atom in these amino-derivatives makes coordinate bond with positive charged metal ions, due to the free electron pairs. Thanks to this, the metal ions removal from treated wastewater is possible. The small particle size of the used adsorbent also increases the process effectiveness. The aniline monomer polymerization leads to production of polyaniline which can be found in one of these three idealized oxidation states – leucoemeraldine, which is white, clear or colorless $(C_6H_4NH)_n$, emeraldine – has dark green color for the emeraldine salt and dark blue color for the emeraldine base $([C_6H_4NH]_2[C_6H_4N]_2)_n$, and (per)nigraniline, which is blue/violet $(C_6H_4N)_n$ [Stejskal, 1995].

The aim of this study is to investigate the possibility of emeraldine to remove copper from model aqueous medium. This research consists of emeraldine synthesis and study of the experimental conditions like metal ion concentration, polymer dosage and contact time for copper ions removal from model aqueous solution. These investigations are needed to determine the removal efficiency.

Materials and methods

Chemicals and solvents

Pure for analysis Aniline ($C_6H_5NH_2$), Hydrochloric acid (HCl) and Ammonium persulfate ($(NH_4)_2S_2O_8$) were used for the polyaniline synthesis. Distilled water was also used. For the emeraldine salt conversion to emeraldine base, pure for analysis sodium hydroxide (NaOH) was used. $CuSO_4.5H_2O$, pure for analysis, with concentration of 1 g/l was used for the preparation of the model solution. Then standard solutions with concentrations of 1.0, 2.0, 4.0, 6.0, 8.0, 10.0, 30.0, 50.0, 70.0 and 100.0 mg/l were prepared. Sodium acetate and acetic acid, pure for analysis, were used for preparing acetate buffer for pH adjustment.

Emeraldine salt synthesis

Polyaniline was synthesized through oxidative polymerization using aniline monomer ($C_6H_5NH_2$) and ammonium persulphate ($(NH_4)_2S_2O_8$) as an oxidant. Distilled aniline (61.4 ml) was diluted with 1 M HCl to 2 liters in a volumetric flask. Ammonium persulphate (168.7 g) was diluted with distilled water to 800 ml. Both solutions were cooled in refrigerator at temperature of 5 ºC. After that the oxidant solution was added dropwise to the 0.5 M aniline solution. The mixture was stirred for 1 hour at room temperature and after that was left to polymerize. The greenish-black suspension of emeraldine salt was filtered through Buckner funnel using continuous stirring with mechanical agitator for better filtrate draining. The precipitate was washed repeatedly with distilled water and after its dewatering was dried in oven at 40 ºC to constant mass. The dried polymer was ground to a fine homogeneous powder.

Emeraldine base synthesis

Protonated emeraldine salt was converted to emeraldine base through washing with 1 M NaOH to pH 10.0 – 11.0. The polymer was dried at 40 ºC to constant mass and after that was ground to a fine homogeneous powder.

Removal technique

In order to establish the influence of the contact time on the copper ions removal as well as the influence of the polyaniline dosage, 50 ml individual samples with initial copper ion concentration of 50 mg/l were prepared. A pre-weighed on an analytical balance amount of polyaniline (m = 0.1 ÷ 1.5 g) and acetate buffer for adjustment of pH to 5 were added to each of the samples [Awual et al, 2014; Igberase et al., 2014; Mansour et al., 2011]. The water samples were poured in iodine flasks and agitated for 24 hours at temperature of 17±1 ºC. At the predetermined time intervals, 20 ml portions of each suspension were taken and filtered through blue ribbon filter paper to remove suspended polymer particles.

In order to establish the influence of the initial copper ions concentration on their removal, 50 ml aqueous samples with different initial copper ion concentration (C_o = 1 ÷ 100 mg/l) were prepared. A certain amount of polyaniline (m = 0.1 g) and acetate buffer for pH adjustment to 5 was added to each of the samples. The water samples were agitated at temperature of 17±1 ºC. At the end of the predetermined period of time, the 20 ml portions of each water samples were taken and filtered through blue ribbon filter paper to remove polymer particles.

Instrument and measurements

Atomic absorption spectrometry was used for copper concentration measurement in the precipitates (Perkin Elmer-323 apparatus).

Removal efficiency

The efficiency of Cu^{2+} removal by polyaniline was calculated according to the formula (1):

$$\mathrm{RE},\% = 100 - \left(\frac{C_t}{C_o}\right) \times 100 \quad (1)$$

where C_o is the initial Cu^{2+} concentration and the C_t is the concentration at time "t" in mg/l.

Results and discussion

Effect of contact time and polyaniline dosage on the removal efficiency.

The binding process between the copper ions and the polymer occurs immediately after mixing of the polymer and the aqueous media, containing copper ions, followed by a complexation reaction delay (Fig. 1). 28 % removal efficiency by 0.1 g emeraldine base was obtained in 15 minutes. After that the Cu^{2+} removal remains constant up to 24 hours. For comparison of the effectiveness of the two forms emeraldine – salt and base, at the same period of time 0.1 g emeraldine salt was used. It was established that the emeraldine salt removes 25 % of the initial 50 mg/l copper ions concentration and after that the removal efficiency also does not change until the 24th hour.

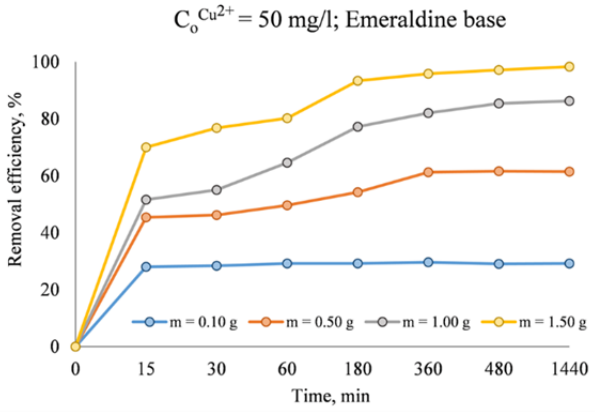

Fig. 1. Effect of the contact time and emeraldine base dosage on the removal efficiency.

In the experiments with the same initial copper ions concentration (50 mg/l) but greater emeraldine base dosage (0.5, 1.0 and 1.5 g), the removal efficiency, achieved in 15 minutes, was as follows: 45.4 %, 51.6 % and 70.0 %, respectively. At the 24th hour the removal efficiency was increased up to 61.4 %, 86.2 % and 98.3 %, respectively for the above mentioned quantities of emeraldine base. The usage of 1.5 g emeraldine base leads to the highest removal efficiency - 98.3 % in 24 hours. It is well-known that the emeraldine base is more effective for metal ions removal due to the more available electron pairs in its structure, compared

to the emeraldine salt, and the obtained results confirmed this statement. Despite that, the emeraldine salt succeeded to catch almost the same amount of copper ions as the emeraldine base in the identical technological conditions. Probably, the removal process with emeraldine salt is a combination of different mechanisms beside the complexation.

Effect of the initial Cu^{2+} concentration on the removal efficiency

The results show, that with initial copper ions concentration increasing, the effect of their removal with 0.1 g of polyaniline is decreasing (Fig. 2). For example, in a period of 30 minutes and the initial copper ions concentrations of 1 mg/l, 10 mg/l and 50 mg/l removal efficiency of 88 %, 60 % and 30 %, respectively, was achieved. The higher removal efficiency achieved in the experiments with lower copper concentration can be explained by the presence of a sufficient number of free electron pairs in the nitrogen atoms of the polymer chain, which have a higher electron density and that those are involved in the complexation with the copper ions. The increasing of the initial metal ions concentration leads to decreasing of the possibility for their attachment to the polymeric structure.

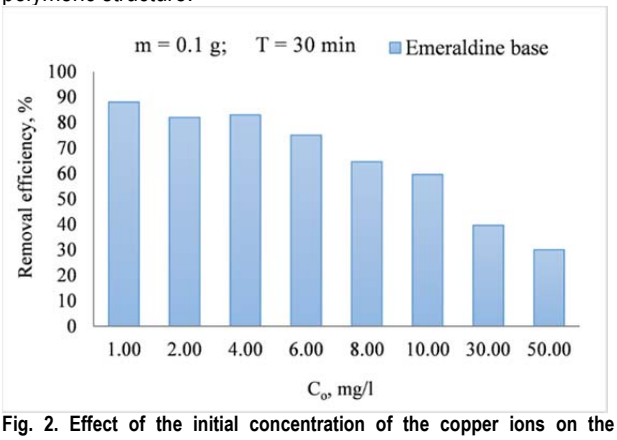

Fig. 2. Effect of the initial concentration of the copper ions on the emeraldine base removal efficiency.

The removal efficiency which was achieved in the experiments with emeraldine salt is lower in comparison with that in the experiments with emeraldine base. For example, in the 30 minute experiment with 10 mg/l initial copper ions concentration, the removal efficiency was 40 %, which is 1.5 times lower than that achieved in the experiment with emeraldine base at the same time and initial copper concentration. With copper ions concentration increasing, the removal efficiency of 0.1 g emeraldine salt is not higher than 27 % (Fig. 3).

Conclusions

The preparation of emeraldine salt and emeraldine base was successfully performed by *in situ* polymerization of aniline. The metal complexation reaction proceeds very quickly and in 15 minutes was achieved 70 % removal efficiency with initial copper ions concentration of 50 mg/l and 1.5 g emeraldine base. The removal efficiency of copper ions increased with the polymer dosage and the contact time increased. The emeraldine base removal efficiency was higher than that of the emeraldine salt.

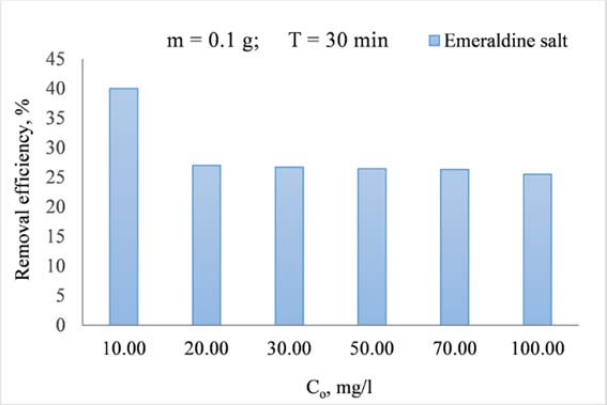

Fig. 3. Effect of the initial copper ions concentration on the removal efficiency of emeraldine salt.

References

Awual, M., Rahman, I., Yaita, T., Khaleque, M., Ferdows, M. pH dependent Cu(II) and Pd(II) ions detection and removal from aqueous media by an efficient mesoporous adsorbent. In: Chem. Eng. J., 236, 2014, 100-109.

Balarama, M., Krishna, H., Karunasagar, D., Rao, S., Arunachalam, J. Preconcentration and speciation of inorganic and methyl mercury in waters using polyaniline and gold trap-CVAAS. In: J. Talanta., 68, 2005, 329-335.

Bhaumik, M., Maity, A., Srinivasu, V., Onyango, M. Removal of hexavalent chromium from aqueous solution using polypyrrole–polyaniline nanofibers. In: J. Chem. Eng., 181-182, 2012, 323-333.

Blázquez, G., Martín-Lara, M., Tenorio, G., Calero, M. Batch biosorption of lead(II) from aqueous solutions by olive tree pruning waste: Equilibrium, kinetics and thermodynamic study. In: J. Chem. Eng., 168, 2011, 170-177.

Chandra, V., Kim, K. Highly selective adsorption of Hg2+ by a polypyrrole reduced graphene oxide composite. In: J. Chem. Commun., 47, 2011, 3942-3944.

Gupta, R., Singh, R., Dubey, S. Removal of mercury ions from aqueous solutions by composite of polyaniline with polystyrene. In: Sep. Purif. Technol., 38, 3, 2004, 225-232.

Hamissa, A., Lodi, A., Seffen, M., Finocchio, E., Botter, R., Converti, A. Sorption of Cd(II) and Pb(II) from aqueous solutions onto Agave Americana fibers. In: J. Chem. Eng., 159, 2010, 67-74.

Henneberry, Y., Kraus, T., Fleck, J., Krabbenhoft, D., Bachand, P., Horwath, W. Removal of inorganic mercury and methylmercury from surface waters following coagulation of dissolved organic matter with metal-based salts. In: Sci. Total. Environ., 409, 2011, 631-637.

Hutchison, A., Atwood, D., Santillian-Jiminez, Q. The removal of mercury from water by open chain ligands containing multiple sulfurs. In: J. Hazard. Mater., 156, 2008, 458-465.

Igberase, E., Osifo, P., Ofomaja, A. The adsorption of copper (II) ions by polyaniline graft chitosan beads from aqueous solution: Equilibrium, kinetic and desorption studies. In: J. Environ. Chem. Eng., 2, 2014, 362-369.

Kagaya, S., Miyazaki, H., Ito, M., Tohda, K., Kanbara, T. Selective removal of mercury (II) from wastewater using polythioamides. In: J. Hazard. Mater., 175, 2010, 1113-1115.

Kumar, P., Chakraborty, S., Ray, M. Removal and recovery of chromium from wastewater using short chain polyaniline synthesized on jute fiber. In: Chem. Eng. J., 141, 2008, 130-140.

Li, X., Feng, H., Huang, M., Strong adsorbability of mercury ions on aniline/sulfoanisidine copolymer nanosorbents. In: Chemistry, 15,18, 2009, 4573-4581.

Mansour, M., Ossman, M., Farag, H. Removal of Cd (II) ion from waste water by adsorption onto polyaniline coated on sawdust. In: Desalination, 272, 2011, 301-305.

Qu, R., Sun, C., Zhang, Y., Chen, J., Wang, C., Ji, C., Liu, X. Syntheses, characterization and Hg (II) adsorption properties of porous cross-linked polystyrene modified with2-aminopyridine via a sulfoxide/sulfone-containing spacer arm. In: J. Chem. Eng. Data., 5, 2010, 4343-4351.

Schiewer, S., Balaria, A., Biosorption of Pb2+ by original and protonated citrus peels: Equilibrium, kinetics, and mechanism. In: J. Chem. Eng., 146, 2009, 211-219.

Stejskal, J., Kratochvil, P., Jenkins, A. Polyaniline: forms and formation. In: Collect. Czech. Chem. Commun., 60, 1995, 1747-1755.

Urgun-Demirtas, M., Benda, P., Gillenwater, P., Negri, M., Xiong, H., Snyder, S. Achieving very low mercury levels in refinery wastewater by membrane filtration. In: J. Hazard. Mater., 215-216, 2012, 98-107.

Vieira, R.,Beppu, M. Dynamic and static adsorption and desorption of Hg(II) ions on chitosan membranes and spheres. In: J. Water. Res., 40, 2006, 1726-1734.

Wang, J., Deng, B., Chen, H., Wang, X., Zheng, J. Removal of aqueous Hg(II) by polyaniline: Sorption characteristics and mechanisms. In: J. Environ. Sci. Technol., 43, 2009, 5223-5228.

Wiatrowski H., Das, S., Kukkadapu, R., Ilton, E., Barkay, T., Yee, N. Reduction of Hg(II) to Hg(0) by magnetite. In: Environ. Sci. Technol., 43, 2009, 5307-5313.

Yu, X., Luo, T., Zhang, Y., Jia , Y., Zhu, B., Fu, X., Liu, J., Huang, X. Adsorption of lead(II) on O2-plasma-oxidized multi walled carbon nanotubes: Thermodynamics, kinetics, and desorption. In: J. ACS Appl. Mater. Interfaces., 3, 2011, 2585-2593.

Zhang, Y., Li, Q., Sun, L., Tang, R., Zhai, J. High efficient removal of mercury from aqueous solution by polyaniline/humic acid nanocomposite. In: J. Hazard. Mater., 175, 2010, 404-409.

This article was reviewed by Prof. Dr. Maria Karsheva and Assoc. Prof. Dr. Svetlana Bratkova.

SULPHATES REMOVAL FROM AQUEOUS MEDIUM USING SURFACE MODIFIED CLINOPTILOLITE

Silviya Lavrova[1], Bogdana Koumanova[1]

[1]University of Chemical Technology and Metallurgy, 8 Kliment Ohridski Blvd., 1756 Sofia, Bulgaria, e-mail engeco2001@uctm.edu

ABSTRACT. Wastewater from mining industry is seriously polluted due to its acidic nature and heavy metals content. In aquatic environment the metal sulphides are oxidised into sulphates, that is a reason for their high concentrations in the outgoing water streams. Experiments for removal of sulphate anions from aqueous medium using natural and modified natural clinoptilolite, respectively, have been carried out. The influence of physico-chemical parameters such as initial sulphate concentration, clinoptilolite mass, contact time, and stirring speed, were investigated. When clinoptilolite modified with barium chloride (particle size of 0.1 - 0.8 mm) was used, the removal efficiency increased up to about 50 %, while the removal efficiency with natural not treated clinoptilolite was about 10 %.

Keywords: acid mine drainage, sulphates, clinoptilolite, surface modification

ОТСТРАНЯВАНЕ НА СУЛФАТИ ОТ ВОДНА СРЕДА ЧРЕЗ ПОВЪРХНОСТНО МОДИФИЦИРАН КЛИНОПТИЛОЛИТ

Силвия Лаврова[1], Богдана Куманова[1]

[1]Химикотехнологичен и металургичен университет, София 1756, бул. Климент Охридски 8
e-mail: engeco2001@uctm.edu

РЕЗЮМЕ. Отпадъчните води от минната индустрия са сериозно замърсени, поради киселия си характер и съдържащите се в тях тежки метали. Във водна среда металните сулфиди се окисляват до сулфати, което е причина за техните високи концентрации в изходящите водни потоци. Проведени са експерименти за отстраняване на сулфатни аниони от водна среда с използването на природен и модифициран клиноптилолит, съответно. Изследвано е влиянието на физико-химични параметри като началната концентрация на сулфатите, масата на клиноптилолита, времето на контакт, както и скоростта на разбъркване. С използването на модифициран с бариев хлорид природен клиноптилолит (размер на частиците 0.1 - 0.8 mm), е постигнат ефект на отстраняване на сулфатните аниони до 50 %, докато ефектът на отстраняване с немодифициран клиноптилолит е около 10 %.

Ключови думи: кисели руднични води, сулфати, клиноптилолит, повърхностна модификация.

Introduction

Wastewater from mining industry is seriously polluted due to its acidic nature and heavy metals content. Because of the oxidation the metal sulphides are converted into sulphates in aquatic environment. As a result their concentrations in the outgoing water streams are very high. There are various methods for metal and sulphates removal. It is possible to achieve their significant removal using some specific microorganisms. During the sulphate reduction the metal ions concentrations are also decreasing [Kiran et al., 2017; Kiran et al., 2017; Bratkova et al. 2013]. There are electrochemical processes for mining wastewater treatment too. Wang et al., using a novel microbial electrolysis cells with intermittent electrical supply, achieve significant decrease of chemical oxygen demand (COD) and sulphates concentration. They found that the electrolysis cells working at intermittent electrical field for longer period of time are more effective in sulphates removal compared to the conventional microbial electrolysis cells. Microbial fuel cells are also used for sulphates reduction [Angelov et al, 2013; Lee et al., 2014; Weng and Lee, 2015]. These ions can be removed from wastewater using fluidized bed crystallization process [De Luna et al., 2017], but the most widely used method for sulphates ions removal from the mine wastewater is the chemical precipitation [Tolonen et al., 2016; Dou et al., 2017]. Using this method the sulphates are precipitated and the formed mineral called ettringite can be used as an adsorbent for subsequent removal of the arsenates contained in this type of wastewaters. Ion exchange, reverse osmosis and electrodialysis are also used for sulphates removal. The high cost of these methods is a limitation for their widespread usage. Adsorption is cost-effective and efficient method for wastewater treatment too. It is well known that its efficiency depends on the type and properties of the sorbent. Widely used sorbents are the zeolites. There are various zeolite types [Wang and Peng, 2010]. The natural zeolites are widely spread and low coast materials. Due to their structure the zeolites belong to the cationic exchangers [Margeta et al. 2014]. They effectively remove the positive charged ions from the wastewater, due to their negatively charged surface, but in slight extent they can trap anions too. After chemical modification with inorganic salts or organic surfactants, the number of positively charged exchange sites on their surface increases [Barczyk et al., 2014; Oliveira and Rubio 2007; Barczyk et al., 2014; Ghiaci et al., 2004; Allen et al., 2009; Samatya et al., 2007; Sun et al., 2011]. So, the anions contained in the wastewater, can be removed. The aim of this study was to examine the possibility for sulphate ions removal from an aqueous solution by modified clinoptilolite.

Materials and methods

Chemicals and solvents

Pure for analysis $BaCl_2.2H_2O$, NaCl, H_2SO_4, $CuSO_4.5H_2O$ and deionized water were used in the experiments. The zeolite used in the experiments is clinoptilolite ($(Na,K,Ca)_{2-3}Al_3(Al,Si)_2Si_{13}O_{36}\cdot 12H_2O$), obtained from the eastern part of the Rhodope mountain in Bulgaria. Two fractions of the material were used (0.1 - 0.8 mm; 0.8 - 2.5 mm).

Clinoptilolite modification

To obtain 10 g of modified clinoptilolite, 10 g of natural clinoptilolite (particle size of 0.1 - 0.8 mm; 0.8 - 2.5 mm) was mixed with 100 mL of 1M NaCl and the resulting suspension was shaken on a plate shaker for 24 hours at room temperature to prepare the surface of the material for further modification. Then the suspension was filtered and the clinoptilolite was washed with 1 L deionized water. The washed material was dried at 105 °C for 24 hours. The modification of the pre-treated clinoptilolite was carried out by contacting the activated clinoptilolite with 100 mL of 1M $BaCl_2.2H_2O$. The suspension was shaken again on a plate shaker for 24 hours at room temperature. After this period of time the suspension was filtered and the modified clinoptilolite was washed with 1 L deionized water and dried at 105 °C for 24 hours.

Preparation of standard solutions of sulphate ions

Initial model solution with concentration 1 g/L of SO_4^{2-} was prepared, by diluting H_2SO_4 with deionized water. Then standard solutions with concentrations of 50.0, 100.0, 150.0, 250.0, 300.0, 350.0 mg/L were prepared.

Removal technique

In order to establish the influence of the initial sulphate ions concentration on their removal, 50 mL of model solutions with different initial sulphate ion concentration (C_o = 50 - 350 mg/L) were prepared. A certain amount of clinoptilolite (m = 1 g) with grain size of 0.1 - 0.8 mm or 0.8 - 2.5 mm, was added to each of the samples, respectively. The samples were agitated at temperature of 17±1 ºC for 96 hours. At the end of this period of time, 20 mL portions of each samples were taken, filtered through blue ribbon filter paper to remove clinoptilolite particles and analyzed.

In order to establish the influence of the contact time on the sulphate ions removal as well as the influence of the clinoptilolite dosage, 2000 mL solution with initial sulphate ions concentration of 100 mg/L was prepared. To the aqueous solution was added a weighed amount of clinoptilolite (m = 3 - 5 g). The suspension was agitated for 1 hour (Heidolph RZR 2100 electronic) at 200 rpm. Samples were taken after 1, 3, 5, 8, 10, 15, 20, 30, 40, 50, 60 min and filtered through blue ribbon filter paper to remove suspended adsorbent particles. Then they were analyzed.

Instrument and measurements

The sulphate concentration was determined using the precipitates standard procedure (APHA, 1992).

Removal efficiency

The efficiency of SO_4^{2-} removal by clinoptilolite was calculated according to the formula:

$$\mathrm{RE},\% = \left(\frac{C_o - C_t}{C_o}\right) \times 100$$

where C_o is the initial SO_4^{2-} concentration and the C_t is the concentration at time "t" in mg/L.

Results and discussion

Effect of the initial SO_4^{2-} concentration on the removal efficiency

In order to estimate the influence of the initial sulphate ions concentration on the removal efficiency, 1 g of the natural and modified clinoptilolite was used, and the initial SO_4^{2-} ions concentration was varied from 50 to 350 mg/L. The results are presented in Figure 1. As shown on the figure, almost twofold decreasing of sulphates concentration was obtained at 50 mg/L initial concentration using 1 g natural clinoptilolite with particle size of 0.1 - 0.8 mm. The results show that with the increasing of the initial sulphate ions concentration, the effect of their removal by 1 g of natural clinoptilolite is decreasing. This is particularly evident at initial sulphate ion concentrations of 50 to 150 mg/L. At higher initial concentrations (from 250 to 350 mg/L) the removal efficiency was not significantly changed. For example, the removal efficiencies obtained at 150 and 350 mg/L were 7.7 and 7.3 %, respectively. About 10 % average sulphate anion removal efficiency using natural clinoptilolite with a particle size of 0.1 - 0.8 mm was obtained. The adsorption capacity of this material increased from 0.47 to 1.21 mg/g with the initial SO_4^{2-} concentration increasing from 50 to 300 mg/L. After that a plateau was reached. After modification of natural clinoptilolite with barium chloride, its removal efficiency significantly increases. Removal efficiency of 69.7 % was achieved using modified clinoptilolite (fraction 0.1 - 0.8 mm) for treatment of aqueous solution with initial sulphate concentration of 50 mg/L. This efficiency is 3.6 times higher than that achieved at the same conditions with nonmodified natural clinoptilolite. After that the removal efficiency was decreasing when the initial concentration was increasing up to 250 mg/L. After this concentration a significant change was not observed. Probably this insignificant change of the removal efficiency after initial concentration of 150 mg/L and of 250 mg/L using natural and modified clinoptilolite, respectively, is a result of specific sites saturation. For example, the removal efficiency obtained at 250, 300 and 350 mg/L were 35.4 %, 34.1 % and 31.8 %, respectively. The adsorption capacity of this material increased from 1.8 to 6.1 mg/g with the increase of the initial SO_4^{2-} concentration from 50 to 350 mg/L. The results show that the adsorption capacity of the modified clinoptilolite is significantly higher than that of the natural clinoptilolite. The same tendency was observed using larger grain size of the clinoptilolite, but the removal efficiency achieved was lower than that achieved with the finer fraction. Treating the aqueous solution with 50 mg/L initial sulphates concentration using natural and modified clinoptilolite (0.8 - 2.5 mm), respectively, the removal efficiencies obtained were 1.6 and 1.1 times lower than that achieved using natural clinoptilolite with the finer fraction. The adsorption capacities were also lower than that achieved with the finer fraction.

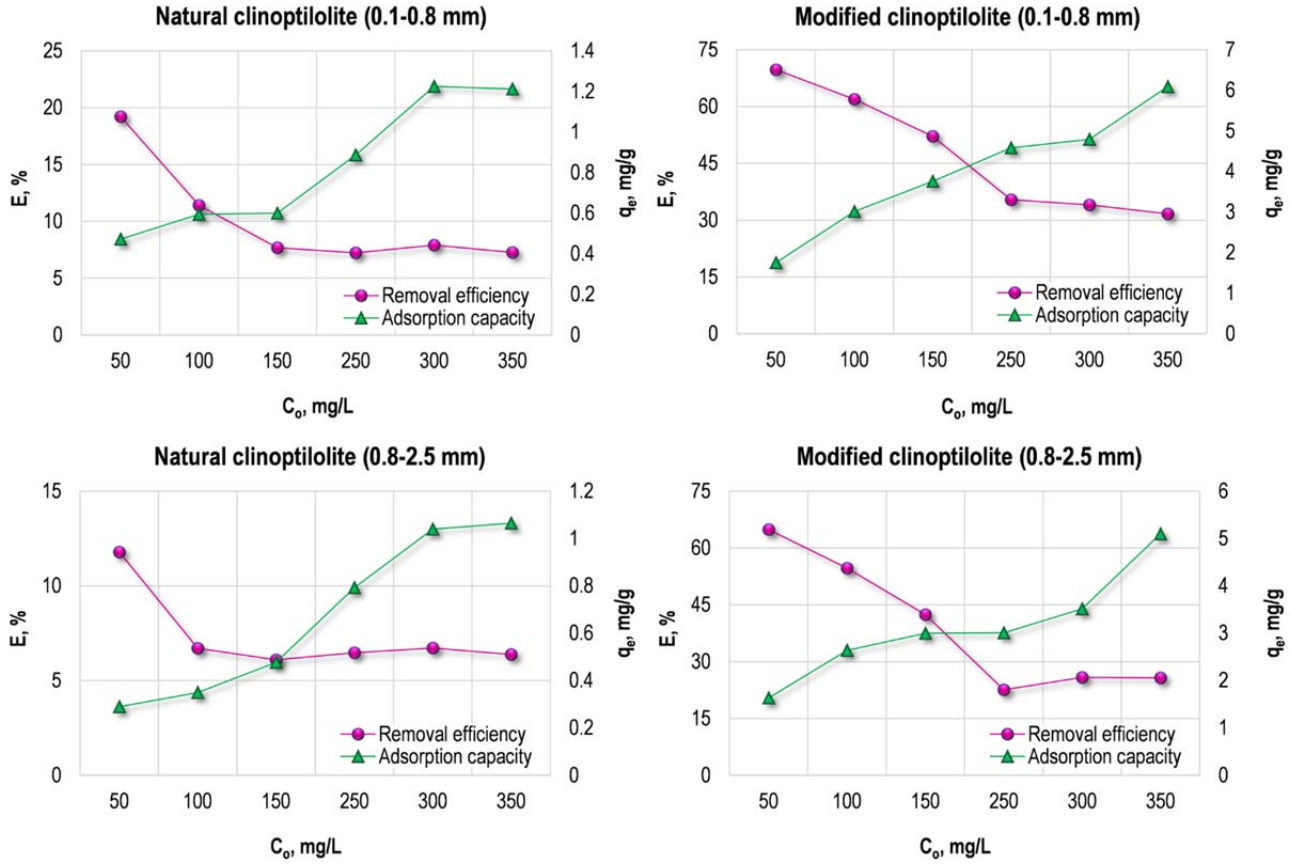

Fig. 1. Removal efficiency and adsorption capacity of the natural and modified clinoptilolite

Its maximal values obtained for model solutions with 350 mg/L initial sulphates concentration, were 1.1 mg/g and 5.1 mg/g, respectively, using natural and modified clinoptilolite, respectively.

Effect of contact time and clinoptilolite dosage on the removal efficiency

The removal of sulphate ions from the solution with 100 mg/L initial concentration with time is shown in Fig. 2. It is observed that the sulphate uptake occurs immediately after the addition of the clinoptilolite to the aqueous solution, followed by a nearly constant values. 66.2 % removal efficiency by 3 g modified clinoptilolite with particle size of 0.1 - 0.8 mm was obtained in the first minute. After that the SO_4^{2-} removal remains without significant change up to the 60th minute. After the 10th minute the removal curve is reaching a plateau, suggesting that equilibrium has been reached. This may be attributed to the lower availability of the specific sites on the modified clinoptilolite surface with time progressing. The removal efficiencies that were achieved at 30th and 60th minutes are 73.9 % and 77.6 %, respectively.

In general, an increase in the amount of clinoptilolite is followed by the increased removal efficiency of sulphate. In the experiments with the same initial sulphate ions concentration (100 mg/L) but greater clinoptilolite dosage (4 and 5 g), the removal efficiency, achieved at the first minute, were as follows: 70.5 % and 81.2 %, respectively. At the 60th minute the removal efficiencies were increased up to 79.7 % and 88.4 %, respectively, using 4 and 5 g of clinoptilolite. The increase of the dosage leads to an increase in the number of the available vacant specific sites, resulted in an increase of SO_4^{2-} removal efficiency by modified clinoptilolite.

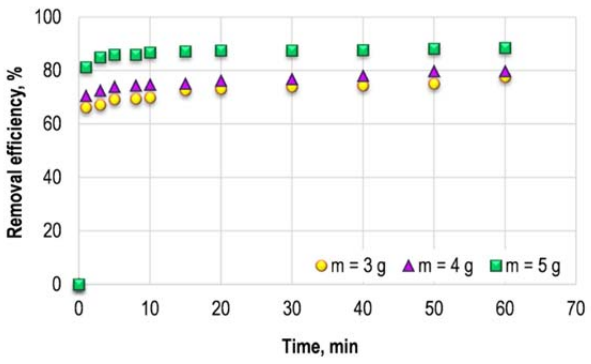

Fig. 2. Effect of the contact time and modified clinoptilolite dosage on the removal efficiency

Effect of the stirring speed on the removal efficiency

Experiments at 200 and 400 rpm were carried out in order to enhance the contact of SO_4^{2-} with the modified clinoptilolite (0.1 - 0.8 mm) (Table 1).

Table 1.
Removal efficiency at different stirring speed

t, min	Removal efficiency, %					
	3 g		4 g		5 g	
	200 rpm	400 rpm	200 rpm	400 rpm	200 rpm	400 rpm
60	77.6	84.1	79.7	86.03	88.4	88.7

The results show that the faster stirring of the system leads to better removal of the sulphates. Thus, for 60 minutes stirring at 400 rpm using 3, 4 and 5 g of the modified clinoptilolite the removal efficiency increases about 1.1 times in comparison to that at 200 rpm stirring.

Conclusions

In situ modification of the natural clinoptilolite was successfully performed. The sulphate removal proceeds quickly and at the first minute 66.2 % removal efficiency was achieved when the initial sulphate ions concentration was 50 mg/L and 3 g clinoptilolite. The removal efficiency of sulphate ions increases with the clinoptilolite dosage, the contact time and the speed stirring increase. The modified clinoptilolite removal efficiency was higher than that with the natural clinoptilolite.

References

Allen, S., Ivanova, E., Koumanova, B. Adsorption of sulfur dioxide on chemically modified natural clinoptilolite. Acid modification. In: Chem. Engin. J., 152, 2009, 389-395.

Angelov, A., Bratkova, S., Loukanov, A. Microbial fuel cell based on electroactive sulfate-reducing biofilm. In: Energ. Convers. Manage., 67, 2013, 283-286.

APHA. 1992. Standard methods for the examination of water and wastewater. Greenberg A.E. (ed.) 18th edition. American Public Health Association (APHA), American Water Works Association (AWWA), and the Water Environment Federation (WEF): Washington, D.C.

Barczyk, K., Mozgawa, W., Król, M. Studies of anions sorption on natural zeolites. In: Spectrochimica Acta Part A: Molecular and Biomolecular Spectroscopy, 133, 2014, 876-882.

Barczyk, K., Mozgawa, W., Król, M. Studies of anions sorption on natural zeolites. In: Spectrochim. Acta Part A: Mol. Biomol. Spectrosc., 133, 2014, 876-882.

Bratkova, S., Koumanova, B., Beschkov, V. Biological treatment of mining wastewaters by fixed-bed bioreactors at high organic loading. In: Biores. Technol., 137, 2013, 409-413.

de Luna, M., Rance, D., Bellotindos, L., Lu, M. Removal of sulfate by fluidized bed crystallization process. In: J. Environ. Chem. Eng. https://doi.org/10.1016/j.jece.2017.04.052.

Dou, W., Zhou, Z., Jiang, L., Jiang, A., Huang, R., Tian, X., Zhang, W., Chen, D. Sulfate removal from wastewater using ettringite precipitation: Magnesium ion inhibition and process optimization. In: J. Environ. Manag., 196, 2017, 518-526.

Ghiaci, M., Kia, R., Abbaspur, A., Seyedeyn-Azad, F. Adsorption of chromate by surfactant modified zeolites and MCM-41 molecular sieve. Sep. Purif. Technol., 40, 2004, 285-295.

Kiran, M., Pakshirajan, K., Das, G. A new application of anaerobic rotating biological contactor reactor for heavy metal removal under sulfate reducing condition. In: Chem. Eng. J., 321, 2017, 67-75.

Kiran, M., Pakshirajan, K., Das, G. An overview of sulfidogenic biological reactors for the simultaneous treatment of sulfate and heavy metal rich wastewater. In: Chem. Eng. Sci., 158, 2017, 606-620.

Lee, D., Liu,X., Weng, H. Sulfate and organic carbon removal by microbial fuel cell with sulfate-reducing bacteria and sulfide-oxidising bacteria anodic biofilm. In: Biores. Technol. 156, 2014, 14-19.

Margeta, K., Logar, N., Šiljeg, M., Farkas, A. Natural Zeolites in Water Treatment – How Effective is Their Use, 2013, Water treatment, Chapter 5, http://dx.doi.org/10.5772/50738.

Oliveira, C., Rubio, J. New basis for adsorption of ionic pollutants onto modified zeolites. I: Minerals Engineering, 20, 2007, 552-558.

Samatya, S., Yuksel, U., Yuksel, M., Kabay, N. Removal of Fluoride from Water by Metal Ions (Al^{3+}, $La^{3+}$and ZrO^{2+}) Loaded Natural Zeolite. In: Sep. Sci. Technol., 42, 2007, 2033-2047.

Sun, Y., Fang, Q., Dong, J., Cheng, X., Xu, J. Removal of fluoride from drinking water by natural stilbite zeolite modified with Fe(III). In: Desalination, 277, 2011, 121-127.

Tolonen, E., Hu, T., Ram, J., Lassi, U. The removal of sulphate from mine water by precipitation as ettringite and the utilisation of the precipitate as a sorbent for arsenate removal. In: J. Environ. Manag., 181, 2016, 856-862.

Wang, K., Sheng, Y., Cao, H., Yan, K., Zhang, Y. A novel microbial electrolysis cell (MEC) reactor for biological sulfate-rich wastewater treatment using intermittent supply of electric field. In: Biochem. Eng. J., 125, 2017, 10-17.

Wang, S., Peng, Y. Natural zeolites as effective adsorbents in water and wastewater treatment. In: Chem. Eng. J., 156, 2010, 11-24.

Weng, H., Lee, D., Performance of sulfate reducing bacteria-microbial fuel cells: reproducibility. In: J. Taiwan Inst. Chem. Eng., 56, 2015, 148-153.

This article was reviewed by Prof. Dr. Maria Karsheva and Assoc. Prof. Dr. Svetlana Bratkova.

BIOREMEDIATION OF ACID DRAINAGE WATERS FOLLOWED BY ELECTRICITY GENERATION

Marina Nikolova[1], Irena Spasova[1], Plamen Georgiev[1], Iliyan Nikolov[1], Stoyan Grudev[1]

[1]University of Mining and Geology "St. Ivan Rilski" Sofia

ABSTRACT. Acid drainage waters generated during the leaching of a copper-bearing sulphide ore and containing toxic heavy metals and arsenic were subjected to treatment by means of a permeable reactive multibarrier under laboratory conditions. The multibarrier was filled by a mixture of crushed limestone and biodegradable organic matter (spent mushroom compost, fresh leaf compost, animal manure and sawdust) and was inhabited by a viable indigenous microflora consisting of various anaerobic microorganisms, mainly sulphate- and iron-reducing bacteria and other interconnected microorganisms. An efficient cleaning of the polluted waters was performed in the multibarrier, mainly by the precipitation of the heavy metals and arsenic as the respective insoluble sulphides. Apart from the natural microflora of the multibarrier effluents, an inoculum consisting of electrochemically selected active microorganisms was added to these effluents. Portions of those were treated in a microbial fuel cell under continuous-flow conditions and this resulted in the generation of electricity with a power of about 1800 – 2100 mW/m^2.

Keywords: acid drainage, microorganisms, electricity generation

БИОРЕМЕДИАЦИЯ НА КИСЕЛИ ДРЕНАЖНИ ВОДИ, ПОСЛЕДВАНА ОТ ГЕНЕРИРАНЕ НА ЕЛЕКТРИЧЕСТВО

Марина Николова[1], Ирена Спасова[1], Пламен Георгиев[1], Илиян Николов[1], Стоян Грудев[1]

[1]Минно-геоложки университет „Св. Иван Рилски" София

РЕЗЮМЕ. Кисели дренажни води, генерирани при излугване на медна сулфидна руда и съдържащи токсични тежки метали и арсен, бяха подложени на третиране посредством пропусклива реактивна мултибариера при лабораторни условия. Мултибариерата беше запълнена със смес от натрошен варовик и биологично разградима органична материя (отработен гъбен компост, свеж листвен компост, животински тор и стърготини) и беше обитавана от жизнена местна микрофлора, състояща се от различни анаеробни микроорганизми, главно сулфатредуциращи и желязоредуциращи бактерии и други взаимно свързани микроорганизми. Ефикасно пречистване на замърсените води беше извършено в мултибариерата, главно чрез утаяване на тежките метали и арсена като съответните неразтворими сулфиди. Освен естествената микрофлора на изтичащите от мултибариерата води, една закваска, съдържаща селекционирани електрохимично активни микроорганизми, беше добавена към тези води. Части от тях бяха третирани в микробна горивна клетка при условия на непрекъснат поток и това доведе до генериране на електричество с мощност около 1800 – 2100 mW/m^2.

Ключови думи: кисели дренажни води, микроорганизми, генериране на електричество

Introduction

The acid drainage waters generated under natural conditions and, very often, as a result of the human activity connected with the recovery and processing of sulphide minerals (mainly pyrite) constitute a very serious environmental problem. This is due to the fact that in most cases, apart from the sulphuric acid, such waters contain different toxic elements, like heavy metals, radionuclides and arsenic. The prevention of this process is usually much more desirable than the subsequent treatment of such waters. Unfortunately, the efficient prevention of acid generation in the huge dumps of low-grade waste ores that are rich-in-sulphides, or of other mineral wastes is usually an extremely difficult and costly process. In some cases, even after total remediation of the environment, it is necessary to treat the polluted drainage waters arising mainly as a result of the activity of some of the indigenous microorganisms inhabiting the relevant territory. Such treatment can be connected with the extraction of some valuable components, like some non-ferrous metals and rare earth elements, and even with the production of electricity by means of especially constructed microbial fuel cells (Spasova et al., 2014, 2016).

This paper contains some data about the possibility to combine the treatment of acid drainage waters generated in mining waters rich in pyrite with the production of electricity by means of a laboratory-scale fuel cell.

Materials and Methods

Acid drainage waters generated during the bioleaching of copper-bearing sulphide ore and containing toxic heavy metals and arsenic were subjected to treatment by means of a permeable reactive multibarrier under laboratory conditions. The multibarrier was a plastic cylindrical column, 120 cm high, with an internal diameter of 30 cm. The column was filled with a mixture of limestone (crushed to particle size of minus 10 mm) and biodegradable organic matter consisting of spent mushroom compost, fresh leaf compost, animal manure and saw dust. The column was inhabited by a viable microflora derived from the natural inhabitants of these organic substrates. This microflora consisted of different anaerobic microorganisms, mainly sulphate-reducing bacteria and other interconnected microbial species. Apart from the natural microflora of the organic substrates mentioned above, an inoculum containing electrochemically selected active

microorganisms was also added to the multibarrier effluents, together with a nutrient solution containing biologically essential elements (a combination of soluble biodegradable organic compounds, vitamins, and trace elements). Such solutions were subjected to continuous-flow circulation from the inlet to the outlet of a microbial fuel cell.

The microbial fuel cell was a Plexiglas cylindrical column, 80 cm high, with a internal diameter of 12 cm. A perforated slab graphite-Mn^{4+} anode and a graphite-Fe^{3+} cathode were located in the bottom and in the top sections of the column, respectively. The two sections were separated by a permeable barrier of 5 cm thickness consisting of a 2.5 cm layer of glass wool and 2.5 cm layer of a glass beads. The feed stream, i.e. the effluents from the multibarrier, was supplied to the bottom anodic section of the column and the effluents passed through the cathodic section and continuously exited at the top. Air was injected during the treatment to the cathodic section.

In the course of time, a biofilm consisting of a consortium of different electrochemically active microorganisms was formed on the anode electrode.

The quality of the waters being treated by means of the permeable reactive multibarrier and by the microbial fuel cell was monitored at different sampling points. Those points were located at the inlet and the outlet of these components of the system for the water cleaning and electricity generation. The parameters measured in situ included: pH, Eh, dissolved oxygen, total dissolved solids, and temperature. Elemental analysis was done by atomic adsorption spectrometry and by inductively coupled plasma spectrometry. The isolation, identification, and enumeration of microorganisms were carried out by the classical physiological and biochemical tests (Karavaiko et al., 1988) and by the molecular PCR methods (Sanz and Köchling, 2007; Escobar et al., 2008).

Results and Discussion

The treatment of the polluted acid drainage waters by means of a permeable reactive multibarrier was very efficient and, in most cases, the acidity and the contents of toxic heavy metals, arsenic and sulphates were decreased below the relevant permissible levels (Tables 1 and 2).

Table 1.
Data about the acid drainage waters before and after their treatment by the permeable multibarrier

Parameters	Before treatment	After treatment	Permissible levels
pH	1.70 - 2.51	6.82 - 7.10	6 - 9
Eh, mV	(+325)-(+512)	(-170)-(-264)	–
TDS, mg/l	2,420 – 5,540	512 – 1,250	1,500
Diss. O_2, mg/l	1.2 – 2.3	0.1 – 0.3	2
Diss. org. C, mg/l	1.7 – 3.2	247 – 486	20
Sulphate, mg/l	640 - 1,544	240 – 415	400
Cu, mg/l	3.7 – 17	<0.05 – 0.32	0.5
Zn, mg/l	9.9 – 37	<0.05 – 0.46	10
Cd, mg/l	0.05 – 0.21	<0.01	0.02
Mn, mg/l	7.1 – 5.3	0.14 – 0.08	0.8
Fe, mg/l	545 – 1,270	2.3 – 6.2	5
As, mg/l	0.05 - 0.28	<0.01	0.2

Table 2.
Microflora of the acid drainage waters before and after their treatment by means of the permeable multibarrier

Microorganisms	Before treatment	After treatment
	Cells/ml	
Acidithiobacillus ferrooxidans	10^7 - 10^9	–
Acidithiobacillus thiooxidans	10^4 – 10^7	–
Leptospirillum ferrooxidans	10^5 – 10^7	–
Aerobic heterotrophic bacteria	10^2 – 10^5	–
Fungi	0 – 10^3	–
Anaerobic heterotrophic bacteria	0 – 10^3	10^6 – 10^8
Denitrifying bacteria	0 – 10^1	10^4 – 10^6
Sulphate-reducing bacteria	0 – 10^3	10^6 – 10^8
Fe^{3+} - reducing bacteria	0 – 10^2	10^2 – 10^4
Mn^{4+} - reducing bacteria	0 – 10^2	10^2 – 10^4
As^{5+} - reducing bacteria	0 – 10^1	10^1 – 10^2
Methanogenic bacteria	0 – 10^1	10^2 – 10^3

At the same time, the content of biodegradable organic carbon in the multibarrier effluents was increased considerably. This made the treatment of these effluents in the microbial fuel cell very efficient (Table 3).

Table 3.
Treatment of the multibarrier effluents by means of the microbial fuel cell

Parameters	Values
Influents in the MFC:	
COD, mgO_2/l.h	520 – 1,650
SO_4^{2-}, mg/l	240 – 1,040
COD/SO_4^{2-}ratio	1.6 – 4.4
pH	7.10 – 7.45
Eh, mV	(-210) - (-255)
Temperature, ^oC	28 – 35
Heavy metals concentrations	Below permissible levels[x]
Voltage of the open circuit, mV	140 – 280
O_2 dissolved in the cathodic section, mg/l	7.7 – 8.2
Power, mW/m^2	1,800 - 2,100

Note: [x] – With the exception of iron – up to 50 mg/l

The microflora in the anodic section of the microbial fuel cell (Table 4) contained considerable amounts of microorganisms able to transfer electrons from the dissolved organic substrates to the anode electrode located in the anoxic section of the microbial fuel cell. The main role in the process was played mainly by two different groups of anaerobic microorganisms: the sulphate-reducing and the iron-reducing bacteria.

Table 4.
Microorganisms in the anaerobic anodic section of the microbial fuel cell

Microorganisms	Cells/ml
Anaerobic heterotrophic bacteria (pH 7)	10^7 – 10^9
Fermenting bacteria	10^6 – 10^8
Sulphate-reducing bacteria	10^7 – 10^8
Denitrifying bacteria	10^4 – 10^5
Fe^{3+} - reducing bacteria	10^7 – 10^8
Mn^{4+} - reducing bacteria	10^4 – 10^6
As^{5+} - reducing bacteria	10^3 – 10^5
Methanogenic bacteria	0 – 10^2

The sulphate-reducing bacteria were able to perform the electron transport by means of secreted metabolites, mainly by the hydrogen sulphide. These microorganisms were related to different genera and species (Table 5) and differed from each other mainly in the rate of their anoxic respiration process, including in the rate of degradation of the different organic substates used as sources of electrons for the final acceptor, i.e. for the sulphate anion.

Table 5.
Sulphate-reducing bacteria in the anodic section of the microbial fuel cell

Sulphate-reducing bacteria	Cells/ml
Desulfovibrio (mainly *D. desulfuricans*)	$10^5 – 10^7$
Desulfobulbus (mainly *D. elongatus*)	$10^3 – 10^7$
Desulfococcus (mainly *D. postgatei*)	$10^2 – 10^5$
Desulfobacter (mainly *D. multivorans*)	$10^2 – 10^6$
Desulfotomaculum (mainly *D. nigrificans*)	$10^1 – 10^3$
Desulfosarcina (mainly *D. variabilis*)	$10^3 – 10^5$
Desulfomonas (non identified species)	$10^2 – 10^4$

It must be noted that some bacteria related to the genus *Pseudomonas*, which were also present in the mixed microbial consortium in the anoxic section of the microbial fuel cell, produced some dissolved organics which were used by the sulphate-reducing bacteria as donors of electrons in their own anoxic respiration process. The iron-reducing bacteria present in some of the microbial consortia in the anoxic section of the microbial fuel cell were related mainly to two different taxonomic genera: *Schewanella* and *Geobacter*. These bacteria were able to transfer electrons from the dissolved organic substrates in the anoxic section via their own respiratory chains and extracellular matrix directly to the anode located also in this section of the microbial fuel cell. It is known that some members of these two genera differ considerably from each other with respect to their mechanisms of the extracellular electron transport from the relevant organic substrates to the cytochromes of c-type present in their respiratory chains. It must be noted that even strains related to one and the same taxonomic species, the well-known *Schewanella oneidensis*, exhibit considerable differences in their current-generating mechanisms.

The iron(III)-reducing bacteria were also well present in the anodic section of the microbial fuel cell, although in relatively low concentrations than the sulphate-reducing bacteria (Table 6).

Table 6.
Ferric iron-reducing bacteria in the anodic section of the microbial fuel cell

Iron(III) – reducing bacteria	Cells/ml
Geobacter metallireducens	$10^4 – 10^7$
Geobacter sulfurreducens	$10^3 – 10^5$
Geobacter sp.	$10^2 – 10^4$
Schewanella oneidensis	$10^4 – 10^6$
Schewanella sp.	$10^2 – 10^4$

It must be noted that the reduction and growth of the iron(III)-reducing bacteria depend considerably not only on the type, composition, and concentration of the organic substrates but also on the structure and surface of the iron(II) minerals. The amorphous Fe(III)-oxyhydroxides are reduced at relatively high rates but the crystalline Fe(III)-oxide minerals, such as goethite [Fe(OH)] and hematite (Fe_2O_3), are reduced incompletely and at lower rates (Johnson and McGinness, 1991).

The results from this study demonstrate that the cleaning of acid drainage waters by means of a permeable multibarrier can be combined with the subsequent electricity generation by the treatment of multibarrier effluents that are rich-in-biodegradable organic compounds. Electricity generation is performed in a microbial fuel cell inhabited by electrochemically active microorganisms (mainly sulphate and iron reducing bacteria).

References

Escobar, B., K. Bustos, G. Morales, O. Salazar. Rapid and specific detection of Acidithiobacillus ferrooxidans and Leptospirillum ferrooxidans by PCR, Hydrometallurgy, 92, , 2008. - 102 – 106.

Johnson, D.B., S, McGinnes. Ferric iron reduction by acidophilic heterotrophic bacteria, Appl. Environ. Microbiology, 57(1), 1991. - 207 – 211.

Karavaiko, G.I., G. Rossi, A. D. Agate, S. N. Grudev, and Z. A. Avakyan, (eds.), Biogeotechnology of Metals. Mannual GKNT Center for International Projects, Moscow, 1988.

Sanz, J. L., T. Köchling, Molecular biology techniques used in wastewater treatment: An overview. Process Biochemistry 42, 2007. - 119–133.

Спасова, И., М. Николова, П. Георгиев, С. Грудев. Пречистване на руднични води, свързано с генериране на електричество, Годишник на МГУ, С., 57 (II), 2014. - 137 – 139. (Spasova, I., M. Nikolova, P. Georgiev, S. Grudev, Prechistvane na rudnichni void, svarzano s generirane na elektrichestvo. In: Godishnik na MGU, Sofia, 57 (II), 2014. - 137 – 139.)

Спасова, И., М. Николова, П. Георгиев, С. Грудев. Биологично излугване на метали от отработена руда, свързано с добив на мед, опазване на околната среда и генериране на електричество, Годишник на МГУ, С., 59 (II), 2016. - 167 – 211.(Spasova, I., M. Nikolova, P. Georgiev, S. Grudev, Biologichno izlugvane na metali ot otrabotena ruda, svarzano s dobiv na med, opazvane na okolnata sreda i generirane na elektrichestvo, In: Godishnik na MGU, Sofia, 59 (II), 2016. - 167 – 211.

This article was reviewed by Assoc. Prof. Dr. Dimitar Mochev and Assist. Prof. Dr. Mihail Iliev.

LEACHING OF VALUABLE METALS FROM COPPER SLAG BY MEANS OF CHEMOLITHOTROPHIC ARCHAEA AND BACTERIA

Plamen Georgiev[1], Marina Nicolova[1], Irena Spasova[1], Albena Lazarova[1], Stoyan Groudev[1]

[1]University of Mining and Geology "Saint Ivan Rilski" Sofia

ABSTRACT. Copper slag containing 0.62% Cu, 1.07% Zn, 0.08% Co, 32.5% Fe, 1.90% S and 16.3% Si as basic components was subjected to leaching by means of chemolithotrophic microorganisms (bacteria and archaea) in flasks on shaker and agitated reactors. Chemolithotrophs of three different groups based on their optimum temperatures for growth and activity were used: mesophilic bacteria and archaeon Ferroplasma acidiphilium at temperature of 35˚ C; moderate thermophilic bacteria at 55˚ C, and the extreme thermophilic archaea at 75˚ C. The optimum conditions for the leaching (temperature, composition of the leaching solution, particle size, pulp density) were determined. It was found that the archaea leach the slag with higher rates than the bacteria but at relatively lower pulp density (up to 6 – 8 %) and the moderate thermophilic bacteria were more efficient at the higher pulp densities (from 10 – to 20 %).

Key words: copper slag, chemolithotrophs, leaching, valuable metals

ИЗЛУГВАНЕ НА ЦЕННИ МЕТАЛИ ОТ МЕДНА ШЛАКА ЧРЕЗ ХЕМОЛИТОТРОФНИ АРХЕИ И БАКТЕРИИ

Пламен Георгиев[1], Марина Николова[1], Ирена Спасова[1], Албена Лазарова[1], Стоян Грудев[1]

[1]Минно-геоложки университет „Свети Иван Рилски" София

РЕЗЮМЕ. Медна шлака, съдържаща 0.62 % Cu, 1.07 % Zn, 0.08 % Co, 32,5 % Fe, 1.90 % S и 16.3 % Si като основни компонети беше подложена на излугване чрез хемолитотрофни микроорганизми (бактерии и археи) в колби на шейкър и в реактори с механично разбъркване. Хемолитотрофи от три различни групи, основани на техните оптимални температури за растеж и активност бяха използвани: мезофилни бактерии и археона *Ferroplasma acidiphilum* при температура в границите 35 °C; умерено термофилни бактерии при 55 °C, и екстремално термофилни археи при 75 °C. Оптималните условия за излугването (температура, състав на излугващия разтвор, размер на частиците, плътност на пулпа) бяха определени. Установено бе, че археите излугват шлаката с по-високи скорости от бактериите, но при сравнително по-ниска плътност на пулпа (до 6 – 8 %) и умерено термофилните бактерии бяха по-ефикасни при по-високи плътности на пулпа (от 10 до 20 %).

Ключови думи: медна шлака, хемолитотрофи, излугване, ценни метали

Introduction

The pyrometallurgical slags are wastes containing significant quantities of valuable components, mainly non-ferrous metals (such as copper, zinc, cobalt and nickel) but also iron and silicon. At present, the slags are used mainly in the construction of roads and for the preparation of cements of different types. In some cases old slags rich-in-valuable metals are mixed with some other rich-in-metals raw materials and wastes and then subjected again to pyrometallurgical treatments for an economically efficient recovery of different valuable components. At the same time, a large number of investigations are connected with the chemical and/or biological leaching of the slags for extraction of some of their residual valuable components (Genchev and Groudev, 1981; Arslan C. and Arslan F., 2002; Banza et al., 2002; Kaksonen et al., 2011, 2016; Panda et al., 2015). It must be pointed that industrial processing of the slags is directly connected with the environment protection due to removal of different toxic components which during the storage of slags as wastes are subjected to the natural processes of solubilization and migration. Some data about the possibility to leach some valuable and, at the same time, toxic metals from a final copper slag by means of different microorganisms are shown in this paper.

Materials and Methods

The slag used in this study contains 0.62 % Cu, 1.07 % Zn, 0.08% Co, 0.09 % Mn, 2.91 % Al, 32,5 % Fe, 1.90 % S and 16.3 % Si as the most essential components of the chemical composition. The fayalite (Fe_2SiO_4) and diopside ($CaMgSi_2O_6$) were the main mineral phases in the slag but some oxides, mainly of iron, such as hematite (Fe_2O_3) and magnetite (Fe_3O_4) were also present, as well as some plagioclases, quartz and calcite. The content of pyrite (FeS_2) was relatively low but considerable portions of the non-ferrous metals were present as the relevant sulphides. Copper was present mainly in bornite (Cu_5FeS_4), covellite (CuS) and chalcopyrite ($CuFeS_2$) but also in oxides and as its elemental form (Cu^0). Zinc was present as the relevant oxide (ZnO) but also in its own elemental form (Zn^0) and as the sphalerite (ZnS).

A large number of microorganisms were tested in the experiments for microbial leaching of the non-ferrous metals from the slag (Table 1).

Table 1.
Ferrous and sulphur oxidizing abilities of different chemolithotrophic microorganisms used in this study

Microorganisms	Fe^{2+}	S^0
	Maximum oxidation rate, mg/L.h[x]	
Mesophilic bacteria		
Acidithiobacillus ferrooxidans	215 – 464	14 – 53
Acidithiobacillus ferrivorans	231 – 435	12 – 46
Acidithiobacillus thiooxidans	–	18 – 62
Leptospirillum ferrooxidans	190 – 394	–
Ferroplasma acidiphilum[x]	203 – 372	–
Moderate thermophilic bacteria		
Sulfobacillus thermosulphidooxidans	275 – 509	44 – 73
Sulfobacillus acidiphilus	246 – 471	46 – 62
Alicyclobacillus sp.	280 – 495	48 – 73
Alicyclobacillus tolerans	302 – 507	53 – 77
Acidithiobacillus caldus	–	47 – 73
Leptospirillum ferriphilum	305 – 503	–
Acidimicrobium ferrooxidans	291 – 495	–
Acidianus sp.	277 – 401	41 – 60
Extreme thermophilic archaea		
Sulfolobus metallicus	415 – 518	51 – 79
Sulfolobus acidocaldarius	–	59 – 84
Sulfolobus solfataricus	–	77 – 86
Metallosphaera sedula	246 – 471	55 – 77
Acidianus infernus	280 – 495	48 – 71
Thermoplasma acidophilum	321 – 460	51 – 64

Note: The maximum oxidation rate is measured at the end of the exponential growth phase on the relevant substrate (Fe^{2+} or S^0).
The oxidation rate of the mesophilic microorganisms was measured at 35° C; of the moderate thermophilic bacteria at 55° C, and of the extreme thermophilic archaea at 75° C. These temperatures are not the real optimum of each of the microorganisms tested in this study but are close to this optimum for all microorganisms of the relevant group.
[x] – the *Ferroplasma* is a mesophilic archaeon.

Most of these microorganisms were acidophilic chemolithotrophs possessing the ability to oxidize the ferrous iron and/or the low-valence form of sulphur (the sulphidic) and its zero-valence elemental form (S^0). These microorganisms were related to three different groups on the basis of the optimum temperature for their growth and activity: mesophilic bacteria, with temperature optimum at 30 – 37° C; moderate thermophilic bacteria, with a temperature optimum at 50 – 60° C, and extremely thermophilic archaea, with a temperature optimum within the range of about 65 – 86° C. In these comparative experiments each of the different microbial species was present by 3 – 7 different strains, at least. The experiments of this type were performed by the shake-flask technique using Erlenmeyer flasks of 300 ml volume containing 100 ml of 9K nutrient medium (Silverman and Lundgren, 1959) with different quantities of slag. Fe^{2+} (added as ferrous sulphate) and/or elemental sulphur (S^0) were used as potential sources of energy for the chemolithotrophs. For the cultivation of archaea, yeast extract (0.5 g in 100 ml nutrient 9K medium) was added.

The comparative experiments for the ability of the different microorganisms to leach the slag were carried out at 35, 55 and 75° C for the mesophilic, moderate thermophilic and extreme thermophilic species, respectively. The effect of the most essential environmental factors, apart from the temperature, was studied with more active strains as follows: pH within the values from 1.0 to 3.7, particle size of the slag - minus 100 and minus 200 microns, pulp density of the slag in the leach solution - from 5 to 20 %, aeration by air enriched with CO_2 to 0.10 – 0.20 %.

The activity of some of the most active strains from the different taxonomic microbial species was increased to different extents by means of consecutive cultivations in the nutrient medium 9K supplied by slag with a step-by-step increasing of the relevant pulp density.

In some experiments the combined chemico-biological leaching of the slag was performed in agitated bioreactors with a volume of 1 L each. Apart from the batch leaching, such bioreactors were used also for performing the continuous-flow leaching. Such leaching was performed not only in a single bioreactor but also in a two-step system consisting of two connected reactors. In the first reactor the initial acidification of the slag was performed by adding sulphuric acid to the relevant pH levels which were optimal for the growth and activity of the microorganisms acting in the second bioreactor.

Elemental analysis of the liquid samples was performed by atomic absorption spectrometry (AAS) and inductively coupled plasma spectrometry (ICP). The isolation, identification and enumeration of microorganisms were carried by the classical physiological and biochemical tests and by the molecular PCR methods (Karavaiko et al., 1988; Sanz and Köchling, 2007; Escobar et al., 2008).

Results and Discussion

It was found that many of the microbial strains used in this study, even some related to one and the same taxonomic species, differed considerably from each other with respect to their ability to leach the heavy metals from the slag (Table 2).

Very active strains from the three temperature groups mentioned above were found. It must be noted, however, that the most efficient extractions of the non-ferrous metals and iron from the slag were achieved by means of microorganisms possessing both ferrous and sulphur oxidizing abilities (Table 1 and 2).

Table 2.
Batch leaching of non-ferrous metals from the slag by means of different microorganisms [x]

Microorganisms	Cu	Zn	Co
	Extraction, %		
Mesophiles at 35 °C			
At. ferrooxidans	82	86	90
At. ferrivorans	77	80	86
At. thiooxidans	37	41	46

L. ferrooxidans	68	73	80
F. acidophilum[x]	64	68	71
Mixed cultures	80 – 84	82 – 89	84 – 92
Moderate themophilic bacteria at 55 °C			
S. thermosulphidooxidans	88	86	93
S. acidophilus	84	81	88
Alicyclobacillus sp.	88	83	91
At. caldus	47	53	56
L. ferriphilum	80	84	88
Ac. ferrooxidans	78	84	86
Acidianus sp.	50	62	68
Mixed cultures	82 – 88	84 – 91	88 – 94
Extreme thermophilic archaea at 75 °C			
S. metallicus	89	87	93
S. acidocaldarius	53	60	64
M. sedula	88	87	93
Ac. infernus	80	85	87
T. acidophilium	77	82	85
Mixed cultures	84 – 93	84 – 90	87 – 95

Note: The most active strains from each species were used in these experiments.

However, even microorganisms possessing the ability to oxidize only the Fe^{2+} (such as the species related to the genera *Leptospirillum, Acidimicrobium* and *Ferroplasma*), as well as microorganisms able to oxidize only the sulphur but not the ferrous iron (such as *Acidithiobacillus thiooxidans* and some species of the genera *Sulfolobus*, such as *S. acidocaldarius* and *S. solfataricus*) were able to leach the slag. It must be noted, however, that the leaching by these microorganisms was not so efficient and the extractions of the non-ferrous metals were similar to these obtained by means of the chemical leaching of the slag with sulphuric acid and ferric ions (Table 3).

Table 3.
Chemical batch leaching of the slag

Leaching system	Cu	Zn	Co
	Extraction, %		
H_2SO_4 (pH 2.0) at 35° C	35	32	44
H_2SO_4 (pH 2.0) at 55° C	42	40	48
H_2SO_4 (pH 2.0) at 75° C	46	44	57
H_2SO_4 + Fe^{3+} (10 g/l); pH 2.0, 35° C	48	46	55
H_2SO_4 + Fe^{3+} (10 g/l); pH 2.0, 55° C	53	50	64
H_2SO_4 + Fe^{3+} (10 g/l); pH 2.0, 75° C	61	59	68

Note: The leaching was performed at initial pulp density of 10 % and Fe^{3+} concentration of 10 g/l; pH was maintained at 2.0 by addition of H_2SO_4. The total concentration of dissolved iron increased during the leaching but the concentration of Fe^{3+} decreased. Duration of leaching 48 hours.

The highest rates of extraction of the non-ferrous metals and iron were achieved by means of some archaea but at relatively low pulp densities (5 – 10 %). It must be noted that the preliminary adaptation of most microbial strains to the slag used in this study increased to some extent the rates and efficiency of leaching. However, in most cases the increase was different at the different strains, even at such related to one and the same taxonomic species.

In any case, the most efficient bioleaching of slag was possible only by means of microorganisms possessing ferrous iron oxidizing ability. These microorganisms oxidized the ferrous ions solubilized from the slag during the leaching to the ferric ions. The ferric ions are efficient oxidizers of most sulphide minerals, including those present in the slag. However, it is essential to be noted that the role of these microorganisms in the leaching of slag was not connected only with the generation of ferric ions *in situ*. Some of these microorganisms, more especially the ones possessing also sulphur-oxidizing ability, were able to oxidize the sulphide minerals in the slag directly, i.e. without the presence of soluble iron ions. This was demonstrated by the fact that the strains of *At. ferrooxidans* possessing both ferrous and sulphur oxidizing abilities were able to leach the slag in the absence of iron ions introduced to the system from outer source at much higher rates than strains of *Leptospirillum ferrooxidans* possessing higher ferrous oxidizing ability but not able to oxidize sulphur in different forms (elemental or sulphidic in some iron-free sulphides such as covellite and chalcocite). This was also demonstrated by the fact that the strains of *At. ferrooxidans* possessing both ferrous and sulphur oxidizing abilities oxidized the slag at higher rates than strains of *L. ferrooxidans* which were able to oxidize the Fe^{2+} at higher rates than *At. ferrooxidans* but not any form of the sulphur in the absence of iron.

The bioleaching of slag under continuous-flow conditions was also very efficient (Table 4 and 5).

Table 4.
Continuous-flow leaching of the slag by means of moderate thermophilic bacteria

Component	Pulp density, %			
	5	10	15	20
	Extraction, %			
Cu	90.7	88.2	84.0	82.4
Zn	88.4	86.0	82.4	80.8
Co	95.0	90.7	88.4	86.8
Fe	52.1	50.5	48.8	47.0
Mn	92.9	90.1	89.4	88.0
Al	58.1	56.5	55.0	53.8

Table 5.
Continuous-flow leaching of the slag by means of archaea

Component	Pulp density, %			
	5	10	15	20
	Extraction, %			
Cu	91.4	87.5	79.0	70.1
Zn	89.4	84.0	76.1	68.0
Co	97.0	89.4	80.2	73.0
Fe	53.0	49.8	44.0	40.4
Mn	93.7	87.3	82.0	77.0
Al	59.0	56.0	51.9	49.5

The pH was maintained at about 1.8 – 2.0 by addition of sulphuric acid. It must be noted, however, that the leaching by some mesophiles and by some moderate thermophilic bacteria at pH 3.0 – 3.5 was also very promising since it was connected with high extractions of the non-ferrous metals but at much lower acid consumption (about 576 g H_2SO_4/kg slag for pH 3.50 versus about 800 g H_2SO_4/kg slag for pH 1.80 – 1.90.

Furthermore, the solubilization of fayalite at pH 3.0 – 3.5 was much lower which resulted in the production of pregnant solutions suitable for processing and recovery of the dissolved non-ferrous metals.

References

Arslan, C. and Arslan, F., 2002. Recovery of copper, cobalt and zinc from copper smelter and converter slags. Hydrometallurgy, 67, 1 – 7.

Banza, A.N., Gock, E. and Kongolo, K., 2002. Base metals recovery from copper smelter slag by oxidizing leaching and solvent extraction, Hydrometallurgy, 94, 18 – 22.

Escobar, B., Bustos K., Morales, G. and Salazar, O., 2008. Rapid and specific detection of *Acidithiobacillus ferrooxidans* and *Leptospirrilim ferrooxidans* by PCR, Hydrometallurgy, 92, 102 – 106.

Genchev, F.N. and Groudev, S.N., 1981. Utilization of copper slags by using combined bacterial and conventional methods, in: XV Scientific Conference on Mineral Processing Krakow, Poland, October 24, 1981.

Kaksonen, A.H., Lavonen, L., Kuusenaho, M., Kolli, A., Närhi, H., Vestola, E., Puhakka, J.A. and Tuovinen, O.H., 2011. Bioleaching and recovery of metals from final slag waste of the copper smelting industry, *Minerals Engineering*, 24, 1113-1121.

Kaksonen, A. H., Särkijärvi, S., Puhakka, J. A., Peuraniemi, E., Junnikkala, S. and Tuovinen, O. H., 2016. *Chemical and bacterial leaching of metals from a smelter slag in acid solutions. Hydrometallurgy, 159*, 46-53.

Karavaiko, G.I., Rossi, G., Agate, A.D., Groudev, S.N. and Avakyan, Z.A. (eds.), 1988. Biogeotechnology of Metals. Manual, GKNT Center for International Projects, Moscow.

Panda, S. Mishra, S., Rao, D.S., Pradhan, N., Mohapatra, U.B., Angadi, S.K. and Mishra, B.K., 2015. Extraction of copper from copper slag: Mineralogical insights, physical beneficiation and bioleaching studies, Korean J. Chem. Eng., 32 (4), 667 – 676.

Sanz, J.L. and Köchling, T. 2007. Molecular biology techniques used in wastewater treatment: An overview. Process Biochem.42, 119–133.

Silverman, M.P. and Lundgren, D.G., 1959. Studies on the chemoautotrophic iron bacterium *Ferrobacillus ferrooxidans.* J Bacteriol. 77, 642–647.

This article was reviewed by Assoc. Prof. Dr. Dimitar Mochev and Assist. Prof. Dr. Mihail Iliev.

EFFECTS OF SOME FACTORS ON THE IRON REMOVAL FROM RICH-IN-IRON WASTE SOLUTIONS BY MEANS OF GOETHITE AND HEMATITE PRECIPITATION PROCESSES

Plamen Georgiev[1,2], Ivelina Zheleva[1], Stoyan Grudev[1], Marina Nicolova[1], Irena Spasova[1]

[1]University of Mining and Geology "St. Ivan Rilski", 1700 Sofia, [2]ps_georgiev@mgu.bg

ABSTRACT: Biohydrometallurgical processing of raw materials enriched with non-ferrous metals is based on the direct and indirect mechanisms of the oxidative leaching of their sulfides, and accumulation of the released ions in the pregnant leach solution. Further, the leached non-ferrous metals are separated from each other and concentrated in rich electrolytes by means of the relevant solvent extraction processes, while the dissolved iron accumulates in raffinate which needs some additional processing steps for its removal from the solution. This study presents some results about the effects of the operating temperatures (25 – 90 °C), pH (2 – 4), and the applied seeding rate on the chemical oxidation of ferrous ions and removal of ferric iron as goethite and hematite from rich-in-iron waste solutions generated during the processing of final copper slags.

Keywords: goethite, hematite, iron, pregnant leach solutions

ВЛИЯНИЕ НА НЯКОИ ФАКТОРИ ВЪРХУ УТАЯВАНЕТО НА ЖЕЛЯЗО ОТ ОТПАДНИ ВОДИ ПОД ФОРМАТА НА ГЬОТИТ И ХЕМАТИТ

Пламен Георгиев[1], Ивелина Желева[1], Стоян Грудев[1] Марина Николова[1], Ирена Спасова[1]

[1]Минно-геоложки университет „Св.Иван Рилски", София 1700, ps_georgiev@mgu.bg

РЕЗЮМЕ: Процесите на преработка на минерални суровини, богати на цветни метали чрез методите на биохидрометалургията се базират на прекия и непряк механизъм на окисление на сулфидите и натрупване на образуваните йони при този процес в продукционните разтвори. Разтворените цветни метали се разделят един от друг и концентрират в богати разтвори посредством съответните процеси на течностна екстракция, докато разтвореното желязо се акумулира в рафината, което налага допълнителни стъпки за неговото отстраняване от разтвора. Настоящето изследване представя някои резултати за влиянието на температурата (25 – 90 °C), pH (2 – 4), и концентрацията на внасяните зародиши върху химичното окисление на феро йоните и утаяването на желязото, като гьотит или хематит от отпадни разтвори, богати на желязо, образуващи се при преработката на крайни медни шлаки.

Ключови думи: гьотит, хематит, желязо, продукционни разтвори

Introduction

Iron plays a main role in the hydrometalurgy where the processing of non-ferrous metals from different types raw materials (low-grade ores, flotation concentrates, technogenic wastes) is carried out usually at acidic pH. At such conditions, ferric iron is stable in solution and because of its strong oxidative properties oxidizes and leaches a wide range of sulfides. Ferrous iron ions generated as a result of that process are regenerated back to ferric state due to the ability of iron oxidizing chemolithotrophic bacteria to gain energy for their growth on the account of that process. Thus, the higher concentration of the chemical oxidant is maintained during the raw material processing, which combined with very acidic pH, determines the higher concentration of non-ferrous metals in the generated pregnant leach solutions (PLS). The next step in the typical hydrometallurgical flowsheet is the solvent extraction process (SX). It is based on the consecutive separation of the base metals in PLS and their many-fold concentration into separate aqueous stream-rich electrolyte. From there, the dissolved non-ferrous metals deposit as zero valent state form under the relevant optimal current and voltage regime supplied to the electrowining cell (Davenport et al., 2002).

The classical way of iron removal from waste solution is the chemical oxidation of ferrous iron, neutralization of the water acidity and iron (hydro)oxides formation as a result of the ferric iron hydrolysis. The latter process is connected with the non-ferrous metals or toxic elements co-precipitation in a different extent and the formed iron minerals, as a result, are with a low quality to other industries, which impose their disposal and long-term storage. The main products of chemical neutralization, in dependence on temperature and pH, are jarozite, schwertmanite, goethite, or hematite. Because of the higher iron content and some properties (color, bulk density and higher settling velocity), goethite and hematite are preferred end products of the iron removal from iron rich waste solutions (Ismael and Carvalho, 2003)

The new approach in the iron removal process from PLS is the iron oxides formation with almost constant mineralogy and a chemical content free from other non-ferrous metals or toxic elements. In that case, the iron oxides could be used as an iron source in the steel industry (Torfs and Vliegen, 1996.) or in preparation of suitable sorbents for treatment of waters polluted by toxic elements (Mohan and Pittman Jr., 2007). That approach imposes the requirement of a preliminary transfer of

dissolved iron from the bulk solution into a separate only-iron-containing water stream which is achieved by means of solvent extraction process. Different kind of compounds are used into the practice for that purpose – organic phosphorous-containing compounds (Hirato et al., 1992) (tributhyl phosphate (TBP), 2-ethylhexyl) phosphate (DEHPA) (Sato et al., 1985), a tertiary carboxylic acids (Versatic acid; Thorsen et al., 1984) or amino-phosphoric acid (phosphonomethylated alkylamine (EU2), Delmas etal., 1996). The transfer of dissolved iron in a separate water stream enables the application of suitable measures for its precipitation as iron oxides with higher iron content and a good filterable characteristic. In most cases, goethite and hematite are preferred end products. Goethite (α-FeOOH) is formed at pH 2-3, temperatures below 70 °C and at lower concentration of ferric iron (Agatzini et al., 1986). Hematite has been reported as an end product at a temperature greater than 100 °C and under pressure oxidation of greater than 5 bar (Dutrizac and Riveros, 1999). In that case, intermediate irons oxides are formed (as akagenite in chloride media), which are transformed later into hematite. When the reaction takes place at lower temperature (50-90 °C) and in the presence of hematite seeds, however, hematite is formed directly (Cohen et al., 2005).

The article presents results about the effect of pH, temperature, and seeding rate on the goethite and hematite precipitation processes from rich-in-iron waste solution generated during bacterial leaching of final copper slags.

Materials and methods

All batch experiments about the iron precipitation from rich-in-iron waste leach solutions were carried out in 1 L reactors supplied with a propeller. The iron precipitation as goethite formation was studied at temperatures 25 and 50°C, while at 90°C the hematite formation was studied. The relevant temperature during the tests were maintained by a water bath. The chemical neutralization of the acidic pH was carried out by means of addition of alkaline solution (5 M NaOH) at a regime of permanent agitation (250 rpm). In the case when goethite formation was studied, the solutions were aerated with mini compressor as the air splurged in the zone determined by the lower propeller level and the reactor`s bottom. pH and Eh values were measured periodically depending on the added bases to the solution.

The effect of seeding rate (0.2 – 5.0 g/L) on the iron precipitation was studied by addition of finely ground samples (below 25 microns) of goethite (or hematite) to the waste solutions in the beginning of the chemical neutralization. The concentration of total and ferric iron in the solutions was determined by means of spectrophotometric method in the presence of sulfosalicylic acid at acidic and alkaline pH, respectively.

Some important characteristics (settling velocity, total suspended solids (TSS) (Eaton et al., 2005a) and sludge volume index (SVI) (Eaton et al., 2005b)) of already formed iron oxides were measured in the graduated sedimentary cone with volume of 1 L at a constant temperature.

Table 1.
Data about the solutions used in this study

Parameter	Pregnant leach solution	Rich-in-iron waste solution
pH	0.48-0.67	1.82 – 1.95
Eh, mV	345 – 360	710 – 770
Fe^{3+}, mg/L	825 – 1050	8650 – 11440
Fe^{2+},mg/L	29370 – 32837	130 – 255
Fe total, mg/L	30195 – 33890	8780 – 11695
Cu, mg/L	225 – 281	< 0.6
Al, mg/L	222 – 250	18.5 – 24.2
Ca, mg/L	1074 – 1326	18– 45
Mg, mg/L	188 – 240	3.3 – 8.8

Table 2.
Data about iron hydrolysis carried out at ambient temperature when the alkaline solution was added gradually during the test

t, min	Parameter			
	Base consumption, ml NaOH/ L	pH	Eh	Fe_{total}, mg/ L
10	6	3.02	625	2320
20	22	3.18	620	990
30	32	3.23	615	970
40	40	3.60	579	690
50	47.6	4.43	440	10.4

Table 3.
Data about iron hydrolysis carried out at ambient temperature when the alkaline solution was added almost at once at the test`s start

t, min	Parameter			
	Base consumption, ml NaOH/ L	pH	Eh	Fe_{total}, mg/ L
10	38.7	3.35	585	2015
20	40.5	3.28	542	720
30	42.3	3.47	503	255
40	44.7	3.55	480	64.2
50	47.6	4.45	415	6.2

Results and discussion

The pregnant leach solution (PLS) generated during the bacterial leaching of final copper slag in a continuously operated bioreactor was used in the study. For that reason, the solution characterized with very high concentration of dissolved iron which ranged between 27 – 34 g/L, as the relative content of ferric iron was around 3 % from the above-mentioned value (Table 1). Copper was the base metal leached easily from the processed raw materials and it separated and concentrated from the PLS into copper-rich solution by means of solvent extraction process with ACORGA LS 4202. The optimal pH for that process was around 2.0 and the copper extraction from PLS was low when the process was realized in the presence of iron. So, the very high iron concentration in PLS imposed the need for a stage of preliminary oxidation of ferrous iron followed by extraction and separation of the generated ferric iron ions into a separate rich-in-iron waste solution. The chemical oxidation of ferrous iron by stabilized hydrogen

peroxide solution (30 %) was applied in that case and the oxidized iron was extracted from the PLS by means of 15 % solution of DEHPA. The formed rich-in-iron waste stream was with acidic pH (in the range of 1.8 – 2.0), as a result, it had deep red color because more than of 97.5 % of the iron in solution was in the ferric state. The copper concentration transferred by this process was negligible (Table 1).

Table 4.
Effect of the temperature during the chemical neutralization of rich-in-iron waste solution on some important characteristics of the produced slimes

Parameter	Temperature		
	25°C	50°C	90°C
Residual iron concentration, mg/	10.4	3.6	4.4
Total suspended solids (TSS), g/L	21.8	21.5	15.7
Sludge volume index (SVI), mL/ g	41.5	27.9	12.3
Settling velocity, cm/ min	0.03	0.04	0.19

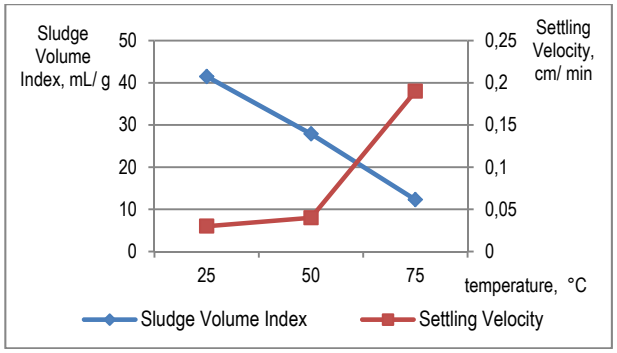

Fig. 1. Effect of the temperature on the iron removal from rich-in-iron waste solution

pH and Eh values were invaluable during the characterization of the ferric iron precipitation. The ferric iron hydrolysis simultaneously decreased the oxidant concentration and generated hydrolytic acidity into the solution. For that reason, Eh values gradually decreased while the pH values remained almost constant despite the added bases (Tables 2-5).

Two different approaches were applied to the process of iron hydrolysis. The first was connected with the gradual addition of alkaline solution as the main aim was to maintain pH in the range of 3.00- 3.20 (Table 2). As an alternative, the already known amount of bases was added at the test beginning and during the next 60 minutes the changes of water chemistry were only monitored (Table 3). However, the results showed that regardless of the way of alkaline solution addition, the iron hydrolysis was carried out with higher rate and more than of 80 % of the iron precipitated during the first ten minutes in both cases. However, the residual lower iron concentration was measured when the needed amount of alkaline solution was added almost all in the beginning of the test in comparison to the variant when it was added serially. For that reason, the needed amount of bases was added at once at the start of all other experiments. In both cases, the formed iron precipitates had yellowish color which is a typical feature of goethite. The freshly formed goethite particles suspended in water for a long time which determined the highest value of sludge volume index (SVI) (more than 40 mg/ L) and their very low settling velocity (Table 6, Fig. 1).

Table 5.
Data about iron hydrolysis carried out at 50 °C from rich-in-iron waste solution

t, min	Parameter			
	Base consumption, ml NaOH/ L	pH	Eh	Fe_{total}, mg/ L
10	37.0	3.00	695	1825
20	41.4	3.26	605	546
30	43.4	3.48	586	72.0
40	46.8	4.00	575	14.3
50	47.3	4.04	386	3.6

Table 6.
Data about iron hydrolysis carried out at 90°C from rich-in-iron waste solution

t, min	Parameter			
	Base consumption, ml NaOH/ L	pH	Eh	Fe_{total}, mg/ L
10	24.7	3.00	645	1510
20	28.3	3.28	590	475
30	30.0	3.52	568	58
40	31.3	3.96	532	9.5
50	31.5	4.06	367	2.2

Table 7.
Effect of the seeding rate with goethite on the iron hydrolysis at 50° and some important characteristics of the produced slimes

Parameter	Goethite seeding rate, g/ L				
	0	0.2	0.5	1.0	5.0
Residual iron concentration, mg/ L	3.6	2.9	3.3	4.2	4.5
Total suspended solids (TSS), g/L	21.5	21.6	22.1	22.6	25.5
Sludge volume index (SVI), mL/ g	27.9	23.7	23.7	19.3	27.8
Settling velocity, cm/ min	0.04	0.10	0.10	0.14	0.14

Slightly different approach for the iron removal from acidic solutions was applied in Kaksonen et al., (2014a, 2014b). It was based on the bacterial oxidation of ferrous iron and the acidity consumption by the mesophilic chemolithrophic consortia, consisting of *Acidithiobacillus ferrooxidans* and *Leptospirilum ferrooxidans,* growing at room temperature in a two-stage continuous stirred bioreactors. The produced ferric iron hydrolyzed instantly as jarosite. An equilibrium between the processes of bacterial oxidation and chemical precipitation existed which determined almost constant pH (2.05- 2.06) in bioreactors. At such conditions, the ferrous oxidation rate was in the range of 1.0 – 1.1 g.L/ h as both rates (ferrous iron oxidation and ferric iron precipitation) increased with increase of the solution`s pH. In the same trend, the particles size

diameter increased also and they were in the range of 14 microns, which determined sludge volume index (SVI) about 12 mL/g.

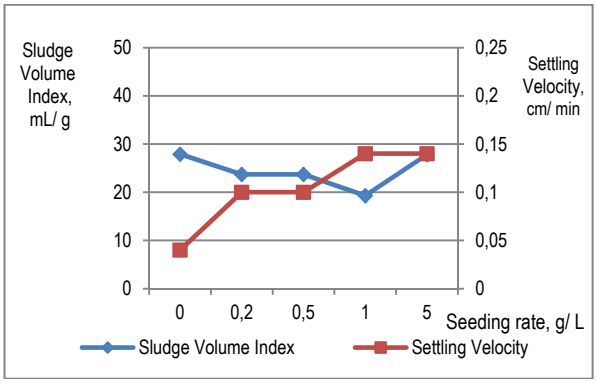

Fig. 2. Effect of the seeding rate with goethite on the iron removal from rich-in-iron waste solution at 50°C

Table 8.
Effect of the seeding rate with hematite on the iron hydrolysis at 90° C and some important characteristics of the produced slimes

Parameter	Goethite seeding rate, g/ L			
	0	0.2	0.5	2.0
Residual iron concentration, mg/ L	4.4	5.2	6.4	3.0
Total suspended solids (TSS), g/L	15.7	15.9	16.2	17.7
Sludge volume index (SVI), mL/ g	12.3	13.1	18.5	20.2
Settling velocity, cm/ min	0.19	0.17	0.16	0.15

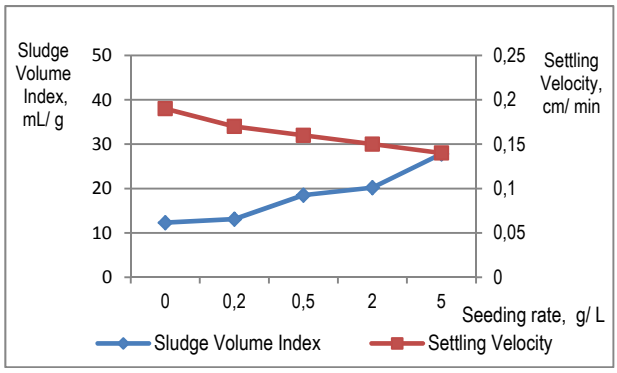

Fig. 3. Effect of the seeding rate with hematite on the iron removal from rich-in-iron waste solution at 90°C

Sasaki and Konno (2000) demonstrated that the particles size distribution of freshly formed iron mineral particles is affected by the rates of their crystallization and agglomeration. Both rates are affected by the local temperature during the process and the concentration of finely minerals particles, which could act as seeds to initiate and to accelerate later the agglomeration rate.

The results about the temperature effect on the rate of agglomeration showed that the higher the temperature was during the test, the higher the rate of iron precipitation was. (Tables 5, 6). The formed iron oxides had dark brown color in that case, had higher bulk density which determined the lower value of SVI (with 33 % and 70.4 % for iron oxides formed at 50 °C and 90 °C, respectively) in comparison to the values measured at ambient temperature. However, the settling velocity of the particles formed at 50 °C was nearly the same as the velocity measured at 25 °C. The results from seeding experiments showed that the factor could improve considerably SVI and the settling velocity of the particles when the accurate dosage is applied. For example, the accurate dosage for the iron precipitation as goethite at 50 °C from solution with iron concentration 11500 mg/ L was 1g/ L. (Table 7). As a result, SVI decreased by 31 % and the settling velocity increased 3.5 time in comparison to the non-seeded variant at the same temperature (Figure 2). The sludge was bulkier when a higher seeding dosage was applied.

Interesting results about ferric iron precipitation as phosphate and hematite from chloride leach solution presented Masambi et al. (2016). In that case, the iron removal process was realized with PLS enriched with copper and nickel. Results showed that the iron removal as hematite reached 99.6 % at temperature 80 °C when pH of solution was 1.0 and the seeding rate was in the range of 10-15 g/ L. Copper and nickel co-precipitation were in range of 3.5 and 1.7 %, respectively.

The experiments about the iron removal at 90 °C from the waste solution with lower iron concentration generated slime consisted of iron oxides with brown-reddish color. The slime itself characterized by the optimal values of sludge volume index (SVI) and settling velocity (SV) (Table 8, Figure 3), was determined during this study. However, all seeding experiments with hematite carried out at 90 °C showed that seeding, irrespective of the applied rate, had a negative effect on the above-mentioned parameters of the produced iron-rich slimes.

Conclusions

1. The experiments about the chemical neutralization of acidic rich-in-iron showed very high iron removal (above 99.5 %) at all tested temperatures.
2. However, the iron precipitates formed only at 50 and 90 °C were characterized with acceptable for the practice values of Sludge Volume Index (SVI) and Settling Velocity (SV).
3. The seeding rate with 1 g/ L goethite at 50 °C had a highly positive effect on the iron removal from waste solution with iron concentration of 11500 mg/ L. The seeding experiments with hematite had a negative effect on the Sludge Volume Index (SVI) and Settling Velocity (SV) of the iron oxides formed from solution with iron concentration of 8650 mg/ L at 90 °C.

References

Agatzini, S., Kontopoulus, A., Maraboutis, P., Xenidis, A., 1986.
Removal of iron–nickel–cobalt solutions by precipitation and solvent extraction techniques. In: Dutrizac, J.E., Monhemius, J.A. (Eds.), Iron Control in Hydrometallurgy. Ellis Horwood, Chichester, pp. 353–373.

Cohen, B., D.S. Shipley, A.R. Tong, S.J.G. Casaroli, and J.G. Petrie. 2005. Precipitation of iron from concentrated chloride solutions: literature observations, challenges and preliminary experimental results. Minerals Engineering, 18, 1344–1347.

Davenport, W.G., M. King, M. Schlesinger, A.K. Biswas. 2002. Extractive metallurgy of copper. 4th edition, Pergamon Press, pp. 11-14.

Delmas, F., M. Ehle, R.O Koch, C. Nogueira, P.C.Oppenlfander, K.H. Ujma, V. Weigel. 1996. Development of a selective extractant for iron in hydrometallurgical process solutions in order to reduce the amount of ferric sludges. In: Shallcross, D.C., Paimin, R., Prvcic, L.M. (Eds.), Proceedings of the International Solvent Extraction Conference, vol. 1, pp. 293–298.

Dutrizac, J.E., and P.A. Riveros. 1999. The precipitation of hematite from ferric chloride media at atmospheric pressure. Metall. Mater. Trans. B 30, 993–1001.

Eaton, A.D., L.S. Clesceri, E.W. Rice, A.E. Greenberg, M.A.H. Franson, 2005a. 2540 D. Total suspended solids dried at 103–105 °C. Standard Methods for the Examination of Water & Wastewater. American Public Health Association, American Water Works Association, Water Environment Federation, Washington DC.

Eaton, A.D., L.S. Clesceri, E.W. Rice, A.E. Greenberg, M.A.H. Franson, 2005b. 2710 D. Sludge volume index, Standard Methods for the Examination of Water & Wastewater. American Public Health Association, AmericanWaterWorks Association, Water Environment Federation, Washington DC.

Ismael, M.R.C and J.M.R. Carvalho. 2003. Iron recovery from sulphate leach liquors in zinc hydrometallurgy. Minerals Engineering 16, 31-39.

Hirato, T., Z.C. Wu, Y. Yamada, H. Majima. 1992. Improvements of the stripping characteristics of Fe(III) utilizing a mixture of di- 2-ethylhexyl phosphoric acid and tributyl phosphate. Hydrometallurgy 28, 81–93.

Kaksonen, A.H., C. Morris, S. Rea, J. Li, J. Wylie, K.M. Usher, M.P. Ginige, K.Y. Cheng, F. Hilario, and C.A. du Plessis. 2014a. Biohydrometallurgical iron oxidation and precipitation: Part I — Effect of pH on process performance. Hydrometallurgy 147 – 148, 255-263.

Kaksonen, A.H., C. Morris, S. Rea, J. Li, J. Wylie, K.M. Usher, M.P. Ginige, K.Y. Cheng, F. Hilario, and C.A. du Plessis. 2014b. Biohydrometallurgical iron oxidation and precipitation: Part II — Jarosite precipitate characterisation and acid recovery by conversion to hematite. Hydrometallurgy 147 – 148, 264-272.

Masambi, S., C. Dorfling, S. Bradshaw. 2016. Comparing iron phosphate and hematite precipitation processes for iron removal from chloride leach solutions. Minerals Engineering 98, 14-21.

Mohan, D. and C.U. Pittman Jr. 2007. Arsenic removal from water/ wastewater using adsorbents – a critical review. Journal of Hazardous Materials 142, 1-53.

Sasaki, K. and H. Konno. 2000. Morphology of jarosite-group compounds precipitated from biologically and chemically oxidized Fe ions. Canadian Mineralogist. 38, 45–56.

Sato, T., T. Nakamura and M. Ikeno. 1985. The extraction of iron (III) from aqueous acid solutions by di(2-ethilhexil)phosphoric acid. Hydrometallurgy 15, 209–217.

Thorsen, G., Svendsen, H.F., Grislingas, A., 1984. The integrated organic leaching-solvent extraction operation in hydrometallurgy. In: Renato, G.B. (Ed.), Hydrometallurgical Process Fundamentals. Plenum Press, New York, pp. 269–292.

Torfs, K.J. and J. Vliegen. 1996. The Union Miniere Goethite process: plant practice and future prospects. In: Dutrizac, J.E., Harris, G.B. (Eds.), Iron Control and Disposal. The Canadian Institute of Mining, Metallurgy and Petroleum, Montreal, Canada, pp. 135–146.

This article was reviewed by Assist. Prof. Dr. Mihail Iliev and Dr. Raliza Ilieva.

POSSIBILITIES TO REDUCE THE NEGATIVE ENVIRONMENTAL IMPACT OF MINING ACTIVITES IN THE RHODOPE MINING BASIN

Emilia Sokolova[1], Velichka Hristova[1]

[1]Kardzhali Branch of the University of Mining and Geology "St. Ivan Rilski" - Sofia, 6600 Kardzhali, emisokolova@abv.bg

ABSTRACT. Mining and processing of natural recources have brought about high levels of pollution, deterioration of the quality of the environment, and depletion of resources. Nowadays, it is imperative to find alternatives for the rational and environmentally friendly use of natural resources. This paper discusses the different mining activities in the Rhodope mining basin that can be sources of environment pollution and the possible measures to prevent their impact.

Keywords: natural recources, mining activities, environmental protection, the Rhodope mining basin

ВЪЗМОЖНОСТИ ЗА НАМАЛЯВАНЕ ВРЕДНОТО ВЪЗДЕЙСТВИЕ ВЪРХУ ОКОЛНАТА СРЕДА НА ОБЕКТИ ОТ МИННО-ДОБИВНИТЕ ДЕЙНОСТИ ОТ РОДОПСКИЯ МИНЕН БАСЕЙН

Емилия Соколова[1], Величка Христова[1]

[1]Филиал Кърджали на Минно-геоложки университет "Св. Иван Рилски" - София, 6600-Кърджали, emisokolova@abv.bg

РЕЗЮМЕ. Добивът и преработването на природните ресурсите са довели до високи равнища на замърсяване, влошаване качеството на околната среда и изчерпване на ресурсите. В днешно време се налага търсене на възможности за рационално използване на природните ресурси, при опазване на околната среда. В настоящата статия се разглеждат различните източници на замърсяване на околната среда от минно-добивната дейност в Родопския минен басейн и възможните мерки за предотвратяване на въздействието им.

Ключови думи: природни ресурси, минно-добивни дейности, опазване на околната среда, Родопски минен басейн

Introduction

The Rhodope Mining Basin is a lead - zinc ore field covering a wide area of the Eastern Rhodopes and the vicinity of the towns of Topolovgrad and Elhovo. Since the 1950s, large lead-zinc deposits have been exploited here. There are several ore areas in the Rhodope Mining Basin, the most significant of which are around the towns of Madan and Madzharovo. The Madan ore region is presented by almost six parallel steep ore-bearing failures that are oriented northwest. Many vein and metasomatic deposits are located along these lines - for example, Ribnitsa - Shahonitsa - Belevitsa, Varba - Krushov dol - Stratiev kamak, Karaalievski dol - Petrovitsa - Erma reka, Sharenka - Borieva reka - Gyudyurska, and Spoluka - Strashimir. The lead-zinc fields near the town of Nedelino also belong to the Madan ore region. The Madzharovo ore region is located along either side of the Arda River south of the town of Harmanli and includes more than 45 ore veins, four of which have a very important industrial importance. The remaining ore areas that are of significance for the mining branch are the Ustrem region (between Topolovgrad and Elhovo), the Davidkovo region, the Persenk - Laki deposits, and others.

The Rhodope basin is an important mining center with a number of active mines and flotation factories.

The mining and metallurgical industries create significant environmental problems with their large-scale development.

The consequences of land disruption and environmental pollution are now at the center of the attention of the global public (Atanasov, 2007).

Industry has a direct impact on all environmental components - air, water, soils. Mostly landscape pollution is associated with releases of harmful substances into air and waters, previous accumulations of harmful substances in the soil, unresolved problems with waste, etc. In mining industry, the risk of contamination is also observed in tailing ponds (acidic and containing heavy metals sewage and sediments). Acidic ore depositions are a long-term problem, as well as the potential danger of accidents and failures .

The extraction and processing of natural resources have led to high levels of pollution, deterioration of the environment and depletion of resources.

Nowadays, it is necessary to search for opportunities for rational utilization of natural resources while preserving the purity of the atmosphere, water and soil.

The rational use of natural resources and the protection of the environment are questions that interest not only scientists, but also governments of many countries and public figures and organizations (Atanasov, 2007).

This paper examines the different sources of environmental pollution from mining activities in the Rhodope Mining Basin.

Pollution of waters from mining activities

One of the most serious environmental problems is the generation of acidic drainage water leaking from different deposits, ore and waste dumps. Because of their high acidity (extremely low pH), these waters lead to the disappearance of the entire flora and fauna in the water intakes where they are discharged.

The formation of acidic ore water is a natural process that goes through all the stages of function of a specific mine working. The oxidation of sulphide minerals, mainly pyrite (FeS2), chalcopyrite (CuFeS2), sphalerite (ZnS), galena (PbS), arsenopyrite (FeAsS), cinnabarite (HgS), etc., leads to generating waters that are acidic and with a high level of sulphates, Fe, Mn, Al, Cu, Zn, Pb, and other toxic elements. All of these heavy metals are soluble, mobile, and can be transported over long distances away from the source of the pollution (Panayotova et al., 2013).

The sources of wastewater are the functioning or the already abandoned open pits and underground mines, the landfill waste, transport roads, etc.

The adverse environmental impact of water discharged from mining activities includes: acidification of water; metal pollution; increasing the concentration of the dissolved salts in water bodies where mine waters are discharged; silting.

The negative impact of acidic ore water is the strongest, since the pH of the water bodies where such water is discharged reduces. Hence, their corrosive effect increases. Acidified waters are not able to support the life of aquatic organisms. Heavy metals (Pb, Cd, Hg, Cu, Zn, Ni), even in very low concentrations, are toxic, especially for the aquatic fauna.

In cases when the mine waters are not acidic, they have high mineralization, high concentrations of suspended solids, and often bacterial contamination. The water in these cases usually contains calcium (Ca), magnesium (Mg), sodium (Na), potassium (K) cations, and basic anions are sulphate (SO_4^{2-}), chlorine (Cl^{1-}), fluoride (F^-), nitrate(NO_3^-), hydrogen carbonate (HCO_3^-), and carbonate (CO_3^{2-}) (Panayotova et al., 2013).

All mining activities require a huge amount of water: dust suppression after blasting, ore processing and transportation, and landfilling of waste and sediments.

Opportunities to reduce water pollution from mining activities

With current technologies, it is almost impossible to stop the generation and prevent the leakage of acidic ore water since fast chemical processes occur. It is necessary to put in more effective means for the treatment of acidic ore water, for discharging and landfilling of sludge. The best opportunity to prevent from acidic ore water is to reduce their generation by contacting sulfide-containing ores with air and water.

For mining waste with high pyrite content, it is necessary to reduce the oxygen flow. The passive prevention is by means of covering the waste with a water layer or a dry mass. For the dry cover layer, waste material is used that is obtained before reaching sulfide ores or materials from abandoned tailings. The water coating is a lagoon that may contain material from the tailing ponds. In both cases, the purpose of the coating is to prevent or reduce the weathering of sulfide minerals to insignificant levels by preventing the flow of oxygen to the pyrite and other sulfide minerals.

The storage of sulfide-containing materials under water reduces the microbial population with oxidizing capabilities and allows the development of sulfate-reducing bacteria. These bacteria contribute to the reverse process - the reduction of sulphate ions to sulphide ions, which help the precipitation of mobile metals in the form of metallic sulphides. The formed sludge is drained through channels or underground drains.

To optimize the effect of the coating, sulfide-containing materials need to be placed below the level of the underground water and the depth of atmospheric oxygen penetration reaches the underground water level to the utmost. One of the most important requirements in designing the coating system is its long-term integrity.

Often, in order to reduce the possibility of generating acidic ore water in waste banks, sulfide-containing waste rock materials are mixed with unslacked lime (CaO), ash, and slag from blast furnaces rich in Al_2O_3, SiO_2, CaO, and MgO.

When mining water is placed into consecutively connected tanks for precipitation, the amount of insoluble suspended solids in the water to be discharged is reduced.

To collect the drainage water from waste banks, it is necessary to construct a drainage ring. The addition of a suitable coagulant helps to precipitate the coarsely dispersed pollutants directly into the drainage ring (Panayotova et al., 2013).

Reclamation of damaged area

Mining industry has a negative impact on the environment, and the restoration of damaged areas is much slower. One of the serious tasks of landscape construction in regions with developed mining industry is the reclamation of damaged areas. Its purpose is to enable "technical lands" to be reused in agriculture and forestry.

According to the normative documents that regulate the preservation and restoration of the environment in the open pit mining process in the whole country, since 1980 it has been obligatory to carry out reclamation works.

The process of reclamation of the damaged areas is regulated by Ordinance №26 of 2/10/1996 on the reclamation of damaged areas, improvement of low-productive lands, removal and utilization of the humus layer (Prom., SG, issue 89 of 22/10/1996, amended and supplemented, issue 30 of 22/03/2002). It covers a complex of engineering, meliorative, agricultural, forestry and other activities, the implementation of which leads to the restoration of damaged areas and to the improvement of the landscape, the harmonious combination of the natural components - relief, climate, soil and vegetation.

The reclamation of damaged areas in the open development of mineral resources can only be successfully carried out in a complex way and provided that are shared enough resources and material equipment from mines for this important activity. The present and future of mining and industrial regions depends largely on the adequate accomplishment of this technological process.

The restoration of damaged natural landscapes is determined by the sanitary, hygienic, moral and aesthetic requirements of modern society and by the public interests in the future of mankind (Atanassov, 2007).

Contamination of water by mineral processing

The main stages in mineral processing are the crushing and grinding of ores, classification, flotation, compression, and filtration. The most significant is the water consumption in the flotation and transport of the concentrate and the waste, as well as a result of evaporation and infiltration in the tailings ponds.

In mineral processing, different types of waste in the liquid and solid phase are generated.

The solid wastes from the flotation are mainly rock materials and small amounts of non-extracted minerals. The liquid phase consists of water, dissolved and suspended substances and compounds, and unused during the flotation reagents. The liquid phase is usually taken to tailings ponds in which the suspended particles precipitate. Certain natural physicochemical processes also lead to the formation of slightly soluble compounds. The clarified liquid can be returned to the mills or to be discharged in natural water sources, provided that it meets the water quality standards. Depending on the processed ore, the used reagents, and the processes, different liquid and solid wastes are generated. The suspensions from grinding and from gravity enrichment are also disposed in tailing ponds.

The added flotation reagents are precipitated, neutralized and adsorbed on the surface of the mineral particles, but in some cases some of them remain dissolved in the wastewater, requiring the application of measures to prevent the pollution of the environment.

The type and concentrations of pollutants in wastewater from flotation depend on the type of enriched material (copper ores, copper-molybdenum ores, iron ores, lead-zinc ores, nickel ores, sulfide ores, oxide ores, mixed type, etc. or industrial minerals, coal). In general, wastewater contains: heavy metal ions (lead, zinc, copper, cadmium, manganese, molybdenum, iron, nickel), increased concentrations of other metals (aluminum, calcium, sodium), increased concentrations of sulphates, arsenic, selenium, sulfides, chlorides, phosphates, cyanides. The main inorganic pollutants in wastewater from the flotation of lead-zinc ores, processed in the Rhodope region are Pb, Zn, Hg, Cd, Cu, Cr, Mn, Fe, CN.

Often the waters are contaminated with organic reagents: collectors (butyric and some aromatic amines, sulfhydryl collectors - with basic xanthogenates, dithiophosphates (aerofloites), dithiocarbamates, products from the distillation of oil and tar); regulators - mercaptans (thioalcohols and thiophenols); Foaming agents – compounds, containing carboxyl (-COOH), carbonyl (= C = O), amine (-NH_2), sulfo group (-OSO_2OH or -SO_2OH) Waters are usually neutral, but some cases of releasing low acid (pH 4.0 - 4.5) or slightly alkaline (pH 8.0 - 8.5) water are also observed (Panayotova et al., 2013).

Measures to reduce water pollution from mineral processing

One or more of the following mechanisms for the efficient use of water are chosen:

• In the processing plant:

- Installation of thickeners to obtain a high density concentrate;
- Installation of filter presses;
- Primary water transport of the concentrate, with subsequent water recovery.

•In tailing ponds:

- Filtration of the waste suspension feeding from the ore-dressing plant to the tailing pond;
- Additional feeding of flocculants and / or alkalizing agents (calcimine) to accelerate flocculation and precipitation;
- Improvement of the tailing pond to achieve a higher water recovery rate, as evaporation and infiltration losses are the greatest;
- The bottom and walls of the tailing pond must be covered with a waterproof material such as gravel, clay or processed ore after leaching;
- A fine waterproof material must be accumulated on the bottom and the walls of the tailing pond to prevent or reduce the infiltration of contaminated water into underground or surface water;
- Installation of drainage in the tailing pond for the reduction of filtration losses (Panayotova et al., 2013).

Conclusion

Finally, it should be pointed out that the above measures do not cover the full list of conservation measures that can be proposed for the protection of the environment damaged by the result of mining and processing activities. The main concern is not just to know but to apply those in practice. It is necessary to move towards economically justifiable solutions and environmentally friendly technologies.

References

Атанасов, А. Екологични проблеми и рекултивация на земите, нарушени от минната промишленост. С., 2007. – 13,24 с. (Atanasov, A. Ekologichni problemi i rekultivatsiya na zemite, narusheni ot minnata promishlenost. Sofia, 2007. – 13,24.)

Наредба № 26 за рекултивация на нарушени терени, подобряване на слабопродуктивни земи, отнемане и оползотворяване на хумусния пласт, Обн. ДВ. бр.89 от 22 Октомври 1996г., изм. ДВ. бр.30 от 22 Март 2002 г. (Naredba № 26 za rekultivatsiya na narusheni tereni, podobryavane na slaboproduktivni zemi, otnemane I opolzotvoryavane na humosniya plast, Obn. DV. br. 89 ot 22 Oktomvri 1996 g., izm. DV. br. 30 ot 22 Mart 2002 g.)

Панайотова, М., Е. Власева, Е. Александрова, С. Браткова. Въздействие на добива и преработването на полезни изкопаеми върху околната среда. С., Издателска къща „Св. Иван Рилски”, 2013. – 48, 55, 64-66. (Panayotova, M., E. Vlaseva, E. Aleksandrova, S. Bratkova. Vazdeystvie na dobiva i prerabotvaneto na polezni izkopaemi varhu okolnata sreda. Sofia, Izdatelska kashta „Sv. Ivan Rilski”, 2013. – 48, 55, 64-66.)

http://eea.government.bg/eea/bg/publicat/2003/economic/prom2.htm (accessed 17 July 2017),

This article was reviewed by Prof. Dr. Marinela Panayotova and Assoc. Prof. Dr. Evgenia Alexandrova.

POSSIBILITIES FOR THE UTILIZATION OF TECHNOGENIC WASTE FROM THE ACTIVITY OF MINING AND PROCESSING PLANTS IN THE RHODOPE REGION

Velichka Hristova[1], Emilia Sokolova[1]

[1]Kardzhali Branch of the University of Mining and Geology "St. Ivan Rilski" - Sofia, 6600 Kardzhali, velichka_hristova@mgu.bg

ABSTRACT. Sustainable and long-term development is a major goal in the use of non-renewable natural resources nowadays. The concept of sustainable development of the mining industry includes the rational and efficient utilization of mineral resources. From an environmental point of view, it is necessary to combine many different approaches for the protection of the environment. One of the most important and complex environmental tasks is the solution to the problems related to the treatment and utilization of the technogenic waste. The aim is to utilize waste as a secondary resource. The issue of "Waste management" is regarded more and more seriously, especially after Bulgaria joined the European Union. This paper presents the possibilities of using the technogenic waste from the mining and processing industries in the Rhodope region as a secondary resource.

Keywords: mining and processing industries, Rhodope region (Bulgaria), technogenic waste, utilization of waste

ВЪЗМОЖНОСТИ ЗА ОПОЛЗОТВОРЯВАНЕ НА ТЕХНОГЕННИ ОТПАДЪЦИ ОТ ДЕЙНОСТТА НА МИННО-ДОБИВНИ И ПРЕРАБОТВАТЕЛНИ ПРЕДПРИЯТИЯ В РОДОПСКИЯ РЕГИОН

Величка Христова[1], Емилия Соколова[1]

[1]Филиал Кърджали на Минно-геоложки университет „Св. Иван Рилски" – София, 6600 Кърджали, velichka_hristova@mgu.bg

РЕЗЮМЕ. Устойчивото и дългосрочно развитие е основна цел при използването на невъзобновимите природни ресурси в днешно време. Концепцията за устойчиво развитие на минната промишленост включва рационално и ефективно усвояване на минералните ресурси. В екологичен план се налага комбиниране на множество различни подходи за опазване на околната среда. Една от най-важните и сложни екологични задачи е решаването на проблемите, свързани с третирането и утилизацията на техногенните отпадъци. Целта е оползотворяване на отпадъците като вторичен ресурс. Темата „Управление на отпадъците" се развива все по-сериозно, особено след присъединяване на страната ни към Европейския съюз. В настоящата статия се разглеждат възможностите за използване на техногенни отпадъци от минно-добивната и преработвателна промишленост в Родопския регион като вторичен ресурс.

Ключови думи: минно-добивна и преработвателна промишленост, Родопски регион (България), техногенни отпадъци, оползотворяване на отпадъци

Introduction

The development of the mining and processing industries makes the mining sector one of the main engines for the economic development of our country. A serious problem in the extraction and processing of natural resources is the generation of large quantities of waste. A National Strategy for the development of the mining industry was adopted in 2015 to meet the existing legal and regulatory framework for underground natural resources in the European Union. The strategy includes the sustainable and balanced management of mining waste and the minimization of waste through its utilization in relevant industrial sub-sectors. The recovery of mining waste will help reduce its amount by using it as a secondary resource for various industries. It will also reduce environmental pollution associated with the extraction and processing of primary raw materials, and will protect human health.

This paper aims at exploring the possibilities for the utilization of technogenic waste by analyzing the mining and processing industry in the Rhodope region. The mining industry is one of the most important economic sectors in this region.

The extraction and processing of minerals, non-metallic minerals, and coal in the Rhodope region is the main subject of the present study. The above are classified as non-renewable natural resources and their processing and efficient recovery is essential because of their depletion. Minerals (lead-zinc and gold-containing ores) and non-ore minerals (bentonite, perlite, zeolite and lignite coal) are extracted and processed in the region. Depending on the minerals that are extracted and processed according to the accepted technological scheme of the individual enterprises, different waste types are obtained. The utilization of these wastes is important both in economic and environmental terms.

The present work examines the types of waste generated by the production and technological processing and the alternatives for their use as raw material. The essence of the problem is to follow the concept of sustainable development of the mineral raw materials sector by limiting the depletion of non-renewable resources and reducing their harmful impact on the environment.

Characterization of mining waste

The characterization of mining waste aims to identify and assess its properties and behaviour, as well as to select management methods that provide: prevention, reduction or minimization the harmful impact of waste on the environment, safety, and human health (Grigorova, 2011). For the characterization of mining waste, information is needed about the region, including: relief, soils and vegetation, surface and underground water, climate, threats of natural disasters (earthquakes, landslides, floods, etc.) and socio-economic data. Technological characteristics of the deposit, closed or being mined, are of great importance (depth, shape, and size of the deposit); applied extraction technologies in the region and their characteristics; applied processing technologies (used reagents, concentration and quantities, requirements for the circulating water, purification technologies in the mineral processing plant; sources of pollution in mine dumps); transport connections (auto transport, conveyor belts, pipelines); opportunities for backfilling of processed mining sites. Consideration should be given to:

- The geological characteristics of the deposit - characterization of the underground resources, the country rocks and waste rock (their type, mass and volume); mineralogical characteristic; granulometric characteristic; chemical properties; hydrothermal changes, as well as changes that occurred as a result of the weathering and supergene processes of the underground resources and the country rocks; physical, engineering and technical characteristics (volumetric weight, density, porosity, strength, elasticity, plasticity, fissuration, hardness, abrasiveness, permeability, filtration properties, moisture, sludge separation, dusting, etc.); risk of acidic water generation; surface water properties, etc .;
- Characterization of mining waste - annual (hourly) output and total quantity; granulometric composition of the solid fraction; solid waste or suspended sludge, pulp density, solid phase density; chemical composition of the liquid phase, metal content.

The geochemical characterization of mining waste includes assessment of the mineral and chemical composition of the waste, the presence of residual chemical compounds (reagents) from its processing, as well as predicting the leakage potential of chemicals polluting the components of the environment and affecting the health and safety of people, also, the leaching of metals leading to soil contamination (Panayotova et al., 2013).

External factors, such as transport, storage, type of storage facility, may also have effect on the characteristics of mining waste.

Each mining company must have a waste management plan compliant with European directives.

Information for the characterization of mining waste is used for the preparation of management plans, working projects for the construction, for the operation and closing down of mining waste facilities, and for the categorization of the mine waste storage facilities (Nishkov, 2010). The treatment and utilization of waste generated by ore beneficiation is less developed than the utilization of metallurgical waste. It is necessary to search alternatives for relatively closed production cycles where it is possible to use waste as a secondary resource.

Generated waste from mining and processing plants and opportunities for its utilization

Waste from the beneficiation of lead-zinc ores in the Rhodope region

In the Rhodope region, the polymetallic lead-zinc ores in the ore fields near the towns of Madan, Rudozem, Laki and Zlatograd, are with the greatest industrial importance. The production of lead-zinc ores is carried out in an underground way with systems of mining adapted to these conditions. The lead-zinc ores in the Rhodope region are processed by a flotation method of beneficiation. During the flotation process, the waste rock and small amounts of non-extracted useful minerals are separated as solid waste; a liquid phase is also formed, consisting of water, suspended solids and residual flotation reagents. The slurry is discharged in the tailing pond, where the suspended particles are precipitated. Some natural physicochemical processes occur, leading to the neutralization of some compounds or to the formation of soluble compounds. The precipitated waste contains valuable components for which extraction is possible when new technologies are introduced. This is particularly important for waste from past productions, since rich ores were processed with less developed technologies then and the accumulated waste contains metals of high concentration. At present, pyrite (FeS_2) is not extracted as a concentrate and it precipitates into the waste because of the content that is currently unprofitable for extraction. With the development of mining waste processing technologies, it is possible to extract metals from sources with low metal content, such as mineral processing waste. The introduction of a new technological scheme will enable the extraction of pyrite which will be used for the production of sulfuric acid.

Secondary pyrite tailings were treated by using an oxidizing-reducing roasting technological flow sheet. The two-stage oxidizing roasting technology is suitable for eliminating S and As. The material was enriched in Fe to more than 64% after treatment at a temperature of over 600 - 700°C and can be used as a fine iron-making raw material (Gu et al., 2008).

It is proposed to process the material from the mine dump of the Bor Mine, in which the main sulfide mineral is pyrite. Before the flotation process, the pre-treatment of the material is essential. For the release of sulfide minerals from the rock formations, better results have been obtained by abrasion of the surface through friction compared to the conventional grinding (Panayotova, 2011).

A mineral admixture with photocatalytic activity is obtained through acid leaching-hydrolyzation and the single calcination method, using industrial waste pyrite tailings and high titanium slag as raw materials in which pyrite tailings were the substrate and high titanium slag was the source of titanium (Zhang, 2017).

It will be possible to extract Mn, Fe, Zn, Pb, Cu, Au, Ag, Ni, Co, and others with the use of modern technologies and technical means.

Waste from the beneficiation of gold-containing ores in the Rhodope mining basin

Since 2006, gold-containing polymetal ores have been extracted from the Chala deposit by means of underground method in the Eastern Rhodopes. Their processing and beneficiation are realized in the Kardzhali Enrichment Factory through gravity technology. In 2012, cyanide technology, the so-called CIL-process (Carbon in leach), was introduced for the processing of the gravitational waste. This technology provides a high level of extraction of gold, over 95% (http://gorubso.bg). Costs of reagents are low and the introduced technology for cyanide destruction in the waste pulp guarantees concentrations of pollutants, including cyanides, that comply with the Bulgarian and European legislation.

The waste, generated by the processes of gravitational beneficiation for the period 2006 – 2012, is shipped from the tailing pond and processed for finishing off the gold extraction.

The mining of polymetallic gold and silver ores from the Sedefche deposit in the municipality of Momchilgrad is being developed. The ore will be extracted by means of open-pit mining and processed in the enrichment plant in the town of Kardzhali.

Mining and processing of gold-containing ores from the Ada Tepe site of the Khan Krum deposit, in the town of Krumovgrad is also envisaged. The main beneficiation process for the extraction of gold and silver from the ore will be realized by means of flotation.

The limited resources of gold in the world, as well as the reduction of its content in the ore, leads to the regulation of the mining of this precious metal and the steady rise in its value due to the increasing demand. The recovery of gold is of importance because of high market prices and huge industrial applications.

Waste from the beneficiation processes, the so-called mineral waste, often contains significant amounts of precious metals, especially when the efficiency of the flotation technologies used in the past to concentrate the target minerals was not so good.

Pyrometallurgical and hydrometallurgical processes are the main methods which are applied for the extraction of gold from ores and technogenic wastes. Recent years have witnessed an increasing interest in the wastes from the metallurgical industries for the extraction of precious metals available in them. These wastes can be utilized and are secondary resource of metals.

Through diverse biosorbents, such as bacteria, yeasts, fungi, actinomycetes, algae, bio-polymers and some bio spent materials, biosorption is considered a promising and efficient technology for the recovery of gold from secondary sources (Syed, 2012).

In long terms, the application of new geotechnological methods for gold extraction is envisaged:
- Heap leaching;
- Heap - biological leaching;
- Combined leaching.

Waste from mining industry can be processed to extract a wide range of minerals by applying technology schemes using chemical and biochemical leaching in heaps, baths, etc., (National Strategy for the Development of the Mining Industry, 2015).

Before the processing of gold-containing ore, the enrichment factory in Kardzhali processed lead-zinc ore through a flotation method. Waste from the factory, accumulated in the tailing pond, is a secondary resource of metals that can be utilized by applying new methods or modified technologies.

Wastes from the extraction and processing of industrial minerals

Of the industrial minerals in the Rhodopes, bentonite, perlite and zeolites are the most important. The deposits of bentonite clays are "Propast-Dobrovolets" and "Enchets". Perlite is extracted from a deposit known as "Schupenata planina", and zeolite from the "Beli Plast" deposit. The extraction is carried out by an open-pit mining and the material is processed to obtain a final product. Their growing consumption is due to their specific qualities (http://bentonite-bg.com). In January 2017, a concession for the extraction of bentonite clays and zeolite from the "Ralitsa" deposit was obtained (Decision No 92/ 26.01.2017 of the Ministry of Energy).

In mining of industrial minerals, significant quantities of rubble are extracted.

The humus layer of the rubble can be separated and subsequently utilized.

As the amount of the earth's mass from the overburden is large, it is possible to return the overburden to fill the space from which the extraction of bentonite, zeolite and perlite is made.

Solid wastes are obtained by the mining and processing industries of industrial minerals. In practice, these are inert materials - rock fragments, limestone, sand, clay and others. These materials can be separated and used as they have a wide-ranging application. Rock materials can be used in road construction; sands can be used in casting, as well as in the production of bricks and tiles; limestone can be used to produce cement, lime, enhancers, colouring agents; clays can be used to create anti-filtration screens of tailing ponds.

Wastes from the extraction and processing of lignite coal

In Bulgaria, the main source of energy is still coal. The largest deposit in the country is the East Maritsa Coal Basin. Lignite coal from this deposit is extracted through open-pit mining and is mainly used for electricity generation and for the production of briquettes. Three thermal power plants in Maritsa - Iztok generate electricity by using this coal.

The overburden that is removed in coal mining is used to re-cultivate the landscape, align the terrain, and build roads. The

humus layer is collected and transported to temporary landfills. After aligning the terrains intended for agricultural use, the humus collected is spread over them. It can be used on lands for agricultural use and in areas for forestry use.

Slags, ashes and cinder are the main wastes from the thermal power plants. Although waste management requirements are adopted and have to be implemented, large quantities of wastes are disposed. The utilization of these wastes can be performed in different areas.

Waste from thermoelectric power plants can be used in the following ways: in the construction of roads, bridges, dams and buildings (as an ash additive in building mortars, in the form of gypsum, gypsum board and other panels for interior lining); for the production of cement, concrete, and other construction mixtures; in the production of bricks and roof tiles; for piling and filling activities, roofing, asphalt roads; as a soil cultivator in agriculture; for the production of paints, adhesives, varnishes (Zarichinova et al., 2016).

The utilization of the ash from thermal power stations can produce glass and glass products using the high temperature method. The ash from thermal power stations is a suitable recourse for the production of zeolites, which can be used for cleaning industrial and household waters (Panayotova et al., 2013).

In order to minimize the waste generated by the thermal power stations, it is necessary to promote its utilization.

Conclusions

- Effective utilization of primary natural resources requires complex and efficient processing;
- Using waste from a single production as a secondary resource (feedstock) for another production would contribute to the efficient and complex use of the raw materials;
- The main factor for waste reduction is the introduction of new high-tech processing using waste-free and low-waste technologies.

References

Григорова, И. Гравитационни технологии при управление на минни отпадъци. Силистра, Издателство РИТТ, 2011. - 33 с. (Grigorova, I. Gravitatsionni tehnologii pri upravlenie na minni otpadatsi. Silistra, Izdatelstvo RITT, 2011. – 33 p.)

Заричинова, Д., И. Попов, Г. Кондарев. Отпадъци от въглищната индустрия. (Zarichinova, D., I. Popov, G. Kondarev. Otpadatsi ot vaglishtnata industria), available at: http://zazemiata.org/v1/fileadmin/content/energy/Otpadatzi_ot_vaglishtna_industria_doklad.pdf (accessed 20 July 2017).

Министерство на енергетиката. Национална стратегия за развитие на минната индустрия (приета с Решение 761 от 29.09.2015 г. на МС). (Ministerstvo na energetikata. Natsionalna strategia za razvitie na minnata industria (prieta s Reshenie 761 ot 29.09.2015 g. na MS)), available at: https://www.me.government.bg/bg/themes/nacionalna-strategiya-za-razvitie-na-minnata-industriya-1575-295.html (accessed 10 July 2017).

Нишков, И. Управление на отпадъци. Силистра, Издателство РИТТ, 2010. - 149 с. (Nishkov, I. Upravlenie na otpadatsi. Silistra, Izdatelstvo RITT, 2010. – 149 p.)

Панайотова, М. Рециклиране на някои цветни метали чрез концентриране и извличане от течни и твърди отпадъци от добива, преработването и употребата им. С., Издателска къща „Св. Иван Рилски", 2011. – 78 с. (Panayotova, M. Retsiklirane na nyakoi tsvetni metali chrez kontsentrirane i izvlichane ot techni i tvardi otpadatsi ot dobiva, prerabotvaneto i upotrebata im. S., Izdatelska kashta "Sv. Ivan Rilski", 2011. – 78 p.)

Панайотова, М., Е. Власева, Е. Александрова, С. Браткова. Въздействие на добива и преработването на полезни изкопаеми върху околната среда. С., Издателска къща „Св. Иван Рилски", 2013. - 117-118, - 122. (Panayotova, M., E. Vlaseva, E. Aleksandrova, S. Bratkova. Vazdeystvie na dobiva i prerabotvaneto na polezni izkopaemi varhu okolnata sreda. Sofia, Izdatelska kashta "Sv. Ivan Rilski", 2013. - 117-118, - 122.)

Gu, Y., W. Xu, T. Yang, H. Peng. Comprehensive treatment of the secondary pyrite tailings by oxidizing-reducing roasting. Multipurpose Utilization of Mineral Resources, 2008-04, available at: http://en.cnki.com.cn/Article_en/CJFDTOTAL-KCZL200804011.htm (accessed 08 July 2017)

Syed, S. Recovery of gold from secondary sources - A review. Hydrometallurgy, Volumes 115-116, 2012. – 30-51 p., available at: https://doi.org/10.1016/j.hydromet.2011.12.012 (accessed 15 July 2017), DOI: 10.1016/j.hydromet.2011.12.012

Zhang, G., Y. Yan, Z. Hu, B. Xiao. Investigation on preparation of pyrite tailings-based mineral admixture with photocatalytic activity. Construction and Building Materials, Vol. 138, 2017. – 26-34 p., available at: https://doi.org/10.1016/j.conbuildmat.2017.01.134 (accessed 12 July 2017), DOI: 10.1016/j.conbuildmat.2017.01.134

http://bentonite-bg.com/bg/index.html (accessed 16 July 2017)

http://gorubso.bg (accessed 11 July 2017)

http://www.me.government.bg/bg/themes/reshenie-92-26-01-2017-g-za-predostavyane-na-koncesiya-za-dobiv-na-nemetalni-polezni-izkopaemi-ind-1829-0.html (accessed 16 July 2017)

This article was reviewed by Assoc. Prof. Irena Grigorova, DSc. and Prof. Dr. Marinela Panayotova.

CARBON NANODOTS COATED WITH OLIGONUCLEOTIDES AS FLUORESCENT HYBRIDIZATION PROBES FOR DNA MICROARRAY

Polina Mladenova[1], Hibiki Udono[2], Anatoliy Angelov[1], Aleksandar Lukanov[1,2]*

[1] Department of Eng. Geoecology, University of Mining and Geology "St. Ivan Rilski" – Sofia, Bulgaria
[2] Graduate School of Science and Engineering, Saitama University, Shimo-Ohkubo 255, Sakura-ku, Saitama 338-8570, Japan
Email: loukanov@mail.saitama-u.ac.jp

ABSTRACT. In this article we report an easy preparation of single stranded oligonucleotides conjugated to highly-fluorescent carbon quantum dots as efficient hybridization probes for DNA microarray. These nanotools enable fast detection and quantification of nucleic acid molecules. The main advantage of carbon nanodots (C-dots) over conventional organic dyes is their photobleaching resistance, which improves the signal intensity and thus lower amount of DNA material can be detected. In addition, the surface passivation of C-dots with ethylenediamine leads to the enhancement of their quantum yield and photoluminescence intensity, which is of great importance because, for many bioassays, the genetic amount is extremely limited. In the current report, nitrogen-doted C-dots were used as effective nanoquencher agents for fluorescent hybridization DNA microarray. Their bio-compatibility and stability make them promising fluorescent probes or DNA markers for bio-labeling and bio-imaging applications.

Keywords: Carbon quantum dots, DNA microarray, hybridization probes.

ВЪГЛЕРОДНИ НАНОТОЧКИ ПОКРИТИ С ОЛИГОНУКЛЕОТИДИ, КАТО ФЛУОРЕСЦЕНТНИ ХИБРИДИЗАЦИОННИ СОНДИ ЗА ДНК МИКРОЧИПОВЕ

Полина Младенова[1], Хибики Удоно[2], Анатолий Ангелов[1], Александър Луканов[1,2]
[1] Катедра „Инженерна геоекология", Минно-геоложки Университет „Св.Иван Рилски" – София, България
2 Университета Сайтама, Шимо-окубо 255, Сакура-ку, Сайтама 338-8570, Япония
Email: loukanov@mail.saitama-u.ac.jp

РЕЗЮМЕ. В настоящия доклад е представено приготвянето на едноверижни олигонуклеотиди конюгирани към високо-флуоресцентни въглеродни квантови точки, като ефикасни хибридизационни сонди за ДНК микрочипове. Тези нано-инструменти позволяват бързо откриване и количествено опредделяне на нуклеинови киселини. Основното предимство на въглеродните квантови точки (C-dots) спрямо конвенционалните органични багрила е тяхната устойчивост към фото-избелване, което подобрява интензитета на сигнала и по този начин може да се детектира по-малки количества ДНК материал. В допълнение, повърхностното пасивиране на C-dots с етилендиамин води до повишаване на квантовия им добив и респективно интензитета на фотолуминесценция, което е от голямо значение, тъй като за много биологични анализи генетичното количество е изключително ограничено. В представения доклад въглеродните точки дотирани с азот са използвани, като ефективни нано агенти за загасване на флуоресценцията при хибидизационните ДНК микрочипове. Тяхната био-съвместимост и стабилност ги прави обещаващи флуоресцентни сонди или ДНК за приложения, като био-маркиране и био-изобразяване.

Ключови думи: Въглеродни квантови точки, ДНК микрочипове, хибридизационни сонди.

1. Introduction

The rapid development of highly sensitive, cheap and easy to perform systems for effective detection of specific nucleic acids, aptamers, and oligonucleotides is necessary due to their widespread biotechnological applications (Gresham et al., 2006; Li et al., 2011; Qiang et al., 2014). The recently increased availability of various nanostructures has created interest in their use for the purposes of biotechnological DNA microaaray application. The efforts are focused on the fabrication of homogeneous fluorescence assays based on fluorescence resonance energy transfer or quenching mechanism for oligonucleotides detection (Zhang et al., 2017). It is interesting to note that these techniques generally compromise the use of a photosensitizer and quencher molecules attached to the opposite terminals of oligonucleotide probe. In the absence of the target analytes, the organic dyes are in close proximity and the emission is suppressed. However, upon the occurrence of specific recognition reaction with the target molecules (in the case with complementary oligonucleotide this reaction is hybridization), the quencher agent becomes physically separated from the photosensitizer molecule and thus visible emission is released. Nevertheless, a basic disadvantage of the conventional organic fluorescent sensor is the requirement for careful selection of a photosensitizer-quencher pair in order to ensure optimum efficiency (Li, et al., 2011). Examples of efficient nanoquenchers could be those with gold nanoparticles, carbon nanotubes, metal-organic frameworks, graphene oxide, etc. One of the main advantages of these nanomaterials is their cytotoxicity behavior (Liao et al., 2011; Kumarathasan et al.,

2015). Therefore, the development of new efficient nanoparticles is needed to replace the above nanomaterials.

Carbon quantum dots (C-dots) are potential candidates as nanoquencher agents for fluorescent hybridization DNA microarray. They have unique properties, like resistance to photo-bleaching, small and well-defined size, biocompatibility, low cytotoxicity, and relatively high quantum yield (Roy et al., 2015). In addition, C-dots possess high water solubility, which allows homogeneous sensing assay. This property is of particular importance for the DNA microarray detection of nucleic acids. The purpose of the current report is to develop the C-dots coated with oligonucleotides as fluorescent hybridization probes for DNA microarray. The nitrogen dotted fluorescent C-dots play a role as nano-quenchers in the detection processes.

2. Experimental Procedures

2.1. Materials.. Citric acid, ethylenediamine, sodium carbonate, and *p*-Phenylene diisothiocyanate were purchased from Wako. Amino-terminated DNA oligonucleotides with the following sequencing 5' Fluorescein-$(CH_2)_6$-AAA AAA AAA AAA AAA AAA AAA-CH_2-CH_2-SH 3' (or FAM-probe) and 5' TTT TTT TTT TTT TTT TTT TTT TTT-CH_2CH_2-N_2H 3' were obtained from Sigma-Aldrich. The used water was ultrapure obtained by Milli-Q ion exchange column (Millipore). Gold nanoparticles with 20 nm of diameter were prepared by standard protocol of Greg Herman (Bioconjugation Techniques, Third Edition).

2.2. Synthesis of Carbon nanodots (C-dots) *by microwave-assisted pyrolysis*. C-dots were prepared by the microwave-assisted pyrolysis method (Loukanov et al., 2016), where 1 g of citric acid was dissolved in 10 ml Milli-Q water. Then 200 μL of 1,2-ethylenediamine was added to the prepared solution and the reaction mixture was exposed to microwave irradiation for about 3 min (in 600 W microwave oven). After the occurred microwave pyrolisys, a yellowish brown gum was formed in the Becker glass. This gum was used in the next step without any preliminary purification.

2.3. Preparation of modified nucleotides. FAM-probe-SH templates were immobilized on the surface of 20 nm gold nanoparticles by following a standard protocol (Dharanivasan et al., 2016). The carbon nanodots were conjugated to 5' TTT TTT TTT TTT TTT TTT TTT TTT-CH_2CH_2-N_2H 3' oligonucleotide via *p*-phenylene diisothiocyanate linkage. For that purpose, 200 mg C-dots were dissolved in 100 mL of 50 mM carbonate buffer with pH 9.5, containing 150 mM NaCl. At this alkaline pH, the amino groups from C-dots surface remain unprotonated. Then, 40 mg of *p*-phenylene diisothiocyanate was added, and the reaction mixture was stirred for 30 min at room temperature. The modified carbon nanodots were purified from the reaction mixture by simple centrifugation with acetone. Thiocyanate modified C-dots were mixed with amino-terminated oligonucleotides in carbonate buffer with pH 9.5 at room temperature. After 30 min of incubation, the modified oligonucleotides were separated from the unreacted C-dots by gel electrophoresis.

2.4. Fluorescence quenching and detection of the hybridized DNA oligonucleotides. A 40 nM Tris-HCl buffer solution was prepared to study the fluorescence quenching reaction. Aliquots of FAM-probe-immobilized on gold nanoparticles and C-dot labeled oligonucleotides were added to the buffer solution and the reaction mixture was incubated for 20 min at ambient temperature and for 30 min at 50 °C. After the incubation, the fluorescence of the reaction solution was measured.

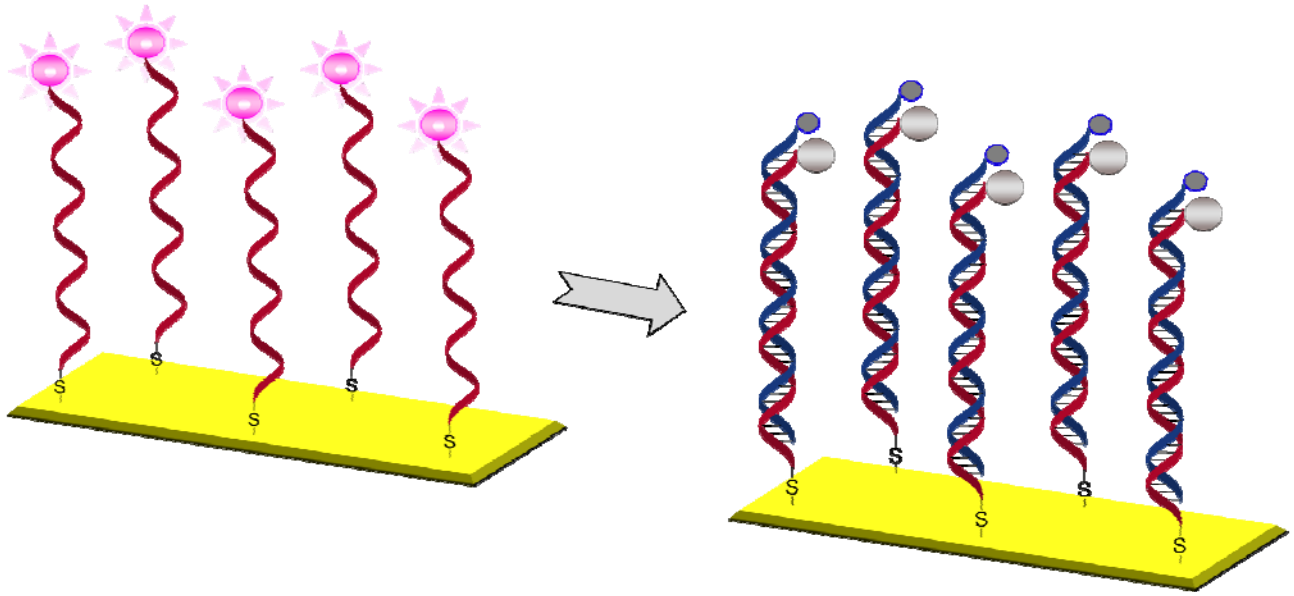

Fig. 1. Schematic illustration of the DNA microarray fluorescent based detection by quenching of fluorescein emission with carbon nanodots

2.5. Analysis and characterization of the nanomaterials and oligonucleotides hybridization. Jasco UV-VIS absorption spectrophotometer (model № V-570) and Jasco analytical spectrofluorometer ((model № FP-6300) were used for the absorption and fluorescence measurements respectively. High resolution X-ray photoelectron spectroscopy (XPS) was performed on an ESCAProbe P spectrometer equipped with a monochromatic aluminum X-ray radiation source (Omicron

Nanotechnology LTD., Taunusstein, Germany). Fourier transform infrared spectroscopy (FT-IR) spectra were recorded using a Tensor II spectrometer (Bruker) with Platinum ATR.

3. Result and discussion

3.1. Principles of C-dots fluorescence-based detection. The general principle of DNA array fluorescence detection in the current report is illustrated in Figure 1. The fluorescein modified oligonucleotide chains were immobilized on the surface of gold nanoparticles. In contact with their complementary oligonucleotides in the buffer, a reaction of hybridization occurred and double stranded DNA (dsDNA) structure was formed. An interaction between dsDNA and the hydrophobic aromatic core of C-dots might have occurred trough π-π stacking. The difference in the electrostatic and hydrophobic properties of FAM-probe and dsDNA leads to a different propensity to adsorb onto the surface of C-dots. Such effect has an impact on the sensitivity and selectivity in the DNA detection microarray. To understand deeply the properties of carbon nanodots, their characterization was performed with X-ray photoelectron spectroscopy (XPS) and Fourier transform infrared spectroscopy (FT-IR).

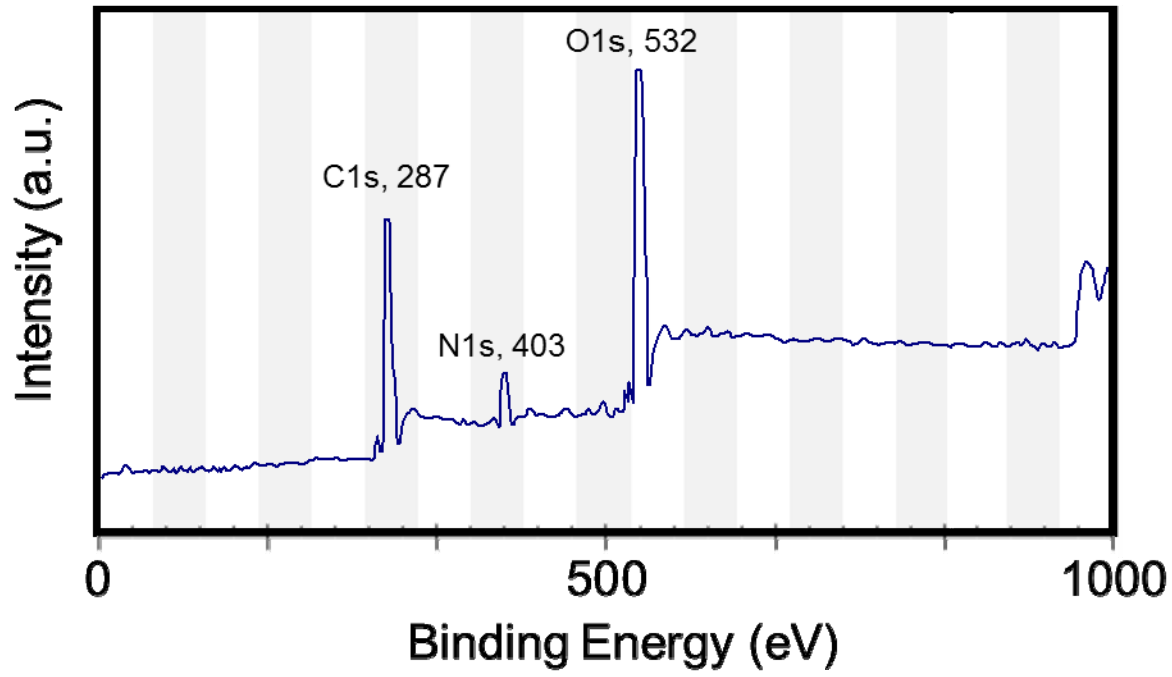

Fig. 2. X-ray photoelectron spectroscopy (XPS) spectrum of carbon nanodots prepared by microwave-assisted pyrolysis

3.2. X-ray photoelectron spectroscopic analysis. XPS is a sensitive and semiquantitive analytical method for studying the nanoparticle surface. It also provides qualitative information for the surface elemental composition and the bonding arrangements of the synthesized carbon nanodots. Hence, survey scans, from a binding energy of 1000 to 0 eV were recorded for C-dots, as shown in Fig. 2, in order to find their overall elemental composition. The binding energy for carbon is 287 eV (C1s), for nitrogen 403 eV (N1s) and for oxygen 532 eV (O1s). As illustrated in the figure carbon-to-oxygen (C/O) ratios of 2.12 and 1.39 was obtained. The values highlight the presence of carboxylic groups and hydrophobic graphitic regions on the surface of C-dots. In fact, the prepared C-dots are also soluble in organic solvents such as acetone, ethanol, methanol, EtOAc and DMSO. However, the high resolution scans revealed that the C-dots also contained C=C, C–C, C–O, C=O and O–C–O peaks on their surface, which might correspond to hydrophilic groups as carboxyl, hydroxyl and esters. A more detailed analysis of the surface chemical groups of C-dots can be achieved by IR spectroscopy.

3.3. FT-IR analysis of the carbon nanodots. As shown in Fig. 3, the absorption band at 3000~3500 cm^{-1} is associated to the combination of stretching vibrations of amino (H_2N–), hydroxyl (HO–), and alkyl (C–H) groups. The band at 3420 cm^{-1} corresponds to N–H; the stretching and bending vibrations of CH_2 and CH_3 groups are at 2975, 2927, 2854, 1460 and 1380 cm^{-1} respectively. The groups C=O and C=N have stretching vibrations at 1720 and 1660 cm^{-1}. There is N–H deformation vibration at around 800 cm^{-1}. The asymmetric and symmetric stretching vibration of C–O–C are 1095 and 1020 cm^{-1}.

3.4. Sensing of complementary oligonucleotide. In order to validate the mechanism described in Fig. 1, the fluorescence behavior of FAM-probe under different experimental condition was investigated. From Fig. 4 it is demonstrated that, in the absence of carbon nanodots, the FAM-probe exhibits strong fluorescence emission (blue line). However, after hybridization with oligonucleotide modified with carbon nanodot, a significant quenching of the fluorescence occurred (red line). This indicates that the presence of C-dot can quench the fluorescent dye effectively. In buffer solution with FAM-probe oligonucleotides and high concentration of C-dots as a control experiment, the quenching effect is much higher in comparison with the hybridization microarray experiment.

Subsequently, another calibration experiment with various concentration of oligonucleotides modified with C-dots was

performed to evaluate the range of detection by this method. With the increase of the concentration of modified oligonucleotide, enhancement of the quenching was observed. This can be attributed to the fact that, with more complementary C-dots-oligonucleotides added, a higher degree of DNA hybridization occurs and more dsDNA were obtained in the solution. The range of detection is established to be within the range of about 0.45 – 500 nM. It is interesting to note that independent studies with carbon nanoparticles and nanospheres were done and the determined range of detection was between 33 – 300 nm (Li et al., 2011).

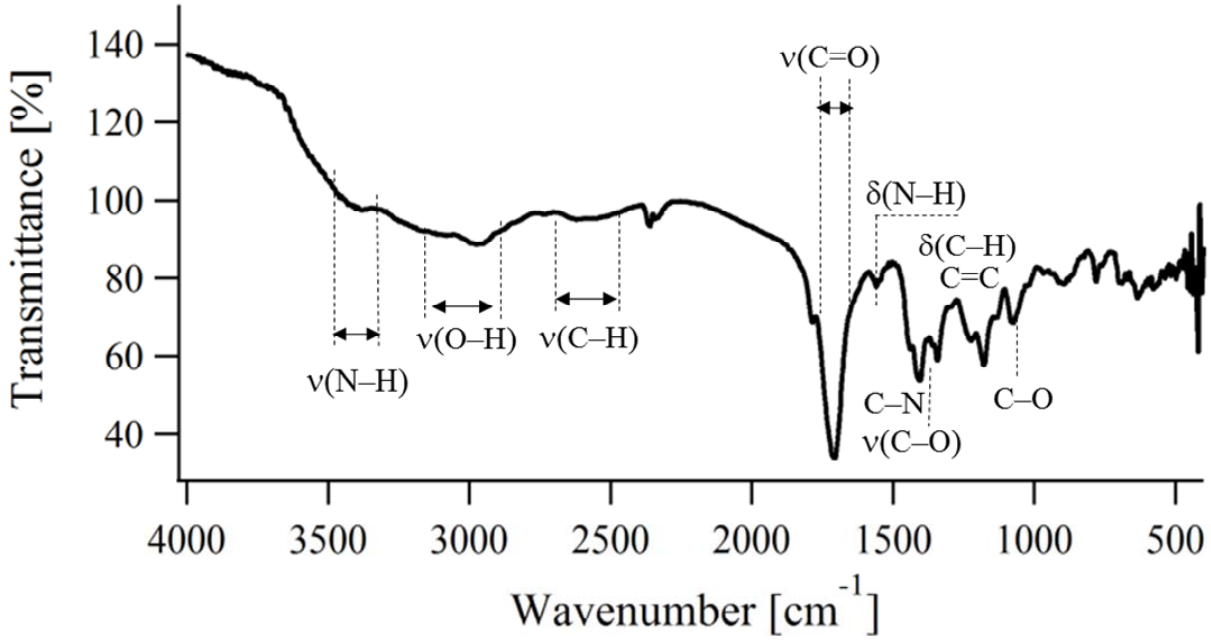

Fig. 3. Fourier transform infrared spectroscopy (FT-IR) spectrum of carbon nanodots prepared from citric acid and ethylenediamine by microwave-assisted pyrolysis

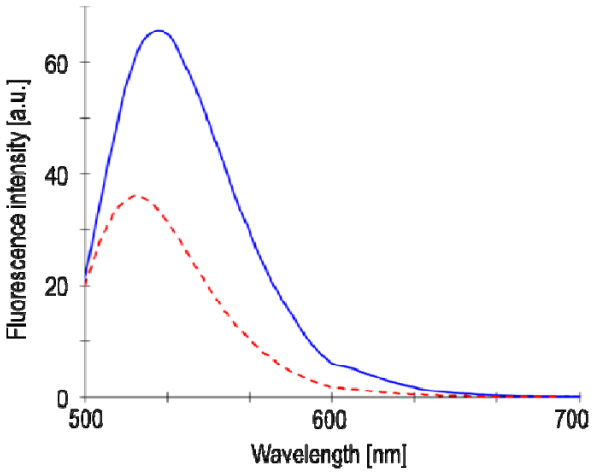

Fig. 4. Fluorescence emission spectra of FAM-probes in Tris-HCl buffer (blue solid line), FAM-probes hybridized with C-dots-oligonucleotides in Tris-buffer (red dotted line)

To investigate the selectivity performance of the proposed detection DNA microarray, single nucleotide polymorphism analysis was performed. This is an analysis in which a single nucleotide that occurs at a specific position in the nucleic chain might be exchanged with another nucleotide. Thus, the two possible variations are said to be alleles for this base. In our control experiment, the enhancement of the fluorescent signal was achieved when C-dots-oligonucleotide with one thymine base was exchanged with cytosine and introduced in the microarray analysis. It suggests that the hybridization did not occur completely in the case of single nucleotide polymorphism analysis.

4. Conclusion

We have developed a novel application of carbon quantum dots as a nanoquencher for DNA microarray analysis. Various nucleic acids can be detected by applying this analytical sensing technique. The linear dynamic range of detection is found to be 0.45 – 500 nM. The conclusions from this study act as the foundation for future works on utilizing this technique for fluorescent detection of essential biomolecules in the practical biotechnology.

Acknowledgment

This study was accomplished thanks to the bilateral agreement between Saitama University-Japan and the University of Mining and Geology "St. Ivan Rilski"-Bulgaria. The authors are grateful to Saitama University for the financial support of the reported investigations.

References

Dharanivasan, G., S. U. Mohamed Riyaz, D. M. I. Jesse, T. R. Muthuramalingam, G. Rajendran, K. Kathiravan. DNA

templated self-assembly of gold nanoparticle clusters in the colorimetric detection of plant viral DNA using a gold nanoparticle conjugated bifunctional oligonucleotide probe. RSC Adv 6, 2016. - 11773–11785.

Gresham, D., D. M. Ruderfer, S. C. Pratt, J. Schacherer, M. J. Dunham, D. Botstein, L. Kruglyak. Genome-wide detection of polymorphisms at nucleotide resolution with a single DNA microarray. Science 311, 2006. -1932–1936.

Kumarathasan, P., D. Breznan, D. Das, M. A. Salam, Y. Siddiqui, et al. Cytotoxicity of carbon nanotube variants: a comparative *in vitro* exposure study with A549 epithelial and J774 macrophage cells. Nanotoxicology 9, . - 148–161.

Li, H., Y. Zhang, Y. Luo, X. Sun. Effective fluorescent sensing platform for biomolecular detection. Small 7, 2011. - 1562–1568.

Li, H., Y. Zhang, L. Wang, J. Tian, X. Sun. Nucleic acid detection using carbon nanoparticles as a fluorescence sensing platform. Chem. Commun. (Cambriadge, U. K.) 47, 2011. - 961–963.

Li, H., Y. Zhang, T. Wu, , S. Liu, L. Wang, X., Sun. Carbon nanospheres for fluorescent biomolecular detection. J. Mater. Chem. 21, 2011. - 4663–4668.

Liao, K.-H., Y.-S. Lin, C. W. Macosko, C. L. Haynes. Cytotoxicity of graphene oxide and graphene in human erythrocytes and skin fibrioblasts. ACX Appl. Mater. Interfaces 3, 2011. - 2607–2615.

Loukanov. A., R. Sekiya, M. Yoshikawa, N. Kobayashi, Y. Moriyasu, S. Nakabayashi. Photosensitizer-conjugated ultrasmall carbon nanodots as multifunctional fluorescent probes for bioimaging. J. Phys. Chem. C 120(29), 2016 . - 15867–15874.

Qiang, W., W. Li, X. Li, X. Chen, D. Xu. Bioinspired polydopamine nanospheres: a superquencher for fluorescence sensing of biomolecules. Chem. Sci. 5, 2014. - 2018–3024.

Roy, P., P.-C. Chen, A. P. Periasamy, Y.-N. Chen, H.-T. Chang. Photoluminescent carbon nanodots: synthesis, physicochemical properties and analytical applications. Materials Today 18(8), 2015. - 447–458.

Zhang, H., J. Lv, Z. Jia. Efficient fluorescence resonance energy transfer between quantum dots and gold nanoparticles based on porous silicon photonic crystal for DNA detection. Sensors (Basel) 17(5), E1078. 2017.

This article was reviewed by Assoc. Prof. Dr. Chavdar Filipov and Prof. Dr. Ryuzo Kawamura.

DIRECT PROBLEM AND THE LIE GROUP ANALYSIS IN THE NON-LINEAR STOCHASTIC EARTH'S SURFACE SUBSIDENCE MECHANICS

Mihail Vulkov

University of Mining and Geology "St. Ivan Rilski", 1700 Sofia, e-mail: mvulkov@abv.bgl

ABSTRACT: The problem is in the field of applied geo-mechanics. The investigation is focused on strata and ground movement over mined-out areas. Using the Lie group analysis of the main equation of the nonlinear stochastic geo-mechanics, a solution to determine the earth's surface subsidence is obtained .The partial differential equation of the nonlinear stochastic geo-mechanics is transformed into an ordinary one. The solution is compared with other existing solutions. The obtained relations may be used to plan and manage mining operations.

Keywords: surface subsidence mechanics, nonlinear stochastic model, Lie group analysis, direct problem

ПРИЛОЖЕНИЕ НА ГРУПОВИЯ АНАЛИЗ НА ЛИИ В МЕХАНИКА НА МУЛДАТА - ПРАВА ЗАДАЧА

Михаил Вълков

МГУ „Св. Иван Рилски",1700 София, e-mail mvulkov@abv.bg

РЕЗЮМЕ: Въз основа на груповия анализ на Лии, приложен към основното уравнение на нелинейната стохастична геомеханика, е предложено решение на задачата за предвиждане на последиците от провеждането на подземни минни работи върху земната повърхност (права задача в механика на минната мулда). Анализирани са предимствата и недостатъците на разгледания метод. Направени са изводи.

Ключови думи: механика на мулдата, групов анализ, пряка задача

Introduction

This paper is in the field of mining geo-mechanics. The investigation is focused on the mining subsidence when mining out underground ore bodies. As a basis, the nonlinear stochastic theory is proposed.

The main differential equation is obtained as a nonlinear parabolic one with the assumption that the rock mass is a stochastic medium consisting of elastic parts.

The basic goal of Lie group analysis of equations is to study the results of the application of the allowed from the equation group on the variety of its solutions.

Using the allowed from the equation group, it is possible to arrange an algebraical structure of the multitude of its solutions. This knowledge may be applied to:

- the description of the general structure of the family of all solutions of the equation;
- the determination of the types of solutions easier to be found in difference to the general solution;
- the construction of new solutions on the basis of the existing solutions, etc.

The problem

To introduce the model of the nonlinear stochastic geo-mechanics, it is assumed that the following axioms are satisfied:

- The rock mass displacements are studied from the viewpoint of the stochastic processes;
- The geo-material is stochastic medium built from elastic parts;
- The characteristics of the mining field allow the model of the new stochastic medium, introduced in (Vulkov 2006), to be applied.

By studying the plane model of cages, shown in Fig.1, and assuming that the rock mass is a stochastic medium built from elastic particles, the general equation for calculating the rock mass subsidence in the influence zone is determined in (Vulkov 1989, 2006).

On the basis of this model and according to the probability mechanisms, the following equation is obtained:

$$\left[A_{11}(P)P_x\right]_x+\left[A_{12}(P)P_x\right]_z+\left[A_{22}(P)P_z\right]_z+B_1(P)P_x+B_2(P)P_z=0 \quad (1)$$

where $P=P(x,z)$ is the probability that a particle of the stochastic medium appears in a point with coordinates (x,z), $P_x=\frac{\partial P}{\partial x}$, $P_z=\frac{\partial P}{\partial z}$, $A_{11}(P)$, $A_{12}(P)$, $A_{22}(P)$, $B_1(P)$ and $B_2(P)$ are rock mass characteristics for the subsiding process.

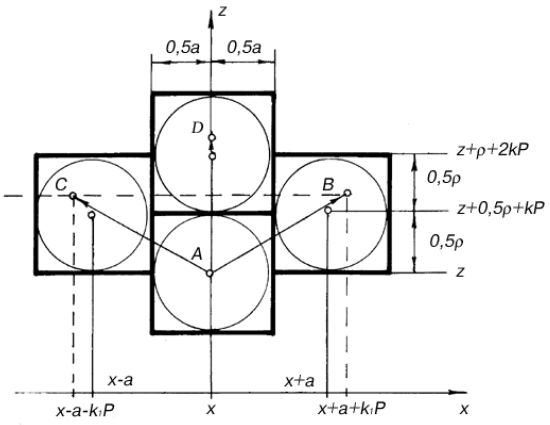

Fig. 1.

By mining out of a horizontal coal seam and by horizontal earth's surface, it is fulfilled:

$$A_{12}(P) = A_{22}(P) = B_1(P) = 0$$
$$B_2(P) = 1 .$$

In this case, equation (1) can be simplified to the form:

$$\left[A_{11} P_x\right]_x + P_z = 0 \qquad (2)$$

The solutions to equation (2) are the objects of this study.

The calculation of the earth's surface displacements, caused by the underground mining of mineral deposits, in given limits, is an important practical problem.

The boundary conditions of the studied problem can be written as follows:

$$P(x,0) = \varphi_o(x) \qquad -\infty \le x \le \infty \qquad (3)$$

$$P(-k,z) = \varphi_1(z) \qquad P(k,z) = \varphi_2(z)$$

$$0 \prec x \le H \qquad (4)$$

The Lie group analysis of the main equation

L.V.Ovsyannicov (1959, 1978) made the Lee group analysis of the equation similar to the main equation of the non-linear stochastic geo-mechanics. The group invariant solutions to that equation may be classified after the type of the non-linear coefficient, which characterizes the heterogeneity of the rock mass:

- when the coefficient $A(w)$ is an arbitrary function, then equation (3) allows three independent operators:

$$\xi_1 = \frac{\partial}{\partial x},\ \xi_2 = \frac{\partial}{\partial z},\ \xi_3 = x\frac{\partial}{\partial x} + 2z\frac{\partial}{\partial z}; \qquad (5)$$

- bigger number of operators may exist only when

$$A(w) = \exp(w) \text{ and } A(w) = w^{2n}. \qquad (6)$$

By constructing the main equation of the non-linear stochastic geo-mechanics, the nonlinear coefficient is obtained in a polynomial form (Vulkov 1989). So, the cases (6) are not interesting for this study.

Generally, the different solutions to equation (2) of ground of one parametric under groups are shown in table 1 (Ovsyannicov 1959).

Table 1

№	Case	$A_{11}(P)$ - arbitrary function
1	I	ξ_1
2	II	ξ_2
3	III	ξ_3
4	IV	$\xi_1 + \xi_2$

The invariant solutions in cases I, II, and IV are not interesting to use in solving geo-mechanical problems connected with the formation of the mining trough.

The attention in this study is concentrated on case III with invariants

$$\eta = \frac{x^2}{z} \text{ and } P(x,z) = V(\eta) \qquad (7)$$

Solving the problem

Let us consider the plane problem for determining the subsidence trough equation in an infinite stripe - Fig. 1.

Using the assumption of J. Litwiniszyn (1974) for proportionality of the probability $P = P(x,z)$ and the vertical displacement of the rock mass $w = w(x,z)$ in the influence zone, the problem (2)- (4) can be written in the following form:

$$\left[A(w) w_x\right]_x + w_z = 0 \quad -\infty \le x \le \infty;\ 0 \prec x \le H; \quad (8)$$

$$w(x,0) = \varphi_o(x) \qquad -\infty \le x \le \infty \quad z = 0 \qquad (9)$$

$$w(0,H) = 0{,}5 w_o,\ x = 0,\ z = H \qquad (10)$$

where $w = w(x,z)$ is the vertical displacement of a point P of the influence zone with coordinates (x,z); $A(w)$ is the coefficient which characterizes the heterogeneity of the rock mass; $\varphi = \varphi(x)$ is a function describing the subsidence of the immediate seam top; *H* is the depth of the coal seam; w_o is the maximal vertical displacement of the immediate seam arising by the existing conditions.

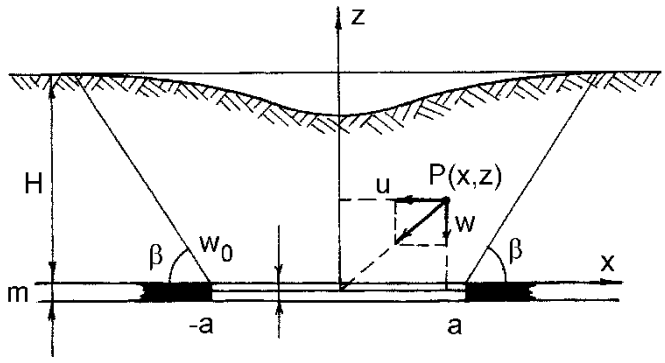

Fig. 2.

The problem for (8) – (10) can be simplified by applying the transformations (6). They transform the quasilinear parabolic partial equation into an ordinary one.

After introducing the following dimensionless variables in equation (8):

$$V = \frac{w}{w_o}; \qquad A(V) = \frac{A(w)}{A(w_o)} \tag{11}$$

and substituting (6) and (11) in problems (1) – (3), it is obtained:

$$-V_\eta = 4\left[A(V)V_\eta\right]_\eta \tag{12}$$

$$V(0) = 0,5; \tag{13}$$

$$V(\infty) = 0, \tag{14}$$

where $V_\eta = \frac{dV}{d\eta}$.

To solve the studied problem, the ordinary equation (12) is integrated once:

$$V - C = -4A(V)V_\eta. \tag{15}$$

After separating the variables, it is obtained:

$$d\eta = -\frac{4A(V)\,dV}{V - C}. \tag{16}$$

Equation (16) is integrated once and the result is the function $\eta = \eta(V)$:

$$\eta = -4\int \frac{A(V)}{V - C}dV + C_1 \tag{17}$$

where C_1 is an integration constant determined by the boundary conditions of the specific problem.

After transforming (17) in the form $V = V(\eta)$, the equation of the mining subsidence trough formed on the earth's surface is obtained.

Conclusion

In the paper, the direct problem connected with predicting the effects on the earth's surface resulting from underground mining activities is solved. This problem is reduced to Cauchy's problem for the nonlinear Fourier equation.

The partial differential equation of the nonlinear stochastic geo-mechanics is reduced into an ordinary one on the basis of the Lie group analysis of main differential equations of the non-linear stochastic mining subsidence theory.

References

Вълков М., Нови стохастични линейни и нелинейни модели в теорията на сляганeто на земната повърхност под влияние на подземни минни работи. Автореферат на дисертацията, София, 1989 г.(Vulkov, M., Novi stohastichni lineiyni i nelineyni modeli v teoriata na slyaganeto na zemnata povarhnost pod vliyanie na podzemni minni raboti, Avtoreferat na dicertatsiata, Sofia,1989.)

Вълков М., Стохастични модели в кинематиката на минната мулда, С., МГУ, 2006г. (Vulkov, M., Stohastichni modeli v kinematikata na minnata mulda, Sofia, MGU, 2006.)

Овсянников, Л. В., Групповые свойства уравнения нелинейной теплопроводности, ДАН, т.125, №3, 1959. (Ovsyannikov, L. V., Gruppovie svoistva uravneniya nelineinoi teploprovodnosti, DAN, 125, 3, 1959.)

Овсянников, Л. В., Групповой анализ дифференциальных уравнении, М., Наука, 1978 г. (Ovsyannikov, L. V., Gruppovoy analiz diferentsialynih uravneniy, Moskva, Nauka , 1978.)

Litwiniszyn J., 1974., Stochastic Methods in Mechanics of granular bodies. Wien, Heidelberg, New York, Springer Verlag.

Kratzsch H., Mining Subsidence Engineering, Berlin, Heidelberg, New York, Springer Verlag, 1983.

This article was reviewed by Assoc. Prof. Dr. Stanislav Topalov and Assoc. Prof. Dr. Violeta Trifonova-Genova.

THE LIE GROUP ANALYSIS AND THE COEFFICIENT PROBLEM IN THE NON-LINEAR STOCHASTIC EARTH'S SUBSIDENCE MECHANICS

Mihail Vulkov

University of Mining and Geology "St. Ivan Rilski", 1700 Sofia, e-mail mvulkov@abv.bg

ABSTRACT. The problem is in the field of applied geo-mechanics. The investigation is focused on strata and ground movement over mined out areas. Using the Lie group analysis of the main equation of the non-linear stochastic geo-mechanics, a transformation is obtained. The partial differential equation of the non-linear stochastic geo-mechanics is transformed into an ordinary one. Applying measurements data for the vertical displacements, the coefficient problem is solved. An algorithm for organizing the solving procedure is described. The obtained relations may be used to plan and manage mining operations.

Keywords: surface subsidence mechanics, nonlinear stochastic model, Lie group analysis, coefficient problem

ГРУПОВИЯ АНАЛИЗ НА ЛИИ ПРИ РЕШАВАНЕ НА КОЕФИЦИЕНТНАТА ЗАДАЧА В МЕХАНИКА НА МУЛДАТА

Михаил Вълков

МГУ „Св. Иван Рилски",1700 София, e-mail mvulkov@abv.bg

РЕЗЮМЕ: Въз основа на груповия анализ на Лии, приложен към основното уравнение на нелинейната стохастична геомеханика, е решена коефициентната задачата в механика на минната мулда. Нейна цел е определянето на коефициента в основното уравнение на нелинейната стохастична геомеханика по данни от полеви измервания. Последният характеризира поведението на подработения скален масив по отношение на мулдообразуването. Представен е алгоритъм за провеждане на решението. Анализирани са предимствата и недостатъците на разгледания метод. Направени са изводи.

Ключови думи: механика на мулдата, групов анализ, коефициентна задача

Introduction

Underground mining of minerals or civil engineering works are the reasons for subsiding the overlying rock mass into the underground cavities. The studied result of that phenomenon is the subsidence of the earth's surface. It creates unfavorable conditions for the functioning of buildings, infrastructure, and equipment and natural objects on the earth's surface.

In order to analyze the subsiding process caused by underground mining, it is important to determine the rock mass properties connected with the studied phenomenon.

The functional coefficient $A(w)$ in the main equation of the non-linear stochastic geo-mechanics (Vulkov 1989, 2006) characterizes the heterogeneity of the rock mass and its behavior in the process of subsiding. In this paper, the problem of determining this functional coefficient is studied.

The plane problem of determining the equation of the mining subsidence trough, (Vulkov 1989, 2006) - Fig.1 - is considered using the Lie group analysis method for the main equation of the non-linear stochastic geo-mechanics.

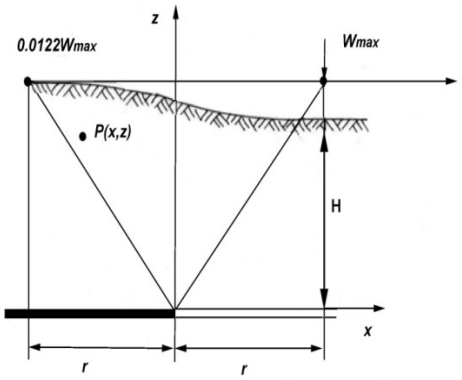

Fig. 1.

The coefficient problem

The problem of determining the non-linear coefficient can be reduced to the following problem for the quasilinear Fourier equation:

$$\left[A(w)\,w_x\right]_x = w_z \quad -\infty \le x \le \infty; \quad 0 \prec x \le H \qquad (1)$$

$$w(x,0)=\varphi_o(x) \qquad -\infty \le x \le \infty \quad z=0 \tag{2}$$

$$w(0,H)=0{,}5w_o\,,\ x=0\,,\ z=H\,, \tag{3}$$

where $w(x,y)$ is the vertical displacement of point P of the influence zone with coordinates (x,y); $A(w)$ is the studied coefficient; $\varphi=\varphi(x)$ is a function describing the subsidence of the immediate seam top; H is the depth of the coal seam; w_o is the maximal vertical displacement on the earth`s surface arising by the existing conditions.

Relationship (3) is experimentally determined.

The Lie group analysis of the main equation

L.V. Ovsyannikov (1959, 1978) made the Lee group analysis of the equation similar to the main equation of the non-linear stochastic geo-mechanics. The group invariant solutions to that equation may be classified after the type of the non-linear coefficient, which characterizes the heterogeneity of the rock mass:

- when the coefficient $A(w)$ is an arbitrary function, then equation (3) allows three independent operators:

$$\xi_1=\frac{\partial}{\partial x}\,,\ \xi_2=\frac{\partial}{\partial z}\,,\ \xi_3=x\frac{\partial}{\partial x}+2z\frac{\partial}{\partial z}\,; \tag{4}$$

- bigger number of operators may exist only when

$$A(w)=\exp(w) \ \text{ and } \ A(w)=w^{2n}\,. \tag{5}$$

By constructing the main equation of the non-linear stochastic geo-mechanics, the non-linear coefficient is obtained in a polynomial form (Vulkov 1989). So, the cases in (6) are not interesting for this study.

Generally, the different solutions of the equation (2) of ground of one parametric under groups are shown in table 1 (Ovsyannikov, 1959).

Table 1

№	Case	$A_{11}(P)$ - arbitrary function
1	I	ξ_1
2	II	ξ_2
3	III	ξ_3
4	IV	$\xi_1+\xi_2$

The invariant solutions in cases I, II, and IV are not interesting to use in solving geo-mechanical problems connected with the formation of the mining trough.
The attention in this study is concentrated on case III with invariants

$$\eta=\frac{x^2}{z} \quad \text{and} \quad P(x,z)=V(\eta)\,. \tag{6}$$

Solution to the coefficient problem

The current investigation is concerned with the problem of obtaining the coefficient *A(w)* using the results of in-situ measurements of the earth's surface displacements.

The coefficient problem for (1) – (3) can be simplified by applying transformations (6).

They transform the quasilinear parabolic partial equation into an ordinary differential equation.

After introducing the following dimensionless variables in equation (8):

$$V=\frac{w}{w_o}\,;\ A(V)=\frac{A(w)}{A(w_o)} \tag{7}$$

and substituting (6) and (11) in problems (1) – (3) it is obtained:

$$-V_\eta=4\left[A(V)V_\eta\right]_\eta \tag{8}$$

$$V(0)=0{,}5\,; \tag{9}$$

$$V(\infty)=0\,, \tag{10}$$

where $V_\eta=\frac{dV}{d\eta}$.

To solve the studied problem, the ordinary equation (12) is integrated once:

$$V-C=-4A(V)V_\eta\,. \tag{11}$$

From (11), the non-linear coefficient is obtained in the form:

$$A(V)=\frac{C-V}{4V_\eta}\,. \tag{12}$$

The constant in (12) is

$$C=4A(V_0)V_\eta(V_0)-V_0 \qquad 0\le V_0\le 1\,. \tag{13}$$

where $V(0)=0{,}5$ is the measured value of the vertical displacement above the border of the mined-out area (Fig. 1).

Finally, for *A(w)* is obtained:

$$A(V)=\frac{A(V_0)V_\eta(V_0)-V_0-0{,}25V}{V_\eta} \tag{14}$$

In order to apply relation (14), the measurements in some points of the horizontal u_0 and vertical w_0 displacements in-situ are needed. Using these values and the Avershin's relationship (1947)

$$u(x,y)=-A(w)\frac{\partial w}{\partial x}\,,$$

the values of the functional coefficient at these points can be calculated:

$$A(V_0)=-\frac{u_0}{(w_0)_x}\,.$$

Result analysis and discussion

The characteristic of the geo-material $A(V_0)$ characterizing the heterogeneity of the rock mass and its behavior in the process of subsiding is determined using the Lee group analysis of the main equation of the non-linear stochastic geo-mechanics and some measurements data. Such information is available in the survey departments of the mines. To adapt relationship (14) to the specific conditions of a mining field, it is necessary to measure the values of the vertical and the horizontal displacements in some points in the zone of subsidence trough. Instead of this, one can use empirical knowledge such as $w(0,H) \approx 0,5w_o$ in fig.1.

By creating the model (1)-(3), it is assumed after S.Knothe (1956) that the following axioms are fulfilled:

- The mining subsidence is caused by the mining out of a single horizontal coal seam;
- The dynamic phase of the process of subsiding is over;
- The mining front is linear and long enough;
- The depth of the seam is $H \geq 150m$;
- The mined-out part of the coal seam is big enough.

The established results show that once the non-linear coefficient is obtained for some zone of the mining field, the same relationship can be used for the whole influence zone of the mining operations, and in mining fields with analogical conditions.

Conclusion

The considerations presented in this paper lead to a new mathematical model which allows the determination of rock mass properties by subsiding, caused by underground excavation of geo-material.

In conclusion, it can be noted that the considerations presented above correspond to a new mechanical method for describing the medium behavior properties by subsiding. The essence of such a model is its adaptation possibility for the specific conditions in a mining field by using measurements data in some points of the influence zone.

References

Авершин С.Г. Сдвижение горных пород при подземных разработках. М., Углетехиздат, 1947. (Avershin, S. G., Sdvizhenie gornih porod pri podzemnih razrabotkah, Moskva, Ugletehisdat, 1947.)

Будрык, В. и др. Вопросы расчета сдвижении поверхности под влиянием горных разработок, Москва, Углетехиздат, 1956, стр.64. (Budrik, V.and others, Voprpsi rascheta sdvizheniy poverhnosti pod vliyaniem gornih razrabotok, Moskva, Ugletehisdat, 1956.)

Вълков, М., Нови стохастични линейни и нелинейни модели в теорията на сляганeто на земната повърхност под влияние на подземни минни работи. Автореферат на дисертацията, София, 1989 г. (Vulkov, M., Novi stohastichni lineyni i nelineyni modeli v teoriata na slyaganeto na zemnata povarhnost pod vliyanie na podzemni minni raboti, Avtoreferat na dicertatsiata, Sofia, 1989.)

Вълков, М., Стохастични модели в кинематиката на минната мулда, С., МГУ, 2006г. (Vulkov, M., Stohastichni modeli v kinematikata na minnata mulda, Sofia, MGU, 2006.)

Овсянников, Л. В., Групповые свойства уравнения нелинейной теплопроводности, ДАН, т.125, №3, 1959. (Ovsyannikov, L. V., Gruppovie svoystva uravneniya nelineynoy teploprovodnosti, DAN, 125, 3, 1959.)

Овсянников, Л. В., Групповой анализ дифференциальных уравнении, М., Наука, 1978 г. (Ovsyannikov, L. V., Gruppovoy analiz diferentsialynih uravneniy, Moskva, Nauka, 1978.)

This article was reviewed by Assoc. Prof. Dr. Stanislav Topalov and Assoc. Prof. Dr. Violeta Trifonova-Genova.